# Improved production of *epi*-cedrol and santalene by fusion protein expression: Stability study and cyclization mechanism of *epi*-cedrol biosynthesis

Thesis Submitted to the AcSIR for the Award of

The Degree of

**DOCTOR OF PHILOSOPHY**

In

Biological Science

By

**Mr. Govinda Ramnath Navale**

(10BB17J26063)

Research Supervisor

**Dr. Mahesh S. Dharne**
Principal Scientist, Head
National Collection of Industrial Microorganisms (NCIM)
Resource Centre,
CSIR-National Chemical Laboratory
Pune – 411008, India

Research Co-supervisor

**Dr. Sandip S. Shinde**
Associate Professor
Department of Industrial and
Chemical Engineering,
ICT, Mumbai, Marathwada Campus
Jalna- 431213, India

**CSIR-National Chemical Laboratory**,
**Pune, India**
March, 2020

*“Science is a way of thinking much more than it is a body of knowledge”*

*-Carl Sagan*

# Certificate

This is to certify that the work incorporated in this Ph.D. thesis entitled ***Improved production of epi-cedrol and santalene by fusion protein expression: Stability study and cyclization mechanism of epi-cedrol biosynthesis*** submitted by ***Mr. Govinda R. Navale*** to Academy of Scientific and Innovative Research (AcSIR) in fulfilment of the requirements for the award of the Degree of ***Doctor of Philosophy***, embodies original research work under my/our supervision/guidance. We further certify that this work has not been submitted to any other University or Institution in part or full for the award of any degree or diploma. Research material obtained from other sources has been duly acknowledged in the thesis. Any text, illustration, table etc., used in the thesis from other sources, have been duly cited and acknowledged.

It is also certified that this work done by the student, under my supervision, is plagiarism free.

**Mr. Govinda R. Navale**
**(Student)**

**Dr. Mahesh S. Dharne**
**(Supervisor)**

**Dr. Sandip S. Shinde**
**(Co-Supervisor)**

(Reg. No. 10BB17J26063)

Date: 16 March 2020

Place: CSIR-NCL, Pune

# *DECLARATION*

I, Govinda R. Navale, hereby declare that the work incorporated in the thesis entitled **"Improved production of *epi*-cedrol and santalene by fusion protein expression: stability study and cyclization mechanism of *epi*-cedrol biosynthesis"** submitted by me to **AcSIR** for the degree of **Doctor of Philosophy** is original and has not been submitted to this or any other University or Institution for the award of Degree or Diploma. Such material, as has been obtained from other sources, has been duly acknowledged.

*Date:* 16th March 2020
*Place:* **Pune**

**Govinda Ramnath Navale**

***Dedicated to my beloved Family…***

# *Acknowledgement*

*With* the name of *God*, I start with, it gives me great pleasure to look over my Ph.D. journey, and remember all who have helped me during my Ph.D. tenure. First and foremost, I greatly accept this opportunity to convey my heartiest thanks and express my deep sense of gratitude to my supervisor and co-supervisor Dr. Mahesh S. Dharne and Dr. Sandip S. Shinde for inspiring guidance, constructive criticism, valuable suggestions and their extensive discussions around my work, without which it would have been improbable for me to have completed my thesis. Thanks were also extended to Dr. H. V. Thulasiram, who have gave me opportunity to learn many things in his laboratory and he always helped me and supported me in various aspects. I am extremely grateful to all of them to have introduced me to the area of isoprenoids or terpene biosynthesis and their structural elucidation. They have also given me the opportunity to explore various in fields such as nanomaterials, ionic liquids etc. I take this opportunity to sincerely acknowledge the Department of Science & Technology (DST), New Delhi, and Council of Scientific and Industrial Research (CSIR), New Delhi, for providing me Ramanujan project funding and Senior Research Fellowship (SRF) which facilitated me to carry out my work. I would like to thank The Director, National Chemical Laboratory (NCL), Pune and HOD, Biochemical Sciences and Division of Organic Chemistry, for infrastructure and support to accomplish my research work. It is probably the best time to express my gratefulness towards my all BSc and M.Sc. professors, Dr. Sushma Chaphalkar, Dr. Nandkumar Khaire, Dr. Rajesh Sharma, Prof. Rupali Shinde and Prof. Priya Sonawani for kindling my scientific interest and encouraging me to explore various dimensions. I am highly obligated to Dr. Tushar Borse for sowing scientific seeds during my M.Sc. dissertation under him at Vidya Pratishthan's School of Biotechnology (VSBT), Baramati.

*I* am extremely obliged to my DAC members, Dr. Syed G. Dastager, Dr. Narendra Kadoo, and Dr. C. V. Ramana for their continuous evaluation of my Ph.D. work and their valuable advice for the same. I would also like to thank my work Collaborator, Dr. Ajali Jha, Dr. Dattatraya J. Late, Dr. Sudha Ramkumar, Dr. Poojadevi Sharma, Dr. Sanjay Borikar for their help and continuous support. I would also like to special thanks

to Dr. Prabhanjan, Dr. Amar Yevhare, Dr. Shruti, Dr. Atul Anand, Dr. Harshal Patil, Dr. Prabhakar Shrivastava, Dr. Krithika Ramkrishnan, , Dr. Avinash Pandreka, Dr. Arthy Thiagaraya, Dr. Aarti Deshmukh, Dr. Reema Banarji, Dr. Chetan Sharma, Ajay, Vijayshree, Vyankatesh, Ashish, Fayaj, Nivedita, Soniya, Chaya, Jennifer, Priti, and Khandekar Kaka for their continuous support and motivation throughout my tenure.

We don't thank friends but still I would like to thank my MSc. friends, Prem, Anagha, Amit, Vivek, Swapnil, Yugant, Manisha, and Pragati for their unconditional love, support and encouragement in my best and worst times. I would like to acknowledge my traveling cum chemistry friends Dr. Ashish Chinchunsure, Arjun Gontalka, Dr. Jayant Rathod, Sagar More, Tushar Valkute, Sandip Wagh, Sagar, Digamber, Balasaheb and Rushikesh Kale. I would like to acknowledge my organic chemistry labmates, Amruta, Trupti, Ashok, Nilesh and specially Madhukar Said for his help and contribution in synthesis and elucidation of cyclization mechanism of enzymes experimental part.

Words fail me when I express my gratitude to Meghana Thorat, Kushal Gohil and Manan Shah for supports, efforts and lab-fun, in completing critical parts of my work specially my all presentations. I would like to extend a huge thanks to my all NCIM staff members and lab-mates, Dr. Jayant Khire, Dr. D. V. Gokhale, Dr. Mamata Singvi, Dr. Monika Dhote, Mrs. Shalaka, Mrs, Ratnamala, Mrs. Kavita, Mrs. Sandhya Sudge, Mrs. Meeta, Dr. Parin, Dr. Kumar Raja, Dr. Priyanka Buddhivant, Dr. Rahul Malavankar, Dr. Gajanan Mehetre, Dr. Hari, Dr. Jaya Chakraborty, Dnyanada, Amit, Rupa, Vinod, Vasu, Bharat, Vibha, Rakesh, Junaid, Pranav, Rachel, Vinay, Vidhyashri, Sayali, Pooja, Ashish, Digheswar, Karthika, Jini, Kaustubh, Alfina, Sneha, Priya, Irfan, Manoj, Raju, Sagar, Ambadaji and Shinde Mama for providing a healthy and pleasant environment in the work place and NCIM laboratory.

My warm thanks to my room-mates, Shrikant Nikam, Santosh Lavhale, Gopal Kalure, Sandip Kadam, for bearing with me for more than 4 years and extending brotherly love towards me. I would like to give a special mention to some of my friends at NCL, namely Dr. Govind, Dr. Amit, Tripuranthaka, Mahendra, Disha, Urmila, Lina,

Manisha, Dnyanoba, Jyoti, Vishwanath, Sachin Survase, Jignesh, Hariprasad, Shiva, Vijay, Dipanjan, Tushar, Mahesh and Monika, for their constant support.

*"Family is the most important thing in the world"*

I would like to pay my highest regards to my beloved family for their constant supports, love, care, understanding and sacrifices. My late father, Mr. Ramnath Sudam Navale, my pillar of strength, motivation; my mother, Mrs. Ratnamala Navale; my elder brother, Mr. Rahul, Mr. Abhijit and Mr. Amol, they have always stood by me, my sister-in-law Mrs. Rashmi, for her care and love and my little nephew, Shriraj and Sumedh, for inspiring me to go on. My beloved sisters Ms Priyanka, for their immensely love, supports and encouragements. I would also like to thank my all my Navale family members, uncles, aunty, and all cousins for their support and encouragement. Last, but not least, I would like to thank God Ganeshji for the strength and courage. He has always blessed upon me in every phase of my life.

*--Govinda R. Navale*

# *Table of Contents*

# *List of Tables*

# *List of Figures*

***Chapter 4***



***Chapter 5***

# *Abbreviations*

| | |
|---|---|
| Å | Angstrom |
| Aa | *Artemisia annua* |
| Amp | Ampicillin |
| AA | Amino acid |
| *Aa*ECS | *Artemisia annua Epi*-cedrol synthase |
| bp | Base pair |
| Cam | Chloramphenicol |
| CDP-ME | 4-Diphosphocytidyl-2C-methyl-D-erythritol |
| CDP-ME-2P | 4-Diphosphocytidyl-2C- methyl-D-erythritol-2-phosphate |
| C-terminal | Carboxy terminal |
| DTT | Dithiothritol |
| DMAPP | Dimethylallyl pyrophosphate |
| DXP | 1-Deoxy-D- xylulose-5-phosphate |
| DXS | DXP synthase |
| DSR | DXP reductoisomerase |
| DPMD | Mevalonate-5-pyrophosphate Decarboxylase |
| EDTA | Ethylene diamine tetra acetic acid disodium salt |
| ERG1 | HMG-CoA reductase |
| ERG10 | Acetoacetyl-CoA thiolase |
| ERG13 | HMG-CoA synthase |
| ERG20 | Yeast FPP synthase |
| ECS | *Epi*-cedrol synthase |
| FPP | Farnesyl pyrophosphate |
| FPPS | Farnesyl pyrophosphate synthase |
| GPP | Geranyl pyrophosphate |
| G3P | Glyceraldehyde 3-phosphate |
| HMG-CoA | 3-hydroxy-3-methyl-glutaryl-CoA |
| IL | Ionic liquid |
| IPP | Isopentyl pyrophosphate |
| IPTG | Isopropyl β-D-1-thiogalactopyranoside |
| IspA | *E. coli* FPPS |
| IspD | 2C-methyl-D-erythritol-4-phosphate cytidylyl transferase |
| IspE | 4-diphosphocytidyl-2C-methyl-D-erythritol kinase |
| IspF | 2C-methyl-D-erythritol-2,4-cyclodiphosphate synthase |
| IspG | 1-hydroxy-2-methyl-2-(E)-butenyl-4-diphosphate synthase |
| IspH | 4-hydroxy-3-methyl-2-(E)-butenyl-4-diphosphate reductase |
| IspS | Isoprene synthase |
| Kan | Kanamycin |
| kDa | Kilo dalton |

| | |
|---|---|
| LA | Luria Bertani agar |
| LB | Luria Bertani broth |
| mg | Milligram |
| mL | Millilitre |
| MVA | Mevalonate (Mevalonic acid) |
| MEP | 2C-Methyl-D-erythritol-4-phosphate) |
| MEC | 2C-Methyl-D-erythritol 2,4-cyclodiphosphate |
| HMBDP | 1-Hydroxy-2-methyl-2-(E)-butenyl-4-diphosphate |
| [mim-$^t$OH][OMs] | Methyl imidazolium ter-butyl alcohol mesylate |
| µg | Microgram |
| µL | Microlitre |
| µM | Micromolar |
| nM | Nanomolar |
| ng | Nanogram |
| NCBI | National Center for Biotechnology Information |
| N-terminal | Amino terminal |
| NADP | Nicotinamide adenine dinucleotide phosphate |
| NADPH | Nicotinamide adenine dinucleotide phosphate reduced |
| OD | Optical density |
| ORF | Open Reading Frame |
| PCR | Polymerase Chain Reaction |
| Pyr | Pyruvate |
| PMSF | Phenyl methyl sulphonyl fluoride |
| Rt | Retention time |
| Sa | *Santalum album* |
| SaFPPS | *Santalum album* Farnesyl pyrophosphate synthase |
| SaSS | *Santalum album* Santalene synthase |
| Sec | Seconds |
| SDS-PAGE | Sodium dodecyl sulfate polyacrylamide gel electrophoresis |
| TB | Terrific broth |

# Thesis Abstract

Isoprenoids are the most abundant and highly diverse family of natural organic compounds often isolated from plant source. Many isoprenoids have useful applications in the pharmaceutical, nutraceutical, and chemical industries. However, they are naturally produced in very low quantity (0.1 % - 1 % of dry wt.). They have higher value as well as more demand. Thus, there is a need of biotechnological interventions to develop a microbial system that produces these metabolites via heterologous expression. The study has been undertaken with interest of fusion enzyme expression in heterologous host systems like *Escherichia coli* and *Saccharomyces cerevisiae* for the production of plant sesquiterpenes *epi*-cedrol and santalene via Methyl-Erythritol Phosphate (MEP) and Mevalonate (MVA) pathway, respectively. Herein, we have constructed a two fusion proteins by linking FPPS gene with sesquiterpenoid synthase genes *epi*-cedrol synthase (ECS) and santalene synthase (SS) with the help of short GSGS linker in bacterial and yeast vector. Fusion constructs FPPS-ECS-pET32a; FPPS-SS-pET32a and FPPS-ECS-pYES2/CT; FPPS-SS-pYES2/CT expressed in *E. coli* BL21 and *S. cerevisiae* INV*Sc*1 respectively. All these constructs were characterized for the single step conversion of corresponding *epi*-cedrol and α/β santalenes respectively, maximum production by heterologous expression. In this study, also includes synthesis of imidazolium based ionic liquids (ILs) functionalized with *ter*-butyl alcohol as anion. These ILs initially these ILs were evaluated for antimicrobial and antibiofilm activity on selected pathogenic microorganisms including bacteria (Gram positive and Gram negative), yeast, and fungi. In that, We observed that the ILs bearing chain lengths lower than the decyl [$C_{10}$-$^{t}$OHim][OMs] length were found to be less effective against most of the tested microorganisms analyzed for their antimicrobial and antibiofilm activity. Later these ILs supplemented in ECS enzymatic assay, which revealed that the hexyl and decyl substituted imidazolium ILs showed good stability and helped in enhanced activity of ECS at various temperature condition. Overall, we conclude that the ILs bearing chain lengths higher than the hexyl ($C_6$) length were found to be effective in ECS enzyme activity. This could be help to improved production of volatile terpenes. Finally, the cyclization mechanism of *epi*-cedrol biosynthesis are elucidated by feeding 21.6 atom % $H_2{}^{18}O$ water and hydrogen ($^{2}H$)/deuterium labelled IPP substrates in chemo-enzymatic reactions. These labelled

oxygen study, revealed that the hydroxyl group of ECS enzymatic product, *epi*-cedrol was derived from water molecule, not from the phosphate moiety of the FPP. In the final elucidation of cyclization mechanism, the GC-EI-MS fragmentation ions was compared with non-labelled ions. These isotopic mass shift fragments suggested that the 2H of C6 migrates to the C7 position during the cyclization mechanism.

## Chapter I: Introduction of isoprenoids and current updates

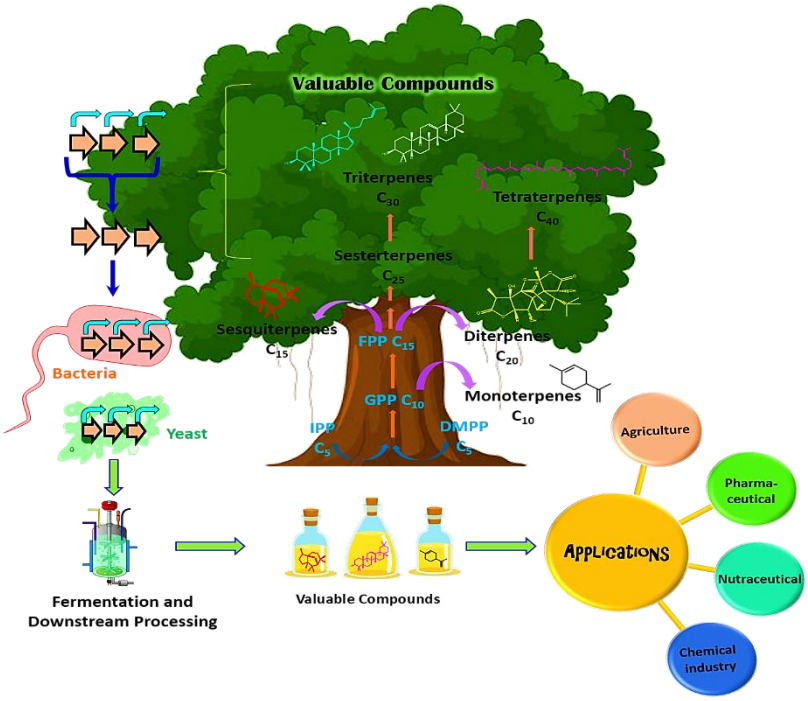


A wide range of secondary metabolites (>70,000) are produced by living things such as plants, bacteria and fungi as a part of their defence system against herbivores, pests and pathogens etc. Isoprenoids often called as terpenoids, are the most abundant and highly diverse family of natural organic compounds. In Plants, they play a diverse part in photosynthetic pigments, hormones, electron carrier, structural components of membrane, as well as an important role in communication and defence. They are often isolated from plants and used as food flavour and additives, low volatile fragrance compounds including santalol, eucalyptol, limonene and menthol; nutraceuticals such as lycopene, vitamin K, and vitamin E. In area of pharmaceuticals the natural antimalarial drugs Artemisinin, anticancer taxol (Paclitaxel) and antiviral Prostratin are some commercially important isoprenoids. Isoprenoids synthesized in living organisms by Methyl D-Erythritol 4-Phosphate (MEP) pathway and Mevalonate (MVA) pathway.

The recent advancement in metabolic engineering and synthetic biology techniques have enabled the engineering of these important isoprenoid biosynthetic pathways in the heterologous host systems like *Escherichia coli* and *Saccharomyces cerevisiae.* Both engineered systems are induced for large scale production of value added isoprenoids. In this chapter, the engineering in MEP pathway and MVA pathway for synthesizing isoprene units ($C_5$) and its poly-isoprene chains for terpenoid productions have been summarized. This introduction chapter particularly emphasised the efforts taken for the production of hemiterpenoids ($C_5$), monoterpenoids ($C_{10}$), and sesquiterpenoids ($C_{15}$) by various metabolic engineering techniques in *E. coli* and *S. cerevisiae* over a decade.

## Chapter 2: Production of *epi*-cedrol and santalene in *E.coli* and *S. cerevisiae*

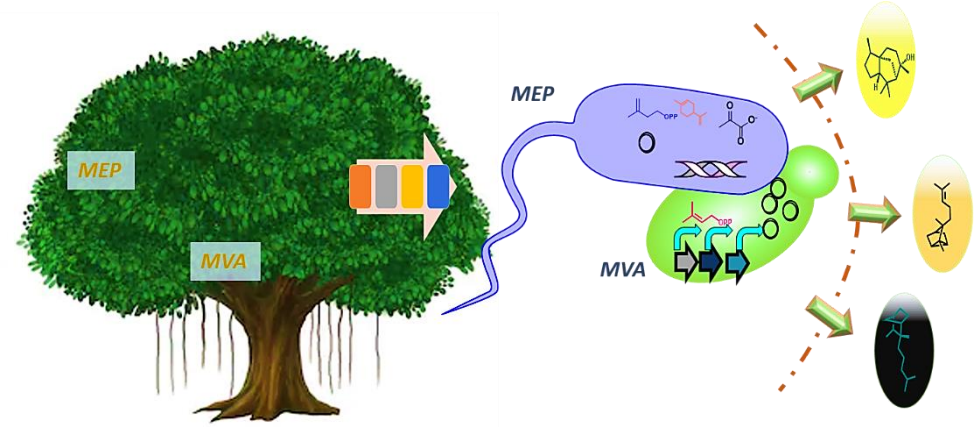


*E. coli* and *S. cerevisiae* are the promising hosts for isoprenoid production, as these systems are the most successful due to a wide range of advantages, including ease of manipulation, high sugar catabolic rate, simple genetic background as well as relatively high growth rate and native isoprenoid pathway flux.

### *Section 2A*- Cloning, expression and characterization of two fusion proteins: FPPS-ECS and FPPS-SS in *E. coli*

Biosynthesis of terpenoid/isoprenoids production in *E. coli* has been carried out by the MEP or DXP pathway. This pathway consists of seven enzymatic steps that convert glyceraldehyde-3-phosphate (G3P) and pyruvate to IPP and DMAPP in a ratio of 5:1. Overexpression of terpene synthases leads to the biosynthesis of respective isoprenoids. Production of *epi*-cedrol and santalene was carried out by cloning and

expression of two fusion proteins of FPPS-ECS and FPPS-SS in pET 32a vector in *E. coli* host organisms respectively. The recombinant purified multifunctional enzymes carried out the efficient and faster conversion of IPP to respective sesquiterpenoids *i.e epi*-cedrol and α/β-Santalene, compared to the corresponding individual enzymes together respectively. In shake flask fermentation, recombinant *E. coli* harbouring fusion plasmids individually produces 1.021 mg/L *epi*-cedrol and 0.433 mg/L santalene (α/β) mixtures in broth respectively by IPTG induction (1mM) for 16 h. The production of *epi*-cedrol in *E. coli* is three times enhanced than previous reports in yeast.

***Section 2B*- Cloning, expression and characterization of two fusion proteins: FPPS-ECS and FPPS-SS in *S. cerevisiae***

Biosynthesis of isoprenoids production in yeast (*S. cerevisiae*) has been carried out by MVA pathway. In this pathway, central carbon metabolism via acetyl-CoA, ATP and NAD(P)H which is the final metabolite of the glycolysis pathway, and synthesized IPP/DMAPP from mevalonate. This makes ease of production of isoprenoids in this host. Heterologous expression of terpene synthases MVA pathway has generally resulted in higher production titers than an endogenous pathway. Although, the MEP/DXP pathway is theoretically more efficient than MVA pathway. For better production of our sesquiterpenes (e*pi*-cedrol and santalenes), fusion of FPPS-ECS and FPPS-SS were carried out in pYES2/CT yeast expression vector and *S. cerevisiae* host cell respectively. Out of both fusion constructs, *epi*-cedrol was detected in yeast broth extracts and also confirmed by crude enzymatic assay experiments. In future, further optimization in production *via* galactose induction needs to be carried out.

***Section 2C*- Structural and docking analysis of two fusion proteins**

In order to gain insight in the fusion proteins and substrate binding, I-TASSER predicted protein model was docked with various substrate by using AutoDock Vina (v4.2) tool. These structural models help to gain insight in the role of synthetic linker in protein structure and function. The enzyme catalyses the formation of multiple products from a single substrate because of the consequences of the highly reactive series of carbocationic intermediates formed during the enzyme assay. FPP was

synthesized from the active pocket of FPPS in fusion protein and easily channelled to α-helical loop over the active site that protects the carbocation from the water.

Overall, our results indicated that fusion of two enzymes may have led to their active pockets closing together and helped in the substrate channeling in fusion enzymes which leading to increase in the overall catalytic activity.

## Chapter 3: Stability of terpene synthases in imidazolium based ionic liquids (ILs)

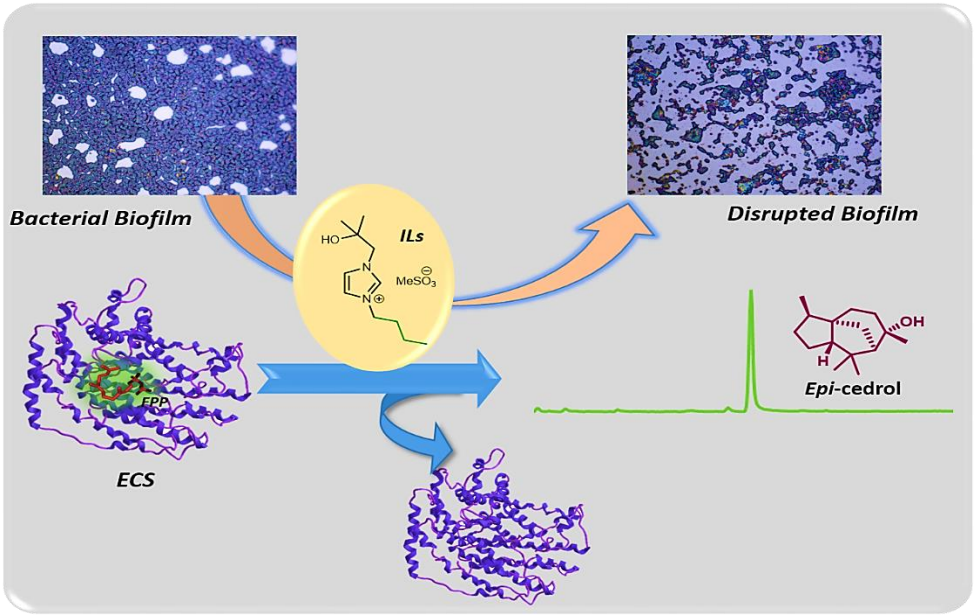


Imidazolium salts or Ionic liquids (ILs) are low-melting-point salts, thus forming liquids that consist of only cations and anions. They are often applied to any compounds that have a melting point less than 100 °C. For the overall environmental impact and economics, they are employed as greener solvents for electrochemistry, analytical chemistry, chemical synthesis, liquid-liquid extractions, and catalysis etc. Their physical, biological and chemical properties such as being liquids at room temperature, reasonable chemical stability, low flammability, insignificant vapor pressure and high ionic conductivity are the main motivating factor behind the vast interest in green chemistry applications. They are widely used in biological fields as antimicrobial, anti-cancer etc. as well as in biomedical fields such as protein based pharmaceuticals and therapeutics, media for bio-catalytic reactions, and biosensors. It also applied in protein stabilization to avoid denaturation and precipitation, to increase protein solubility, adjusting osmolality of the solutions, protecting hydrophobic regions

of the proteins and single alternatives for sugar, salts, and amino acids to provide stability. They are act as an antioxidant or antimicrobial agents and also applied as bio-preservation/bio-protectant (Replacement of DMSO/Glycerol). Herein we have synthesised various alkyl chain based imidazolium based ILs which has good antimicrobial and antibiofilm properties. We have conducted an experiment which could help to optimize the stability of terpene synthase enzymes at various temperature conditions. Terpene cyclases, *ECS* from *A. annua* plant spp. have been used as primary terpene cyclase enzyme to check the stability and catalytic activity in ILs. Among all seven imidazolium ILs, hexyl and decyl alkyl chain containing IL gives better stability as well as enhanced the catalytic activity of ECS at various temperature conditions. This could be used as best enzyme protectant in future.

## Chapter 4: Elucidation of cyclization mechanism of e*pi*-cedrol biosynthesis

### *Section 4A*- Source of oxygen atom in *epi*-cedrol biosynthesis

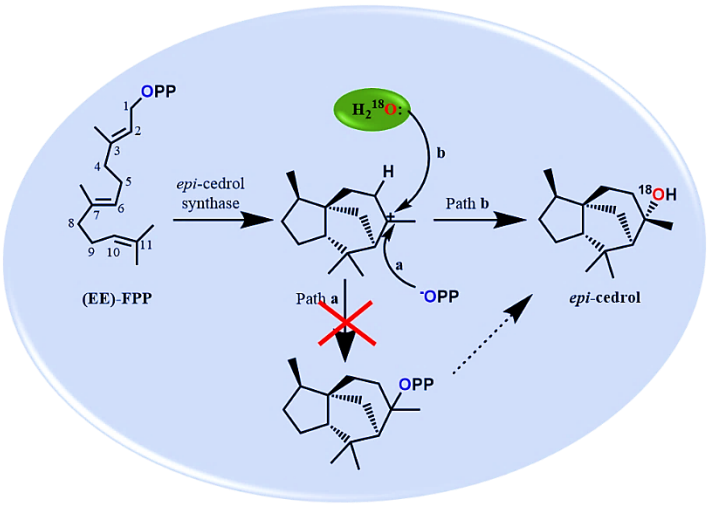


Sesquiterpene synthases catalyses the cyclization of the FPP into complex hydrocarbon skeletons through a series of reactions involving electrophilic cyclization's, Wagner-Meerwein re-arrangements etc. The oxygen atom of sesquiterpenes is derived either from a water molecule or from the oxygen of diphosphate anion of FPP. Herein we have studied the source of oxygen atom in *epi*-cedrol biosynthesis by carrying out the enzyme assay in $H_2{}^{18}O$. In conclusion, we have demonstrated that the oxygen atom of the hydroxyl functionality of *epi*-cedrol is derived from a water molecule, not from the oxygen of diphosphate anion of farnesyl

diphosphate. The attack of water to obtain the isotopically labelled *epi*-cedrol is preferred due to the steric blocking effects of the proximal geminal dimethyl groups in cedryl carbocation. The detection of traces of isotopically labelled cedrol implies that attack on the unbound carbocation is at least partially responsible for the observed product mixture.

***Section B*- Elucidation of cyclization mechanism of *epi*-cedrol biosynthesis by chemo-enzymatic deuterium labelling method**

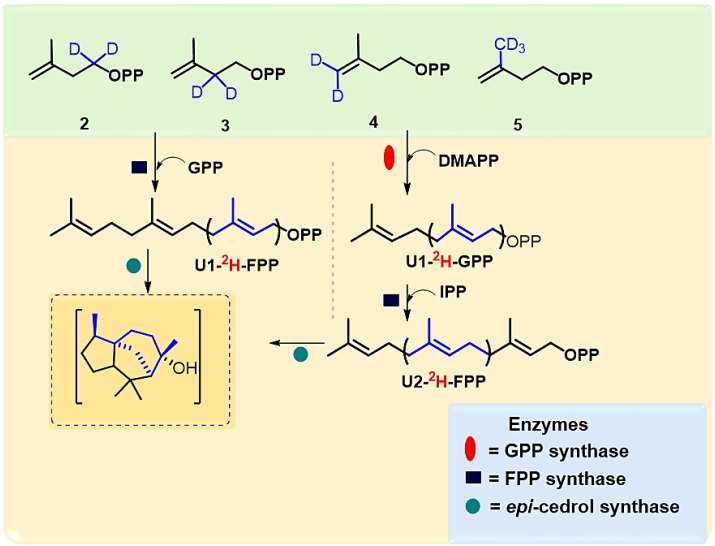


Sesquiterpene synthases catalyses the cyclization of the FPP into complex hydrocarbon skeletons. The biosynthesis mechanisms of these enzymes have been investigated by feeding isotope-labelled precursors to terpene cyclase. These isotopes include deuterium, ($^{2}$H), carbon ($^{13}$C) and tritium ($^{3}$H). The conventional method to trace isotopically-labelled products derived from enzyme catalysts is NMR spectroscopy, which generally requires milligram amounts of product for complete analysis, thus to synthesis sufficient amount of product requires high quantities of labelled precursors and enzymes. Herein, we successfully labelled eight specific positions of FPP followed by a chemo-enzymatic strategy which biosynthesized ($^{2}$H) *epi*-cedrol and GC-EI-MS fragmentation based mechanism of *epi*-cedrol demonstrated that the 1, 2-migrations of the hydride while cyclization of *epi*-cedrol biosynthesis. The strategy is highly sensitive and provides sufficient information of proton/hydride migrations by mass of fragmented ion analysis, also the rapid synthesis of any desired

deuterium labelled poly-prenyl chain can be achieved by using all the four specifically labelled IPPs.

### Chapter 5: Summary and future perspectives

In this chapter, summary of thesis chapters and the future perspectives and challenges of work has been discussed.

# Chapter 1
# Introduction of isoprenoids and current updates

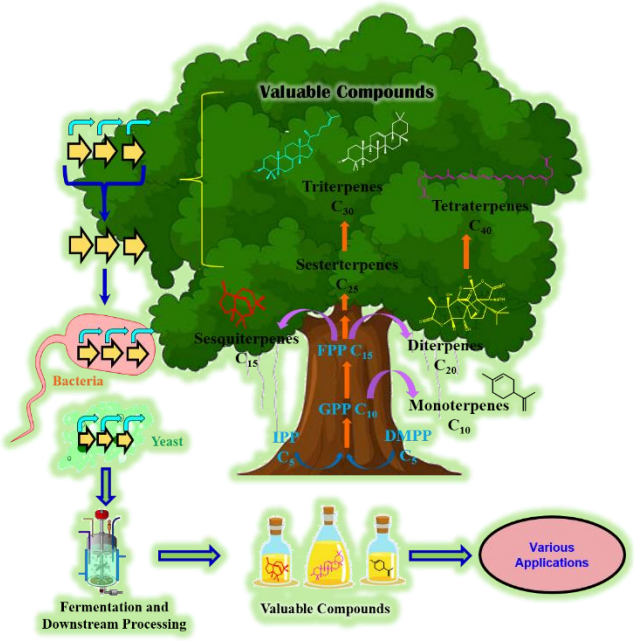

**Abstract**

A wide range of secondary metabolites are produced by living organisms such as plants, bacteria and fungi as a part of their defense system against herbivores, pests and pathogens etc. Isoprenoids often called as terpenoids, are the most abundant and highly diverse family of natural organic compounds. In Plants, they plays a diverse part in photosynthetic pigments, hormones, electron carrier, structural components of membrane, as well as an important role in communication and defense. Many isoprenoids have useful applications in the pharmaceutical, nutraceutical, and chemical industries. Isoprenoids synthesized in living organisms by Methyl D-Erythritol 4-Phosphate (MEP) pathway and Mevalonate (MVA) pathway. The recent advancement in metabolic engineering and synthetic biology techniques have enabled the engineering of these important isoprenoid biosynthetic pathways in the heterologous host systems like *Escherichia coli* and *Saccharomyces cerevisiae.* Both engineered systems are induced for large scale production of value added isoprenoids. In this chapter, the engineering in MEP pathway and MVA pathway for synthesizing isoprene units ($C_5$) and its poly-isoprene chains for terpenoid productions have been summarized. This introduction chapter particularly highlighted the efforts taken for the production of hemiterpenoids ($C_5$), monoterpenoids ($C_{10}$), and sesquiterpenoids ($C_{15}$) by various metabolic engineering techniques in host *E. coli* and *S. cerevisiae* over a decade.

## 1. Introduction

Isoprenoids are the class of secondary metabolites, and the most abundant structurally diverse (>60,000 different structures) family of natural products in plants and microorganisms (Tholl, 2015; Yamada et al., 2015). Classification of isoprenoids are divided on the basis of number of $C_5$ isoprene units and its poly-chains, such as hemiterpenes ($C_5$), monoterpenes ($C_{10}$), sesquiterpenes ($C_{15}$), diterpenenes ($C_{20}$), sesterterpenes ($C_{25}$), Triterpenes ($C_{30}$), and Tetraterpenes ($C_{40}$) (**Fig. 1**). Isoprenoids often isolated from plants, are used as food flavours and additives; low volatile fragrance compounds including santalol, eucalyptol, limonene and menthol; nutraceuticals such as lycopene, vitamin K, and vitamin E. In area of pharmaceuticals the natural antimalarial drugs Artemisinin, anticancer taxol (Paclitaxel) and antiviral Prostratin are the some commercial important isoprenoids (**Fig. 2**) (Singh and Sharma, 2015; Vickers et al., 2017).

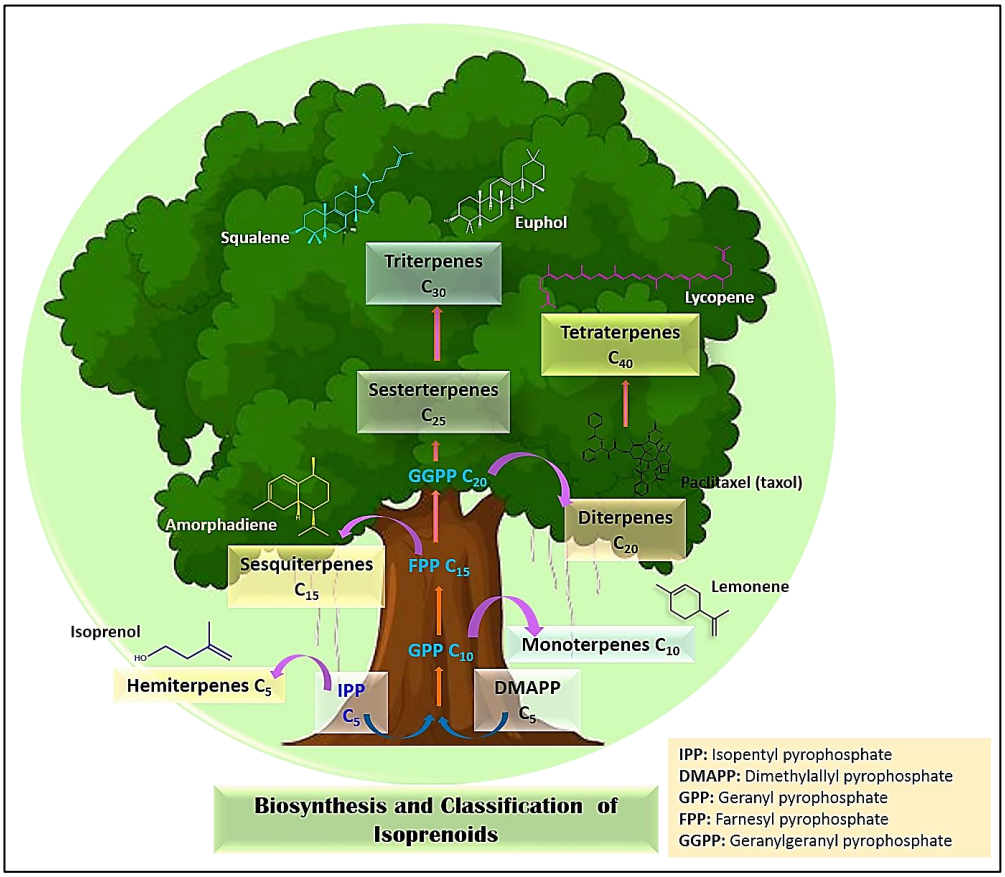


**Figure 1.** Biosynthesis pathway of isoprenoids.

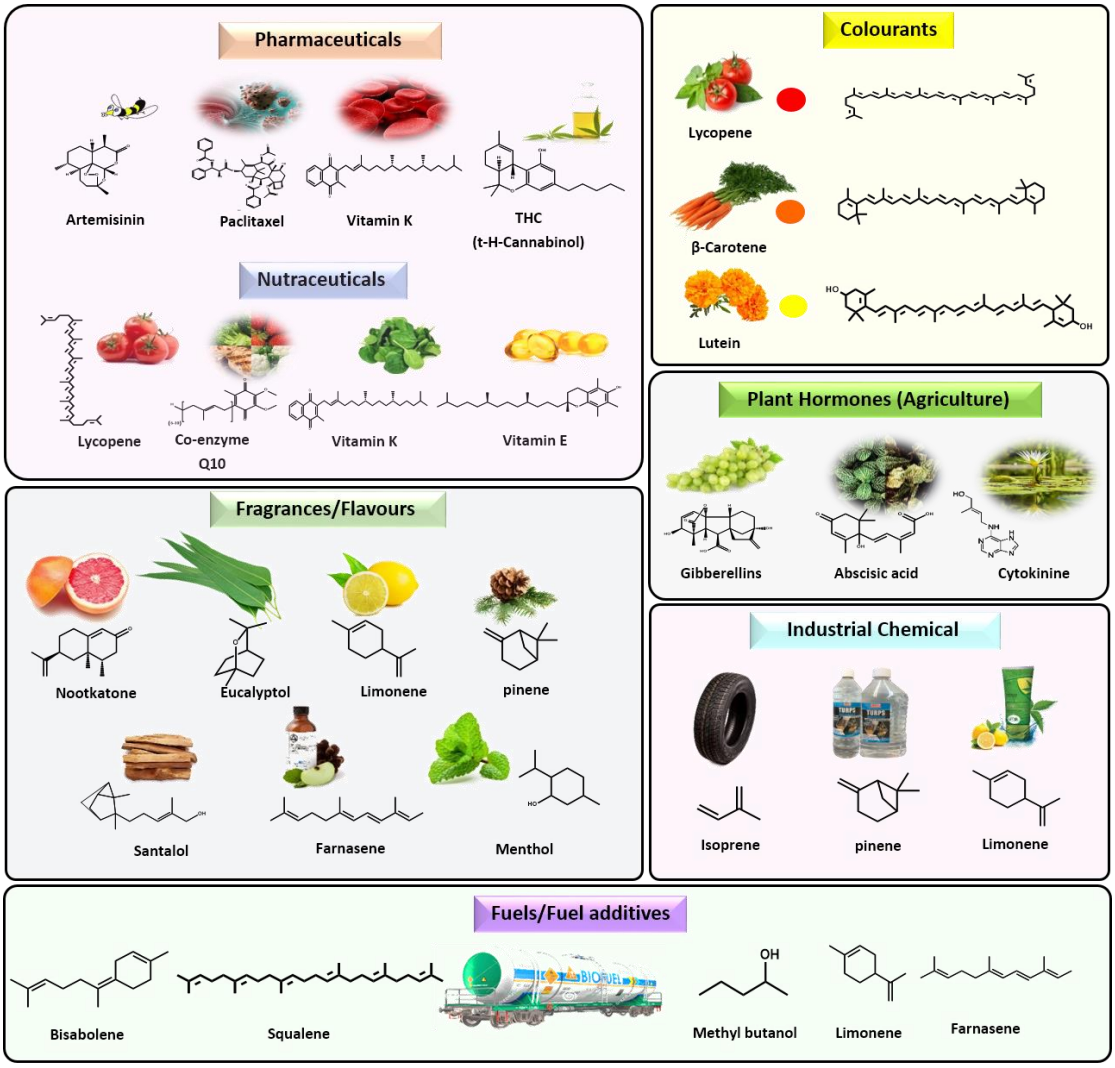


**Figure 2**. Applications of isoprenoids in various fields (Singh and Sharma, 2015; Vickers et al., 2017).

Isoprenoids are synthesized in plants *via* Mevalonate (MVA) and Non-mevalonate or Methyl D-Erythritol 4-Phosphate (MEP) or 1-deoxy-D-xylulose-5-phosphate (DXP) pathways (Vranová et al., 2013). MEP pathway is carried out in plastids while MVA pathway carried out in cytosol as shown in **Fig. 3**. Recently numerous isoprenoids reported for their potential uses in advanced biofuel industry due to the methyl branching and cyclic hydrocarbons chain (Tippmann et al., 2013). The extraction of mature *Artemisia annua* (sweet wormwood) plant yields 1.5 % of artemisinin of their dry weight (Weathers et al., 2011), while four year mature Pacific yew trees (*Taxus brevifolia*) yields only 1 g of paclitaxel (Liu and Khosla, 2010) from natural sources which is infeasible to complete the demand of current world population.

However, the production of isoprenoids in natural sources are insufficient concentrations. Considering the importance of commercial value of isoprenoids, hampering industrially viable in large scale production (Pickens et al., 2011). Chemical synthesis of these natural isoprenoids is difficult and costly because of their structural complexity and gives low yields. Engineering of metabolic pathway in microbial systems for the production of isoprenoids in large scale presents a cost-effective alternative tool for isoprenoid biosynthesis. Therefore, significant metabolic engineering in a microbial host (*e.g. Escherichia coli, Bacillus subtilis, cyanobacteria-Synechocystis sp.*.) with transplantation of heterologous pathway from a natural source (plants) is generally required to achieve appropriate amounts and yields for industrial or commercial applications, are a key solution for this issue. Yeast (*Saccharomyces cerevisiae* and *Pichia pastoris*) is an alternative eukaryotic model system, widely used in peptide production and metabolic engineering. It has also the ability to produce isoprenoids, with the biosynthesis of hydrocortisone from the sterol pathway (Szczebara et al., 2003; Zhang et al., 2017b).

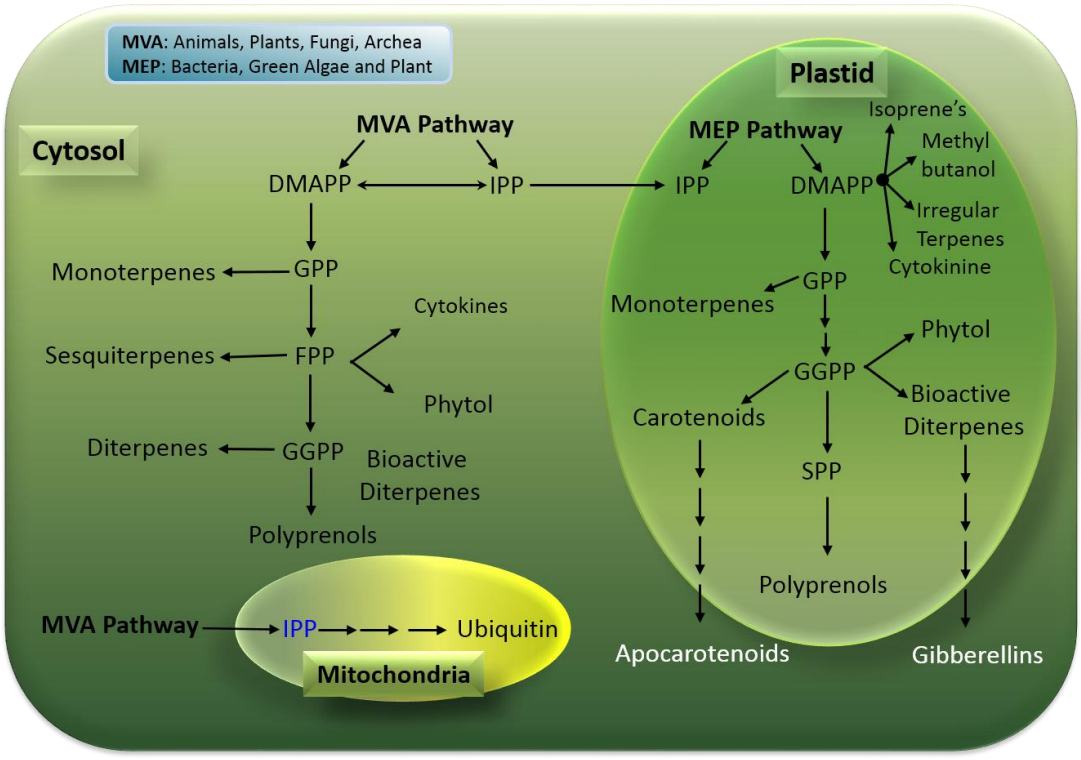


**Figure 3**. Sub-cellular localization of MEP and MVA pathways in plants (Vranová et al., 2013).

*E. coli* and *S. cerevisiae* are the promising hosts for isoprenoid production, as this host systems are the most successful among other organisms due to a wide range of advantages, including ease of manipulation, high sugar catabolic rate, simple genetic background as well as relatively high growth rate and native isoprenoid pathway flux. The capacity to engineer improved isoprenoid pathway flux to introduce complex functional modifications of products and amenability to industrial bio-process conditions (Ignea et al., 2011). Both microbes having precursors for biosynthesis of building blocks of isoprenoids via MEP pathway (*E. coli*) and MVA (*S. cerevisiae*) pathway. *S. cerevisiae* biosynthesized the precursors of isoprenoids naturally by the sterol biosynthetic pathway, which helps in the improvement of plant terpenoid production (Gonzalez et al., 2017). There are many tools or pathway engineering way available for the production of natural metabolites in *E.coli* and *S. cerevisiae*, such as advances in chromosome integration by CRISPR-*Cas9* aid tool, promoters, trans-acting factors and novel terminators, RNAi and riboswitches, developments in small molecule sensing strategies for optimizing pathway engineering, overexpression of isoprenoid synthase genes, and fusion protein expression *etc*. (Besada-Lombana et al., 2018; Donohoue et al., 2017; Keasling, 2012; Li et al., 2015; Shi et al., 2016; Tong et al., 2019).

Over the past decades, efforts have been made in metabolic engineering and synthetic biology to enhance the production of numerous isoprenoids in hosts *E. coli* and *S. cerevisiae*. This introduction chapter covers the recent development in the biosynthetic pathways of isoprenoids in genetically engineered of hemiterpenoids ($C_5$), monoterpenoids ($C_{10}$), and sesquiterpenoids ($C_{15}$) in *E. coli* and *S. cerevisiae* and also commented on the future perspectives on commercially valuable plant isoprenoid production by microbial host are summarized.

## 2. Isoprenoid Biosynthetic Pathways in *E. coli* and *S. cerevisiae*

Isoprenoids are composed of branched isoprene units ($C_5$), derived from two basic building blocks, isopentenyl pyrophosphate (IPP) and dimethylallyl pyrophosphate (DMAPP) (Withers and Keasling, 2007). There are two distinct pathways for IPP and DMAPP synthesis from metabolites of the glycolytic pathway, which is a major metabolic pathway in cells: the MVA pathway is present mainly in

eukaryotes (plants), archaea, few insect species, and eubacteria; and the Non-mevalonate or MEP or DXP pathway is found mainly in prokaryotes, algae and plant plastids (Miziorko, 2011). Therefore, the pathways providing the isoprene units, IPP and DMAPP, for the synthesis of isoprenoids are termed as the "stem pathways". The building blocks of IPP and DMAPP are condensed or cyclized in a head-to-tail manner to form geranyl pyrophosphate (GPP, $C_{10}$), farnesyl pyrophosphate (FPP, $C_{15}$), geranylgeranyl pyrophosphate (GGPP, $C_{20}$), and decaprenyl pyrophosphate (DPP, $C_{50}$). These are the intermediates finally required for the conversion into diverse and complex structural isoprenoid compounds by sequential cyclization reactions via various terpene cyclases. These condensation and modification pathways are termed as the "branch pathways". Generally, isoprenoid production has been achieved by increasing the intracellular pool of basic building block elements IPP and DMAPP by engineering of the DXP and MVA pathways as well as isoprenyl pyrophosphate synthases (*Isp*S) and terpene synthases (or phosphatases) (*Tsp*S). They can also be engineered through knock-down of next cyclase gene to get more flux in isoprenoid biosynthetic pathway (Lange et al., 2000).

### 2.1. Generation of isoprenes (IPP and DMAPP) in *E. coli* and *S. cerevisiae*

Biosynthesis of isoprenes in *E. coli* has been carried out by the MEP or DXP pathway. The DXP pathway consists of seven enzymatic steps that convert glyceraldehyde-3-phosphate (G3P) and pyruvate to IPP and DMAPP in a ratio of 5:1 (Rohdich et al., 2003). It initiates with enzyme DXP synthase (DXS) which catalyzes the condensation of G3P and pyruvate to form DXP. This step is crucial and is rate limiting step (Zhao et al., 2013). Further DXP reduced into methyl D-erythritol 4-phosphate (MEP) by DXP reductoisomerase (DXR). MEP undergoes series of reactions, MEP cytidylyl transferase (*Isp*D) catalyses MEP to 4-diphosphocytidyl-2-C-methyl-D-erythritol (CDP-ME), CDP-ME phosphorylate into 4-diphosphocytidyl-2-C-methyl-D-erythritol-2-phosphate (CDP-MEP) by 4-diphosphocytidyl-2-C-methyl-D-erythritol kinase (*Isp*E). Further cyclilization are carried out by MEcPP synthase (*Isp*F) and (*Isp*G) to form 2-C-methyl-D-erythritol-2,4-cyclodiphosphate (MEcPP), 4-hydroxy-3-mehtyl-butenyl 1-diphosphate (HMB-PP), respectively. The two iron-sulfur proteins, 4-hydroxy-3-methyl-2-butenyl pyrophosphate synthase (*Isp*G) and reductase

(*Isp*H), finally catalyze the reduction of MEcPP to IPP and DMAPP (**Fig. 4a**) (Rohmer et al., 1993; Wang et al., 2017). Both *Isp*G and *Isp*H require flavodoxin (Fld) and flavodoxin/ferredoxin reductase (Fldr) to modulate the redox potential of their [$Fe_4$-$S_4$] cluster (Wang and Oldfield, 2014). IPP isomerase (IDI) isomerised IPP and DMAPP. The total seven genes (*DXS*, *DXR*, and *Isp*-D-E-F-G-H) encoding the MEP/DXP pathway in the *E. coli* genome and regulated by different promoters. This pathway is affected by various aspects of the intracellular metabolites including available carbon, ATP, the reducing power, and accumulation of intermediates of the pathway (Banerjee and Sharkey, 2014).

On the other hand, the yeast has MVA pathway for the isoprenoid biosynthesis as mentioned above, which is connected to central carbon metabolism via acetyl coenzyme A (acetyl-CoA), ATP (energy) and NAD(P)H (reducing power) which is the final metabolite of the glycolysis pathway, two molecules of acetyl-CoA are sequentially are condensed to form acetoacetyl-CoA by an acetoacetyl-CoA thiolase (encoded by *ERG10*) and HMG-CoA synthase (*ERG 13*) to form 3-hydroxy-3-methylglutaryl-CoA (HMG-CoA), which is then reduced to mevalonate by HMG-CoA reductase (ERG 1) (**Fig. 4b**). These three catalytic steps are referred to as the upper portion of the MVA pathway, while the remaining steps of conversion of mevalonate to IPP/DMAPP synthesis are referred to as the lower portion. Mevalonate is phosphorylated twice at the 5'-OH position by mevalonate kinase (MK) and mevalonate-5-phosphate kinase (PMK) and then decarboxylated to IPP by mevalonate-5-pyrophosphate decarboxylase (DPMD) (Farhi et al., 2011; Lv et al., 2014). This pathway is further connected to the steroid biosynthesis.

Recently, both pathways have been successfully engineered in *E. coli* and *S. cerevisiae* for isoprenoid production, heterologous expression in MVA/MEP pathway are generally depend on the selection of promoter and cyclase enzymes for the production of different isoprenoids. Although, the MEP/DXP pathway is theoretically more efficient with a carbon yield of 1.255 mol of glucose per mole of IPP than the MVA pathway with 1.5 M glucose per mole IPP (Ajikumar et al., 2010).

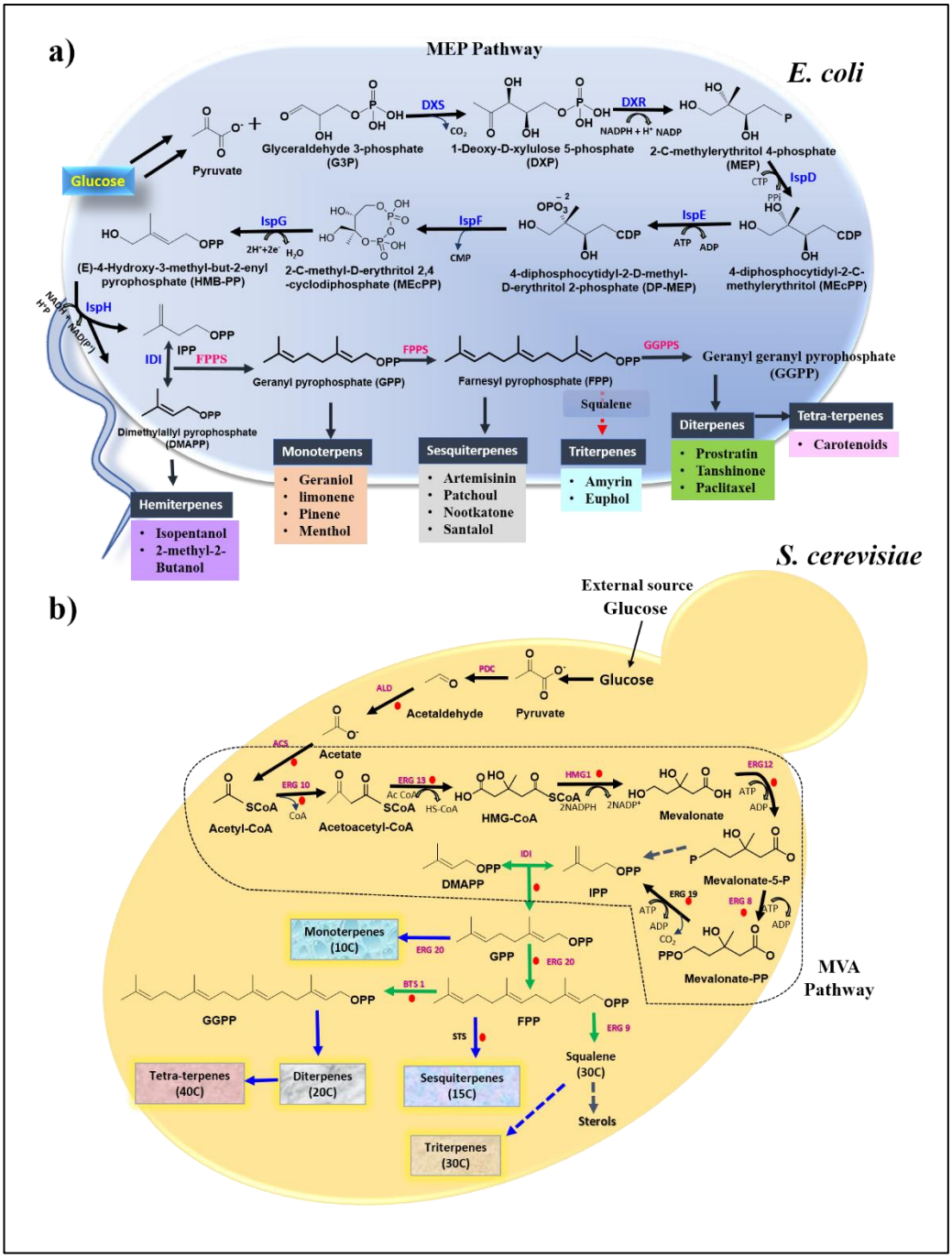


**Figure. 4 a)** Isoprenoid biosynthesis pathway MEP/DXP in *E. coli*. **b)** MVA pathway in *S. cerevisiae* (red dots represent the enzyme/gene targets for metabolic engineering) (Singh and Sharma, 2015; Vickers et al., 2017).

## 2.2. Biosynthesis of various isoprenoids

Biosynthesis of IPP ($C_5$) and DMAPP ($C_5$) are either by DXP/MEP pathway or MVA pathway, these linear isoprenyl pyrophosphates are generated by head-to-tail condensations. Further they are converted by various terpene synthases to form

hemiterpenes (1 isoprene unit, $C_5$), monoterpenes (2 isoprene units, $C_{10}$), sesquiterpenes (3 isoprene units, $C_{15}$), diterpenes (4 isoprene units, $C_{20}$), Sesterterpenoids, (5 isoprene units, $C_{25}$), Triterpenoids (6 isoprene units, $C_{30}$), tetra-terpenoids (8 isoprene units, $C_{40}$). Isoprene synthases (*Isp*S) catalyses the de-phosphorylation of DMAPP to isoprene, the simplest hemiterpene. GPP, FPP, and GGPP are catalyses by GPP synthase (GPPS), FPP synthase (FPPS), and GGPP synthase (GGPPS) into numerous isoprenoids via carbocationic reaction and forms a carbon skeletons in the structure (Christianson, 2017). They are also utilizes these substrates to form various isoprenoids such as squalene ($C_{30}$) and phytoene which are the precursors of triterpenoids, cholesterols, and carotenoids (Ghimire et al., 2009).

These skeletons regio-/stereo-selectively catalysed by many tailoring enzymes such as cytochrome P450 (P450s), acyltransferase, cleavage, cyclization, oxidation, acylation and glycosyltransferase by combinatory manner and finally formed into various functions to isoprenoids (e.g., artemisinin, taxol, retinol and ginkgolide) (King et al., 2016). The structural diversity of isoprenoids depends on various terpene synthases and consecutive steps. Therefore, the microbes, which is a better host and several genetic engineering techniques are available for them, can be easily engineered to synthesize valuable isoprenoids by collecting together for the precursor synthesis, isoprenyl chain elongation, structural rearrangement and enzymatic reactions. Recently advancements and achievements in metabolic engineering in microbial host *E. coli* and *S. cerevisiae* for the heterologous production of hemiterpenes, monoterpenes, and sesquiterpenes are elaborated further in following sections.

## 3. Biosynthetic Isoprenoids

There is enormous interest in the production of terpenoids from microbial sources. Till date, many efforts have been taken in this direction using metabolic engineering and synthetic biology approach by various scientific groups in the world. Various isoprenoid production in *E. coli* and *S. cerevisiae* has been achieved by modifying DXP and MVA pathway by increasing pool between terpene synthases and, IPP and DMAPP (**Fig. 4**). Isoprenoids are usually derived from plants and microbial sources, but they are in less quantity (Niu et al., 2017; Wang et al., 2018). *In vitro* production of isoprenoids using plant tissue culture and plant metabolic engineering, have a complexity in downstream processing, because of the interference of phenolic

and other products, though they have received some success in development (Nosov et al., 2014). For the synthesis of isoprenoids, some of the common targets in *S. cerevisiae* are as follows: **i**) for all classes of terpenes (mono-, di-, ses-) overexpression of *tHMG1*, *ERG20*, *upc2-1*, Site-directed mutagenesis such as Upc2p (G888A). **ii**) For mono-, di- and sesquiterpenes repression of ERG9 by replacement of the native promoter with a repressive methionine promoter, a mutation in ERG20p (K197G). **iii**) In the case of di- and tetraterpenes, overexpression of BTS1 (Krivoruchko and Nielsen, 2015; Paramasivan and Mutturi, 2017). **iv)** Yeast homologous recombination cloning (Joska et al., 2014). **v**) Machine-learning workflow in conjunction with YeastFab Assembly strategy (MiYA) for optimizing of heterologous metabolic pathway (Zhou et al., 2018).

### 3.1 Biosynthetic Hemiterpenoids

Hemiterpenoids or isoprene ($C_5H$) are the simplest form of isoprenoid. They are used in the commercial manufacturing of millions of tons of synthetic rubber for tires and various other applications, such as elastomers and adhesives. It is also suggested as liquid fuel (Isopentanol, methyl-butanol) (Niu et al., 2017). Several IspS or terpene cyclases (TcS) have been isolated from various plant species, and their heterologous expression enables *E. coli* and *S. cerevisiae* to produce isoprene as summarised in **Table 1**.

| Hemiterpenes | Strategy Used | Host | Culture Conditions | Yield/ Titre | Ref. |
|---|---|---|---|---|---|
| Isoprene | Combination of MVA and DXP, optimized with gas-phase recovery | *E. coli* | Fed-batch fermentation | 60 g/L | (Whited et al., 2010) |
| Isoprene | Expressing *P. nigra IspS* and *B. subtilis* DXS and DXR | *E. coli* | Fed-batch fermentation | 314 mg/L | (Zhao et al., 2011) |
| Isoprene | Engineered MVA pathway from *S. cerevisiae* and IspS from *P. alba* | *E. coli* | Shake-flask fermentation | 532 mg/L | (Yang et al., 2012b) |
| Isoprene | Replacement of an upper portion of MVA from *S. cerevisiae* with *E. faecalis* | *E. coli* | Fed-batch fermentation | 6.3 g/L | (Yang et al., 2012a) |

| | | | | | |
|---|---|---|---|---|---|
| Isoprene | Compared five different MEP feeding module (EMP, EDP, PPP *etc*.) | *E. coli* | Shake-flask fermentation | 221 mg/L | (Lv et al., 2013) |
| Isoprene | Engineering of the native acetyl-CoA and MVA with a push-pull-restrain strategy | *S. cerevisiae* | Shake-flask fermentation | 37 mg/L (782 fold) | (Lv et al., 2014) |
| Isoprene | Expressing *DXS, DXR* and *IDI* | *E. coli* | Shake-flask fermentation | 17.5 mg/L | (Lv et al., 2016a) |
| Isoprene | Dual metabolic engineering of cytoplasmic and mitochondrial acetyl-CoA utilization | *S. cerevisiae* | Fed-batch fermentation | 2.5 g/L | (Lv et al., 2016b) |
| Isoprene | *P. trichocarpa ispS* and the Engineered MVA pathway, deleted several genes and preventing the waste of acetyl-CoA | *E. coli* | Shake-flask fermentation | 1.8 g/L | (Kim et al., 2016) |
| Isoprene | Synergic effect of DXP and MVA simultaneously | *E. coli* | Fed-batch fermentation | 24 g/L | (Yang et al., 2016a) |
| Isoprene | Heterologous expression of MVA upper pathway | *E. coli* | Fed-batch fermentation | 620 mg/L | (Yang et al., 2016b) |
| Isoprene | Optimises ribosome sequences and screened IDI, MK and *Isp*S enzymes from various organisms | *E. coli* | Shake flask fermentation | 698 mg/L | (Li et al., 2019) |
| Isoprene | Overexpr,MVA pathway genes *mvaE, mvaS, mvk, pmk, mvaD,* and *idi* to accelerate DMAPP | *E. coli* | Fed-batch fermentation | 587 mg/L | (Liu et al., 2019) |
| Isoprene | NADPH redox cofactor balance by coupling the production with 1,3-Propandiol | *E. coli* | Shake-flask fermentation | 665 mg/L | (Guo et al., 2019) |
| Prenol/ Isoprenol | Engineered MVA pathway and blocking the conversion of IPP to | *E. coli* | Shake-flask fermentation | 1.3 g/L | (Zheng et al., 2013) |

| | | | | | |
|---|---|---|---|---|---|
| | DMAPP and employing *B. subtilis NudF* | | | | |
| Isopentanol | Overexpr. of *NudF* and *yhfR* from *B. subtilis;* and (MEP pathw) *IspG* and *Dxs* | *E. coli* | Fed-batch fermentation | 69 mg/L | (Liu et al., 2014) |
| Isopentanol | Engineered MVA, Shorter 3 step, Mevalonate kinase (*MK*), *DPMD* and *AphA* (instead of *NudB/F*) | *E. coli* | Shake-flask fermentation | 836 mg/L | (Kang et al., 2016) |
| Isopentanol | CRISPRi-mediated silencing of multiple repressor endogenous genes | *E. coli* | Shake-flask fermentation | 1.2 g/L | (Tian et al., 2019) |
| Methylbutenol | Engineered MEP by modifying Nud B and MK (mevalonate kinase) expression | *E. coli* | Shake-flask fermentation | 2.2 g/L | (George et al., 2015) |

**Table 1.** Biosynthetic production of various isoprenoids by engineered microorganisms *(E. coli /S. cerevisiae*).

Improving hemiterpenoids production mainly depends on increasing the DMAPP supply. Combination of pathway engineering strategy with gas-phase recovery optimized the production of 60 g/L isoprene in a fed-batch culture (Whited et al., 2010). Zhao *et al.,* improved the isoprene production up to 314 mg/L in fed-batch culture by expressing *Populus nigra Isp*S as well as *Bacillus subtilis* DXS (DXP synthase) and DXR (DXP reductoisomerase) in *E. coli* (Zhao et al., 2011). The engineered MVA pathway in *S. cerevisiae* and *Populus alba IspS* in *E. coli* produces 532 mg/L of isoprene in a fed-batch culture (Yang et al., 2012b). The production was further improved up to 6.3 g/L by replacement of the upper portion of the MVA pathway from *S. cerevisiae* with *Enterococcus faecalis* (Yang et al., 2012a). The DXP pathway utilizes G3P and pyruvate in the same molar ratio; however, the Embden-Meyerhof pathway (EMP), Entner-Doudoroff Pathway (EDP), Pentose Phosphate Pathway (PPP) and Dahms pathway generates an imbalanced distribution of G3P and pyruvate in *E. coli*, which compromises the efficiency of the pathway. Liu *et al.*, analysed and compared five different MEP feeding module for isoprene production. Engineering of

the feeding module EDP and PPP results in a 3.1-fold increase in isoprene titer to 221 mg/L compared to the EMP pathway only in same strain (Liu et al., 2013). Further Lv *et al.*, reported isoprene production by co-expressing *DXS*, *DXR*, and *IDI* genes in order to improve the DXP pathway (Lv et al., 2013). Later, the same group reported 37 mg/L isoprene production in *S. cerevisiae* by engineering of the native acetyl-CoA and mevalonic acid pathways with a push-pull-restrain strategy (Lv et al., 2014). further increased up to 60% production of isoprenes by using the expression of the non-evolved *DXS*, *DXR* and *IDI* genes (Lv et al., 2016a). Later, by using dual metabolic engineering of cytoplasmic and mitochondrial acetyl-CoA utilization and fed-batch fermentation in *S. cerevisiae* isoprene was increased up to 2.5 g/L (Lv et al., 2016b). In another study, *E. coli* MG1655 harbouring *Populus trichocarpa* isoprene synthase (*PtispS*) and the engineered MVA pathway, produced 1.8 g/L isoprene by deleting several genes and preventing the waste of acetyl-CoA in the form of fermentation byproducts in a flask culture (Kim et al., 2016). Yang *et al.*, reported 24 g/L isoprene production in a fed-batch culture by synergy effect of the dual pathway, DXP and MVA simultaneously (Yang et al., 2016a).

Apart from these usual methods, the expression of *Jeotgalicoccus* fatty acid decarboxylase and *Elizabethkingia meningoseptica* oleate hydratase form isoprene from mevalonate, although at a very low titer 2.2 mg/L in a flask and 680 mg/L in fed-batch culture as compared to previous reports (Yang et al., 2016b). Li *et al.*, screened key enzymes such as *IDI*, *MK* and *Isp*S, from other organisms and optimized their ribosome-binding site (RBS) sequences to reduce translation initiation rate value of non-key enzymes, *ERG*19 and *Mva*E. Optimized strain showed 2.6 fold increase production of isoprene (698 mg/L) to the original strain (Li et al., 2019). Liu *et al.*, reported 587 mg/L of isoprene production in fermentation by over expressing MVA pathway genes from various sources (*mvaE, mvaS, mvk, pmk, mvaD,* and *idi*) to accelerate the DMAPP production in *E. coli* (Liu et al., 2019). Recently, Guo *et al.*, reported a new strategy by coupling production of isoprene with 1,3-Propandiol (PDO) fermentation by redox cofactor (NADPH) balancing. The introduction and optimization of the dual pathways in an recombinant *E. coli* G05, simultaneously produced 665.2 mg/L isoprene and 2532.1 mg/L 1,3-PDO under flask fermentation condition (Guo et al., 2019).

Branched $C_5$ alcohols, Isopentenols (isoprenol and prenol) are promising biofuels with favourable combustion properties and can be produced via the hydrolysis of DMAPP and IPP by the phosphatases, *NudB*, and *NudF* (Chou and Keasling, 2012; Withers and Keasling, 2007). In another study, Zheng *et al.*, reported the expression of the MVA pathway and *B. subtilis NudF* in *E. coli* was found to result in the production of 1.3 g/L of isoprenol in a flask culture by blocking the conversion of IPP to DMAPP and employing the Bs*NudF* (Zheng et al., 2013). Recently, microbial production of isopentenols has been developed via metabolically engineered *E. coli*. Liu *et al.,* used *NudF* and *yhfR* genes from *B. subtilis*, and expressed in *E. coli* W3110 for the isopentenol production. They also overexpressed two key enzymes *Isp*G and *DXS* to optimize nave MEP pathway, which led to production of 61.9 mg/L isopentenol from 20 g/L of glucose (Liu et al., 2014). Isopentenol synthesis from mevalonate can be shortened to a three-enzymatic-step process involving Mevalonate kinase (MK), phosphomevalonate decarboxylase (PMD) and an *E. coli*-endogenous phosphatase (*Aph*A), by which Kang *et al.*, reported 836 mg/L titre of isopentenol in a shake-flask culture, further the production was optimized by 50% of theoretical yields by phosphatase activity of *Aph*A, which gives complete hydrolysis of IPP generated by *Nud*B or *Nud*F (Kang et al., 2016). Recently, Tian *et al.*, silenced the transcription of several endogenous genes to increase precursor availability in a heterologous biosynthesis of isopentenol by using CRISPRi-mediated multiplex repression system. They increased 98 % enhancement in isopentanol biosynthesis in *E. coli*. Engineered strain produced about 1.2 g/L isopentanol in shake flask fermentation (Tian et al., 2019).

*E. coli* was heterologously engineered for the isoprenoid pathway for the high-yield production of 3-methyl-3-buten-1-ol, 3-methyl-2-buten-1-ol, and 3-methyl-1-butanol, three C5 alcohols, which serve as potential biofuels, yielded 2.2 g/L isoprenol in a flask culture (George et al., 2015). Isopentanols can be formed from Isopentenols by reducing it by additional expression of the reductase NemA (Chou and Keasling, 2012; George et al., 2015).

### 3.2 Biosynthetic Monoterpenoids

Terpene synthases convert one molecule of DMAPP and one molecule of IPP to numerous terpenes via carbocationic intermediate cascades and/or hybridization of carbon atoms, which generate a number of carbon skeletons containing several stereocenters are present in their diverse structure (Christianson, 2017). The condensation of DMAPP and IPP leads to the formation of GPP, the $C_{10}$ precursor, by association with various monoterpene synthases (GPP synthase), monoterpenoids have formed. They are the major component of essential oils and used as a fragrances (*e.g.*, geraniol, limonene, menthol), biofuel alternatives (e.g. pinene, cymene, limonene and myrcene), and industrial chemicals (e.g. limonene, pinene), and are synthesized from GPP by associated monoterpene synthases (Koziol et al., 2015). The recent metabolic engineering of numerous monoterpenes in *E. coli* and *S. cerevisiae* are summarised in **Table 2.** The most basic requirement for monoterpenoids production in *E. coli* and *S. cerevisiae* depends on *in-vivo* availability of GPP, because both the systems do not have GPPS, mutant FPP synthase (FPPS) (*ERG 20)* and plant GPPS were used to construct a monoterpenoids synthetic pathway in both systems (Carter et al., 2003; Reiling et al., 2004).

| Monoterpenes | Strategy Used | Host | Culture Conditions | Yield/Titre | Ref. |
|---|---|---|---|---|---|
| Geraniol | Deleted Alc. dH (YjgB) and produced | *E. coli* | Shake flask<br>Fermentation | 183 mg/L | (Zhou et al., 2014) |
| Geraniol | Optimizing GPPS expr. by engineering of its ribosome binding site (RBS) | *E. coli* | Shake flask<br>Fermentation | 1.1 g/L | (Zhou et al., 2015) |
| Geraniol | Overexpr. of *Ocimum* geraniol synthase, *Abies grandis* GPPS | *E. coli* | Fed-batch fermentation | 2.0 g/L | (Liu et al., 2016) |
| Geraniol | Overexpressed truncated GPPS from *C. acuminate* | *E. coli* | Shake-flask fermentation | 74 mg/L | (Yang et al., 2017) |

| | | | | | |
|---|---|---|---|---|---|
| Geraniol | Control of ERG20 expression and deletion of *OYE2* | *S. cerevisiae* | Fed-batch fermentation | 1.69 g/L | (Zhao et al., 2017) |
| Limonene | Regulating the expres-sion levels of the MVA pathway enzymes | *E. coli* | Shake-flask fermentation | 435 mg/L | (Alonso-Gutierrez et al., 2013) |
| Limonene | Over expression of DXS and IDI | *E. coli* | Shake flask Fermentation | 17.4 mg/L | (Du et al., 2014) |
| Limonene | Optimization of carbon sou-rce and strain species | *E. coli* | Fed-batch fermentation | 2.7 g/L | (Willrodt et al., 2014) |
| Limonene | Degrading *FPPS* mechanism for increasing monoterpenes | *S. cerevisiae* | Shake-flask fermentation | 76 mg/L & Linalool (18 mg/L) | (Peng et al., 2018) |
| Limonene | Mutation in Mevalonate Synthase (*EfMvaS*) and use *NPPS* | *E. coli* | Fed-batch fermentation | 1.29 g/L | (Wu et al., 2019) |
| Linalool | Fusion of *S*-linalool synthase (*AaLS1*) and plant *FPPS* | *S. cerevisiae* | Shake-flask fermentation | 240 µg/L | (Deng et al., 2016) |
| Linalool | Chromosomal mutation in native *FPPS* | *E. coli* | Shake-flask fermentation | 505 mg/L | (Mendez-Perez et al., 2017) |
| Linalool | Engineered *S. clavuligerus LS* and 1,8-cineole synthase (*bCinS*) | *E. coli* | Shake-flask fermentation | 300 fold yield | (Karuppiah et al., 2017) |
| Linalool | Synthetic grape juice medium without of plant genes | *S. cerevisiae* | Shake-flask fermentation | >750 µg/L | (Camesasca et al., 2018) |
| Linalool | Overexp.. of MVA pathway in mitochondria and cytoplasm, Down-regulation of *ERG20* and overexp. t*HMG*1 | *S. cerevisiae* | Batch fermentation | 23 mg/L | (Zhang et al., 2020) |

| | | | | | |
|---|---|---|---|---|---|
| Menthol | Co-expressing ene-reductase (NtDBR from *Nicotiana tabacum* and two menthone dehydrogenases (MMR and MNMR from *Mentha piperita* | *E. coli* | Shake-flask fermentation | menthol (79.1% pure) and neoment hol (89.9 % pure) | (Toogood et al., 2015) |
| Myrcene | Expressing *GPPS* and myrcene synthase (*MS*) along with MVA pathway | *E. coli* | Shake-flask fermentation | 58 mg/L | (Kim et al., 2015) |
| Pinene | Co-expressed native GPPS (*IspA*) and α-pinene synthase (Pt30) from *Pinus taeda* | *E. coli* | Shake-flask/Fed-batch fermentation | 5.44 mg/L & 0.97 g/L (Fed-batch) | (Yang et al., 2013) |
| Pinene | Fusion of GPPS with pinene synthase (*PIS*) | *E. coli* | Shake-flask fermentation | 32 mg/L | (Sarria et al., 2014) |
| Pinene | Directed evolution of *PIS* controlled of its manganese dependency | *E. coli* | Shake-flask fermentation | 140 mg/L | (Tashiro et al., 2016) |
| Sabinene | Synthetic Dominant Negative GPPS | *S. cerevisiae* | Shake-flask fermentation | 17 mg/L | (Ignea et al., 2014) |
| Sabinene | Combining expression of *GPPS* and sabinene synthase genes | *E. coli* | Fed-batch fermentation | 2.65 g/L | (Zhang et al., 2014) |

**Table 2.** Biosynthetic production of various Monoterpenes by engineered microorganisms *(E. coli* /*S. cerevisiae*).

Geraniol is a valuable monoterpene alcohol which is widely used in cosmetics, perfume, pharmaceutical industries, and it is also has potential alternatives to gasoline. Zhou *et al*. research group engineered *E. coli* and deleted alcohol dehydrogenase (YjgB) gene and produced 183 mg/ L geraniol in nearly pure form (~98%) in a flask culture system, because of geraniol can be isomerized to geranial, neral, and nerol (Zhou et al., 2014). *GPPS* has already known as a key factor in the improvement of monoterpene production. Optimization of *GPPS* expression by engineering of RBS strength can improve the yield of geraniol by 6 folds to 1.1 g/L (Zhou et al., 2015). Recently geraniol yield was obtained 2.0 g/L in fermentation process by overexpression of *Ocimum*

*basilicum* geraniol synthase, *Abies grandis* GPPS, and a heterotic mevalonate pathway in *E. coli* BL21 (DE3) (Liu et al., 2016). In another study, Yang *et al.,* overexpressed truncated GPPS from *Camptotheca acuminate* in *E. coli*, and produces 74.6 mg/L geraniol production (Yang et al., 2017). Zhao *et al.,* constructed *S. cerevisiae* strain with highest production of geraniol by engineering the MVA pathway and GPPS. In optimised strain they had deleted of OYE2 (encoding an NADPH oxidoreductase) or ATF1 (encoding an alcohol acetyltransferase) both involving endogenous conversion of geraniol to other terpenoids and down-regulated *ERG*20 expression which finally improved geraniol production up to 1.69 g/L with pure ethanol feeding in fed-batch fermentation (Zhao et al., 2017). The production of limonene up to 435 mg/L was achieved by regulating the expression levels of the MVA pathway enzymes (Alonso-Gutierrez et al., 2013). Overexpression of *IDI* and *DXS* in *E. coli*, up to 17 mg/L limonene was produced (Du et al., 2014). Further, optimization of carbon source and strain species resulted in 2.7 g/L limonene in a fed-batch culture was produced (Willrodt et al., 2014). In addition, this limonene was hydroxylated to form a perillyl alcohol (100 mg/L) by coupling with a cytochrome P450 (Alonso-Gutierrez et al., 2013). In addition, Peg *et al.,* engineered *S. cerevisiae* by silencing FPPS mechanism for increasing production of monoterpenes limonene (76 mg/ L) and linalool (18 mg/L) (Peng et al., 2018). Recently, Wu et al., engineered *E. coli* and enhanced production of limonene up to 1.29 g/L by site directed mutation of EfMvaS, expression of *MmMK* with *ScPMK*, *ScPMD*, and *ScIDI* genes under FAB80 promoter. They used first time NPPS for the higher production monoterpenoids (Wu et al., 2019).

Monoterpenes are high energy density fuels and low boiling compounds. Fusion of (*S*)-linalool synthase (AaLS1) from *Actinidia argute* plant *spp.* with FPPS resulted in the 240 µg/L linalool in *S. cerevisiae* (Deng et al., 2016). Mendez-Perez *et al.,* did a chromosomal mutation in native FPPS of *E. coli* to improve the availability of GPP for the production of monoterpenes using a heterologous MVA pathway. The optimized strains produced two jet fuel precursors 1,8-cineole (653 mg/L) and linalool (505 mg/L) in batch cultures (Mendez-Perez et al., 2017). Recently, Karuppiah *et al.,* engineered *Streptomyces clavuligerus* linalool synthase (*bLinS*) and 1,8-cineole synthase (*bCinS*) into *E. coli* and produces a 300-fold production of linalool as compared to plant linalool synthase. Obtained 96% pure 1,8-cineole as compared to

from plant species which having only (67%) (Karuppiah et al., 2017). Recently, Camesasca *et al.,* successfully overproduced of linalool (>750 µg/L), geraniol, α-terpineol from *S. cerevisiae* in a synthetic grape juice medium without the use of plant genes (Camesasca et al., 2018). Recently, Zhang *et al.,* increased the linalool production in *S. cerevisiae* by dual metabolic engineering of the MVA pathway in both mitochondria and cytoplasm. They down-regulated endogenous *ERG20* to prevent the competitive loss of precursor. The recombinant strain produced 23.45 mg/L titer of linalool in a batch fermentation with sucrose as carbon source. This is the first report on combinatorial engineering strategy which may provide hints for biosynthesis of other

monoterpenes (Zhang et al., 2020).

Menthol and its isomers are high-value monoterpenoid chemicals, produced naturally by *Mentha spp*. Toogood *et al.,* developed a one-pot biosynthesis of menthol (79.1% pure) and neomenthol (89.9 % pure) from pulegone (naturally occurring organic compound), using engineered *E. coli* extracts by co-expressing the biosynthetic genes for an ene-reductase (NtDBR from *Nicotiana tabacum*) and two menthone dehydrogenases (MMR and MNMR from *Mentha piperita*) (Toogood et al., 2015). Myrcene has been successfully engineered in *E. coli* by expressing GPPS and myrcene synthase along with MVA pathway produces optimal up to 58 mg/L of myrcene in shake flask (Kim et al., 2015). α-Pinene is widely used in industry and it is mainly produced either by tapping trees (gum turpentine) or as a by-product of paper pulping (crude sulfate turpentine). This extraction is tedious and inefficient and requires extensive expenses of natural resources. Yang *et al.,* co-expressed native GPPS (IspA) from *E. coli* and α-pinene synthase (Pt30) from *Pinus taeda*, and then to increase the geranyl diphosphate (GPP) content in the cells they had introduced GPPS 2 from different origin. The final *E. coli* strain, YJM28, harboring the novel biosynthetic pathway, produces α-pinene up to 5.44 mg/L and 0.97 g/L under shake-flask and fed-batch fermentation conditions, respectively (Yang et al., 2013). Sarria *et al.,* used fusion technique to produce pinene, by fusing GPPS with pinene synthase (*PIS*) generated a fused chimera that enabled *E. coli* to produce 32 mg/L pinene (Sarria et al., 2014). In another study, directed evolution of PIS controlled to the alteration of its manganese dependency and yielded 140 mg/L pinene from the engineered *E. coli* strain (Tashiro

et al., 2016). Ignea *et al*., engineered *ERG20*p into a GPPS and achieved a significant increase (350 fold) sabinene in *S. cerevisiae* (Ignea et al., 2014). Later, Production of sabinene up to 2.7 g/L of titre in *E. coli* was produced by fed-batch fermentation (Zhang et al., 2014).

### 3.3 Biosynthetic Sesquiterpenoids

Sesquiterpenoids are the $C_{15}$-hydrocarbon scaffolds of the thousands of structurally diverse natural products which are synthesized from FPP by sesquiterpene synthases. This class acquires the largest number of isoprenoids than other classes. Sesquiterpene synthase enzymes bind the pyrophosphate group of FPP at the active site *via* $Mg^{2+}$ ion, which is characteristic metal ion binding motifs are universally conserved and coordinated by two conserved aspartate-rich motif DDXXD/E and NSE/DTE (N/DD*XX*S/T*XX*(K/R)E) in all sesquiterpene cyclases. These motifs are responsible for the formation of the $Mg^{2+}$-diphosphate-enzyme complex, as well as the ionization of the substrate (Davis and Croteau, 2000). These are used in various sectors, pharmaceuticals, agricultural, flavors, and fragrance industries (*e.g*. artemisinin, Paclitaxel, bisabolol, santalol, and farnesol), and biofuel alternatives (*e.g*. farnesene, bisabolene and humulene). The important sesquiterpenes products are origin from FPP dephosphorylation by various sesquiterpene synthases as shown in **Fig. 5** (Lange and Ahkami, 2013).

Though isoprenoid biosynthetic pathway was discovered in microbes in 1996, but the production of isoprenoids reported in 2013 by Martin *et al.* They reported the first microbial (bacterial) production of amorphadiene (AD) sesquiterpene by heterologous MVA pathway and overexpression of amorphadiene synthase (*ADS*) into *E. coli* from *Artemisia annua*. They obtained 24 µg/L titre of amorphadiene in shake flask medium (Martin et al., 2003). This became the milestone achievement in the microbial production of isoprenoids. Their efforts gave the opportunity for the thousands of new isoprenoids engineering in microbes via MVA and MEP pathway. All these metabolic engineering in important sesquiterpene productions are summarised in **Table 3**.

| Sesquiterpenes | Strategy Used | Host | References |
|---|---|---|---|

| | | | **Culture Conditions** | **Yield/Titre** | |
|---|---|---|---|---|---|
| Amorphadiene | Overexpressing amorphadiene synthase (*ADS*) and MVA pathway from yeast into *E. coli* | *E. coli* | Shake-flask fermentation | 24 µg/L | (Martin et al., 2003) |
| Amorphadiene | Overlay of dodecane to prevent vaporization of the volatile product | *E. coli* | Fed-batch fermentation | 0.5 g/L | (Newman et al., 2006) |
| Amorphadiene | HMG-CoA synthase & HMG-CoA *redc*. replaced with equivt. genes from *S. aureus* and Optimizing fermentation process | *E. coli* | Fed-batch fermentation | 27 g/L | (Tsuruta et al., 2009) |
| Amorphadiene | optimizing MVA pathway and the use of variant HMG-CoA reductases | *E. coli* | Shake-flask fermentation | 700 mg/L | (Ma et al., 2011) |
| Amorphadiene | Regulating FPP-responsive promoters (*PgadE* and *PrstA*) in the MVA | *E. coli* | Shake-flask fermentation | 1.4 g/L | (Dahl et al., 2013) |
| Amorphadiene | Optimized the MVA pathway by modulating the RBS strengths of the pathway genes | *E. coli* | Shake-flask fermentation | 3.6 g/L | (Nowroozi et al., 2014) |
| Amorphadiene | Systematic optimization of the DXP pathway and glucose uptake | *E. coli* | Shake-flask fermentation | 201 mg/L | (Zhang et al., 2015) |
| Amorphadiene | *In vitro* metabolic engineering of the accumulation of inhibitory metabolites | *E. coli* | Shake-flask fermentation | >6 fold | (Chen et al., 2017) |
| Amorphadiene | Increasing metabolic flux of MVA pathway towards FPP | *S. cerevisiae* | Shake-flask fermentation | 22 mg/L | (Farhi et al., 2011) |
| Amorphadiene | Overexpressed every enzyme of the MVA pathway to *ERG20* | *S. cerevisiae* | Fed-batch fermentation | 40 g/L | (Westfall et al., 2012) |

| | | | | | |
|---|---|---|---|---|---|
| | (also synthesized artemisinin) | | | | |
| Bisabolene | Overexpression of bisabolene synthases (*BS*) | *E. coli* and *S. cerevisiae* | Shake-flask fermentation | ~912 mg/L | (Peralta-Yahya et al., 2011) |
| Bisabolene | Overexpression of bisabolene synthases (*BS*) | *S. cerevisiae* | Shake-flask & Fed-batch fermentation | 800 mg/L & 5.2 g/L | (Özaydin et al., 2013) |
| Bisabolene | Overexpression of bisabolene synthases (*BS*) | *E. coli* | Shake-flask fermentation | 9 mg/g DCW | (Kirby et al., 2015) |
| α-bisabolol | Engineering MVA pathway and *BS* from *Matricaria chamomilla* | *E. coli* | Fed-batch fermentation | 9.1 g/L | (Han et al., 2016) |
| *β*-eudesmol | Introduced a gene cluster, six enzymes of the MVA pathway and co-expressed it with *BIS* gene | *E. coli* | Shake-flask fermentation | 100 mg/L | (Yu et al., 2008) |
| Caryophyllene | Overexpression MVA pathway genes with a caryophyllene synthase | *E. coli* | Fed-batch fermentation | 100 mg/L | (Wu et al., 2018) |
| Cubebol | Deletion of GDH1 (NADPH-dependent) | *S. cerevisiae* | Shake-flask fermentation | 85 % increased than wild | (Asadollahi et al., 2009) |
| *Epi*-cedrol | Engineered *ERG 20* in MVA | *S. cerevisiae* | Shake-flask fermentation | 290 µg/L | (Jackson et al., 2003) |
| *Epi-cedrol* | Fusion expression of ECS and FPPS genes, Utilization of MEP pathway | *E. coli* | Shake-flask fermentation | 1.1 mg/L | (Navale et al., 2019) |
| Farnesene | Fusion of farnesene synthase (FS) and FPPS | *E. coli* | Shake-flask fermentation | 380 mg/L | (Wang et al., 2011) |
| Farnesene | Pathway optimization (DXP) and reconstruction of enzymes | *E. coli* | Shake-flask fermentation | 1.1 g/L | (Zhu et al., 2014) |

| | | | | | |
|---|---|---|---|---|---|
| Farnesene | Overexpre. of three terpene synthases from distinct plant origins | *S. cerevisiae* | Fed-batch fermentation | 170 mg/L | (Tippmann et al., 2016) |
| Farnesene | Used the affibodies for enzyme tagging and scaffolding | *S. cerevisiae* | Fed-batch fermentation | 400 mg/L | (Tippmann et al., 2017) |
| Farnesol | Overexpression of the truncated HMG-CoA reductase | *S. cerevisiae* | Fed-batch fermentation | 145 mg/L | (Ohto et al., 2009) |
| Farnesol | *IspA* over expressed without FPPS , utilised MVA pathway | *E. coli* | Shake-flask fermentation | 135 mg/L | (Wang et al., 2010) |
| Farnesol | Overexpression of FPP synthase (*IspA*) and PgpB, along with a heterologous MVA pathway | *E. coli* | Shake-flask fermentation | 526 mg/L | (Wang et al., 2016) |
| Germacrene | Over expressed HMG-CoA reductase and fusion of FPPS with germacrene synthase (GAS), | *S. cerevisiae* | Shake-flask fermentation | 190 mg/L | (Hu et al., 2017) |
| Humulene | Overexpression of humulene synth. (HMS) and MVA pathway with acetoacetate-CoA ligase | *E. coli* | Shake-flask fermentation | 945 mg/L | (Harada et al., 2009) |
| Nerolidol | Overexpression of the truncated HMG-CoA reductase | *S. cerevisiae* | Fed-batch fermentation | 99 mg/L | (Ohto et al., 2009) |
| Nerolidol | Silencing or degrading squalene synthase | *S. cerevisiae* | Shake-flask fermentation | 100 mg/L | (Peng et al., 2017) |
| Patchoulol | Fusion FPPS coupled with patchoulol synthase (PS) | *S. cerevisiae* | Fed-batch fermentation | 110 mg/L | (Albertsen et al., 2011) |
| Protoilludene | Sequential variation of the MVA and MEP pathway genes | *E. coli* | Shake-flask fermentation | 1.2 g/L | (Yang et al., 2016c) |
| Protoilludene | Engineering IDI, Fpr-FldA redox proteins, and NADPH | *E. coli* | Shake-flask fermentation | 513 mg/L | (Zhou et al., 2017) |

| | | | | | |
|---|---|---|---|---|---|
| | regenerators for boosting the metabolic flux | | | | |
| Santalene | Optimized the FPP branch point, MVA pathway, enhanced the activity of a transcriptional activator | *S. cerevisiae* | Fed-batch fermentation | 92 mg/L | (Scalcinati et al., 2012) |
| Santalene | SS from *Clausena lansium* with various combinations | *S. cerevisiae* | Fed-batch fermentation | 163 mg/L | (Tippmann et al., 2016) |
| Valencene | Targeting CsTPS1 and FDPS to the yeast mitochondria. | *S. cerevisiae* | Shake-flask fermentation | 1.5 mg/L | (Farhi et al., 2011) |
| Valerenadiene | Valerenadiene Synthase gene (VS) under strong Ptrc and PT7 promoters and co-expression of MVA pathway | *E. coli* | Fed-batch fermentation | 62 mg/L | (Nybo et al., 2017) |
| Valerenadiene | MVA pathway engineering | *S. cerevisiae* | Shake-flask fermentation | 140 mg/L | (Wong et al., 2018) |

**Table 3.** Biosynthetic production of various sesquiterpenes by engineered microorganisms *(E. coli* /*S. cerevisiae*).

This isoprenoid (AD) is the precursor for the synthesis of well-known antimalarial drug artemisinin (Garcia, 2015). This artemisinin was isolated from a Chinese medicinal plant *Artemisia annua L.* in 1972 by a Chinese Professor Tu YouYou, who awarded the 2015 Nobel Prize in Physiology or Medicine for the discovery of this potent antimalarial drug. Till date artemisinin has saved millions of lives and represents one of the significant contributions of China to world-wide health (Su and Miller, 2015; Tu, 2016; Wang et al., 2019).

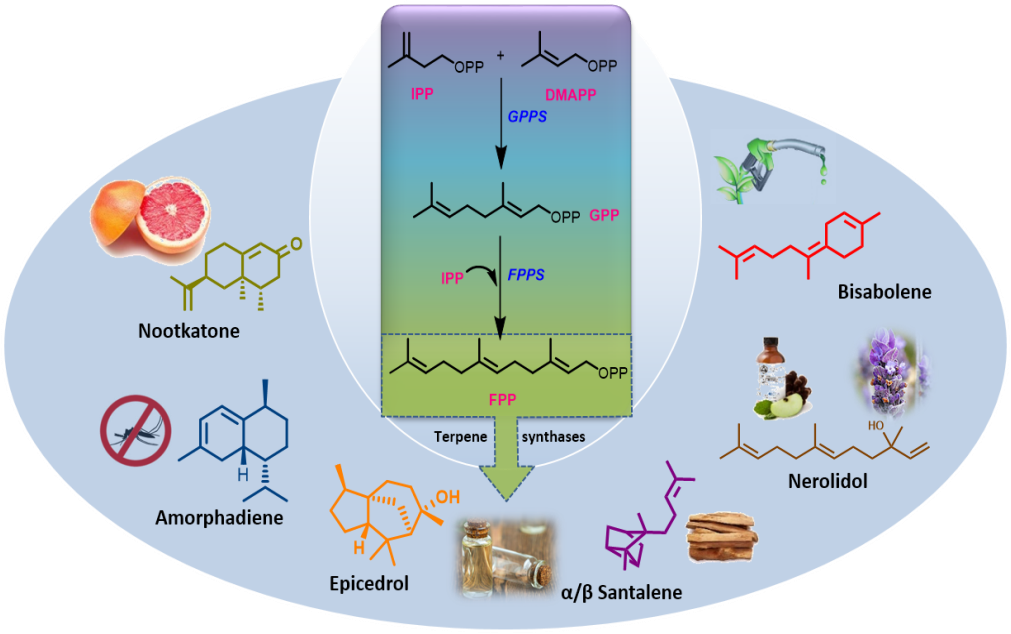


**Figure 5**. Synthesis of some important sesquiterpenes and their applications (Lange and Ahkami, 2013).

.

The precursor for artemisinin AD was further engineered through various tools and host for improved production. After the first report, 3 years later, the yield was increased to 0.5 g/L in *E. coli* with an overlay of dodecane to prevent vaporization of the volatile product (Newman et al., 2006). Paradise et al., increases five-fold production of amorphadiene by down-regulating squalene synthase (*ERG 9*) flux at FPP branch point in *S. cerevisiae* (Paradise et al., 2008). Catania *et al*., showed that if the *ADS* gene deleted, 95 % of artemisinin production was reduced in glandular secretory trichrome and it only increases FPP pool in the cell, not other terpene production (Catania et al., 2018). In fermenter by fed-batch culture, Tsuruta *et al*., produces 27 g/L titre of amorphadiene (Tsuruta et al., 2009). By optimizing heterologous MVA pathway and the use of variant HMG-CoA reductases, resulted in 700 mg/L of amorphadiene after 48h of fermentation (Ma et al., 2011). In another study, by regulating FPP-responsive promoters (*Pgad*E and *Prst*A) in the MVA pathway, which enabled the production of 1.4 g/L amorphadiene (Dahl et al., 2013). The DXP pathway has also been engineered for amorphadiene production by using Cross-Lapping *In-Vitro* Assembly (CLIVA) method (Zou et al., 2013). Further, Nowroozi *et al.* optimized the

MVA pathway by modulating the RBS strengths of the pathway genes and produce 3.6 g/L amorphadiene (Nowroozi et al., 2014). The systematic optimization of the DXP pathway and glucose uptake, which resulted in the production of 201 mg/L amorphadiene in a flask culture (Zhang et al., 2015). Chen *et al.*, used an alternative approach for cell-based biosynthesis of amorphadiene production by *In vitro* metabolic engineering of the accumulation of inhibitory metabolites which resulted in higher yields (>6 fold) of the AD (Chen et al., 2017). The amorphadiene engineering in yeast initiated by Farhi *et al*., by increasing metabolic flux of the MVA pathway towards FPP, valencene and amorphadiene production was resulted in 8 and 20-fold higher in *S. cerevisiae* host , respectively (Farhi et al., 2011). Westfall *et al.,* engineered *S. cerevisiae* in which overexpressed every enzyme of the MVA pathway to *ERG20*. After the development of fermentation processes, 10 times higher >40g/L amorphadiene than artemisinic acid was obtained. They also developed a chemical process to convert amorphadiene into dihydro-artemisinic acid, which could subsequently be converted to artemisinin and filed a US patent of this work (Westfall et al., 2012). The precursor of artemisinin synthesis, artemisinic acid (1.6 g/L) was produced by metabolic engineering in *S. cerevisiae* (Paddon et al., 2013). Engineering of artemisinin in *S. cerevisiae* summarised in **Scheme 1, 2.**

**3.3.1 Microbial engineering for the production of Artemisinin:** A sesquiterpene lactone, artemisinin extracted from *A. annua* plant, is an antimalarial drug and highly effective against multidrug resistant strains of P. falciparum185. It is accumulated in glandular trichome of the plant producing 0.01-1 % of their dry weight. Supply of this drug from natural resource is limiting because of low yield. Although, chemical synthesis is possible, structural complexity, multiple time-consuming steps and low yield makes it economically nonviable for drug production (Keasling, 2012). Till 2020, Westfall *et al.*, reported the highest production of amorphadiene (AD) (40 g/L) in *S. cerevisiae*, a precursor for artemisinin drug synthesis. They have further converted into dihydro-artemisinic acid and artemisinin also. Here, the key strategy for the production of artemisinin by synthetic biology are highlighted.

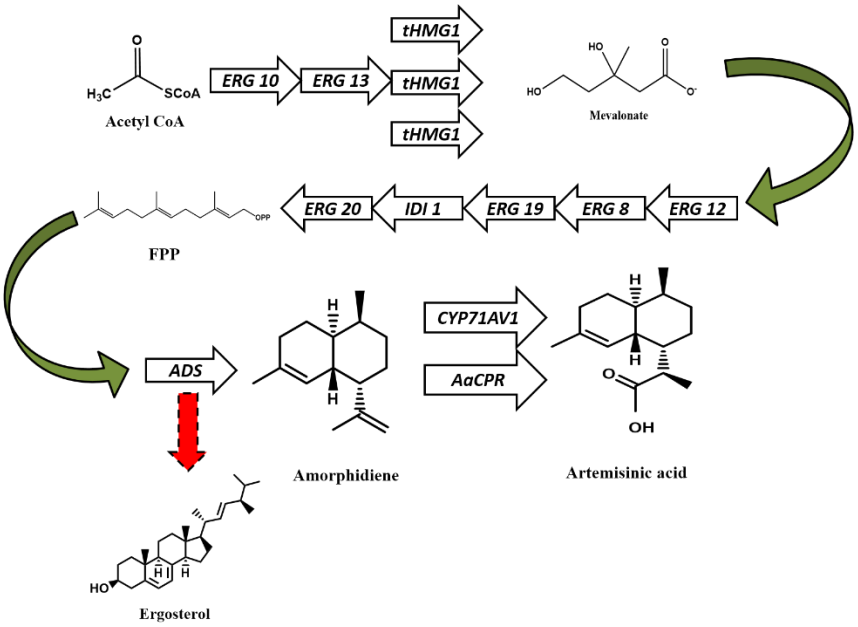


**Scheme 1.** Schematic of the mevalonate pathway showing genes overexpressed in *S. cerevisiae* strains from *GAL1* or *GAL10* promoters in block arrows. Dashed arrow represents the ergosterol pathway transcriptionally restricted at *ERG9* (Westfall et al., 2012)**.**

**3.3.2 Chemical Conversion of Amorpha-4,11-diene to Dihydroartemisinic Acid:** Amorpha-4,11-diene (AD) (**1)**, was converted to dihydroartemisinic acid, compound (**4)**, in three steps beginning with selective hydroboration of the double bond at the 11-position (**Scheme. 2**). Using the hindered borane 9-borabicyclo [3.3.1] nonane (9-BBN) a 79.3% yield of alcohol compound (**2)** was achieved as an 85:15 mixture of epimers with the desired R-epimer predominating. A two-step oxidation sequence was employed in which $SO_3$ pyridine complex oxidized compound (**2)** to aldehyde compound (**3)** (76.4 %) followed by treatment of compound (**3)** with the oxidant $NaOCl_2$ in DMSO to form to dihydroartemisinic acid (**4)** (79.9%). The overall yield of (**4**) from compound (**1)** by this route they reported 48.4% c.

Overall, this work links together the complete process for the production of semisynthetic artemisinin. MVA pathway construction under strong promoter along with optimized fermentation process gave rise high production of AD in *S. cerevisiae*. Combining high-level production of AD with successful conversion to dihydroartemisinic acid represents a significant milestone in the development of an

economically feasible production of the semisynthetic artemisinin (Westfall et al., 2012).

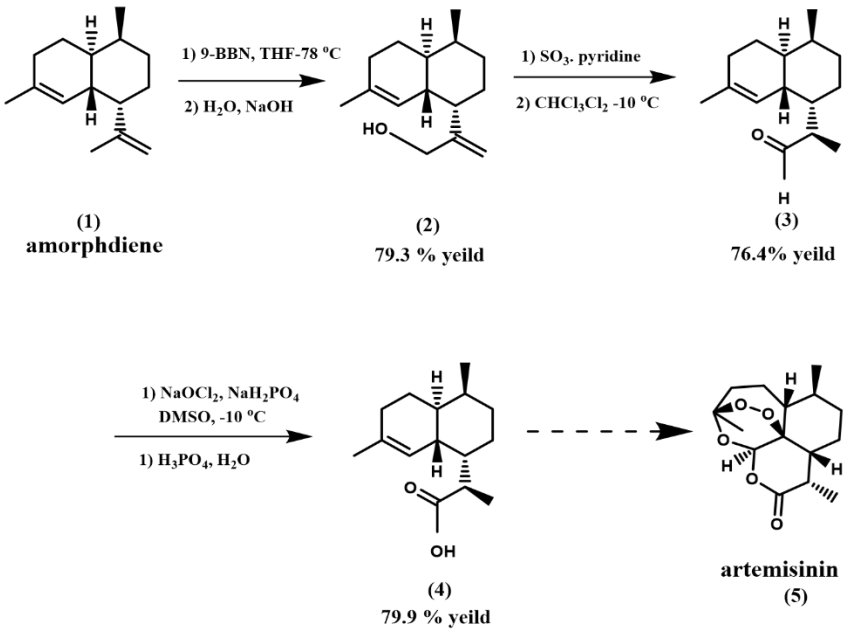


**Scheme 2.** Synthesis of dihydroartemisinic acid from amorpha-4,11-diene. Only the R isomer is shown (Westfall et al., 2012)**.**

Apart from amorphadiene/artemisinin, many more important sesquiterpenes have been engineered in heterologous host. Bisabolene is a monocyclic sesquiterpene, which is a precursor to a potential D2 diesel fuel. To obtain higher titres of bisabolene, bisabolene synthase (*BIeS*) genes from *Arabidopsis thaliana*, *Pseudotsuga menziesii*, *A. grandis* and *Picea abies* have been expressed in *E. coli* (harbouring the entire MVA pathway in a single plasmid) and *S. cerevisiae* (Peralta-Yahya et al., 2011). Overexpression of the codon-optimized *AgBIeS* in an engineered *E. coli*, resulted in production of 912 mg/L of bisabolene. The same level titre of bisabolene was also obtained in the engineered *S. cerevisiae* (Peralta-Yahya et al., 2011). Ozaydin *et al.*, improved the titres of bisabolene more than 20-fold to 800 mg/L in a shake-flask and 5.2 g/L in a fed-batch fermentation by using deletions of the genes that affects isoprenoid biosynthesis and modification of MVA pathway in *S. cerevisiae* (Özaydin et al., 2013). Kirby et al. reported a novel route from ribulose 5-phosphate (Ru5P) to DXP synthesis. Expression of fusion protein (Dxr-RibB) in *E. coli* improved bisabolene titres more than 4-fold (Kirby et al., 2015).

Bisabolol is a skin-whitening agent in cosmetics. Initially, it was produced by using various plant species, optimized by *Abies grandis*, Recently, 9.1 g/L bisabolol was produced by engineering the MVA pathway and *Matricaria chamomilla* bisabolol synthase (*BIoS*) in *E. coli* by fed-batch culture (Han et al., 2016). Apart from *E. coli*, cyanobacteria *Synechocystis sp.* PCC 6803 was used to improve enzyme expression and increase the production of the α-bisabolene, a precursor to bisabolane, which has combustion properties similar to other fuels by utilizing ribosome binding site tools and codon optimization (Sebesta and Peebles, 2017). *β*-eudesmol (100 mg/L) was obtained by introducing a gene cluster encoding six enzymes of the MVA pathway into *E. coli* and co-expressed it with sesquiterpene synthase gene (ZSS2) from *Zingiber zerumbet Sm* plant spp. which in India, is popularly known as "Ghatian" and "Yaiimu" (Yu et al., 2008). Caryophyllene and its derivatives not only exhibit biological activities but also have desired potential jet fuel applications. Recently, the caryophyllene and caryolan-1-ol were produced by an engineered *E. coli* with heterologous expression of MVA pathway genes with a caryophyllene synthase and a caryolan-1-ol synthase. Metabolic flux and optimized fermentation parameters, 449 mg/L of total terpene, including 406 mg/L sesquiterpene with 100 mg/L caryophyllene and 10 mg/L caryolan-1-ol. They also obtained these metabolites by feeding algal biomass (75 mg/L caryophyllene) (Wu et al., 2018). Asadollahi *et al.*, deleted the NADPH-dependent glutamate dehydrogenase (GDH) encoded by GDH1 resulted the target sesquiterpene biosynthesis in *S. cerevisiae.* Deletion of the GDH1 result in an approx. 85 % increase in the final cubebol production (Asadollahi et al., 2009).

Several fusion enzyme approaches were used in *E. coli* and *S. cerevisiae* for sesquiterpene productions. *Epi*-cedrol sesquiterpenes from *Artemisia annua*, was successfully engineered in yeast and resulted in an optimum 390 µg/L *epi*-cedrol in shake flask culture (Jackson et al., 2003). Our group recently, produced *epi*-cedrol up to 1.1 mg/L by fusion of epi-cedrol synthase (ECS) and FPPS enzymes (Navale et al., 2019). Similarly, farnesene synthase (FS) and FPPS fusion for channelling FPP to Farnasene resulted in the production of 380 mg/L farnesene in *E. coli* (Wang et al., 2011). After pathway optimization and reconstruction of enzymes, which led to the production of 1.1 g/L farnesene (Zhu et al., 2014). Tippmann *et al.*, tried three terpene synthases from distinct plant origins and engineered for farnesene production in *S.*

*cerevisiae*. It was raised from 4 mg/L to 170 mg/L farnesene in fed-batch fermentations (Tippmann et al., 2016). For reducing substrate loss and accumulation of toxic intermediates instead of enzyme fusion, enzymes can be co-localized through attachment to a synthetic scaffold via non-covalent interactions. Later, same group Tippmann *et al.*, used the affibodies for enzyme tagging and scaffolding. It was first activated for co-localization of FPPS and farnesene synthase in *S. cerevisiae*. The yield of farnesene was improved by 135% in fed-batch cultures. This versatile affibody could be used for various metabolic engineering purposes (Tippmann et al., 2017). Farnesol is an important $C_{15}$ isoprenyl alcohol. Overexpression of the truncated HMG-CoA reductase in yeast *S. cerevisiae* resulted in 145 mg/L of farnesol production in 5L fed-batch culture for 7 days (Ohto et al., 2009). *IspA* overexpressed without FPPS in *E. coli* and to utilize the MVA pathway resulted in the farnesol (FOH) production 135 mg/L by the promiscuous phosphatase activity (Wang et al., 2010). These phosphatases were screened in *E. coli*, and amongst them, phosphatase *Pgp*B, was used to over express in *E. coli* to produce 526 mg/ L of farnesol (Wang et al., 2016).

Germacrene, is one of the volatile sesquiterpenes, sesquiterpenes, typically produced by numerous plant species. They are playing a role as insect pheromones. There are two prominent molecules are produced germacrene-A and germacrene-D. These are reported for their anti-inflammatory, antibacterial, and antifungal properties, which can be a great topical application for the cuts, scrapes, or wounds *etc* (Noge and Becerra, 2009). For the production of germacrene, Hu *et al.*, overexpressed 3-hydroxyl-3-methylglutaryl-CoA reductase and fusion of FPPS with germacrene synthase (GAS), resulted in 6 fold increase in germacrene (190.7 mg/L) (a precursor of β-elements) production in *S. cerevisiae* (Hu et al., 2017). Humulene, also known as α-humulene or α-caryophyllene, is a naturally occurring monocyclic sesquiterpene, acetoacetate-CoA ligase which converts acetoacetate to acetoacetyl-CoA, has been used to synthesize IPP via the MVA pathway. Recombinant *E. coli* harbouring humulene synthase (HMS) and a heterologous MVA pathway together with acetoacetate-CoA ligase successfully produced 945 mg/L of humulene from acetoacetate (Harada et al., 2009). Overexpression of the truncated HMG-CoA reductase in yeast *S. cerevisiae* resulted in 99 mg/L nerolidol production in 5L fed-batch culture (Ohto et al., 2009). Recently, nerolidol was produced up to 100 mg/L by silencing or degrading squalene synthase in

*S. cerevisiae* (Peng et al., 2017). Patchoulol (110 mg/L) was obtained in *S. cerevisiae* through fusion strategy by using yeast FPPS coupled with patchoulol synthase (*PTS*) of *Pogostemon cablin* plant *spp*. (Albertsen et al., 2011). Protoilludene is a valuable sesquiterpene and serves as a precursor for many medicinal compounds like illudins, which are used as anticancer agents, 1.2 g/L protoilludene yield was achieved using a sequential variation of the MVA and MEP pathway genes in order to optimize its efficiency (Yang et al., 2016c). In addition, 512.7 mg/L, protoilludene was produced by engineering IDI, Fpr-FldA redox proteins, and NADPH regenerators for boosting the metabolic flux toward a recombinant MEP pathway (Zhou et al., 2017).

Sandalwood oil has huge commercial value owing to its use in the perfume industry and as a flavour component in many food products, including alcoholic as well as non-alcoholic beverages (Wang and Kim, 2015). The main components of this oil are santalene and santalol a sesquiterpene derivatives, are worldwide famous for pleasant and woody odour (Jones et al., 2011). It also has great economic value as it possesses promising pharmacologically relevant biological activities (Misra and Dey, 2012; Misra and Dey, 2013). Scalcinati *et al*. optimized the FPP branch point, modified the MVA pathway, the ammonium assimilation pathway and enhanced the activity of a transcriptional activator. This approach has resulted in an overall 4 fold improvement of α-santalene yield of a 92 mg/L or 0.0052 Cmmol (Cmmol glucose)$^{-1}$ as compare to reference strain in a fed-batch culture (Scalcinati et al., 2012). Metabolic engineering of sesquiterpenes from sandal wood was not up to the level (Wang and Kim, 2015). Tippmann *et al.,* expressed santalene synthase from *Clausena lansium* with various combinations in *S. cerevisiae* along observed 163 mg/L, santalens using the highest producing strain in fed-batch fermentations (Tippmann et al., 2016). Metabolic engineering and co-expression of terpene synthases resulted in 80 mg/L of sesquiterpenes in *S. cerevisiae* (Takahashi et al., 2007) as yeast gives the higher plant sesquiterpenes (Nguyen et al., 2012).

Rodriguez *et al.,* briefly reported Production, quantification, and extraction of sesquiterpenes or isoprenoids from *S. cerevisiae* (Rodriguez et al., 2014). *Valeriana officinalis* is a medicinal herb useful for the treatment of anxiety and insomnia. The root extracts having sesquiterpene valerenic acid and valerena-1,10-diene. Valencene was produced up to 1.5 mg/L by targeting Cs*TPS1* and FPPS to the yeast mitochondria

(Farhi et al., 2011). *E. coli* was metabolically engineered to produce valerenadiene in shake flask fermentation with decane overlay. At optimal conditions and codon-optimization, valerenadiene synthase gene under strong Ptrc and PT7 promoters and via co-expression of an exogenous (MVA) pathway, produced 62.0 mg/L valerenadiene. Currently, this was increased up to 200 mg/L (abstract presented) by the same group (Nybo et al., 2017). In addition, recently, Wong *et al.*, synthesized of valerenic acid in *S. cerevisiae* by *De novo* synthesis and resulted in 140 mg/L of valerenadiene and 4 mg/L of valerenic acid (Wong et al., 2018).

As a general precursor of triterpenoids ($C_{30}$), squalene is synthesized by squalene synthase (*SqS*) in a head-to-head condensation of two FPP molecules. It has been successfully produced in *E. coli* with the introduction of *SqS* resulted in 12 mg/L of squalene by overexpression of *DXS* and *IDI* via the DXP pathway (Ghimire et al., 2009) and further 230 mg/L of squalene was produced via the MVA pathway (Katabami et al., 2015). Recently, Han *et al.*, developed an *S. cerevisiae* Y2805 strain having the potential of producing squalene up-to 2.011 g/L and 1.026 g/L from 5-L fed-batch fermentations in the presence and absence of terbinafine supplementation, respectively (Han et al., 2018).

## 4. Concluding Remarks

In conclusion, due to the importance of natural isoprenoids in pharmaceuticals, nutraceuticals, and other chemical industries, several biochemical methods were applied to improve their production. Over the past two decades, the advances in emerging tools and technologies in synthetic biology has paved way for microbial genetic manipulation along with the identification of their metabolic pathways. The heterologous expression in *E. coli* and *S. cerevisiae* also gave the promising metabolic engineering strategies for the production of various isoprenoids. (Gruchattka et al., 2013)(Gruchattka et al., 2013). *In silico* comparative genome analysis, pathway predictions and its engineering are also helped in improvement of production of isoprenoids in any other host organisms. Among the all available microbial hosts, *E. coli* and *S. cerevisiae* are the most attractive and economic platforms due to editable, easy to modify, sustainable at optimum conditions for the bulk production value-added isoprenoids. Therefore, recent achievements in have brought up great potential of ($C_5$-$C_{15}$) isoprenoid biosynthesis by *E. coli* and *S. cerevisiae*. The literature survey revealed that isoprenoids such as *epi*-cedrol and santalene are not engineered sufficient in heterologous host. Their studies has yet to be done. According to literature survey, we have decided to work on these sesquiterpenes production in this two host. Also we have tried to possible mechanism study of *epi*-cedrol synthase enzyme. There are vast opportunity to increase remaining un-engineered isoprenoid production and in future, expand the catalogue of isoprenoid synthesis.

# Chapter 2:
# Production of epi-cedrol and santalene in *E. coli* and *S. cerevisiae*

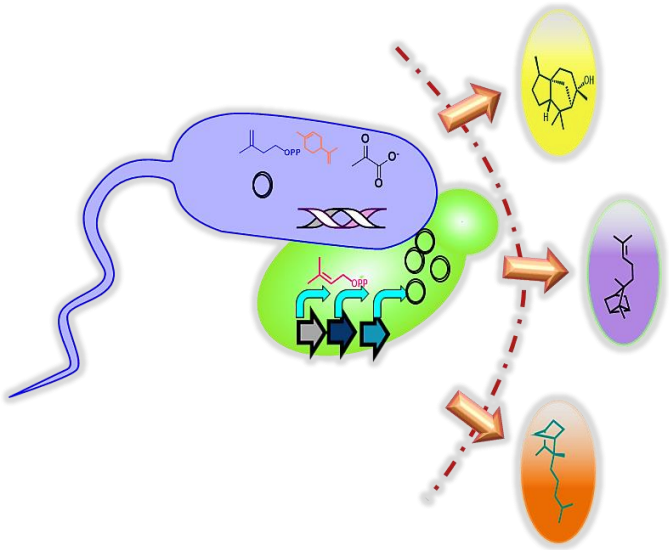

## Abstract

Terpene synthase enzymes catalyzes acyclic diphosphate farnesyl diphosphate (FPP) into desired sesquiterpenes. In this study, fusion enzymes were constructed by linking *Santalum album* farnesyl pyrophosphate synthase (*SaFPPS*) individually with two terpene synthases, *Artemisia annua epi*-cedrol synthase (*AaECS*) and *Santalum album* santalene synthase synthase (*SaSS*). The stop codon at the N-terminus of *SaFPPS* was removed and replace by a short peptide (GSGGS) to introduce a linker between the two ORFs. The fusion clones were expressed in *E. coli* Rosseta DE3 cells. The fusion enzymes FPPS-ECS produced 8-*Epi*-cedrol and the FPPS-SS produced mixture of α- and β-santalenes, respectively from substrates isopentenyl diphosphate (IPP) and dimethylallyl pyrophosphate (DMAPP) through sequential reactions. The Km values of FPPS-ECS and FPPS-SS fusions for IPP were 4.71 µM and 1.8 µM, respectively. Both fusion enzymes carried out the efficient conversion of IPP to respective sesquiterpenoids *i.e epi*-cedrol and α/β-Santalene at a 1.66 and 1.45 fold higher and faster, in comparison to single enzymes *SaFPPS* & *AaECS; SaFPPS* & *SaSS* when combined together in enzyme assay over time. Further, the recombinant *E. coli* BL21 strain harboring fusion plasmids successfully produced *epi*-cedrol and santalenes in fermentation medium. The strain having fusion plasmids (pET32a-FPPS-ECS and pET32a-FPPS-SS) produced 1.084±0.09 mg/L titre *epi*-cedrol and 227 µg/L santalene mixture in fermentation medium by overexpression and MEP pathway utilization. Same fusion constructs were cloned in yeast vector pYES2/CT, and expressed in *Saccharomyces cerevisiae* INV*Sc* 1 cells. Sesquiterpenes were extracted from the fermentation medium. Structural analysis of both fusion proteins were done by I-TASSER server and docking by AutoDock Vina software, which suggested that secondary structure of the N- C terminal domain and their relative positions to functional domains of the fusion enzyme was greatly significant to the catalytic properties of the fusion enzymatic complex than individual enzymes.

## Introduction

Terpenes are chemically and structurally diverse class of metabolites playing a major role in plants primary and secondary metabolism (Withers and Keasling, 2007). Sesquiterpenes are diversified $C_{15}$ containing terpenes which have found vast commercial applications in flavours, fragrances, pharmaceuticals, nutraceuticals, and industrial chemicals (Chappell, 1995; Fraga, 2013). However, these produced in very low concentrations in natural sources, hampering industrially viable commercial production. Therefore, biotechnological intervention considered as a key solution to this issue (Daviet and Schalk, 2010). For the same, a detailed outline of the biosynthetic pathway of terpenoids in source plant, including genes and enzymes involved in the pathway is mandatory (Pickens et al., 2011).

Since last two decades, several hundreds of genes encoding sesquiterpene synthases have been isolated from different plant source. Many of these genes or pathways have been transferred from their natural producer organisms to well characterized microbial host. Further, additional engineering of these genes and pathway has aided to process of achieving higher product titre (Markus Lange et al., 2013). Fusion of different enzymes catalysing sequential reactions of metabolic pathway is an emerging strategy on the horizon in the field of metabolic engineering (**Scheme 1**) (Elleuche, 2015; Orita et al., 2007; Yu et al., 2015). The fusion protein is a protein produced by fusing sequences of two genes together under a single promoter, which offers the advantage of producing larger protein with two or more functions. It may catalyses consecutive steps more efficiently than a simple mixture of the individual free enzymes in metabolic pathway (Conrado et al., 2008; Elleuche, 2015; Orita et al., 2007; Sarria et al., 2014). Possibly, the proximity of fusion enzymes influences the efficiency of sequential reactions (Conrado et al., 2008). Use of fusion proteins also reduces the number of vectors in heterologous expression system. The construction of bi-functional enzyme also can reduce the cost of recombinant protein purification and enhance the cofactor regeneration rate, which simplifies the reconstitutions of metabolic pathways (Yu et al., 2015; Zhang et al., 2017a). Fusion protein strategy has also been explored earlier for metabolic engineering of sesquiterpenoids, such as fusion of patchoulol synthase (*PTS*) and farnesyl diphosphate synthase (*FPPS*) which

channelled more metabolic flux to patchoulol production (Albertsen et al., 2011), *FPPS-epi*-aristolochene synthase (*eAS*) for *epi*-aristolochene production (Brodelius et al., 2002), and fusion of (*S*)-linalool synthase (Aa*LS1*) which led to enhancement in the production of linalool in yeast host (Deng et al., 2016).

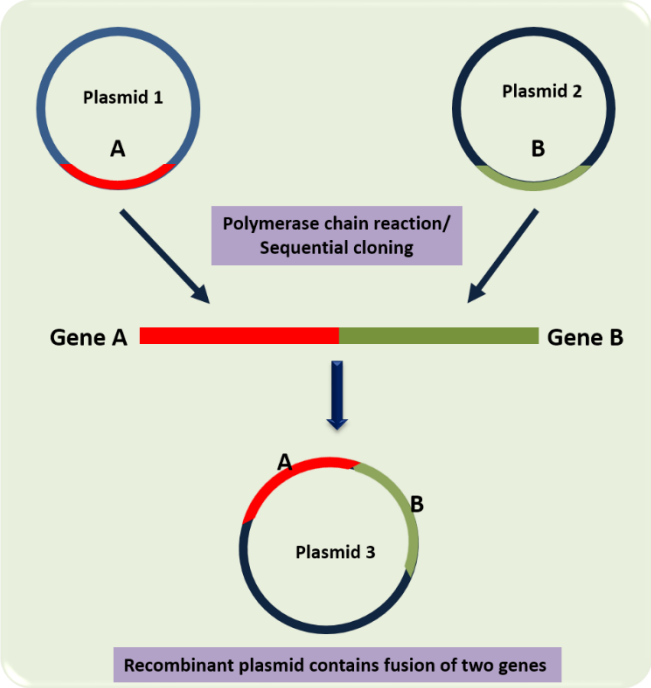


**Scheme 1**. Strategy for fusion genes construction in single plasmid.

Sesquiterpenes from *Artemisia annua L* and *Santalum album L*. have received significant interest on account of wide variety of pharmacological properties like antibacterial, antiviral, antifungal, insecticide, anticancer activity etc. (Abad et al., 2012; Ćavar et al., 2012; Garcia, 2015; Misra and Dey, 2012; Misra and Dey, 2013). Amongst the metabolites from *A. annua*, artemisinin, a sesquiterpene lactone is most widely used as an antimalarial drug (Klayman, 1985). Immense commercial interest has brought about many investigations to explore sesquiterpene biosynthesis in *A. annua* and its biotechnological manipulation. As result, artemisinin has been successfully produced at industrially desired scales in alternative microbial host via metabolic engineering of artemisinin biosynthesis related sesquiterpene synthase genes (Paddon et al., 2013; Wang et al., 2013; Westfall et al., 2012). In due course of time, exploration of *A. annua* sesquiterpene biosynthesis inevitably led to many sesquiterpene synthase genes being cloned and characterized from this plant including

those producing *epi*-cedrol, β-caryophyllene, β-copaene, germacrene, etc. (Shen et al., 2007). On the other hand, *S. album* is a sacred Indian medicinal plant which is famous worldwide for its fragrant oil, composed of santalol, a sesquiterpene derivative that has a pleasant and woody odour (Jones et al., 2006). Sandalwood oil has a huge commercial value owing to its use in perfume industry and as a flavour component in food industry, including alcoholic as well as non-alcoholic beverages (Burdock and Carabin, 2008). It also possesses promising pharmacologically relevant applications like antibacterial, antifungal, antiviral anti-inflammatory, anticancer, antipyretic, anti-ulcerogenic, antioxidant, anti-spasmodic (muscle relaxant), astringent and diuretic activities which are beneficial for human health care (Baldovini et al., 2011; Jones et al., 2006; Rani et al., 2013; Tippmann et al., 2016).

Among the sesquiterpenes, *epi*-cedrol and santalene are least explored metabolite with high-untapped commercial potential. *Epi*-cedrol is potential precursor to cedrenes, which are being used as an important source materials for generation of advanced high density jet and diesel biofuels development (Harrison and Harvey, 2017). Further, cedrol is widely used in pharmaceutical industries for sedative, anti-inflammatory and cytotoxic activities (Bhatia et al., 2008; Luo et al., 2019; Zhang et al., 2016). Santalene is well known fragrance molecule and high pharmaceuticals value (Srivastava et al., 2015). Therefore, *epi*-cedrol and santalene yield enhancement signals industrial benefit and biotechnological solution should be ventured. Fusion protein strategy can be implement with sesquiterpene synthase to enhance yield by fusion of *FPPS*-with a sesquiterpene synthase gene. Such a fusion protein would catalyse one step production of corresponding sesquiterpenes from IPP and DMAPP with enhancement in *FPPS* precursor pool towards sesquiterpene synthase genes via mevalonate (MVA) and non-mevalonate (MEP) pathways that operate in the cytosol and plastid, respectively (Dubey et al., 2003). Isoprenoids synthesis in *Escherichia coli* and *Saccharomyces cerevisiae* are carried out by MEP and MVA pathway, respectively. So production of sesquiterpenes via fusion enzyme might help to get higher yield in both the systems (Zhou et al., 2017).

We have cloned and functionally characterized sesquiterpene synthase gene *epi*-cedrol synthase (*AaECS*) from *A. annua* and farnesyl pyrophosphate synthase

(*SaFPPS*) from *S. album* in the bacterial host (Shinde et al., 2016; Srivastava et al., 2015). In this study, we have constructed two fusion proteins by linking *SaFPPS* gene with sesquiterpenoid synthase genes *AaECS* as well as *SaSS* with the help of short Gly-Ser-Gly-Gly-Ser linker (for *E. coli*) Gly-Ser-Ser-Gly-Gly (for *S. cerevisiae*). Both constructs were made in bacterial vector pET32a and yeast vector pYES2/CT. Fusion proteins were expressed in *E. coli (section A)* and *S. cerevisiae (section B),* then characterised for the single step conversion of corresponding 8-*epi*-cedrol and α-santalenes, β-santalenes, respectively in maximum production by metabolic engineering. Molecular modelling of fusion proteins and substrate docking were shown in *section c*.

## Materials, Reagents and Kits

- Polymerase AccuPrime™*Pfx* Supermix (Invitrogen-Thermo Fischer)
- GelRed™ dye (Sigma-Aldrich)
- Agarose (Himedia)
- JumpStart™ (Sigma-Aldrich)
- T4 DNA ligase (New Englands Biolabs)
- Novex pre-stained protein ladder (Invitrogen-Thermo fischer)
- 1 kb DNA Ladder (Bangalore Genei)
- Alkaline phosphatase (CiP) (New Englands Biolabs)
- High-Fidelity (HF) Restriction enzymes (New England Biolabs)
- Dimethylallyl pyrophosphate (DMAPP) (Sigma-Aldrich)
- Isopentyl pyrophosphate (IPP)
- Geranyl diphosphate (GPP)
- Farnesyl diphosphate (FPP)
- Isopropyl thio-β-D-thiogalactopyranoside (IPTG) Sigma-Aldrich
- Antibiotics (*viz.* Kanamycin, Chloramphenicol, Ampicillin) Sigma-Aldrich
- Luria Bertani Broth/Agar (Himedia, India)
- Terrific Broth (TB) (Himedia, India)
- Nuclease Free Water (Himedia, India)
- Tris-HCl (Himedia, India)
- Glycine (Sigma-Aldrich)
- Ammonium bicarbonate (Himedia, India)
- Dithiothreitol, DTT (Sigma-Aldrich)
- Rubidium chloride (RbCl) (Sigma-Aldrich)
- Manganese (II) chloride tetrahydrate (Sigma-Aldrich)
- Potassium acetate (Himedia, India)
- Calcium chloride dihydrate (Himedia, India)
- CHAPS (Himedia, India)
- PMSF (Himedia, India)
- MOPS (Sigma-Aldrich)
- Glycerol (Himedia, India)

- Acetic acid (Fisher Scientific)
- Sodium hydroxide (Himedia, India)
- Galactose (Spectrochem Lab)
- Raffinose (Spectrochem Lab)
- D-Glucose (Himedia)
- Lithium Acetate (LiAc) (Himedia)
- PMSF (Himedia, India)
- Sodium phosphate (Himedia)
- Dimethyl sulfoxide, DMSO (Merck)
- Bovine serum albumin, BSA (Himedia)
- Phosphate Buffer Saline pH 7.4 (Himedia)
- Tween 20 (Merck)
- Glass beads (0.4–0.6 mm size) (Sigma–Aldrich)
- Nuclease Free Water (Himedia)
- Complete supplementary mixture w/o Ura, CSM-URA (Himedia)
- Yeast Nitrogen Base with ammonium bicarbonate (Himedia)
- YPD Medium (Yeast extract- 10 g/L; Peptone- 20 g/L; Dextrose- 20 g/L)
- Induction medium (CSM-URA 0.667 g/L, 20 g/L galactose- 100 mL stock of filter sterile 20 % galactose or autoclaved at 10 psi for 15 min)
- Desalting bag (10-15 kDa)
- Desalting filter column (10 kDa, 30 kDa) (Merck)
- GenElute™ PCR Clean-Up (Sigma-Aldrich)
- Hexane (Spectrochem Lab)
- Ponceau S stain (Sigma-Aldrich)
- Dimethyl sulfoxide, DMSO (Merck)
- Polyethylene glycol, PEG-3350 (Sigma-Aldrich)
- Distilled petroleum ether (NCL, facility)
- $Ni^{2+}$-NTA agarose (Invitrogen-Thermo fischer and Quagen)
- pET 32a plasmid (Invitrogen-Thermo fischer)
- pYES2/CT yeast plasmid (Invitrogen-Thermo fischer)
- *Escherichia coli*

Strains: DH5α, Mach1™ $T1^R$, Top10, BL21, rosetta DE3 (Thermo Fisher Scientific)

- Yeast strain: *Saccharomyces cerevisiae* INV*Sc* 1
- Deoxyribonucleic acid sodium salt from salmon testes (Salmon single stranded Sperm DNA (Sigma-Aldrich)
- Primary antibody (1º Ab) Anti-His (C-term) (Invitrogen-Thermo fischer)
- Secondary Ab (2º Ab) Anti-His(C-term)-HRP (Invitrogen-Thermo fischer)
- Yeast Breaking Buffer: 50 mM sodium phosphate, pH 7.4 (1 mM EDTA, 5% glycerol, 1 mM PMSF)
- Transfer buffer (Tris-base/glycine in 20% MeOH)
- Blocking buffer (3 % BSA, 3 g of BSA in 100 ml mili Q water)
- Saponification solution (10 % of KOH solution in 80 % of EtOH)
- Competent cell Buffer **I** (50 ml per 500 ml culture)
  100 mM RbCl (12 g/L); 50 mM $MnCl_2 \cdot 4H_2O$ (9.89 g/L); 30 mM potassium acetate (2.94 g/L); 10 mM $CaCl_2 \cdot 2H_2O$ (1.47 g/L); 15% (v/v) glycerol (150 ml/L)
  Adjust pH to 5.8 with dilute acetic acid and filter sterilize. (*Note: Store at 4 °C, protect from light*)
- Competent cell Buffer **II** (25 ml per 500 ml culture)
  10 mM MOPS (2.09 g/L); 10 mM RbCl (1.2 g/L); 75 mM $CaCl_2 \cdot 2H_2O$ (11 g/L); 15% (v/v) glycerol (150 ml/L)
  Adjust pH to 6.5 with dilute NaOH and filter sterilize.
  (*Note: Store at 4 °C and protect from light*)
- Lysis Buffer **A**: 50 mM Tris/HCl pH 7.8, 300 mM NaCl and 10% glycerol, 5 mM imidazole, 1 mM DTT
- Lysis Buffer **B**: 50 mM HEPES pH 7.8, 300 mM NaCl and 10% glycerol, 5 mM imidazole
- Wash Buffer **A**: 50 mM Tris/HCl pH 7.8, 300 mM NaCl and 10% glycerol, 25 mM imidazole
- Wash Buffer **B:** 50 mM HEPES pH 7.8, 300 mM NaCl and 10% glycerol, 35 mM imidazole

- Elution Buffer **A**: 50 mM Tris/HCl pH 7.8, 300 mM NaCl and 10% glycerol, 250 mM imidazole
- Elution Buffer **B:** 50 mM HEPES pH 7.8, 300 mM NaCl and 10% glycerol, 250 mM imidazole
- Enzyme Assay Buffer: pH 8.5, 25 mM Tris-HCl, 5 mM DTT, 10 mM $MgCl_2$, 20% glycerol
- GenElute™ PCR Clean-Up (Sigma-Aldrich)
- PureLink™ Quick Plasmid Miniprep Kit (Invitrogen-Thermo fischer)

# Section 2A

# Cloning, Expression and Characterization of fusion proteins FPPS-ECS and FPPS-SS in E. coli

## 1. Methodology

### 1.1 Preparation of Competent *E. coli* Cells (TOP10, DH5α, BL21, Rosetta DE3) by Using Rubidium Chloride Method

#### 1.1.1 Background

The protocol by (Sharma et al., 2017) allows the preparation of highly competent cells (~$10^6$-$10^8$ CFU/µg DNA). While other protocols require cells to be grown at low temperature (19-22 °C), this protocol involves growing cells at 37 °C. Thus, the cells grow faster and reach log phase within 4 h as compared to 18-24 h. This protocol is highly reproducible.

#### 1.1.2 Preparation of competent cells

*Note: All steps are carried out in sterile conditions.*

**1. Day 1** (1 h preparation + overnight)

Streak *E. coli* strain (*e.g.*, TOP10 or DH5α) on an LB agar plate in a 3 streak fashion and incubate overnight at 37 °C.

**2. Day 2** (10 min preparation + overnight)

Pick a single *E. coli* colony and culture in 5 ml LB broth in a 10 ml culture tube at 37 °C overnight at 200 RPM.

**3. Day 3 (7 h)**

a. Inoculate 500 ml LB broth in a 1 L flask with 500 µl overnight *E. coli* culture and grow at 37 °C (200 RPM) until OD600 = 0.5 (about 4 h).

b. Chill cells on ice for 10 min.

c. Centrifuge *E. coli* cells at 2,000 x g for 10 min at 4 °C.

d. Remove supernatant and re-suspend the pellet in 50 ml ice-cold competent buffer **I** (see Recipes). Keep the cells on ice for the entire time and shake manually in circular motions on ice. It will take 20-30 min to re-suspend the cells.

*Note*: Do not pipette the cells up and down, but you may break the pellet with a pipette for faster resuspension.

e. Centrifuge cells at 2,000 x g for 10 min at 4 °C.

f. Remove supernatant and re-suspend the pellet in 25 ml ice-cold competent cell buffer II by shaking. Keep the cells on ice for the entire time. It will take some time (20-30 min) to re-suspend the cells.

*Note*: Do not pipette the cells up and down, but you may break the pellet with a pipette for faster resuspension.

g. Aliquot 50 µl cells into pre-chilled Eppendorf tubes on ice and immediately freeze the tubes in liquid nitrogen. Work quickly through this step.

h. Store competent cells at -80 °C.

### 1.2 Cloning of fusion of FPPS-ECS and FPPS-SS into pET 32a

#### 1.2.1 PCR Cloning of FPPS from *S. album* into pET 32a

Cloned cDNA of *FPPS* (Srivastava et al., 2015) (*Genbank* Acc. No. KF011939) from *S. album* was used to amplify wild-type FPPS without a stop codon and linker fragment (Gly-Ser-Gly-Gly-Gly-Ser) at 3' end including *Bam* HI site which encodes for Glycine and Serine. Wild-type FPPS was initially amplified by using blunt P1 and P2 primer and further amplified using P3 (forward) and P4 (reverse) containing *Nco* I and *Bam* HI restriction sites, respectively (**Table 1**). PCR was carried out in a total volume of 50 µL with the following reagents: 45 µL Accuprime *Pfx* polymerase (Invitrogen), 20 pmol of each primer and 10 ng of cloned plasmid. PCR program was: 1 cycles of 95 °C (5 min); 35 cycles of 95 °C (30 s), 54 °C (30 s), 68 °C (1.1 min); 68 °C (5 min). The FPPS-wild-type fragment was digested with *Nco* I and *Bam* HI. The bacterial expression vector pET32a (Novagen) was cleaved with the same enzymes and treated with alkaline phosphatase (NEB).Vector and the fragment were purified by using the GenElute PCR Clean-Up kit (Sigma-Aldrich). Ligation of the fragment in frame with a multifunctional His-tag in the vector was carried out using T4 DNA ligase (Thermo Fisher Scientific). The ligation mixture of pET32a FPPS was transformed into *E. coli* Mach1 $T1^R$ (Thermo Fisher Scientific). Colonies were analyzed by PCR using P3 primer and T7 vector specific reverse primer to confirm the presence of the FPPS gene. Positive colonies were grown in LB medium containing ampicillin (100 µg/mL) and the plasmid was purified using the plasmid GenElute Plasmid Miniprep kit (Sigma-Aldrich) and used as a template for insertion of another gene for constructing fusion.

#### 1.2.2 ECS from *A. annua* into FPPS-pET32a

For fusion of *FPPS* and *ECS*, *ECS* gene fragment without start codon was amplified by using blunt P5 and P6 primer from a cloned plasmid (*Genbank* No. AF157059) and further amplified using P7 (forward) and P8 (reverse) containing a *Bam*

HI and *Not* I restriction sites, respectively (**Table 1**). PCR was carried out in a total volume of 50 µL with the following reagents: 45 µL Accuprime *Pfx* polymerase, 20 pmol of each primer and 10 ng of cloned plasmid. PCR program was: 1 cycles of 95 °C (5 min); 35 cycles of 95 °C (30 s), 54 °C (30 s), 68°C (1.30 min); 68 °C (5 min). The ECS-wild-type fragment was digested with *Bam* HI and *Not* I. The newly constructed FPPS-pET32a cloned bacterial expression vector was digested with the same enzymes and treated with alkaline phosphatase for inhibiting self-ligation. Vector and the fragment were kit purified and ligated by using T4 DNA ligase (Invitrogen) as mentioned above. Transformed colonies were analyzed by using PCR with P7 forward primer and T7 vector specific reverse primer to confirm the presence of the wild-type ECS gene. Positive colonies were grown in Luria–Bertani medium containing ampicillin (100 µg/mL) and the plasmid was purified using the plasmid GenElute Plasmid Mini-prep kit (Sigma-Aldrich). This fusion plasmid was used for protein expression.

| **Primer** | **Sequence (5'-3')** | **Template** | **RE*** |
|---|---|---|---|
| P1 | ATGGGCGATCGGAAAACCAAA | SaFPPS F | - |
| P2 | CTTCTGCCGCTTGTATATCTTCGC | SaFPPS R | - |
| P3 | GAGACCATGGGCGATCGGAAAACC | SaFPPS F | *Nco* I |
| P4 | AA**GGATCCGCCGCTGCC**CTTCTGCCGCTTGTATA | SaFPPS**Lnk** R | *Bam* HI |
| P5 | AGCCTGATTGTTGAAGATGTTATTCGTCCG | AaECS F | - |
| P6 | TTAGGTGATGATGGCATCCACAAACAG | AaECSR | - |
| P7 | ACGGGATCCAGCCTGATTGTTGAAGATGTTA | AaECS F | *Bam* HI |
| P8 | AAGCGGCCGCTTAGGTGATGATGGCATC | AaECS R | *Not* I |
| P9 | GATTCTTCCACCGCCACC | SaSS F | - |
| P10 | CTACTCCTCGCCGAGAG | SaSS R | - |
| P11 | CAAGGATCCGATTCTTCCACCGCCACCGCC | SaSS F | *Bam* HI |
| P12 | ATGCGGCCGCCTACTCCTCGCCGA | SaSS R | *Not* I |

**Table** 1. Primers used in cloning. (Restrictions sites are underlined and Linker sequence in bold)

### 1.2.3 SS from *S. album* into FPPS-pET32a

Similarly, for the fusion of *FPPS* and *SS*, the *SS* gene fragment without start codon was amplified by using blunt P9 and P10 primer from *SaSS* cDNA(Srivastava et al., 2015) (*Genbank* Accession: KF011938) and further amplified using P11 (forward) and P12 (reverse) containing *Bam* HI and *Not* I restriction sites, respectively (**Table 1**). PCR and ligation reactions were carried as mentioned above. This fusion plasmid was used for protein expression.

### 1.2.4 Transformation of Plasmid into competent cells

**1. Day 1** (2 h preparation + overnight)

a. Thaw two tubes of competent cells on ice for 5 min. Add 1 ng positive control plasmid (pUC19/pET 28a) to one tube and 1 µL water to the other tube as a negative control.

c. Incubate on ice for 30 min. Heat-shock the cells at 42 °C in a water bath for 30 sec and immediately put the tubes on ice for 2 min.

d. Add 200 µl LB broth/ SOS/ TB medium to the cells and grow the cells at 37 °C for one hour at 200 RPM.

e. Plate 50 µl (1/5th of total volume) on an LB agar plate with appropriate antibiotic.

f. Grow the cells overnight at 37 °C.

**2. Day 2** (Observations)

Check the efficiency of competent cells by counting the number of colonies on both positive and negative control.

### 1.3 Optimization of expression and purification of the recombinant proteins

The constructed recombinant plasmids were transferred into *E. coli* Rosetta DE3α cells. The cells carrying the plasmids FPPS-pRSETB, (Srivastava et al., 2015) ECS-pET28a, SS-pET32b,(Srivastava et al., 2015), FPPS-ECS-pET32a and FPPS-SS-pET32a were grown in 500 mL Terrific broth, with ampicillin (100 µg/mL) and chloramphenicol (34 µg/mL), at 37 °C. At $OD_{600}$ of ≈ 0.8, IPTG was added to the final concentration of 1 mM. The cells were harvested after overnight incubation at 16 °C,

by centrifugation at 6500×g for 10 min at 16 °C, and pellets were re-suspended in 15 mL lysis buffer (For Fusion Plasmid buffer system A and for single plasmids buffer system B were used), lysozyme (1 mg/mL), CHAPS (0.01%) and Triton X 100 (0.1%) were added. The cells were disrupted by sonication (Braun-Sonic 2000 microprobe at maximum power for 10×30s bursts with a 30s chilling period on ice between bursts). The sonicated crude was centrifuged at 10,000×g for 15 min at 4 °C. The supernatant was collected and used for His-Tag $Ni^{2+}$-NTA affinity purification. Wash buffer was used for washing undesired proteins and elution buffer was used to eluting the final pure proteins. Fractions of 0.4 mL were collected and checked by using 10 % SDS-PAGE analysis and further desalted by using GE-ÄKTA instrument or desalting bag (Himedia) 10 kDa size. Desalted proteins were stored at -80 °C. Protein concentrations and purified recombinant enzymes were determined according to Bradford using BSA as standard (Bradford, 1976).

Optimization of expression was carried out for both fusion proteins *i.e.* pET32aFPPS-ECS and pET32aFPPS-SS constructs. The parameters investigated were IPTG concentration (0.25, 0.5, 0.75, and 1.0 mM) used for induction, induction temperature (16, 25 and 30 °C) and time of harvest after induction (16 h, 12 h, and 8 h) respectively.

### 1.4 Enzyme assays and Kinetics

Enzyme activity of single FPPS, SS, and ECS was assayed by using IPP, GPP as a substrate for FPPS and FPP as a substrate for SS and ECS. The newly constructed proteins were monitored by measuring the amount of sesquiterpene *8-epi*-cedrol and α-santalene, β-santalene were released from IPP, DMAPP and IPP, GPP by the enzymatic reaction (**Fig. 1**). For ECS, A 400 µL enzymatic reaction mixture containing assay buffer pH 8.5 (25 mM Tris-HCl, 5 mM DTT, 10 mM $MgCl_2$, 20% glycerol), 15 µL purified fusion protein (25 µg), 100 µM IPP, 50 µM DMAPP (for control GPP+ IPP or 100 µM FPP used), incubated in shaker bath incubator (Brunswick, Eppendorf) at 30 ºC for 45 min at 70 rpm. The enzymatic reaction was stopped by an addition of 10 µl absolute ethanol (95%) followed by vortexing for 30s. For SS, The assay mixture contained purified recombinant protein (100 µg) in buffer (25 mM HEPES, 10% v/v glycerol, 5 mM DTT, 10 mM $MgCl_2$, pH 7.4) with IPP, DMAPP, GPP and FPP as substrates (100 µM) in a final reaction volume of 400 µL. Incubated at 30 ºC for 2 h,

all the products were extracted with hexane (3× 0.5 mL), The organic layers containing sesquiterpene products were dried over anhydrous $Na_2SO_4$ and reduced to ~50 µL with a stream of dry nitrogen. The samples were identified by GC-MS analysis by using Agilent Technology 5975-7890 GC-MS system with a HP-5MS capillary column (30m x 0.250 mm x 0.25 µ coating of 5% phenyl methyl siloxane). Injections were made as cool column at 40 ºC with oven programming from 40 °C (50 °C/min) to 50 °C (5-min hold), then 10 °C/min to 250 °C, then 50 ºC/min to 300 ºC. Separations were made under a constant flow of 1 ml He y min. Mass spectral data were collected at 70 eV and analyzed by using MSD Chem station software.

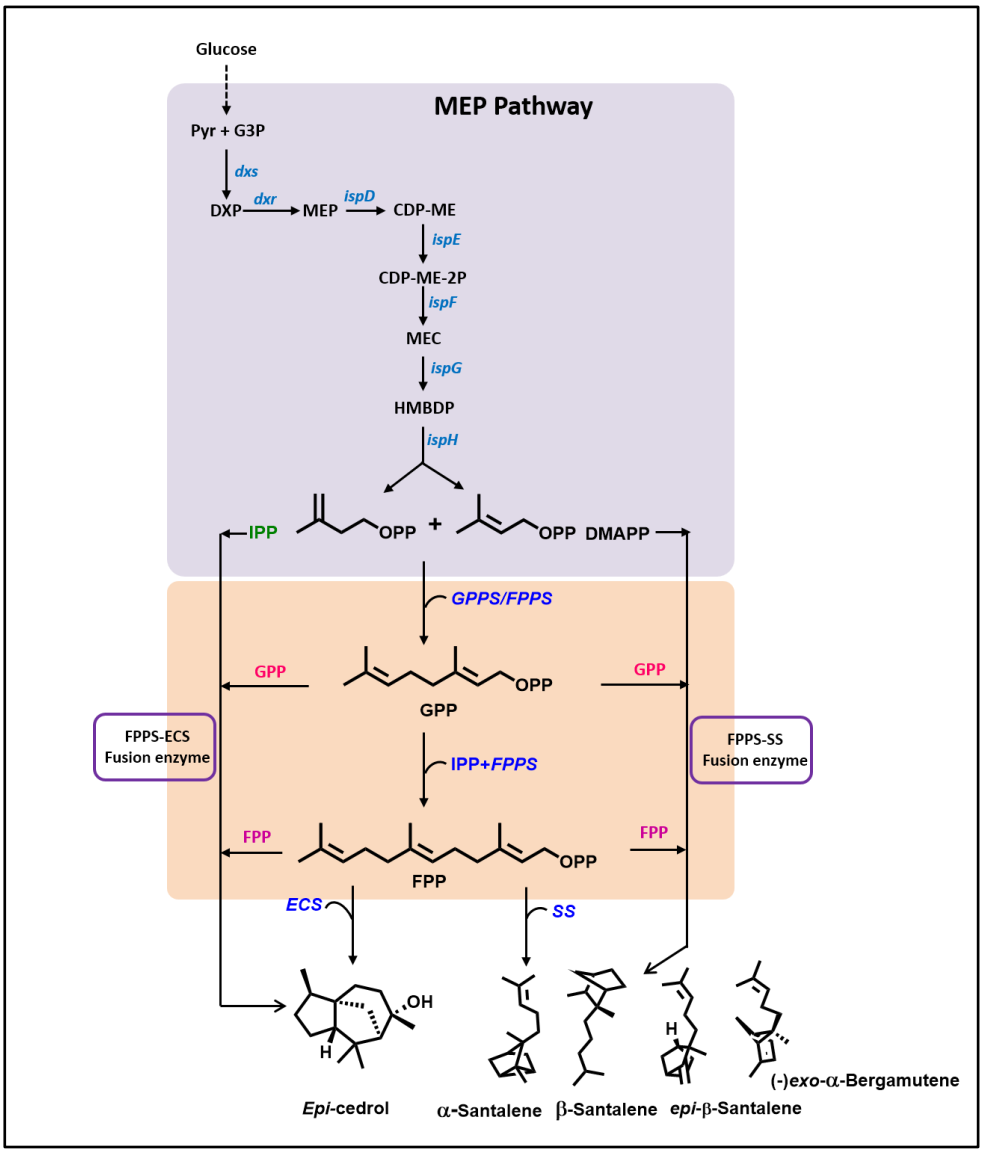

**Figure 1.** Schematic diagram of MEP pathway (blue); *epi*-cedrol, santalene biosynthetic pathway in recombinant *E. coli*. **G3P**, glyceraldehyde 3-phosphate; **3Pyr**, pyruvate; **DXP**, 1-deoxy-D- xylulose-5-phosphate; **MEP**, 2C-methyl-D-erythritol-4-phosphate; **CDP-ME**, 4-diphosphocytidyl-2C-methyl-D-erythritol; **CDP-ME-2P**, 4-diphosphocytidyl-2C- methyl-D-erythritol-2-phosphate; **MEC**, 2C-methyl-D-erythritol 2,4-cyclodiphosphate; **HMBDP**, 1-hydroxy-2-methyl-2-(E)-butenyl-4-diphosphate; **IPP**, isopentenyl pyrophosphate; **DMPP**, dimethylallyl pyrophosphate; **FPP**, farnesyl pyrophosphate; **GPPS**, geranyl pyrophosphate synthase; **FPPS**, farnesyl pyrophosphate synthase; **ECS**, *epi*-cedrol synthase; **SS**, santalene synthase.

For the enzyme kinetic study, the substrate IPP 1-50 µM and DMAPP 0.5-25 µM were used for the conversion into sesquiterpenes *epi*-cedrol and santalene mixture by both fusion enzymes and individual enzymes, respectively. The enzyme concentration was 1.5 nM for all the reactions and the farnesol was used as a standard. The comparative study and the coupled activity were done by relative peak percentage area of respected sesquiterpenes in the GC-MS analysis.

### 1.5 Substrate channeling effect

For the analysis of substrate channeling effect of fusion enzymes as compared to mixed enzymes (FPPS+ECS and FPPS+SS) together, time dependant enzyme assay was carried out with the IPP and DMAPP as a substrate. In a typical 400 µL enzymatic reactions containing equimolar concentrations of mixed enzymes (FPPS+ECS and FPPS+SS) and both fusion enzymes (1.5 nM) with 200 µM IPP and 100 µM DMAPP substrates were used. The assay products were harvested in different time of interval (30, 60, 90, 120, 150, 180 min) and quantified by GC-MS analysis as per above mentioned method and program. The experiments were carried out in three replicates.

### 1.6 Sesquiterpenes *epi*-cedrol and santalene production

The recombinant *E. coli* BL21 strain individually harbouring pRSETB-FPPS, pET28a-ECS, pET32b-SS, pET32a-FPPS-SS and pET32a-FPPS-ECS fusion plasmids were cultured in 1000 mL TB medium supplemented with appropriate antibiotics. Working concentrations of ampicillin and kanamycin were 100 and 50 µg/mL, respectively. Starter cultures were grown at 37 ºC and induced with 1 mM IPTG

($OD_{600}$~ 0.8) and allowed to continue grow at 30 ºC, for 20 h. 50 mL of dodecane was overlaid on medium to capture volatile compounds. 100 mL of samples (cells) were harvested after 2 h of time interval up to 20 h after induction. Optical density (OD) measurements were conducted on a UV–vis spectrophotometer (Thermo-Fisher Scientific Evolution 200) operating at 600 nm. Supernatant broth medium was used for the extraction of *epi*-cedrol and santalenes by 4 wash of 100 mL of distilled petroleum ether. Solvent was evaporated by rota-evaporator (Heidolph, Germany). Samples were analysed and quantified by using GC-MS analysis as per mentioned method. Farnesol was used as internal standard. The experiments were performed as well as analysed in triplicates.

### 1.7 Sesquiterpenes *epi*-cedrol and santalene production

The recombinant *E. coli* BL21 strain individually harbouring pRSETB-FPPS, pET28a-ECS, pET32b-SS, pET32a-FPPS-SS and pET32a-FPPS-ECS fusion plasmids were cultured in 1000 mL TB medium supplemented with appropriate antibiotics. Working concentrations of ampicillin and kanamycin were 100 and 50 µg/mL, respectively. Starter cultures were grown at 37 ºC and induced with 1 mM IPTG ($OD_{600}$~ 0.8) and allowed to continue grow at 30 ºC, for 20 h. 50 mL of dodecane was overlaid on medium to capture volatile compounds. 100 mL of samples (cells) were harvested after 2 h of time interval up to 20 h after induction. Optical density (OD) measurements were conducted on a UV–vis spectrophotometer (Thermo-Fisher Scientific Evolution 200) operating at 600 nm. Supernatant broth medium was used for the extraction of *epi*-cedrol and santalenes by 4 wash of 100 mL of distilled petroleum ether. Solvent was evaporated by rota-evaporator (Heidolph, Germany). Samples were analysed and quantified by using GC-MS analysis as per mentioned method. Farnesol was used as internal standard. The experiments were performed as well as analysed in triplicates.

## 2. Results and Discussion

For expression of recombinant fused enzymes, the bacterial expression vector pET32a was used (cloning shown in **Fig. 2** and **Fig. 3**). whereas, for the production of single enzymes, different expression vectors (ECS-pET28a, SS-pET32b, FPPS-pRSETb) were used (Shinde et al., 2016; Srivastava et al., 2015). This selection was

made because of increased protein solubility due to the presence of thioredoxin tag in the vector (Rosano and Ceccarelli, 2014). The sequence also contains an enterokinase cleavage site for removal of the fusion tag. All plasmids *FPPS*-pRSETb, *ECS*-pET28a, *SS*-pET32b, *FPPS-ECS*-pET32a, and *FPPS-SS*-pET32a were isolated from cloning host *E. coli* Top 10 cells and transferred into *E. coli* Rosetta (DE3) for production of the recombinant enzymes. The transformed *E. coli* was grown and induced with IPTG (0.5 mM), and purified by $Ni^{+2}$-NTA affinity chromatography column.

All the purified desalted proteins were evaluated for *FPPS*, *ECS*, and *SS* activity. These two recombinant multifunctional enzymes showed both activities, as the linker GSGGS is of ideal size to permit the two enzymes to fold properly. When fusing two multimeric enzymes without linker or short linker could lead to the formation of multimeric protein network which cause steric hindrance of the active domain, whereas, if a linker is too long it may be sensitive to proteolytic attack and also lead to reduced channeling of substrates between two active sites (Elleuche, 2015; Mótyán et al., 2013).

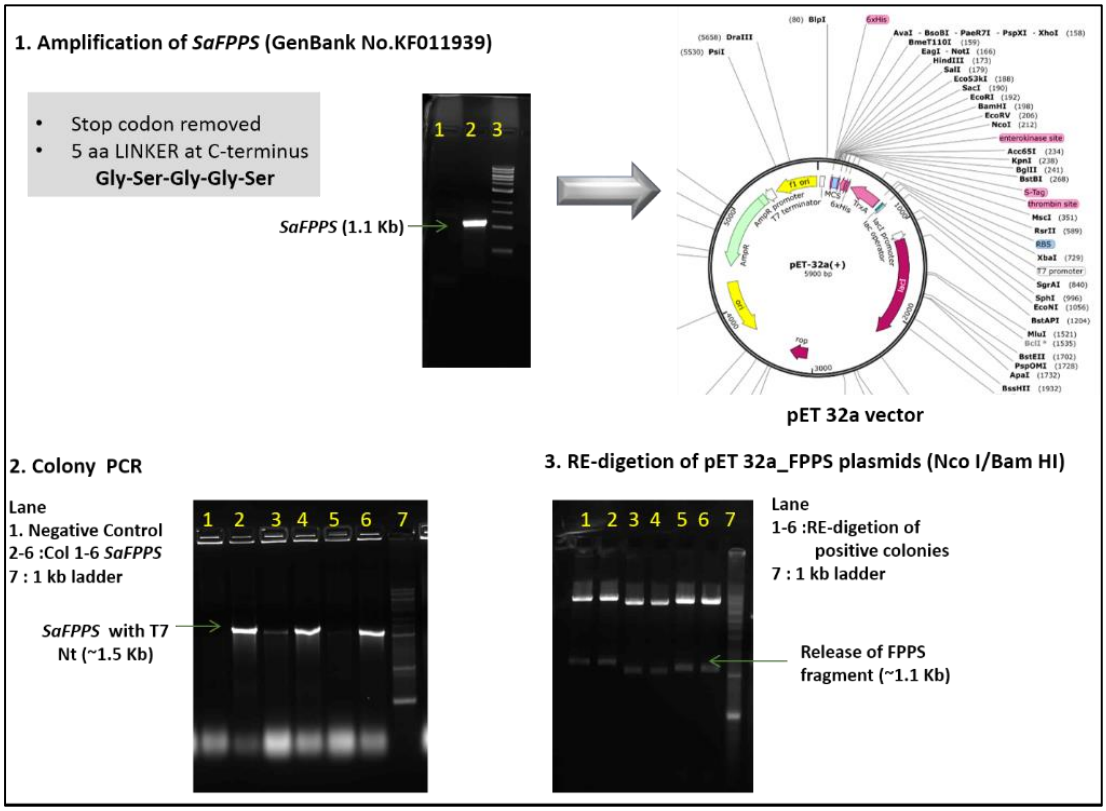


**Figure 2.** Cloning of *SaFPPS* in pET32a vector

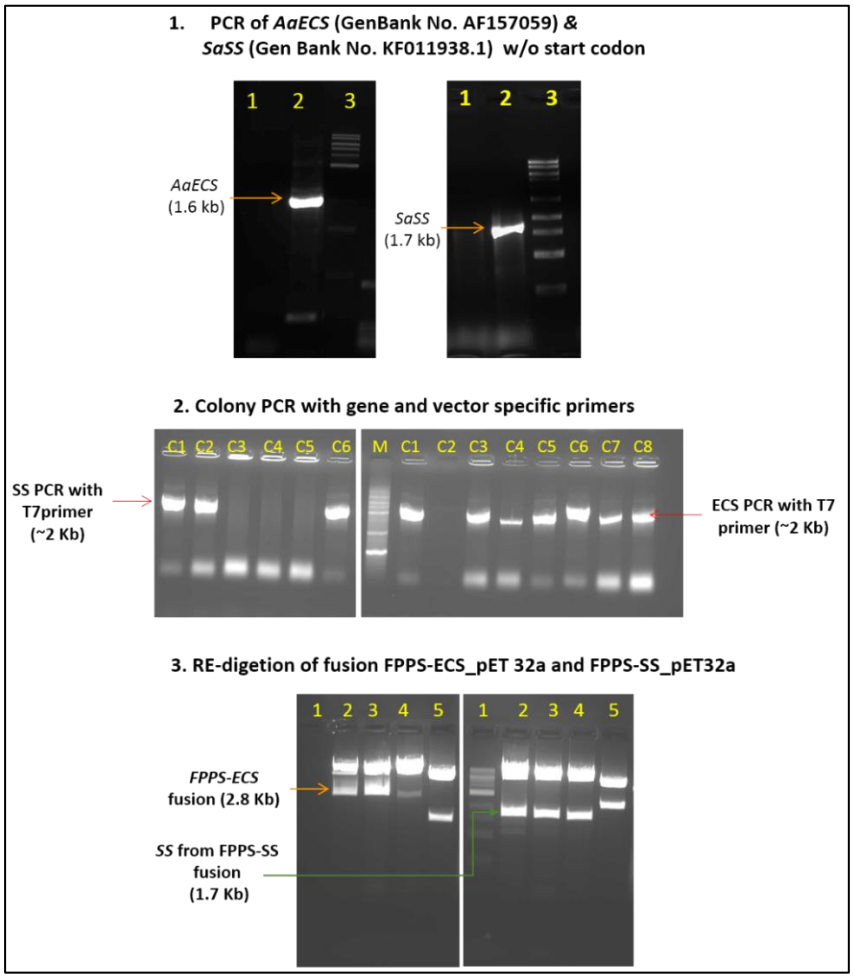


**Figure 3.** Cloning of *Aa*ECS and *Sa*SS in *Sa*FPPS-pET32a plasmid.

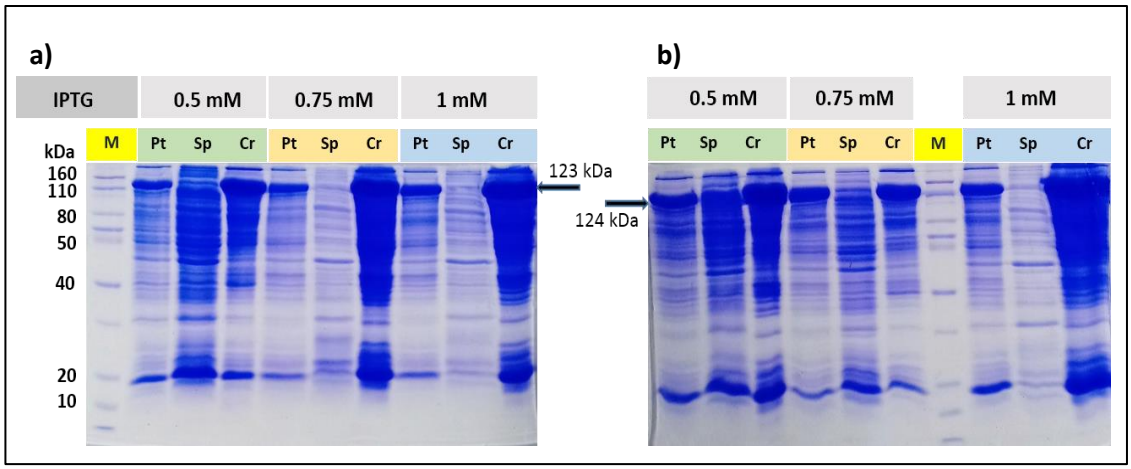


**Figure 4. a)** SDS-PAGE gel image of expressed recombinant FPPS-ECS (**a**) and FPPS-SS (**b**) fusion enzyme with induction of various IPTG concentration (0.25-1.0mM,). (**M**. Protein Marker/ladder; **Pt**= Pellet fraction, **Sup**= Supernatant fraction; **Crd**= Crude sonicated fraction).

Optimization of expression was carried out for the new fusion constructs as mentioned in materials and methods, 0.5 mM IPTG induction and 16 ºC overnight (12-14 h) incubation showed the optimum level of expression in SDS gel (optimization shown in **Fig. 4**), 1 mM IPTG was used for other previously reported constructs. Fused enzymes were expressed as a fusion with the thioredoxin protein tag, which helps to improve the solubility of expressed proteins (Rosano and Ceccarelli, 2014; Young et al., 2012). SDS-PAGE images of all fractions of FPPS-ECS (Fig 5a) and FPPS-SS (**Fig.** 5b) fusion proteins are showed in **Fig. 5**. All the proteins (including individual proteins) were produced in large scale (2× 1000 mL TB broth) using the condition mentioned above and purified by $Ni^{+2}$NTA affinity chromatography. For better and enhanced purification of fusion proteins, size exclusion chromatography (SEC) was used. Partially purified protein were passed through a size exclusion chromatography. The characterization of recombinant protein was carried out with thioredoxin-Stag-His-tag as N-terminal fusion.

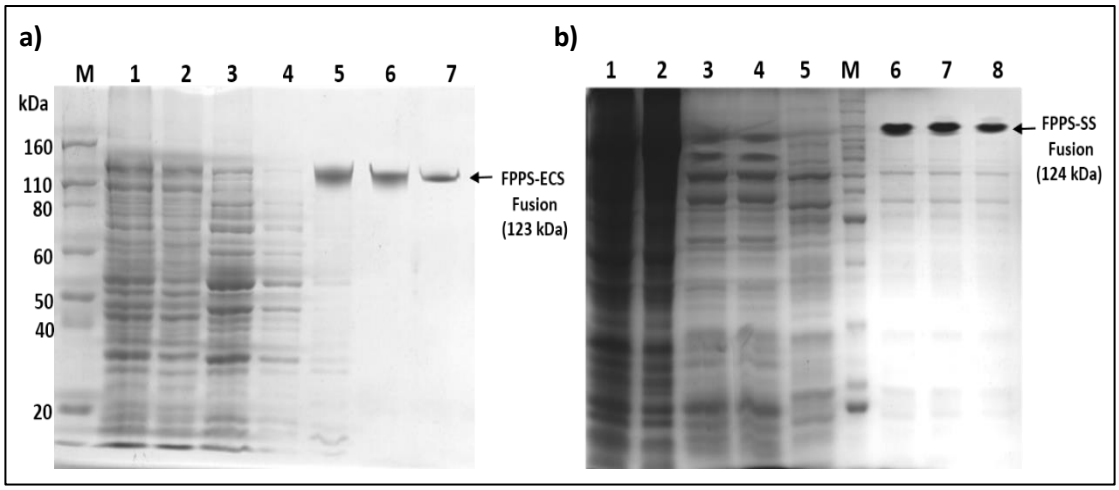


**Figure 5.** SDS-PAGE gel image of purified expressed recombinant **a**. FPPS-ECS and **b**. FPPS-SS fusion enzymes.

### 2.1 Kinetic Properties of Recombinant Enzymes

The SEC-purified pure enzymes were used to determine Km value according to standard techniques (**Fig. 6**) (Srivastava et al., 2015). Enzyme assay for both the fusion enzymes were optimized as per **Table 2**. In kinetics study, the Km values of *ECS* and SS for FPP were 3.74 µM and 0.58 µM, respectively. Whereas, Km values of fusion enzymes *FPPS-ECS* and *FPPS-SS* for IPP were calculated to be 4.71 µM and 1.8 µM

respectively. A slightly higher Km values were observed for the single enzymes together than the fused enzyme for IPP as a substrate. Km value for DMAPP was half of the Km for IPP as the half concentration of DMAPP was used with the IPP in the kinetics study (kinetics shown in **Fig 8**). **Table 3** reveals the catalytic potential of fused enzymes over individual enzymes together. In case of fusion enzymes, $k_{cat}/k_m$ ratio significantly increased compared to the combination of single enzymes which shows the fused enzymes has the catalytic efficiency more than individual enzymes together. Overall, these results correlated to those previously reported fusion proteins for *FPPS* and sesquiterpene synthases from other sources (Albertsen et al., 2011; Brodelius et al., 2002; Deng et al., 2016).

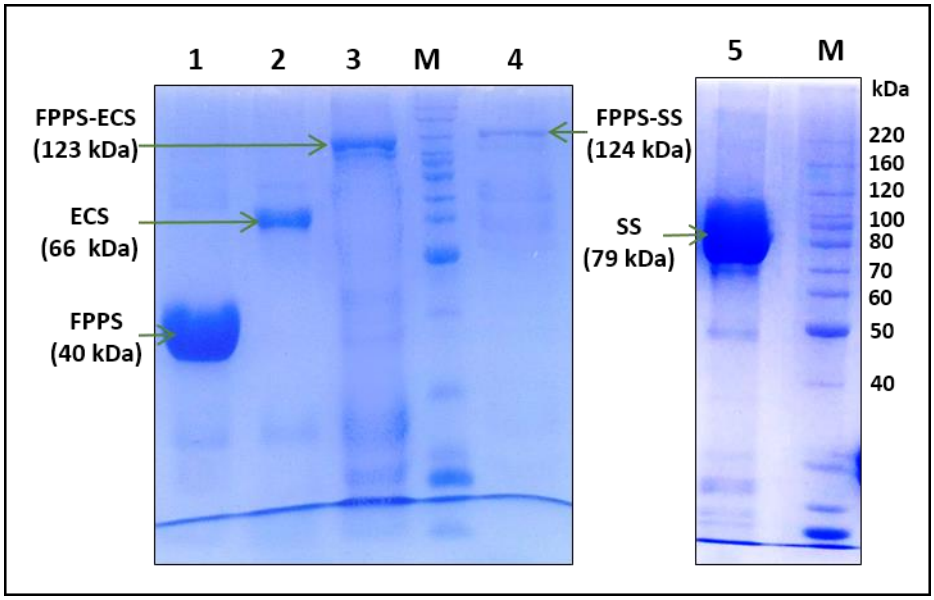


**Figure 6.** SDS-PAGE gel image of all purified fractions of single and fusion enzymes. 1. *Sa*FPPS 2. *Aa*ECS 3. FPPS-ECS fusion, 4. FPPS-SS fusion, 5. *Sa*SS M. Protein ladder.

<table>
<tr><th>Assay</th><th>Substrate/enzyme</th><th>Buffer<br><br>(400 µL)</th><th>pH</th><th>Activity Result</th></tr>
<tr><td rowspan="2">FPPS-ECS Fusion OR FPPS-SS fusion</td><td>• IPP (300 µM) &<br>• DMAPP (150 µM)<br>• GPP (150 µM) &<br>IPP (100 µM)<br>Enzyme- 10 µg/20 µg/ 50 µg/100 µg</td><td rowspan="3">• Tris- 25 mM, $MgCl_2$ 10 mm, DTT 2.5 mM/5mM Glycerol – 10%<br><br>• HEPES 25 mM $MgCl_2$ 10 mm, DTT 2.5 mM/BME 10 mM Glycerol – 10%<br><br>• Phosphate 25 mM $MgCl_2$ 10 mm, DTT 2.5 mM Glycerol – 10%<br><br>• Tris 25 mM, $MgCl_2$ 15 mm, BME 5 mM Glycerol – 20%</td><td rowspan="3">8.0 & 8.5</td><td>Low activity</td></tr>
<tr><td>• IPP (300 µM) &<br>• DMAPP (150 µM)<br>• GPP (150 µM) &<br>• IPP (100 µM)<br>Enzyme- 10 µg/20 µg/ 50 µg/100 µg</td><td>Low activity</td></tr>
<tr><td>Control expt. ECS/SS (Incubation for 4 h)</td><td>IPP - 10 µL (150 µM),<br>GPP 3 µL (150 µM)<br>FPPS- 15 µL (100 µg)<br>ECS- 20 µL (100 µg)</td><td>High Activity</td></tr>
</table>

**Table 2**. Optimization of fusion enzymes assay with various buffer and parameters.

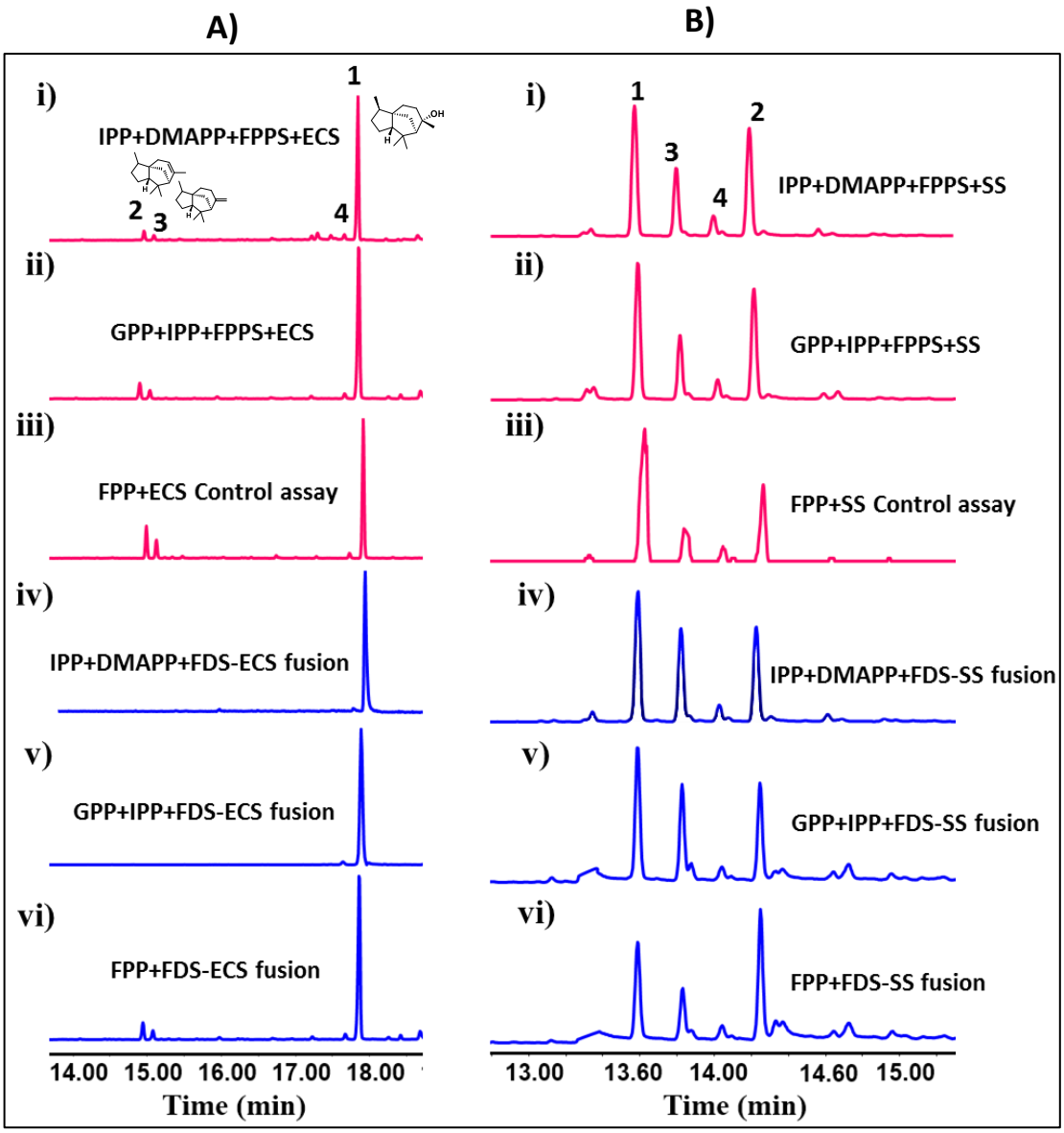


**Figure 7.** GC-FID chromatogram for the assay extracts: **A)** ECS, FPPS and FPPS-ECS fusion with (i) 2×IPP+DMAPP, (ii) GPP+IPP, (iii) FPP, (iv) 2xIPP+DMAPP (v) GPP+IPP and (vi) FPP, respectively. Products were *epi*-cedrol (**1**), *α*-cedrene (**2**), *β*-cedrene (**3**), cedrol (**4**). **B)** SS, FPPS and FPPS-SS fusion with (i) 2×IPP+DMAPP, (ii) GPP+IPP, (iii) FPP, (iv) 2xIPP+DMAPP (v) GPP+IPP and (vi) FPP, respectively. Products were *α*-santalene (**1**), *β*-santalene (**2**), *exo*-α-bergamotene (**3**), *epi*-β-santalene (**4**).

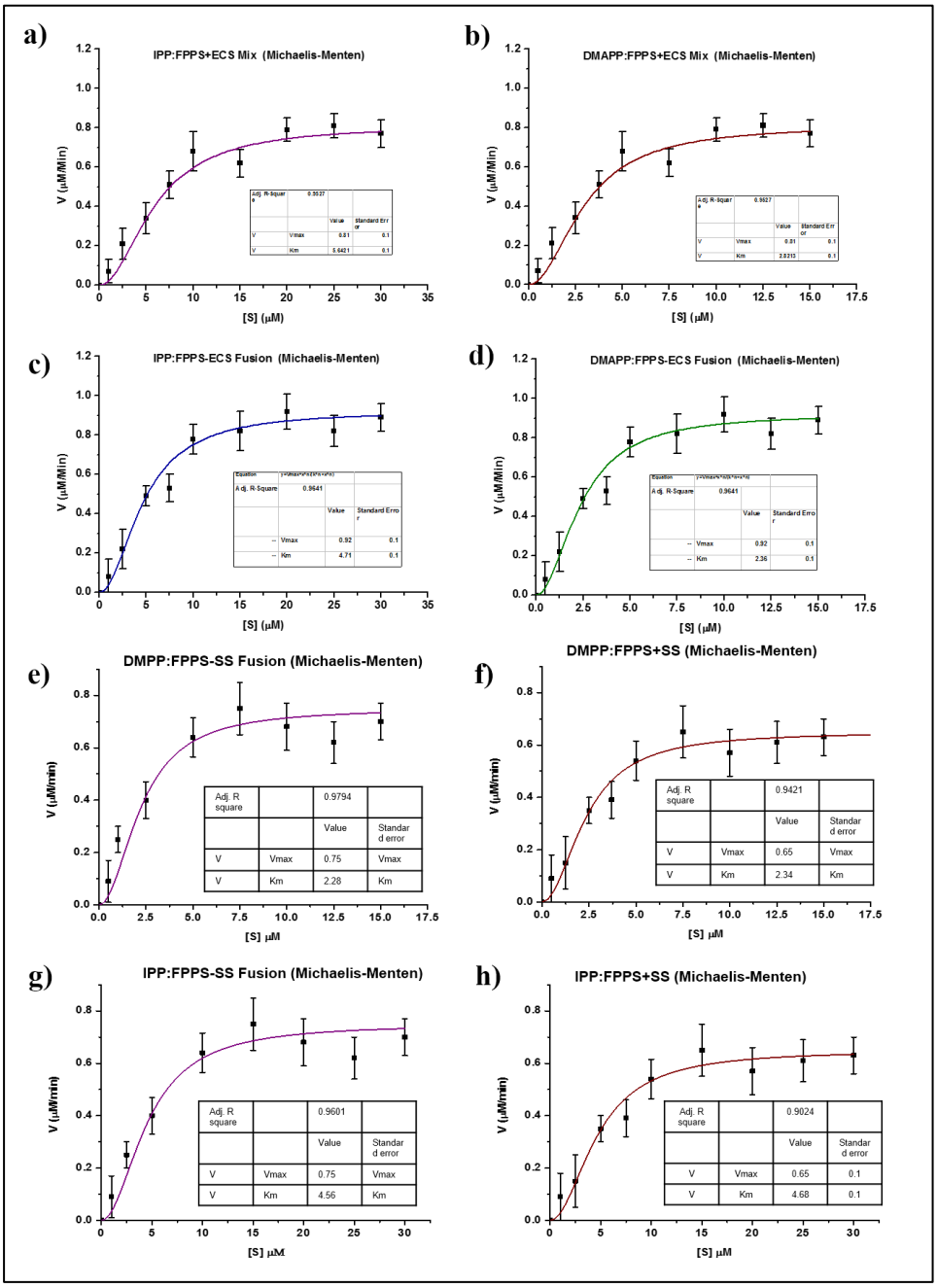


**Figure 8. a-b)** Michaelis Menten graph for kinetics of fusion enzymes (FPPS-ECS, FPPS-SS) and mixed enzymes (FPPS+ECS, FPPS+SS) with IPP and DMAPP as substrates. (Kinetics of single ECS for FPP substrate are shown in Chapter 3).

| Enzymes | $K_m$ (µM) | $V_{max}$ ( µM/min) | $k_{cat}$ ($sec^{-1}$) | $k_{cat}/K_m$ ($\times 10^6$ $M^{-1}S^{-1}$) |
|---|---|---|---|---|
| **For IPP** | | | | |
| *FPPS+ECS* | 5.64±0.2 | 0.81±0.1 | 1.4±0.1 | 0.24±0.1 |
| *FPPS-ECS* Fusion | 4.71±0.1 | 0.92±0.1 | 1.88±0.1 | 0.40±0.1 |
| *FPPS+SS* | 4.68±0.2 | 0.65±0.1 | 1.34±0.05 | 0.28±0.1 |
| *FPPS-SS* Fusion | 4.56±0.2 | 0.75±0.1 | 1.55±0.1 | 0.34±0.1 |
| **For DMAPP** | | | | |
| *FPPS+ECS* | 2.82 ±0.2 | 0.81±0.1 | 1.4±0.1 | 0.49±0.1 |
| *FPPS-ECS* Fusion | 2.35 ±0.1 | 0.92±0.1 | 1.88±0.1 | 0.80±0.1 |
| *FPPS+SS* | 2.34±0.2 | 0.65±0.1 | 1.34±0.05 | 0.57±0.1 |
| *FPPS-SS* Fusion | 2.28±0.2 | 0.75±0.1 | 1.55±0.1 | 0.68±0.1 |

**Table 3.** Kinetic parameters of free enzymes and fusion enzymes**.**

| | **Enzyme assay with individual enzymes** | | | **Enzyme assay with fusion Enzyme (FE & FS)** | | |
|---|---|---|---|---|---|---|
| **Substrates** | DMAPP+IPP | GPP+IPP | FPP | DMAPP+IPP | GDP+IPP | FPP |
| **a) *ECS* Products** (%) | | | | | | |
| *epi*-cedrol | 88.2 ±2.3 | 85.1 ±2.1 | 80.7 ±3.5 | **97.6 ±0.9** | **97.8 ±1.2** | **83.2 ±2.1** |
| α-cedrene | 5.8 ±0.9 | 8.5 ±1.1 | 12.8 ±2.1 | 1.1 ±0.3 | 0.3 ±0.3 | 8.7 ±2.1 |
| β-cedrene | 3.1 ±0.6 | 4.2 ±0.8 | 4.9 ±1.3 | 0.4 ±0.1 | 0.2 ± 0.1 | 4.6 ±0.6 |
| Cedrol | 2.6 ±0.3 | 2.1 ±0.2 | 1.5 ±0.4 | 0.8 ±0.2 | 1.7 ±0.4 | 3.5 ±1.3 |
| **b) *SS* Products (%)** | | | | | | |
| α-santalene | 41.4 ±0.1 | 42.9 ±0.7 | 51.8 ±0.6 | 40.3 ±0.3 | 41.0 ±0.4 | 35.0 ±0.2 |
| β-santalene | 34.2 ±0.2 | 34.7 ±0.3 | 29.8 ±0.2 | 28.9 ±0.2 | 30.1 ±0.6 | **44.6 ±0.4** |
| *exo*-α-bergamotene | 19.1 ±0.2 | 17.3 ±0.2 | 12.7 ±0.1 | 26.3 ±0.2 | 25.2 ±0.1 | 15.9 ±0.2 |
| *epi*-β-santalene | 5.2 ±0.1 | 5.0 ±0.3 | 5.7 ±0.2 | 4.3 ±0.1 | 3.6 ±0.1 | 4.4 ±0.1 |

**Table 4**. Comparisons between (%) ratios of sesquiterpenes (%) formed from various substrates (DMAPP/IPPP/GPP/FPP) with **a)** Enzyme assay with individual enzymes (*FPPS*, *ECS*) and fusion enzymes (*FPPS-ECS*, FP*PS-SS*). **b)** Enzyme assay with individual enzymes (*FPPS*, *SS*) and fusion enzymes (*FPPS-SS*) reaction.

## 2.2 Coupled Enzyme activity

The fused enzymes *FPPS-ECS* and *FPPS-SS* converts DMAPP and IPP or GPP or FPP to respective sesquiterpenes *i.e epi*-cedrol and α/β santalene as a major product respectively (**Fig. 1**). The fusion assay was kept for 1h, as the longer incubation time affects the activity of the fusion protein and the stability of the sesquiterpenes. In case of *FPPS-ECS* fusion, the enzyme assay with DMAPP/IPP or GPP, the side products such as α-cedrene, β-cedrene were found in trace amount as compared to individual assay with FPP, but in the fusion enzyme assay with FPP, these products were observed with certainty (**Fig. 7A, Table 4**). Similarly, in case of *FPPS-SS* fusion the ratio of the products was slightly different with various substrates; single *SS* produces slightly higher proportion of α/β santalenes while FPPS-SS fusion produces higher proportion of *exo*-α-bergamotene than *epi*-β-santalene as depicted (**Fig. 7b, Table 4**). Although the ratios were different, but the relative amount of sesquiterpenoids formed from fusion enzyme was higher than the individually produced by two single enzymes with various substrate combinations. Same results were obtained in the time dependent enzymatic assay with fusion enzymes and free enzymes together. The relative amount of sesquiterpenoids formed from fusion enzyme was higher than the individually produced two single enzymes together over different time of interval with IPP and DMAPP as a substrate, as indicated by relative peak percent area (**Fig 9**).

This Time-dependent experiment was performed for confirming channeling effect. If there is channeling effects, the product percentage will be more as compared to individual enzymes together. This is because of protein-protein interactions may also increase metabolic efficiency either by channeling intermediates between enzymes or by localizing two active sites in close proximity (Zhang, 2011). The larger portion of the FPP produced by the *FPPS* part of the enzyme is converted to final product by *ECS* or *SS*. This may be expected as the building-up of the intermediate FPP is more rapid at higher amounts of *FPPS* and the subsequent *ECS* or *SS* experiences a higher substrate concentration, *i.e.* a steady-state condition is approached. As per previous reports, the orientation of the two enzymes does not affect the activity as well as Km value of the fusion enzymes (Brodelius et al., 2002). Finally, the performance of the multifunctional enzymes, the level of sesquiterpenoid produced from IPP by *FPPS-ECS* and *FPPS-SS*

was compared with that produced by corresponding amounts of two single enzymes (equal molar concentrations) over time (experiment only done in case of ECS). As *FPPS* has active domains for GPP synthesis from DMAPP and IPP, further GPP with IPP converted into FPP by this enzyme. The amount of FPP was higher in fusion enzyme than individual enzymes in minimum time of interval. Therefore, the amount of *epi*-cedrol produced was considerably higher for the fusion enzyme than for the mixture of single enzymes respectively. The amount of *epi*-cedrol and α/β-santalene produced were considerably 1.66 and 1.45 fold higher for the fusion enzymes, respectively than for the mixture of single enzymes together after 1 h of incubation (**Fig. 9**). Fusion enzymes consumes maximum amount of substrates present in the buffer leading to increase in the amount of desired metabolites. This results showed that the FPP produced by the first enzyme is transferred to the active site of *ECS* or *SS* with limited diffusion into surrounding solution. A proximity effect and substrate channeling operates in the fusion enzymes and increases the overall catalytic activity of the enzymatic reaction. Similar substrate channeling has also been observed in previously constructed artificial bifunctional enzymes (Elleuche, 2015; Zhang, 2011).

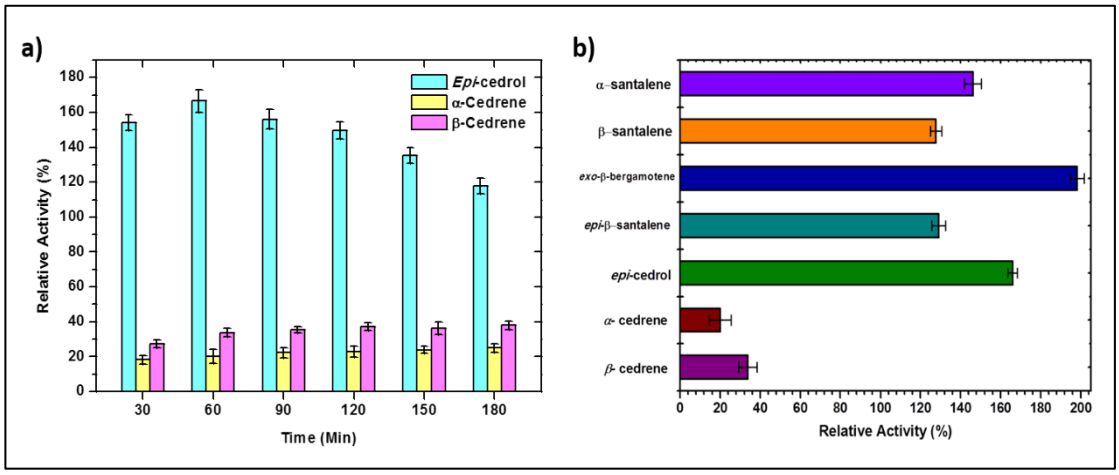


**Figure 9.** a. Time dependant enzyme activity of the *FPPS-ECS* fusion enzyme. b. Relative activity (%) of both fusion enzymes as compare to single enzymes together. The relative activity expressed in comparison of the percentage of the activity of free enzymes *i.e FPPS+ECS* or *FPPS+SS* with IPP and DMAPP substrates only.

## 2.3 *Epi*-cedrol Production

Biosynthesis of terpenoid production in *E. coli* has been carried out by the MEP or DXP pathway (**Fig. 1**). This pathway consists of seven enzymatic steps that convert glyceraldehyde-3-phosphate (G3P) and pyruvate to IPP and DMAPP in a ratio of 5:1 (Rohdich et al., 2003). It initiates with enzyme DXP synthase (DXS) which catalyses the condensation of G3P and pyruvate to form DXP. These total seven genes (*dxs*, *dxr*, and *Isp-DEFGH*) encoding the MEP/DXP pathway in the *E. coli* genome (**Fig. 1**) are regulated by various promoters (Wang et al., 2017). Overexpression of terpene synthases leads to the biosynthesis of respected isoprenoids. This pathway affected by various aspects of the intracellular metabolites including available carbon, ATP, the reducing power, and accumulation of intermediates of the pathway (Banerjee and Sharkey, 2014).

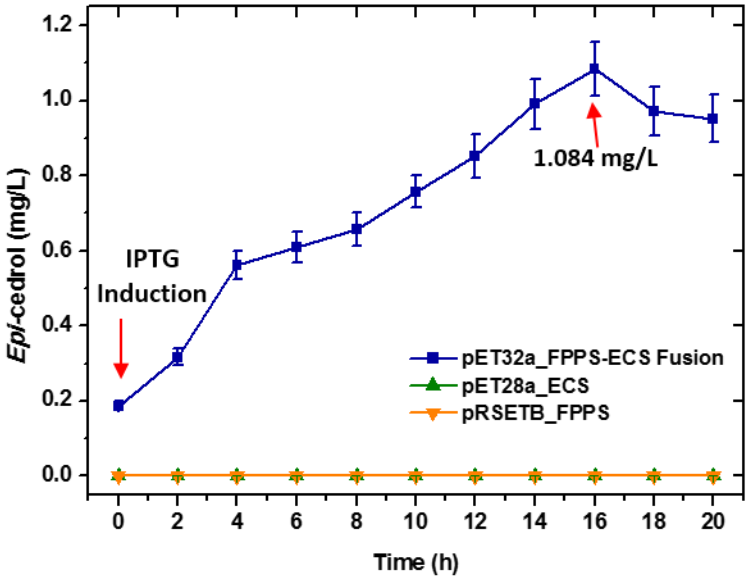


**Figure 10**. Production of *epi*-cedrol over time by *E. coli* BL21 strains harbouring pET32a-FPPS-ECS fusion, pRSET-b-FPPS, and pET28a-ECS plasmids (Error bars represent standard deviation (n = 3))

Production of *epi*-cedrol and santalene were carried out by transferring all plasmids individually into the *E. coli* BL21 cells. Batch culture of was initiated and recombinant cells were harvested over different time of interval (*FPPS-SS* fusion over different time was not carried out due to low yield in fermentation medium), *epi*-cedrol and santalene were extracted from fermentation media and analyzed by GC–MS as

mentioned in methodology section. Out of four recombinant strains, only both fusion plasmids showed the good titre of sesquiterpenes (*epi*-cedrol and santalene mixture) in the fermentation medium. Strain harboring pRSETB-FPPS plasmid produced only FPPS which was utilized for the production of FPP in the cells, however, single pET28-ECS plasmid harboring strain produced negligible amount of *epi*-cedrol after 12-14h of induction (**Fig. 10**). For comparing activity, *E. coli* showed good amount of *epi*-cedrol titre in batch fermentation although maintaining of multiple plasmids may increases the metabolic loads on the cell from DNA, RNA, and protein synthesis as well as the various antibiotic resistance proteins in the cell must produce (Rozkov et al., 2004), and leads to affect the production of the desired final products (Tyo et al., 2009). But the expression levels of two plasmids may vary in the cell. *E. coli* harboring fusion plasmids individually produced maximum 1.084 mg/L *epi*-cedrol while 0.433 mg/L of santalene mixture after 16 h of incubation. This is because of the different expression levels of genes, and the substrate channeling effects. The recombinant strain overexpressing fusion as well as mixed plasmids, were three times higher the titer of *epi*-cedrol than previously reported in engineered yeast (0.370 mg/L) (Jackson et al., 2003).

# Section 2B

# Cloning, Expression and Characterization of fusion proteins FPPS-ECS and FPPS-SS in S. cerevisiae

## 1. Methodology

### 1.1 Cloning of Fusion Enzymes *FPPS-ECS* and *FSS-SS* in Yeast Vector and Expression in *S. cerevisiae*

For the construction of fusion protein in yeast, pYES2/CT yeast vector and for expression, *S. cerevisiae* INV*Sc* 1 host were used. Sequential cloning methodology was used as per described in previous *section 2A*.

#### 1.1.1 PCR Cloning of FPPS from *S. album* into pYES2/CT

A previously constructed cloned cDNA of FPPS (*Genbank* Acc. No. KF011939) from *S. album* was used to amplify FPPS with consequence/signaling sequence and without a stop codon and with or without linker fragment (GSGGS) at 3' end including *Bam* HI site which encodes for Glycine and Serine. Wild-type FPPS was initially amplified by using blunt P1 and P2 primer and further amplified using P3 (forward), P4 (reverse), P5 (reverse with linker Nt.) contained a *Kpn I* and *Bam* HI sites, respectively (**Table 1**). PCR was carried out in a total volume of 50 µL with the following reagents: 45 µL Accuprime *Pfx* polymerase (Invitrogen), 20 pmol of each primer and 10 ng of cloned plasmid. PCR program depicted in fig 2. Product was digested with *Kpn* I and *Bam* HI. The yeast expression vector pYES2/CT was also cleaved with the same enzymes and treated with alkaline phosphatase (NEB). Ligation was carried out using T4 DNA ligase. The ligation mixture of pYES2/CT_FPPS and pYES2/CT_FPP-linker were transformed into *E. coli* TOP10 (Thermo Fisher Scientific). Colonies were analyzed by PCR using (P14) T7 forward primer and Cyc1 (P16) vector specific reverse primer to confirm the presence of the FPPS gene. Positive colonies were grown in Luria-Bertani medium containing ampicillin (100 µg/mL) and the plasmid was purified using the plasmid PureLink Quick Plasmid Miniprep Kit ((Invitrogen-Thermo fischer) and used as a template for insertion of another gene for constructing fusion.

#### 1.1.2 Sequential cloning of sesquiterpene synthase genes (*ECS* and *SS*)

##### 1.1.2.1 PCR cloning of *ECS* from *A. annua* into FPPS-pYES2/CT and FPPS-LNK-pYES2/CT

For fusion of *FPPS* and *ECS*, *ECS* gene fragment without start codon was amplified by using blunt P6 and P7 primer from a cloned plasmid (*Genbank* No.

AF157059) and further amplified using P8 (forward primer) and P9 (reverse primer) containing a *Bam* HI and *Not* I restriction sites, respectively (**Table 1**). PCR was carried out in a total volume of 50 µL with the following reagents: 45 µL Accuprime *Pfx* polymerase (Invitrogen), 20 pmol of each primer and 10 ng of cloned plasmid. PCR program was kept same as per **Fig.** 1. The PCR product and cloned vector was digested with *Bam* HI and *Not* I and ligated by using T4 DNA ligase. Further proceed as mentioned above. This fusion plasmid FPPS-L_ECS-pYES2/CT was be used for protein expression and characterization in *S. cerevisiae*.

| Code | Primer Name | Primer Sequence 5' to 3' |
|---|---|---|
| P1 | FPPS_Cons_F | **AACACAATGTCT**GATCGGAAAACCAAA |
| P2 | FPPS_blnt_R | CTTCTGCCGCTTGTATATCTTCGC |
| P3 | FPPS_KpnI_F | GAGA**GGTACC**AACACAATGTCTGATCGGAAAA |
| P4 | FPPS_BamHI_R | CT**GGATCC**CTTCTGCCGCTTGTATA |
| P5 | FPPS_BamHI-LnkR | AA**GGATCC**GCCGCTCTTCTGCCGCTTGTATA |
| P6 | ECS_bnt_F | AGCCTGATTGTTGAAGATGTTATTCGTCCG |
| P7 | ECS_blnt_R | GCAGCCGGATCTCAGTGGTGGTG |
| P8 | ECS_BamHI_F | ACG**GGATCC**AGCCTGATTGTTGAAGATGTTA |
| P9 | ECS_Not I _RP | AA**GCGGCCGC**GCAGCCGGATCTCAGTGGTGGTGGTG |
| P10 | SS_blunt F | ACAGCTCCATTCATTGATCCTACTG |
| P11 | SS_blunt R | CTCCTCGCCGAGAGGAATAGGG |
| P12 | SS_BamHI_F | CAA**GGATCC**ACAGCTCCATTCATTGATCCTA |
| P13 | SS_Not I_R | AT**GCGGCCGC**CTCCTCGCCGAGAGGAAT |
| P14 | T7 FP | TAATACGACTCACTATAGGG |
| P15 | Gal 1 FP | AATATACCTCTATACTTTAACGTC |
| P16 | CYC 1 RP | GCGTGAATGTAAGCGTGAC |

**Table 1.** Primers used in yeast cloning (Restriction sites and consequences sequence showed in bold.

### 1.1.2.2 PCR cloning of SS from *S. album* into FPPS-pYES2/CT and FPPS-LNK-pYES2/CT

Similarly, for the fusion of *FPPS* and *SS*, the *SS* gene fragment without start codon was amplified by using blunt P10 and P11 primer from *SaSS* cDNA (Gen-Bank Accession: KF011938) and further amplified using P12 (forward) and P13 (reverse)

containing *Bam* HI and *Not* I restriction sites, respectively (**Table 1**). PCR was carried out in a total volume of 100 µL with the following reagents: 90 µL Accuprime *Pfx* polymerase (Invitrogen), 20 pmol of each primer and 20 ng of cloned plasmid. PCR and ligation reactions were carried as mentioned above (**Fig.** 1). This fusion plasmid FPPS-L_SS-pYES2/CT was used for protein expression in *S. cerevisiae*.

- PCR programs used for gene amplification.

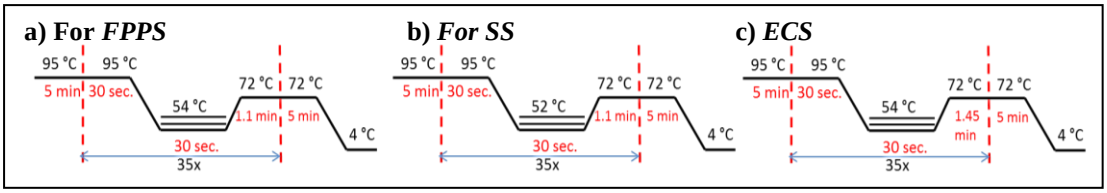


## 1.2 Preparation of competent cells and transformation into *S. cerevisiae* (INV*Sc* 1)

1. Single colony of *S. cerevisiae* INV*Sc*1 was inoculated in 10 mL of YPD medium and kept for overnight at 30°C at 200 rpm.
2. $OD_{600}$ of culture was determined. The culture was diluted to an $OD_{600}$ of 0.4 in 50 mL of YPD medium and incubated for an additional 2–4 h.
3. Cells pellet was down at 1,500 × *g* and re-suspended in 40 mL 1x TE.
4. Again cell pellet was down at 1,500 × *g* and re-suspend the pellet in 2 mL of 1x LiAc/0.5x TE. Finally, the cells were incubated at RT for 10 min. (competent cells were used within 1 week if stored in -80 °C or made freshly each time of expression)
5. For each transformation, 10 µL of Salmon single stranded sperm DNA mixed together with 1 µg fusion plasmid DNA (ECS-pYES2/CT or SS-pYES2/CT) with 100 µL of the yeast suspension from Step 4.
6. Solution of 1x LiAc/40% PEG-3350/1x TE 700 µL was added and mixed well and incubated this solution at 30°C for 30 minutes.
7. DMSO, 88 µL was added, mixed well, and gave heat shock at 42°C for 15 min.
8. Cells were pellet down at high speed centrifuge (in a microcentrifuge) for 10 sec and supernatant was discarded.
9. Pellet was re-suspended in 1 mL 1x TE and step 8 was repeated.
10. Finally, the cell pellet was re-suspended in 50-100 µL 1x TE and plated on a selective SC-minimal medium plate (YNB-CSM-URA-Amp-LA).

11. Plate was incubated for 48 h at 30 °C. The colonies were confirmed by colony PCR.

### 1.3 Expression of fusion proteins in *S. cerevisiae* INV*Sc*1

1. Single colony of INV*Sc*1 containing fusion pYES2/CT construct inoculated into 15 mL of the CSM-URA SC selective medium containing 100 µg/mL ampicillin, 2% glucose or 2% raffinose and incubated overnight at 30°C with 180 RPM.
2. Optical density $OD_{600nm}$ were Determined of overnight culture. For setting 0.4 $OD_{600nm}$ in 50 mL of induction medium (SC selective medium containing 2% galactose) the amount of overnight culture necessary was calculated.
3. Calculated amount of overnight culture was removed and pellet down the cells at 1,500 × g for 5 minutes at room temperature. Pellet was re-suspended in 50 mL of induction medium. (See recipe for induction medium in materials section). Incubated culture at 30°C with shaking.
4. Cells were harvested at 24 h, 48 h, 72 h and 90 h hours after addition of induction medium. For each time point, 10 mL of culture from the flask was removed and $OD_{600}$ was determined of each sample.
5. The cells were centrifuged at 1,500 × g for 5 minutes at 4°C. The supernatants were used for extraction of sesquiterpenes, while pellets were re-suspended in 500 µL of sterile water.
6. Cells were transferred to a sterile microcentrifuge tubes and centrifuged for 30 sec at 12000 rpm in the microcentrifuge. The supernatant of all samples were removed and the cell pellets were stored at –80°C until further use/ for next step.

### 1.4 Identification of Recombinant Fusion Proteins, Extraction and Characterization

#### 1.4.1 Detection of recombinant fusion protein

1. Fresh or frozen cell pellets were re-suspended in 500 µL of yeast breaking buffer (50 mM sodium phosphate, pH 7.4, 1 mM EDTA, 5% glycerol, 1 mM PMSF).
2. Centrifuge the cells at 1,500 × *g* for 5 minutes at 4°C. Supernatant were removed and cells re-suspended in a volume of breaking buffer (Set $OD_{600}$ of 50–100).
3. Equal volume of acid-washed glass beads (0.4–0.6 mm size) were added. Mixtures were vortex for 30 seconds, followed by 30 seconds on ice. Four times

repeated this step for lyse the cells. Cells were lysed by shear force. Lysis of cells were checked by taking a small aliquot and observed under the optical microscope (Leica DM2500).

4. Centrifuge the samples at high speed for 10 min and supernatant was removed and transferred to a fresh microcentrifuge tube.
5. Samples were checked by running in 10 % SDS-PAGE gel electrophoresis.

### 1.4.2 Western blotting for *his*-tag proteins

1. Gel was removed from electrophoresis apparatus and transfer the gel on nitrocellulose or PVDF membrane. PVDF membrane was activated by keeping in methanol for 1 min and rinsed with transfer buffer (Tris-base/glycine in 20% MeOH) before preparing the stack. Transfer all the protein samples to the membrane checked by using the Ponceau S staining before the blocking step.
2. The membrane was blocked for 1 h at RT or overnight at 4°C by using blocking buffer (3% BSA).
3. Membrane was incubated with primary antibody Anti-His (Invitrogen 1:2000 dilutions in 3 % BSA) in blocking buffer. Kept for 1 h on rocker at RT.
4. Primary $1^{o}$ Ab was removed and wash of PBS-T (PBS-0.1% Tween) gave for 3 times.
5. The membrane was washed three times by PBS for 5 min each. Further the membrane was incubated with $2^{o}$ Ab (secondary antibody) in blocking buffer at room temperature for 1 h on rocker.
6. The $2^{o}$ Ab was discarded and the membrane was washed three times with PBS-T, followed by 5 times with PBS for 5 min.
7. For signal development, chemiluminescent dye (luminal + hydrogen peroxide 1:1 ratio) was added. Excess reagent was removed and the membrane was covered in transparent plastic wrap.
8. Image was acquired by using darkroom development techniques for chemi-luminescence, or normal image scanning methods for colorimetric detection.

### 1.4.3 Extraction of sesquiterpenes from expressed *S. cerevisiae* broth (pellet/supernatant)

1. Expressed culture was centrifuged at 5000×g for 10 min at RT. Supernatant and pellet were collected.
2. The sesquiterpene products were extracted by using distilled pet ether solvent (3x). The extracts were concentrated by vacuum evaporator. The products were analyzed and quantified by GC-MS and Farnesol as a standard.
3. Pellet was disturbed by using saponification method. Pellet was suspended in (1:5 dilution; 1 g : 5 mL solution) saponification solution (10 % of KOH solution in 80% of EtOH). Vortex it, 1-2 mL hexane was added, and keep at 72 °C for 2 h. Vortex it in each 15 min of time interval.
4. Volatile compounds were extracted by using hexane or petroleum ether solvent (3x wash). The extracts were concentrated by vacuum evaporator. The products were analyzed by GC-MS.

### 1.4.4 Characterization of sesquiterpenes from expressed crude *S. cerevisiae* supernatant

For the characterization recombinant fusion enzyme FPPS-ECS from yeast, the pellet was lysed by acid washed glass beads and yeast breaking buffer, the supernatant of lysed pellet was used for the characterization of fusion enzyme. *S. cerevisiae* did not have *epi*-cedrol synthase gene in their genome, therefore the enzyme assay was kept in this, enzyme activity was tested by using a only substrate FPP for the cyclization into final product *epi*-cedrol. A 500 µL enzymatic reaction mixture containing assay buffer pH 8.5 (25 mM Tris-HCl, 5 mM DTT, 10 mM $MgCl_2$, 10% glycerol), 100 µL crude fusion enzyme, 100 µM FPP was used, this enzyme assay was incubated in shaker bath incubator (Spire, India) at 30 ºC for 2 h at 70 rpm. The enzymatic reaction was stopped by an addition of 10 µl absolute ethanol (95%) followed by vortexing for 30s. The volatile products were extracted with hexane (3× 0.5 mL), The organic layers containing sesquiterpene products were dried over anhydrous $Na_2SO_4$ and reduced to ~50 µL with a stream of dry nitrogen. The samples were identified by GC-MS analysis by using Agilent Technology 5975-7890 GC-MS system with a HP-5MS capillary column (30m x 0.250 mm x 0.25 µ coating of 5% phenyl methyl siloxane). Injections

were made cool on-column at 40 ºC with oven programming from 40 °C (50 °C/min) to 50 °C (5-min hold), then 10 °C/min to 250 °C, then 50 ºC/min to 300 ºC. Separations were made under a constant flow of 1 ml He/min. Mass spectral data were collected at 70 eV and analysed by using MSD Chem station software.

## 2. Results and discussion

### 2.1 Cloning and expression of fusion proteins in *S. cerevisiae* INV*Sc* 1

For expression of recombinant fused enzymes, the yeast *S. cerevisiae* INV*Sc* 1 cells and pYES2/CT plasmid were used. Sequential cloning of both fusion enzymes *i.e.* FPPS-ECS and FPPS-SS were done in above plasmid. Cloning of fusion enzyme in yeast plasmid showed in **Fig. 1** and **Fig. 2**. All the positive colonies were confirmed by colony PCR by T7 FR and gene specific reverse primer for *FPPS* and gene specific forward and Cyc1 reverse primers for *ECS* and *SS*. Plasmids were isolated from positive clones and again re-confirmed by restriction digestion and sequencing. For the good expression, in yeast small signaling or consensus sequence was added, where the ATG translation initiation codon (AACACA**ATG**TCT) sequences was added in 5' terminal of *FPPS* gene. Two constructs were cloned with linker at 3' end of FPPS.

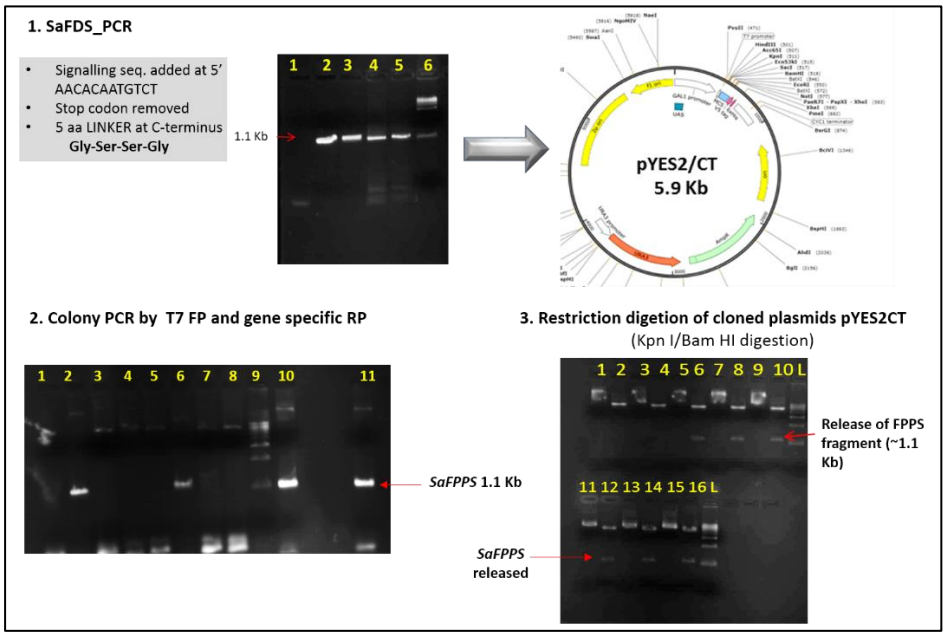


**Figure 1.** Cloning of *Sa*FPPS into pYES2/CT.

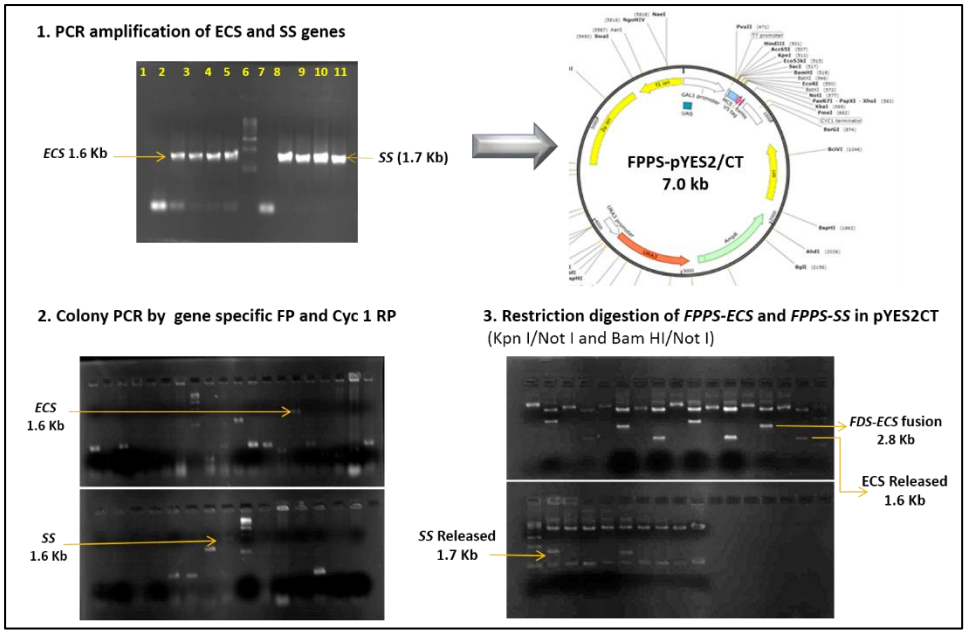


**Figure 2.** Cloning of *AaECS* and *SaSS* into FPPS-pYES2/CT.

Competent cells of yeast *S. cerevisiae* INV*Sc* 1 was prepared as per mentioned protocol. This cells usually used fresh in each expression. Cloned fusion plasmids FPPS-ECS-pYES2/CT and FPPS-SS-pYES2/CT were transformed and induced by using 2 % galactose. In the expression of *S. cerevisiae* INV*Sc* 1, GAL 1 promoter was used in the plasmid which was repressed in the presence of glucose as per reports (West Jr et al., 1984). Transcription can be induced by only removing glucose and adding galactose as a carbon source (Giniger et al., 1985). Maintaining these cells in glucose containing SC medium, gave the most complete repression and the lowest basal transcription of the GAL1 promoter. Transferring these cells from glucose- to galactose-CSM-URA containing medium causes the GAL1 promoter to become de-repressed and allows transcription to be induced. Here, we had initially used glucose, later we used raffinose as a carbon source instead of glucose. Because the presence of raffinose does not repress or induce transcription from the GAL1 promoter. Addition of galactose to the medium induces transcription from the GAL1 promoter even in the presence of raffinose. The media separation step was excluded. We observed that the induction of the GAL1 promoter by galactose was more rapid in the yeast cells maintained in raffinose, when compared to those maintained in glucose. Only thing was the glucose was cost effective than raffinose.

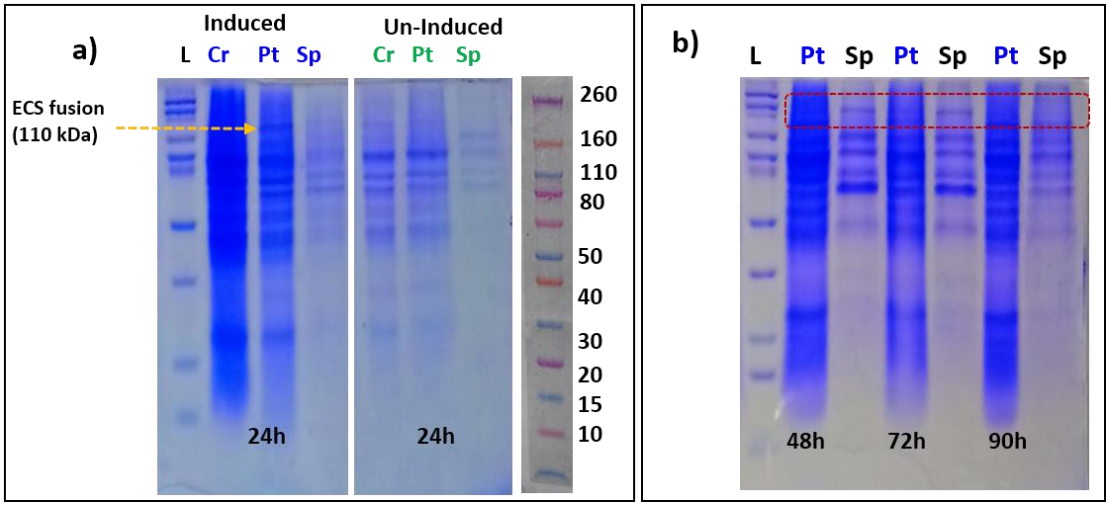


**Figure 3.** SDS-PAGE image of expressed induced and un-induced (a) with galactose fusion enzymes in *S. cerevisiae* INV*Sc* 1 cells after a. 24 h and b. after 48 h, 72 h and 90 h of post induction. Where, **L**: Novex pre-stained protein ladder, **Cr:** Crude lysed fraction, **Pt**: Pellet fraction, **Sp**: Supernatant fraction.

After induction with filter sterilized 2% galactose, yeast samples were collected after 24, 48, 72 and 90 h. Cells were lysed in breaking buffer as mentioned in materials and method section, after lysis, cell fractions were loaded on to 10 % SDS-PAGE gel. The expression was observed in galactose induced yeast cells as shown in **Fig 3**. There no much difference were seen in the expression of ECS fusion proteins after longer incubation. Therefore, we have expression yeast cells only for 24 h of post induction at 30 ºC.

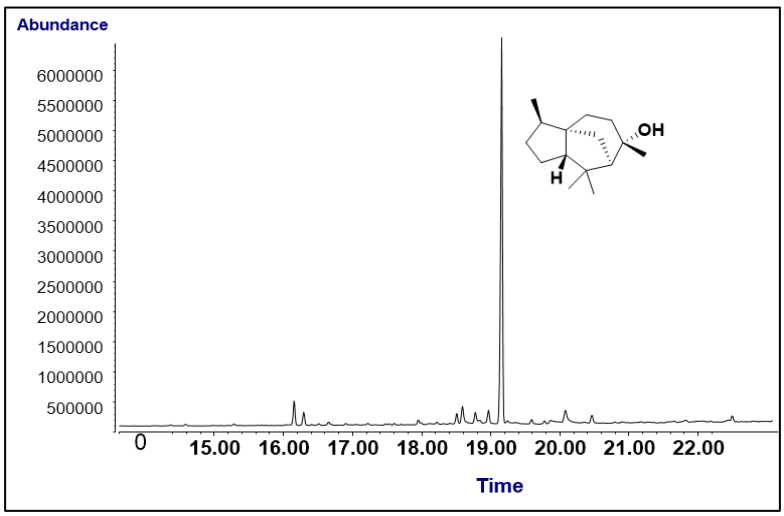


**Figure 4.** GC-MS analysis of recombinant yeast extracts showing *epi*-cedrol in enzyme assay with FPP as a substrate.

## 2.2 Characterization of fusion protein

Recombinant *S. cerevisiae* INV*Sc* 1, expressed in CSM-URA selective medium with galactose. Pellet was separated and lysed as per mentioned protocol, supernatant was collected and crude enzyme used for the characterization of expression of fusion enzymes. After extraction with hexane, the product was analyzed in Agilent GC-MS as per mentioned GC method/program. *Epi*-cedrol peak was seen at 19.18 min retention time (retention time was changed due to the GC-MS instrument change) and which was also correlates with standard enzymatic assay product *epi*-cedrol as shown in **Fig 4**. This results showed that the recombinant *S. cerevisiae* INV*Sc* 1 expressed FPPS-ECS-fusion enzyme which has activity to produced epi-cedrol from IPP and DMAPP a basic building block of sesquiterpene isoprenoids synthesis.

## 2.3 Production and extraction of fusion enzyme

*S. cerevisiae* have the precursors of isoprenoids biosynthesis by MVA pathway and they are naturally synthesized by the sterol biosynthetic pathway, which helped in the improvement of plant terpenoid production (Gonzalez et al., 2017). MVA pathway has been connected to central carbon metabolism via acetyl-CoA, ATP, and NAD(P)H which are the final metabolites of the glycolysis pathway. The generation of final IPP and DMAPP has been sequentially carried out by six terpene synthase enzymes (ERG10, ERG13, HMG1, ERG12, EGR8, ERG19) from two molecules of acetyl-CoA (discussed in chapter 1). For the synthesis of FPP, ERG20 enzymes are in steroid biosynthetic pathway in yeast. Apart from this we have fused sesquiterpene ECS with FPP synthase (FPPS) from *S. album* plant sp. to get maximum flux of FPP in the cell, which enhanced the production of final product *epi*-cedrol.

*Epi*-cedrol was extracted from the supernatant of recombinant *S. cerevisiae* INV*Sc* 1 culture (500 mL) with distilled pet ether with 3 times (300 mL×3). Extracted volatile terpenes were concentrated on rota evaporator (Hedolf, Germany) and analyzed by GC-MS as per mentioned method. We have observed *epi*-cedrol along with many volatile compounds. We have extracted chromatogram on the basis of MSD-Chem software as showing in **Fig. 5**. The amount of epi-cedrol was not observed as good as *epi*-cedrol from the *E. coli*. But the product quantity was much better than previously reported *epi*-cedrol from yeast (Jackson et al., 2003) because of the fusion expression

in the cell. In case of FPPS-SS fusion construct, we have not observed santalene sesquiterpenes in the broth extraction as well as in the enzymatic assay.

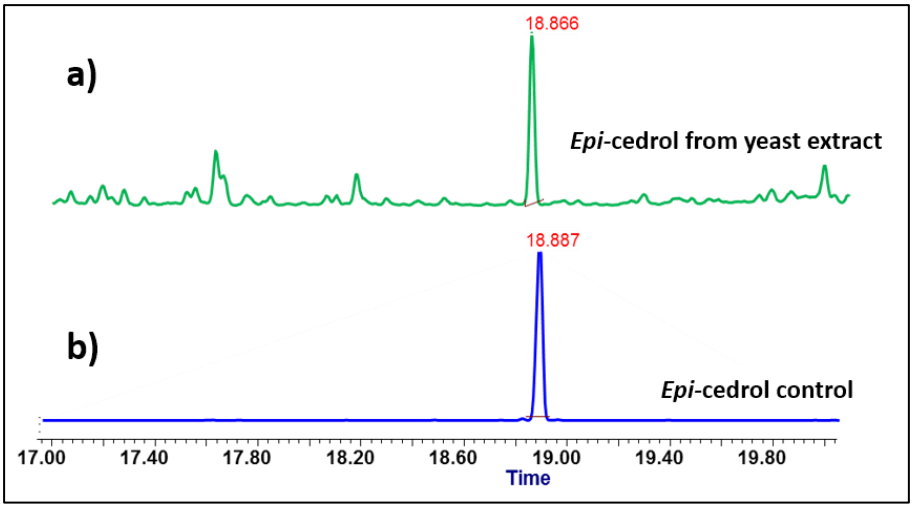


**Figure 5.** a) GC-MS analysis of *epi*-cedrol (18.86 min $R_t$) extracted from recombinant yeast. b) Positive control of e*pi*-cedrol (18.88 $R_t$).

# Section 2C

# Structural and docking study of fusion enzymes

## 1. Protein Modelling and docking simulations

### 1.1 Methodology

Homology modeling of FPPS-ECS and FPPS-SS fusion proteins were carried out utilizing the Swiss Model automated comparative protein modeling server (http://swissmodel.expasy.org) (Arnold et al., 2006). According to the amino acid sequence homology, FPPS (*AsFPPS*) from *A. spiciformis* (PDB ID: 4KK2, sequence identity: 78.87 %) for *SaFPPS*; α-Bisabolol synthase (*AaBOS*) from *A. annua* (PDB ID.: 4GAX, sequence identity: 53.65 %) for *AaECS*, and (+)-Limonene Synthase from *Citrus sinensis* (PDB ID.: 5UV0, Sequence identity: 45.49 %) for *SaSS* were selected as potential structural templates to obtain the homology based structural models. The three-dimensional (3D) structural models of both the fusion enzyme complex with linker incorporation were built up using the web-based I-TASSER server (Yang et al., 2014). I-TASSER server gives the C-score which is a confidence score for estimating the quality of predicted models by I-TASSER and calculated based on the significance of threading template alignments and the convergence parameters of the structure assembly simulations. It also provides TM-score and RMSD values, which are known standards for measuring the structural similarity between two structures which are usually used to measure the accuracy of structure modeling when the native structure is known. The server predicted the cluster density, which is defined as the number of structure decoys at a unit space in the SPICKER cluster. A higher cluster density means the structure occurs more often in the simulation trajectory and, therefore, signifies a better quality model (Yang et al., 2014). Molecular graphics software program PyMOL 2.0.0 was used for illustration (DeLano, 2002).

For docking simulations, initially the substrate binding pockets in FPPS-ECS and FPPS-SS fusion protein models were identified using CASTp, Pocket-Finder and QSite Finder. Further, docking simulations were carried using AutoDock Vina (v4.2) with all the three substrates (IPP, DMAPP and FPP) taken one at a time with grid box spacing at 1 Å. The docking parameters were set with grid box size of (64 x84 x 110), (84 x 84 x 90), and center at x = 87.528, y = 82.500, z = 83.944, and x = 84.415, y = 91.917, z = 78.889 for FPPS-ECS and FPPS-SS, respectively. The ligand protein

interactions were analyzed and visualized using Discovery Studio 4.5 Visualizer and Pymol (BIOvIA, 2015; DeLano, 2002).

## 2. Results and Discussion

The FPPS-ECS and FPPS-SS fusion protein models were predicted by I-TASSER server and gave a C-score of -1.31 and -1.15. In order to gain insight in the fusion proteins and substrate binding, I-TASSER predicted protein model was docked with various substrate by AutoDock Vina. The structures of fusion proteins (FPPS-ECS & FPPS-SS), and individual proteins (FPPS, ECS and SS), homology based models were predicted.

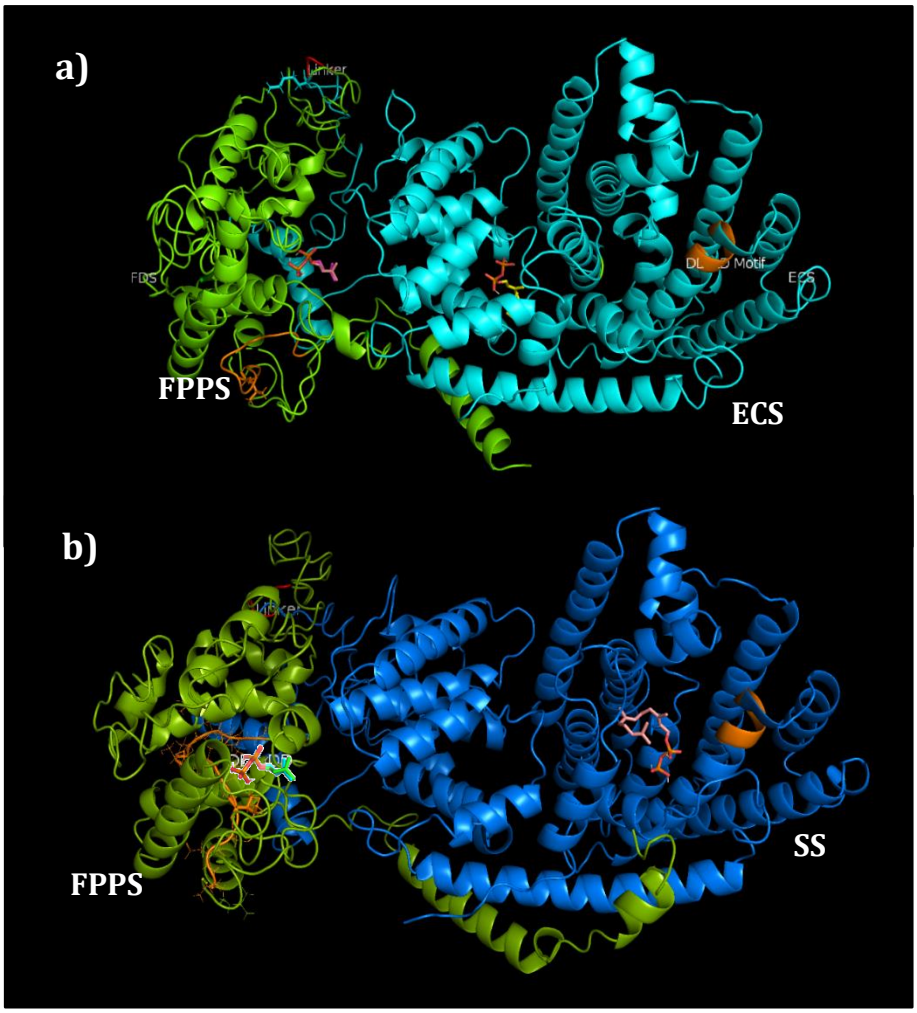


**Figure 1.** Docking of a) FPPS-ECS and b) FPPS-SS with IPP, DMAPP and FPP. Models were made by using I-TASSER server. FPPS displayed in green and its linker between two proteins was depicted in red. ECS and SS were displayed in cyan and blue

colour, respectively. All the catalytic DDxxD motifs present in the proteins displayed in orange.

FPPS were identified using co-ordinates of FPPS from *Artemisia spiciformis* and the sequence identity was 78.87%. In the current study out of the three proteins**,** the crystal structure have been resolved only for plant FPPS (Chan et al., 2017), however *epi*-cedrol synthase structure have been predicted based on homology modelling. These structural models would help to gain insight in the role of synthetic linker in protein structure and function. Terpene synthases are a diverse class of enzyme family with their specificity and activity being highly dependent on small number of amino acids present inside or near the active site cleft. To further understand cyclization of *epi*-cedrol and santalens, the amino acid residues present in and around the active site were identified using the co-ordinates of α-Bisabolol synthase for *epi*-cedrol and (+)-Limonene Synthase (PDB ID.: 5UV0) for santalene as a template with Swiss Modeling server, having a 53.65 % and 45.49 % of sequence similarity of the amino acids, respectively. Numerous studies have revealed that even though terpene synthases vary in sequence similarity but their active sites are highly conserved (Degenhardt et al., 2009). Recently reported FPPS protein sequence has seven highly conserved regions (region I-VII) present, from which Region II (**L**, X4LDDxxDxxxxRRG) and VI (GxxFQxxDDxxD....GK) are the most significant regions due to aspartate-rich motifs and are involved in binding of both homo-allylic (IPP) and allylic diphosphate substrates (GPP and DMAPP) and the divalent $Mg^{2+}$ metal binding at $G_{104}$ and $W_{108}$ (Chan et al., 2017; Shrivastava, 2014). FPPS are joined with a flexible linker ($G_{343}S_{344}G_{345}G_{346}S_{347}$) as shown in **Fig. 1** (red colour) with ECS (**Fig. 1a)** and SS (**Fig. 1b)**. In an analysis of ECS structure, the enzyme catalyses the formation of multiple products including two by-products, from a single substrate because of the consequences of the highly reactive series of carbocationic intermediates formed during the enzyme assay (Mercke et al., 1999). FPP was synthesized from the active pocket of FPPS in fusion protein and easily channelled to an α-helical loop over the active site that protects the carbocation from the water (Shinde et al., 2016). This loop helps the hydrophobic interactions between $W_{273}$ and $Y_{527}$ (Mercke et al., 1999; Shrivastava, 2014) These are a conserved loop in the fusion of ECS as $F_{872}$ and $W_{617}$. Loop was closure together by $R_{606}$ and $R_{786}$ near to each other. This possibly assists in ionization

of the substrate diphosphate ester and helps to move diphosphate anion away from the generating carbocation. The common aspartate-rich motif DDxxDD is located at 642-646 positions. DDxxDD motif has showed in orange colour (**Fig. 1**). The Estimated TM-score, RMSD and cluster density for FPPS-ECS fusion are 0.55±0.15, 11.8± 4.5Å and 0.0473 respectively, predicted by I-TASSER server as details are mentioned in methodology section.

In another FPPS-SS fusion model with the same FPPS sequences, SS structure entirely consists of α-helices connected by small loops and organized into two domains ($NH_2$ terminal domain and COOH terminal domain). The active site of SS was identified by the presence of same highly conserved DDxxD motif as in ECS located in the upper edge of the C-terminal helical barrel domain (**Fig. 1**) (Shrivastava, 2014). This is involved in substrate binding whereas, opposite wall of the active site is composed of highly conserved residues (D/N)Dxx(S/T)xxxE which are involved in divalent metal ion, $Mg^{2+}$ binding (Rynkiewicz et al., 2001). Active site cavity of SS is flanked by six α-helices connected with small loops, making the active site cavity 14Å wide and 20Å deep. Bottom of the active site cavity is mainly composed of aromatic and aliphatic hydrophobic residues such as $W_{639}$, $F_{884}$, $F_{891}$, $Y_{885}$, $I_{768}$, $L_{773}$ which help in giving shape to the active site pocket for the binding of substrate FPP in a correct orientation for cyclization, whereas top site of the pocket is mainly composed of polar amino acids such as, $N_{809}$, $T_{813}$, $E_{817}$, $R_{806}$, $R_{820}$, $K_{820}$, $D_{667}$, $D_{668}$ and thought to be involved in binding the phosphate end of the substrate (**Fig. 1b**) (Shrivastava, 2014). For FPPS-SS fusion protein model estimated TM-score are 0.57±0.15 and RMSD are 11.5±4.5Å. Despite the low level of sequence similarity, the majority of the active site residues are common in SS model and 5UV0 structure whose functions are assigned.

| Substrates | | FPPS | ECS | SS | FPPS-SS fusion | FPPS-ECS fusion |
|---|---|---|---|---|---|---|
| 1. | IPP | -5.6 | - | - | -6.0 | -6.2 kcal/mol |
| 2. | DMAPP | -5.6 | - | - | 5.7 | -6.2 kcal /mol |
| 3. | FPP | - | -7.0 | -6.5 | -6.8 | -7.2 kcal/mol |

**Table 1**. Binding energies between substrates and enzymes in kcal/mol (FPPS, ECS and FPPS-ECS fusion).

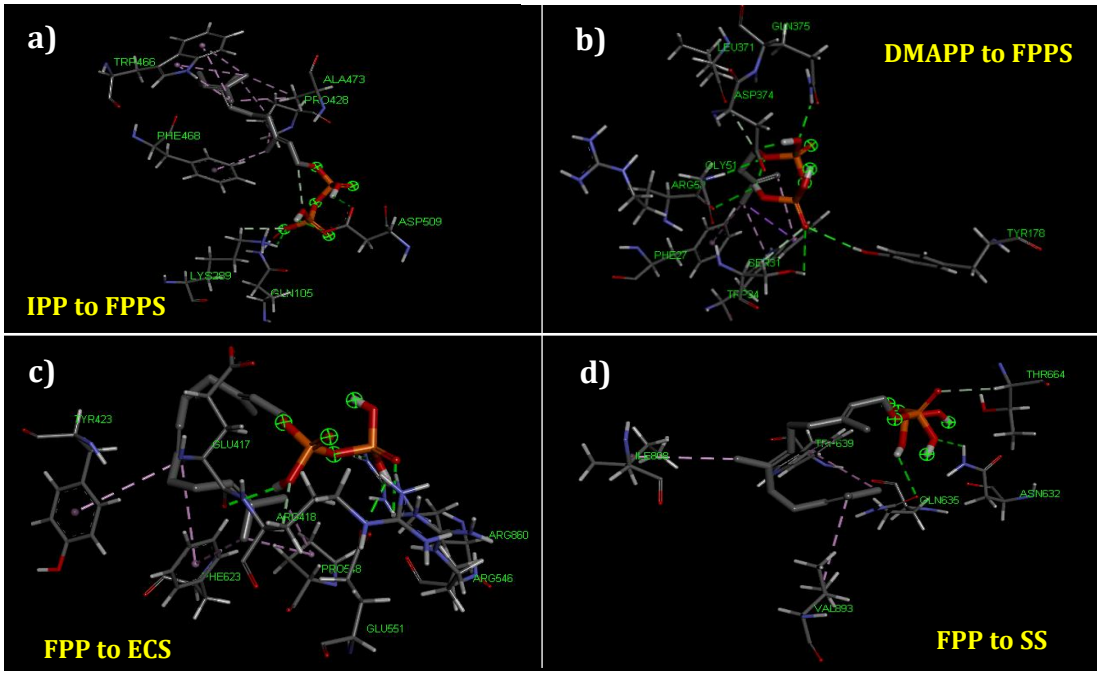


**Figure 2.** Amino acids of fusion proteins interactions to substrate; a. IPP to FPPS; b. DMAPP to FPPS; c. FPP to ECS; and d. FPP to SS.

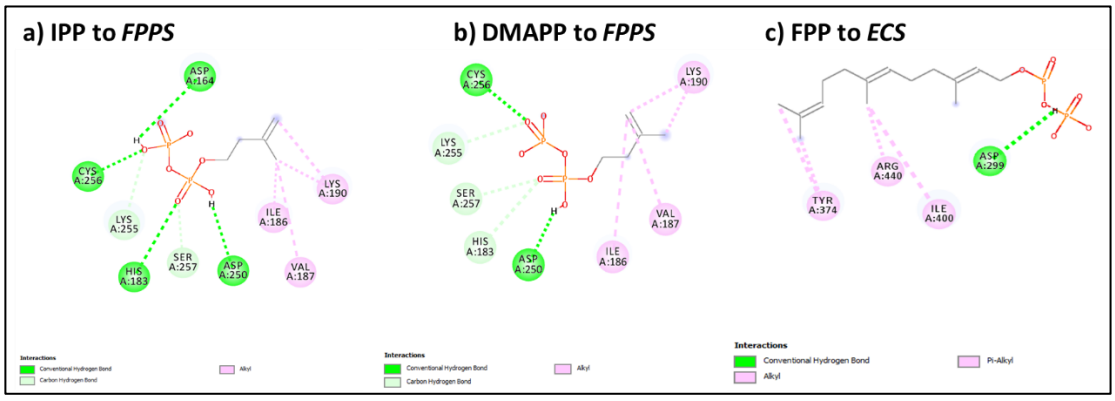


**Figure 3.** Amino acids of single protein interactions to substrate; a. IPP to FPPS; b. DMAPP to FPPS; and c. FPP to ECS. (FPP to single SS was not done).

In docking of both fusion proteins FPPS-ECS and FPPS-SS, total 90 poses were generated for each ligand (IPP, DMAPP and FPP) with protein and further analyzed according to minimum binding energy. The binding energies for fusion enzymes for substrates are mentioned in **Table 1**. This results indicated that the fusion protein bind to the substrates at a lower binding energy in comparison to their respective individual

counterparts. This result is in concurrence with the experimental data, where the *Km* of FPPS-ECS Fusion enzyme for IPP was 4.71 whereas Km of mixed enzymes together for IPP was 5.64 (**Section 2a, Table 3**). This showed that individual enzymes having less binding energies towards respective substrates. The interactions of amino acids were also changed in case of individual enzymes (individual interactions shown in **Fig. 2**). Finally, the results, indicate that the fusion of two enzymes may have led to their active pockets closing together and helped in the substrate channeling in the fusion enzymes leading to increase in the overall catalytic activity.

## Conclusion

We have successfully constructed two unnatural multifunctional fusions of sesquiterpenoid synthases which produces a higher amount of *epi*-cedrol and santalenes from basic building block of isoprenoid biosynthesis pathway, *i.e* IPP and DMAPP when compared to utilizing two different enzymes together. Both fusion proteins were expressed and characterized in bacteria (*E. coli*) and yeast (*S. cerevisiae*). The results of this study clearly indicate that fusion protein strategy has a promising potential to improve product yield by using all substrates of the sesquiterpenoid pathways in heterologous expression. For the production of *epi*-cedrol, because of higher expression and cell biomass, *E. coli* showed better production than the yeast, *S. cerevisiae* host. Yeast host need further engineering for improvement. The fusion protein products were secreted in growth media indicating that an industrially friendly harvesting system for sesquiterpenes can be developed during downstream processing. It also reduces the time and cost of recombinant protein purification. Structural studies showed that the relative positions to functional domains of the fusion enzyme are greatly significant to the catalytic properties of the fusion enzymatic complex than individual enzymes. Fusion of two enzymes may have led to their active pockets closing together and helped in the substrate channeling effect in the enzymes which leads to increase in the overall catalytic activity.

# Chapter 3
# Stability and Catalytic activity of *epi*-cedrol synthase enzyme in Imidazolium based ionic liquids

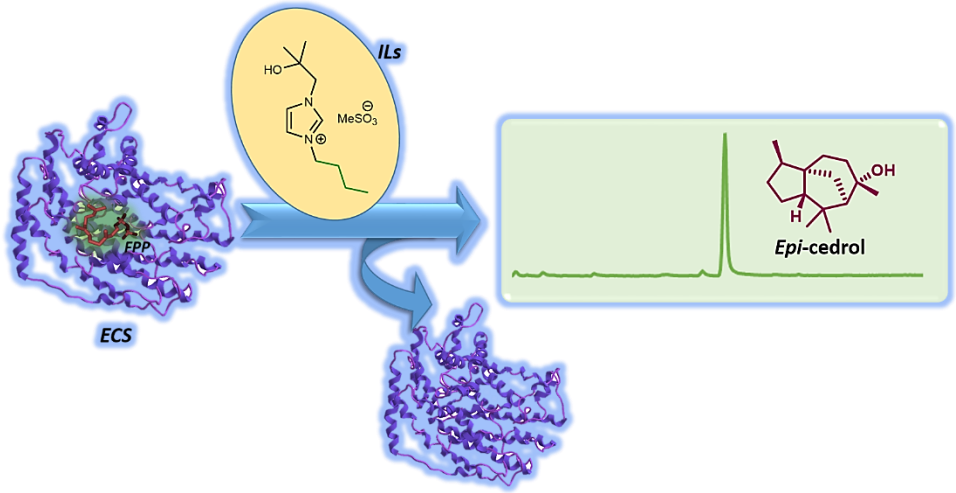

## Abstract

In past decades ionic liquids (ILs) are plays an important role in chemical and biotechnological applications due to their unique and tunable physico-chemical properties. It is used as eco-friendly solvent medium and catalyst in many enzymatic reactions. Terpene cyclases are the key enzymes for the conversion of acyclic intermediate substrate into a complex cyclic isoprenoids/terpenes. Terpene cyclase enzyme such as *epi*-cedrol synthase (ECS) from *Artemisia annua* plant spp. are involved in the biosynthesis of *epi*-cedrol, a sesquiterpenes from farnesyl pyrophosphate (FPP) in aqueous medium. In this study A series of varying alkyl chain length substituted *tert*-BuOH-functionalized-imidazolium mesylate salts [alkyl-$^{t}$OHim][OMs] were synthesized. Initially these imadizolium salts were evaluated for antimicrobial and antibiofilm activity on selected pathogenic microorganisms including bacteria (Gram positive and Gram negative), yeast, and fungi. In that, We observed that the ILs bearing chain lengths lower than the decyl [$C_{10}$-$^{t}$OHim][OMs] length were found to be less effective against most of the tested microorganisms. Further, these ILs were checked for their effect on stability and catalytic activity on terpene synthase ECS enzyme in aqueous medium. Overall, this study revealed that the hexyl and decyl substituted imidazolium ILs [alkyl-$^{t}$OHim][OMs] showed good stability and helped in the enhanced activity when ECS was pre-incubated at various temperature condition. We conclude that the ILs bearing chain lengths higher than the hexyl ($C_6$) length were found to be effective in ECS enzyme activity.

## Introduction

Ionic liquids (ILs) are organic salts, liquid at room temperature with low melting points, (below 100 °C) (Lei et al., 2017; Vekariya, 2017). Over a millions of combinations of cations and anions has been used for the synthesis of an ILs (Venkatraman et al., 2019). They are well known for their unique physico-chemical properties include insignificant vapour pressure, high thermal stability, non-flammability, high ionic conductivity, and biocompability. They are designed for almost all the applications such as in electrochemistry, catalysis, biotechnology etc. (Ghavre et al., 2014; Venkatraman et al., 2019). Imidazolium ILs widely applied in the academic and industry sector as greener solvents or catalyst reactions (Ranke et al., 2004; Shinde et al., 2015). These properties are the main motivating factor behind the vast interest in green chemistry applications (Armand et al., 2009; Marrucho et al., 2014; van Rantwijk and Sheldon, 2007). The tuneability nature of ionic liquids introduces an unparalleled flexibility in the design of reagents for a specific functional role. ILs are often called tailor made solvent or considered "task-specific" due to their possibility to be modified according to the specific required that can result in unique solvent properties, as catalyst and promoter for specific reactions. Over the last decade, there has been increasing developing of numerous task-specific imidazolium-based ionic liquids such as ether, amide, ketone or alcohol functionality (Ghavre et al., 2014; Shinde and Patil, 2014; Xu et al., 2017). These task-specific ionic liquids were applied in a specific reaction, have become an intrigue research area for green impact in various fields (**Fig. 1**).

To date, numerous studies have demonstrated the biological activity of various tailor made ionic liquids against both environmental and health concern microorganisms. This fact has been proven by many toxicological research studies concerning ionic liquids undertaken in the past decade, and the results hopeful in point of clinical applications. The toxicity evaluation of ILs creates possibilities of developing new disinfectants, antiseptics and preservatives. A study of the toxicity and eco-toxicity of these ILs salts yields valuable information for their use as pharmaceuticals as well as impact on the environment (Elliott et al., 2009; Ranke et al., 2004; Wells and Coombe, 2006). Task-specific liquid containing an ester functional

group with alkyl side chain possesses higher adsorption efficiency compared to the simple alkyl chain containing ILs due to enhance the hydrophobicity of the amphiphilic nature of cation (Pernak et al., 2003) (**Fig. 2**). Similarly the antimicrobial activity of imidazolium ionic liquid bearing with various alkoxy methyl side chain, lactate anion against clinically important pathogenic fungi and bacteria (Gore et al., 2013; Swatloski et al., 2003) Recently, the ionic liquid of sulfonate anion exhibited the potential application in drug delivery and as active pharmaceutical ingredients (APIs). Tuning of Lidocaine and Ranitidine drug with docusate (sulfonate dioctylsuccinate) anion prepared ILs significantly enhance the biological properties, resulted in longer pain relief and slow-release mechanism of drug delivery (Marrucho et al., 2014; Mitkare et al., 2013).

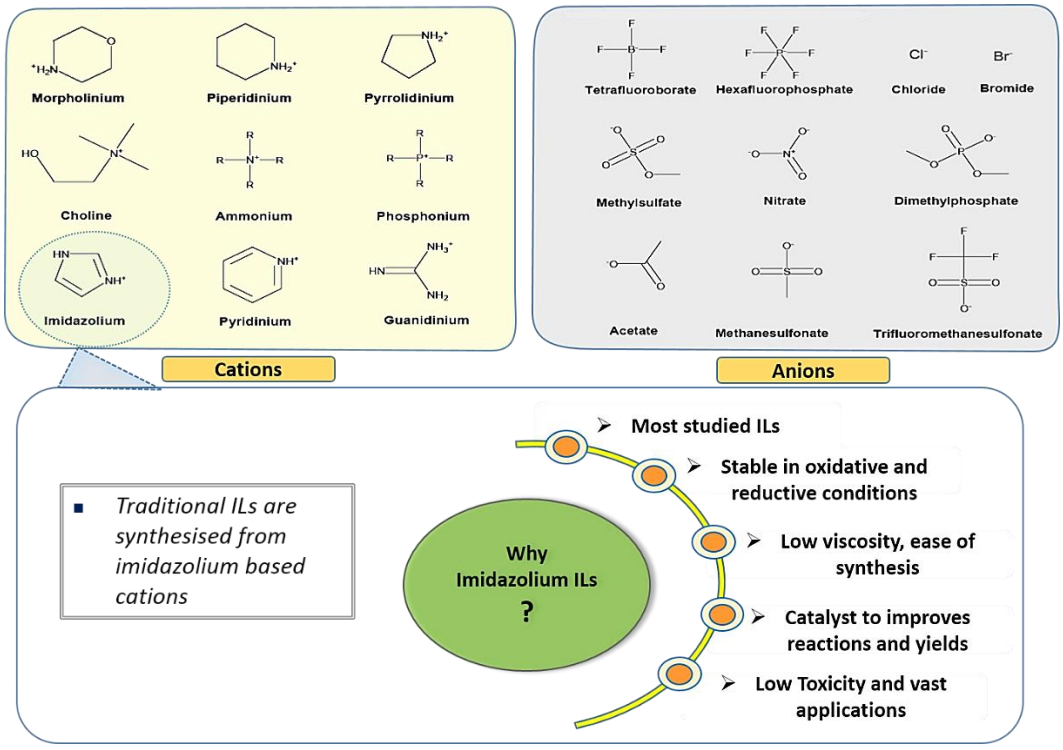


**Figure 1.** Cations and anions used in synthesis of ILs and importance of imidazolium ILs.

The microbial biofilm represent a major survival mechanism for microbial populations and are the cause of a host of industrially and clinically relevant complications specially related to medical devices and microbial-influenced bio-corrosion (Dean et al., 2009). The pathogenic bacterial cells when stick to each other on a surface and forming a self-produced matrix of extracellular polymeric substance,

collectively known as biofilm. Biofilm communities generally exhibit considerable tolerance or resistance to antibiotics and antimicrobial/biocidal agents compared to planktonic bacteria of the same species. NIH already estimated that up to 80% of all chronic human infections are biofilm mediated and that 99.9% of bacteria in aquatic ecosystems live as biofilm communities. Moreover, the IL containing more than ten carbons in the alkyl group exhibiting highest antibiofilm activity (Carson et al., 2009; Lellouche et al., 2009; Nobile and Johnson, 2015).

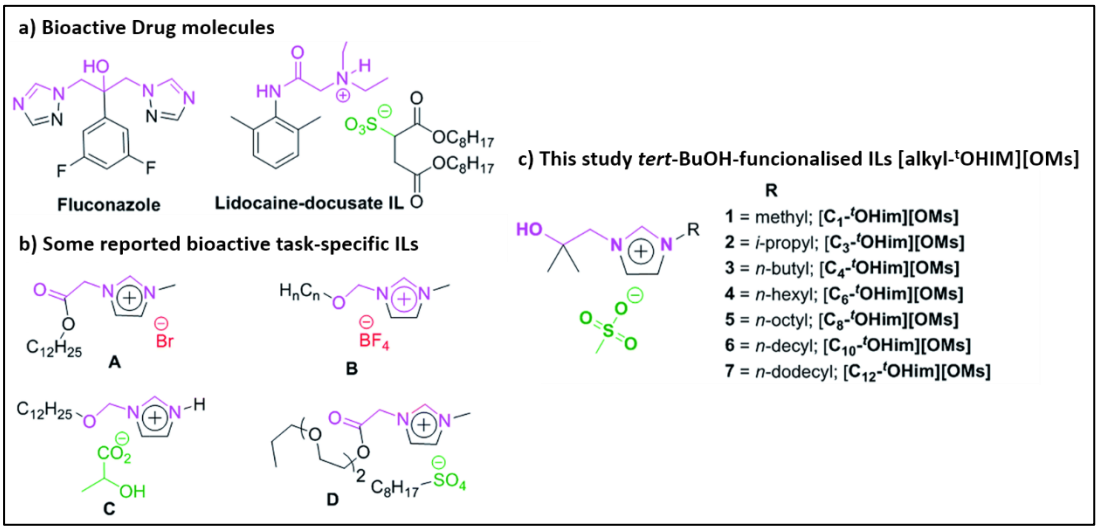


**Figure 2.** Some examples of previously reported bioactive compounds (drugs) (a), and ILs (b) with our newly designed imidazolium ILs (c).

Recently, these imidazolium based ILs have been gained tremendous focus in enzyme biotechnology as catalysts particularly for the enhancement of stabilization of proteins and enzymes (Bisht et al., 2016; Feder-Kubis and Bryjak, 2013; Zhao et al., 2019). Many enzymatic reactions have been carried out in neat ILs and solutions. It includes various hydrolases (e.g. lipases, β-glycosidase, thermolysin, lysozyme, cellulases and proteases etc.), oxidoreductases (e.g. horseradish peroxidase, alcohol dehydrogenase, lignin peroxidase and laccase), lyases (e.g. oxynitrilase), and whole cells (Brogan et al., 2018; van Rantwijk and Sheldon, 2007). Enzyme stability and activity are the main factor for any production of desired industrial products. To improve the stability and activity of enzymes various methods have been used like immobilization, IL-microemulsion, IL coating and the enzyme specific compatible design of ILs (Kumar et al., 2017; Sivapragasam et al., 2016; Solhtalab et al., 2015).

Several research groups have highlighted some important properties, mechanistic overviews on enzyme-ILs behaviours included, hydrogen-bond (H-bond) basicity and nucleophilicity of anions, polarity, Hofmeister series, hydrophobicity, and ILs viscosity, etc. (Paul and Fernández, 2016; Xu et al., 2018; Yang, 2009; Zhao, 2012)**.** Various applications of ILs in biological fields are depicted in **Fig. 3**.

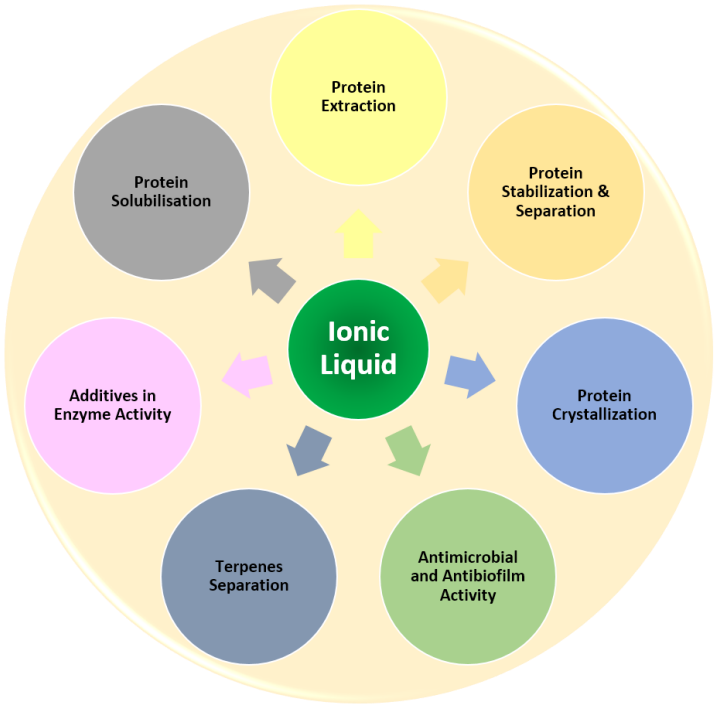


**Figure 3.** Applications of ILs in various biological sectors.

The biocatalyst, enzymes, such as terpene synthase are involved in the cyclization of acyclic isoprene's into chemically and structurally diverse terpenoids. They are mostly involved in primary as well as secondary metabolism in living organisms. These terpenes are applied in various sectors such as chemical, flavour, fragrance, pharmaceutical, nutraceutical industries. Stability and significant catalytic activity of these terpene synthases aiming to get higher production of terpenes at scale up. *Epi*-cedrol synthase (ECS, *Genbank* No. AF157059) was isolated from *Artemisia annua* plant spp. is a sesquiterpene synthase comes under the class of lyses enzymes (EC 4.2.3.39) which catalyses acyclic farnesyl pyrophosphate ($C_{15}$, FPP) into 8-*epi*-cedrol (Navale et al., 2019; Shinde et al., 2016). It also produces monoterpenes from geranyl pyrophosphate ($C_{10}$, GPP). Till date the scale up of *epi*-cedrol and its

applications are remains unexplored. Its precursors like cedrenes, used in jet fuel (Harrison and Harvey, 2017) and cedrol are widely applied in pharmaceutical industries as sedative, anti-inflammatory, and cytotoxic activities (Bhatia et al., 2008; Zhang et al., 2016).

Our research group are interested to continue in developing greener protocols by using IL and task-specific ILs (**Fig. 2c**) in various nucleophilic substitution reactions. We designed a t*ert*-BuOH-functionalized ILs for various applications in organic synthesis, catalysis and biological fields (Navale et al., 2015b; Shinde et al., 2008; Shinde et al., 2015; Shinde and Patil, 2014). In this chapter, *section A*, as per environmental pollution and health concern, the novel designed ionic liquids has to be thoroughly evaluated the toxicity before their potential biological applications. We have evaluated the antimicrobial and antibiofilm activities of a series of *tert*-BuOH group functionalized ionic liquids having methyl ($C_1$), isopropyl ($C_3$), *n*-butyl ($C_4$), *n*-hexyl ($C_6$), *n*-octyl ($C_8$), *n*-decyl ($C_{10}$), n-dodeyl ($C_{12}$) alkyl chains against a panel of clinically revelant pathogens *viz. Staphylococcus epidermidis, Staphylococcus aureus, Salmonella typhimurium, Vibrio fischeri, Fusarium moniliforme, Fusarium proliferatum and Candida albicans*. This is also the first assessment of the antimicrobial and antibioflim efficacy of *tert*-alcohol functionalized-imidazolium cation with methylsulfonate counterion ILs. In *section B,* we have checked the stability and catalytic efficiency of sesquiterpene synthase *epi*-cedrol synthase in presence *tert*-BuOH functionalised imidazolium ILs [alkyl-$^t$OHim][OMs] except ILs with *n*-dodecyl ($C_{12}$) alkyl chains. As per our knowledge, this is first time study on stability and catalytic study of terpene synthase enzyme in any ILs.

## Materials, Reagents and Microbial Strains

- Imidazole (Sigma-Aldrich)
- Dimethyloxirane (Merck)
- Acetonitrile (Fisher Scientific, India)
- Methyl methanesulfonate (Sigma-Aldrich)
- Diethyl ether (Fisher Scientific, India)
- D-Chloroform (Sigma-Aldrich)
- D-methanol (Sigma-Aldrich)
- Goat blood/erythrocytes (dpt. of Microbiology, SPPU, Pune)
- Luria Bertani Broth/Agar (Himedia, India)
- Tripticase Soya broth (Hi-media, India)
- Potato dextrose broth (Himedia, India)
- MGYP (Malt extract-Glucose-Yeast extarct Peptone) medium (See appendix)
- Muller Hington (MH) broth (Himedia, India)
- Nuclease Free Water (Himedia, India)
- Phosphate buffer saline (pH 7.6)
- Fluconazole (Himedia, India)
- Novex pre-stained protein ladder (Invitrogen-Thermo fischer)
- Farnesyl diphosphate (FPP)
- Isopropyl thio-β-D-thiogalactopyranoside (IPTG) Sigma-Aldrich
- Antibiotics (*viz.* Kanamycin, Chloramphenicol) Sigma-Aldrich
- Luria Bertani Broth/Agar (Himedia, India)
- Terrific Broth (TB) (Himedia, India)
- Muller Hington (MH) broth (Himedia, India)
- Nuclease Free Water (Himedia, India)
- Tris-HCl (Himedia, India)
- Glycine (Sigma-Aldrich)
- Ammonium bicarbonate (Himedia, India)
- Dithiothreitol, DTT (Sigma-Aldrich)
- CHAPS (Himedia, India)

- Phenyl-methyl-sulphonyl-fluoride (PMSF) (Himedia, India)
- Glycerol (Himedia, India)
- Acetic acid (Fisher Scientific)
- Sodium hydroxide (Himedia, India)
- Magnesium chloride (Merck, India)
- Manganese chloride (Merck, India)
- Zinc chloride (Merck, India)
- Cupric chloride (Merck, India)
- Nickel Chloride (Merck, India)
- Cobalt chloride (Merck, India)
- 200-mesh copper grids (Tedpella, USA)
- Desalting bag (3-15 kDa)
- Desalting filter column (10 kDa, 30 kDa) (Merck)
- Hexane (Spectrochem Lab)
- $Ni^{+2}$-NTA agarose (Invitrogen-Thermo fischer and Quagen)
- *Epi*-cedrol synthase (ECS) (*GeneBank* No. AF157059) cloned in pET 28a plasmid (synthesized from *Life Technology ,Germany*
- Miniprep Plasmid purification kit (Thermo Fisher Scientific)
- Lysis Buffer **A**: 50 mM Tris pH 7.8, 300 mM NaCl and 10% glycerol, 5 mM imidazole
- Lysis Buffer **B**: 50 mM Phosphate ($Na_2HPO_4$) pH 7.8, 300 mM NaCl and 10% glycerol, 5 mM imidazole
- Lysis Buffer **C**: 50 mM HEPES pH 7.8, 300 mM NaCl and 10% glycerol, 5 mM imidazole
- Wash Buffer **C:** 50 mM HEPES pH 7.8, 300 mM NaCl and 10% glycerol, 35 mM imidazole
- Elution Buffer **C:** 50 mM HEPES pH 7.8, 300 mM NaCl and 10% glycerol, 250 mM imidazole
- Assay Buffer: pH 8.5, 25 mM Tris-HCl, 5 mM DTT, 10 mM $MgCl_2$, 20% glycerol
- **Microbial Strains**

- *E. coli* Strains: Mach1™ $T1^R$, Top10, BL21, rosetta DE3 (Thermo Fisher Scientific)
- Gram Positive bacteria: *Staphylococcus epidermidis* NCIM 2493 (biofilm forming), *Staphylococcus aureus* NCIM 5021,
- Gram negative bacteria: *Salmonella typhimurium* NCIM 2501, *Vibrio fischeri* NCIM 5269,
- Fungi: *Fusarium moniliforme* NCIM 1100, and *Fusarium proliferatum* NCIM 1103
- Yeasts: *Candida albicans* NCIM 3471, *Candida albicans* NCIM 3628

- Flash chromatography was carried out using Merck silica gel 60 (230–400 mesh).
- Analytical thin layer chromatography (TLC) was performed with Merck Silica gel-60, F-254 aluminum-backed plates.
- Visualization on TLC was monitored by UV light
- $^{1}H$ and $^{13}C$ NMR spectra were recorded using Bruker and calibrated using residual un-deuterated solvent or tetra-methylsilane as an internal reference.

# Section 3A

# Synthesis of *tert*-BuOH functionalized ionic liquids and its antimicrobial activity

## 1. Methodology

### 1.1 Synthesis of *ter*-BuOH-functionlized ILs

#### 1.1.1 1-(2-Hydroxy-2-methyl-*n*-propyl)-3-methylimidazolium mesylate ([$C_1$, mim-$^t$OH][OMs], 1)

All the ILs are synthesized as per previous reports from our group (Shinde et al., 2008; Shinde and Patil, 2014) (**Scheme 1**). In a typical experiment, a mixture of imidazole (2.00 g, 29.3 mmol) and dimethyloxirane (2.90 mL, 32.3 mmol) was stirred in reaction vial at 55 ºC for 12 h. The resulting thick liquid was dried under high vacuum at room temperature, which afforded intermediate 1-(2-hydroxy-2-methyl-n-propyl)-3-ethylimidazole dissolved in 20 mL acetonitrile ($CH_3CN$), then methyl methane sulfonate (0.80 mL, 8.8 mmol) was added drop-wise to the solution. The reaction mixture was stirred at 90 ºC for 24 h and evaporated under reduced pressure to remove. The residue was repeatedly washed with diethyl ether (5 mL×15) and dried under high vacuum for 12 h at room temperature to afford 1.17e **1):** $^1$H NMR (chloroform-d, 400 MHz) d 1.19 (s, 6H), 2.74 (s, 3H), 3.97 (s, 3H), 4.25 (s, 2H), 7.32 (s, 1H), 7.41 (s, 1H), 9.51 (s, 1H); $^{13}$C NMR (chloroform-d, 100 MHz) d 26.4, 36.4, 39.6, 59.6, 68.7, 121.8, 123.8, 138.6.

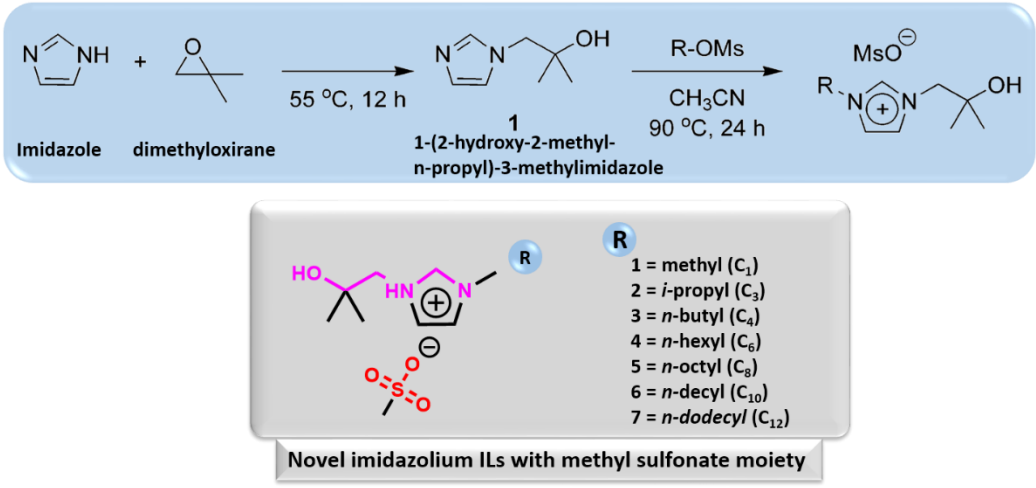


**Scheme 1**. Synthesis of novel[alkyl-$^t$OHim][OMs] ILs.

#### 1.1.2 1-(2-Hydroxy-2-methyl-*n*-propyl)-3-isopropylimidazolium mesylate ([$C_3$, *i*pim$^t$OH] [OMs], 2)

1H NMR ($CDCl_3$, 400 MHz,) G 1.10 (s, 6H) 1.57 (d, $J$ = 6.8 Hz, 6H) 2.75 (s, 3H), 4.28 (s, 2H), 4.57-4.69 (m, 1H), 7.30 (s, 1H), 7.43 (s, 1H), 9.65 (s, $^1$H); $^{13}$C NMR (100 MHz, $CDCl_3$) G 22.8, 26.3, 39.6, 52.8, 59.2, 68.5, 118.7, 124.2, 136.4.

### 1.1.3 1-(2-Hydroxy-2-methyl-*n*-propyl)-3-*n*-butylimidazolium mesylate ([$C_4$-bim-$^t$OH][OMs], 3)

$^1$H NMR (400 MHz, $CDCl_3$) $\delta$ 0.94 (t, $J$ = 7.2 Hz, 3H) 1.20 (s, 6H), 1.32-1.36 (m, 2H), 1.86 (q, $J$ = 7.6, 2H ), 2.74 (s, 3H), 4.22 (t, $J$ = 7.2 Hz, 2H), 4.27 (s, 2H), 7.38 (s, 1H), 7.60 (s, 1), 9.46 (s, 1). $^{13}$C (100 MHz, $CDCl_3$) $\delta$ 13.2, 19.2, 26.2, 31.7, 39.5, 49.4, 59.3, 68.6, 120.7, 124.2, 137.4;

### 1.1.4 1-(2-Hydroxy-2-methyl-*n*-propyl)-3-*n*-hexylimidazolium mesylate ([$C_6$-him-$^t$OH][OMs], 4)

$^1$H NMR (400 MHz, $CDCl_3$) G 0.86 (t, $J$ = 6.4 Hz, 3H), 1.22 (s, 6H), 1.26- 1.39 (m, 6H), 1.88 (q, $J$ = 6.8 Hz, 2H), 2.78 (s, 3H), 4.19 (t, $J$ = 7.2 Hz, 2H), 4.33 (s, 2H), 7.21 (s, 1H), 7.40 (s, 1H), 9.77 (s, 1H); $^{13}$C NMR (100 MHz, $CDCl_3$) G 13.8, 22.3, 25.8, 26.5, 30.0, 31.0, 39.6, 50.1, 59.6, 68.6, 120.2, 123.8, 138.3.

### 1.1.5 1-(2-Hydroxy-2-methyl-*n*-propyl)-3-*n*-octylimadazolium mesylate ([$C_8$, oim-$^t$OH][OMs], 5)

Liquid, $^1$H NMR ($CDCl_3$, 400 MHz) 0.62(t, 3H), 0.938 – 1.07(m, 18H), 1.63(s, 2H), 2.50 (s, 3H), 3.98 (m 2H), 4.04(s 2H), 7.07 (s, 1H), 7.31(s, 1H), 9.24(s, 1H); $^{13}$C NMR(chloroform *d*, 100 MHz), 13.93, 24.44, 22.44, (26.07), 28.78, 28.89, 29.97, 31.53, 39.54, 49.83, 59.42, 68.66, 120.56, 124.18, 137.65. Anal. Calcd for $C_{16}H_{32}N_2O_4S$: C, 55.14; H, 9.26; N, 8.04. Found: C, 55.20; H, 9.29; N, 8.16.

### 1.1.6 1-(2-Hydroxy-2-methyl-*n*-propyl)-3-*n*-decylimadazolium mesylate ([$C_{10}$-dim$^t$OH][OMs], 6)

Liquid, $^1$H NMR ($CDCl_3$, 400 MHz) 0.87(t, 3H), 1.93 – 1.13(m, 21H), 1.88(s, 2H), 2.76 (s, 3H), 4.20(m, 2H), 4.29(s, 2H) 7.29 (s, 1H), 7.41(s, 1H), 9.59(s, 1H); $^{13}$C NMR (chloroform *d*, 100 MHz), 14.04, 22.62, 26.62, 26.43, 28.90, 29.31, 2(29.44), 29.53, 30.01, 31.83, 39.58, 50.00, 59.62, 68.65, 120.40, 123.95, 138.10. Anal. Calcd for $C_{18}H_{36}N_2O_4S$: C, 57.41; H, 9.64; N, 7.44. Found: C, 57.43; H, 9.74; N, 7.61.

### 1.1.7 1-(2-Hydroxy-2-methyl-n-propyl)-3-n-dodecylimadazolium mesylate ([$C_{12}$-ddim$^t$OHim][OMs], 7)

Liquid, $^1$H NMR (chloroform-d, 500 MHz) d 0.85 (t, J ¼ 6.8 Hz, 3H), 1.39–1.23 (m, 24H), 1.90 (bs, 2H), 2.78 (s, 3H), 4.14 (bs, 1H), 4.23 (t, J¼ 7.3 Hz, 2H), 4.32 (s, 2H), 7.36–7.28 (m, 1H), 7.60 (s, 1H), 9.54 (s, 1H); $^{13}$C NMR (chloroform-d, 125 MHz) d 13.8, 22.4, 26.93, 26.17, 28.69, 29.02, 29.08, 29.09, 29.15, 29.29, 29.85, 31.59, 39.47,

49.61, 59.14, 68.53, 120.56, 124.28, 137.27. Anal. calcd for $C_{20}H_{40}N_2O_4S$: C, 59.37; H, 9.97; N, 6.92. Found: C, 59.40; H, 10.03; N, 6.69. Copies of $^{1}H$ and $^{13}C$ NMR spectra are added in the end of the chapters.

## 1.2 Antimicrobial and antibiofilm activity

### 1.2.1 Bacterial Strains and growth media

For antimicrobial activity of ionic liquids the micoorganisms used in this study were Gram positive bacteria (*Staphylococcus epidermidis* NCIM 2493 (biofilm forming), *Staphylococcus aureus* NCIM 5021), Gram negative bacteria (*Salmonella typhimurium* NCIM 2501, *Vibrio fischeri* NCIM 5269), Fungi (*Fusarium moniliforme* NCIM 1100, and *Fusarium proliferatum* NCIM 1103) and yeasts (*Candida albicans* NCIM 3471, *Candida albicans* NCIM 3628). These microbial strains were procured from National Collection of Industrial Microorganisms (NCIM), Pune, india. All bacterial strains were grown in Muller Hington (MH) Broth whereas fungi were grown in Potato Dextrose Broth and yeast were grown in MGYP (Malt extract-Glucose-Yeast extarct Peptone) medium.

### 1.2.2 MIC/MBC determination for antibacterial activity

Broth microdilution tests were carried out according to NCCLS guidelines (Wyne, 2008), different concentration of seven ILs [alkyl-$^{t}$OHim][OMs] (**1–7**) were prepared in MH broth (bacteria), PD broth (fungi) and MGYP (yeast); filtered by 0.22 mm sterile filter. Microorganisms under investigation were grown over 18–24 h at 37 ºC in MH Broth (bacteria) and over 48 h at 30 ºC in PD Broth (Fungi and yeast), from which an inoculum was taken and this suspension was further diluted to give a final inoculum density of 2 x$10^{6}$ CFU $mL^{-1}$, as verified by total viable count (TVC). The microtitre plate for determination of minimum inhibitory concentration (MIC) and minimum bactericidal concentration (MBC) was set up as described. A negative control (growth medium without microorganism) was included. All [alkyl-$^{t}$OHim][OMs] IL's with different concentartions along with controls and test concentrations were prepared in three replicates. The microtitre plates were then incubated for 24 h at 37 ºC for bacteria and 48 h at 30 ºC for fungi and yeast in a shaking plate incubator (Hedolf, Germany). Presence and absence of growth of the micro-organisms was determined visually after incubation. The lowest concentration at which there was no visible growth

(turbidity) was taken as the MIC and MBC derived by transferring 20 µL of the suspension from the wells, which displayed no signs of growth to specified agar plates (as per growth condition). Then plates were incubated in a stationary incubator at 37 ºC for 24 h (bacteria) and 30 ºC for 48 h (fungi) and examined for 99.9% killing. Fluconazole used as standard antifungal drug.

Further, experiment to check inhibitory effect of IL's towards bacterial viability was tested by method reported previously by *Docherty et al.,* (Docherty and Kulpa, Jr., 2005). Pure cultures in MH broth were then diluted to 5 x $10^7$ CFU $mL^{-1}$ in sterile saline solution. Culture was then inoculated into 3 replicates of 5 mL of saline (positive control) and 1000 ppm each of 1-7 ILs (1) Mim-$^t$OH, (2) *i*Pim-$^t$OH, (3) Bim-$^t$OH, (4) Him-$^t$OH, (5) Oim-$^t$OH (6) Dmim-$^t$OH, (7) DDim-$^t$OH ILs. Immediately after inoculation and after each 2 h of time, was serially diluted to $10^{-2}$, $10^{-3}$, $10^{-4}$ and $10^{-5}$ in sterile saline solution. Then 100 µL of each dilution was plated on LB (Luria Bertani agar, Himedia India) agar plates. Plate's cultures were allowed to grow for 18 h at 37 ºC and CFU $mL^{-1}$ (Colony forming unit per mL) was calculated.

### 1.2.3 Antibiofilm Activity

The ability of bacteria to form biofilm was assayed as described earlier with some modifications (Zhang et al., 2009). In brief, the fresh colony of *S. epidermidis* bacteria was inoculated in TSB (Tripticase Soya broth, Hi-media, India) incubated it at 37 °C for overnight, next day 1:100 dilution of culture was made in TSB supplemented with 0.5 % glucose. In sterile 24-well tissue culture plates (Non-treated, Eppendorf, USA) was filled with 1.5 mL of TSB broth per well (containing *S. epidermidis* Cells) and kept it for 24 h at 37 °C. After incubation, the content of each well was gently removed by pipette. The wells were washed three times with 1.5 ml of sterile PBS (Phosphate buffer saline, pH 7.6) to remove free-floating bacteria and other cell debris. After that 1 ml of different concentrations (10, 50, 100, 250 and 500 µM) of IL's in PBS was added in each well separately along with control (without IL's). Then the plate was kept for 4 h at 37 ºC. After 4h incubation biofilm was mixed properly and each replicate of culture in IL treated was serially diluted to $10^{-2}$, $10^{-3}$, $10^{-4}$ and $10^{-5}$ in sterile saline solution. Then 100 µL of each dilution was plated on LB agar plates. Plates were allowed to grow for 18 h at 37 ºC and CFU $mL^{-1}$ was calculated.

The percentage (%) inhibition of biofilm activity was calculated using the following equation: [CFU per mL of cells treated with IL's/CFU per mL of control cells (non-treated)] ×100. Experiments were performed in triplicate. The data are expressed as means ± SD. The morphological changes was observed under optical microscope (Nikon Eclipse LV150NL) after growing biofilm on silicon substrate and incubated with 100 µM ILs for 4 h.

### 1.3 Haemolysis Assay

In order to scrutinize any lysis of the RBC membrane by alkyl *tert*-alcohol TMS ionic liquids a hemolytic assay was per-formed. The [alkyl-$^{t}$OHim][OMs] **1**–**7** were spectrophotometrically assayed for their ability to induce hemoglobin release from blood erythrocytes method from Shin and group was applied (Shin et al., 2001). Essentially, fresh (Goat) blood was received from department of Microbiology, Savitribai Phule University, Pune, collected in a heparinised tube and centrifuged for 20 min at 3000 rpm (503g). After centrifugation, the erythrocytes were washed with PBS (pH 7.4). To obtain a 5 % haematocrit, the packed erythrocytes were re-suspended in PBS and rinsed three times with equal volumes of PBS, following centrifugation for 15 min at 3000 rpm (503g). Equal volumes (100 µL) of the erythrocyte suspension were added to each well of a 96-well microtiter plate. Erythrocytes were subsequently exposed to selected ionic liquid concentrations (50, 100, 250 and 500 µM), incubated at 37 ºC for 1 h and After incubation the cells were kept in an ice bath for 60 seconds, followed by centrifugation at 3000 rpm (503g) for 5 min. Aliquots of the supernatant were transferred to a fresh 96-well microtiter plate, and hemoglobin release measured spectrophotometrically at 405 nm. As a positive control (100% hemolysis), erythrocytes were treated with 0.1% Tween 80, whilst PBS (0% hemolysis) acted as a negative control. All samples (and controls) were assayed in quadruplicate. Percentage hemolysis was calculated according to *Seddon et al.,* reported procedure.

**% Hemolysis** =

$$\frac{\text{Abs405nm ILs sample} - \text{Abs405nm erythrocytes PBS}}{\text{Abs405nm 0.1\% Tween 80} - \text{Abs405nm erythrocytes PBS}} \times 100$$

## 2. Result and Discussion

### 2.1 Antimicrobial activity of ILs

The various alkyl chain length such as methyl, *i*-propyl, *n*-butyl, *n*-hexyl, *n*-octyl, *n*-decyl and *n*-dodecyl group into the side chain of *tert*-BuOH functionalized imidazolium-based cation with methylsulfonate anion IL were synthesized (**Fig. 2**). The precursor *tert*-BuOH group substituted imidazole was achieved by reaction of isobutylene oxide with imidazole **Scheme 1**, then the series of various length of alkyl chain were introduced by N-alkylation reaction of various alkyl chain length of methylsulfonate esters to afforded the series of ILs: 1-alkyl-3-tert-alcohol substituted imidazolium mesylate anion salts: 1-(2-hydroxy-2-methyl-n-propyl)-3-methylimidazolium mesylate ([$C_1$-$^t$OHim][OMs], **1**), 1-(2-hydroxy-2-methyl-n-propyl)-3-isopropylimidazolium mesylate ([$C_3$-$^t$OHim][OMs], **2**), 1-(2-hydroxy-2-methyl-n-propyl)-3-n-butylimadazolium mesylate ([$C_4$-$^t$OHim][OMs], **3**), 1-(2-hydroxy-2-methyl-n-propyl)-3-n-hexylimadazolium mesylate ([$C_6$-$^t$OHim][OMs], **4**), 1-(2-hydroxy-2-methyl-n-propyl)-3-n-octylimadazolium mesylate ([$C_8$-$^t$OHim][OMs], **5**), 1-(2-hydroxy-2-methyl-n-propyl)-3-n-decylimadazolium mesylate ([$C_{10}$-$^t$OHim][OMs], **6**), 1-(2-hydroxy-2-methyl-n-propyl)-3-n-dodecylimadazolium mesylate ([$C_{12}$-$^t$OHim][OMs], **7**). All of these IL-$^t$OH are in liquid state at room temperature and were characterized by $^1$H, $^{13}$C NMR spectroscopy and elemental analysis.

Initial screening of these synthesized ILs was examined by MIC and MBC were estimated, results are summarized in **Table 1**. The examined ILs exhibited significant biological activity at lower concentration in IL **6** and **7,** and at higher concentrations in ILs **1**–**5**. These results indicates that the shorter chain lengths ILs were less inhibitory effects than decanol chain bearing IL **6** and dodecane bearing IL **7**. This results were similar to the previously studied alkyl chain length dependence antimicrobial activity of other ILs. Compounds **6** and **7** manifested a more prominent bacteriostatic activity, *i.e.* lower MIC values than microbiocidal activity measured by MBC. Out of all the examined salts, the most pronounced microorganism growth-inhibiting effect on *S. epidermidis* was shown by ILs containing carbons lengths 6, 8, 10 or 12 in side chain. Interestingly, ILs bearing longer than 10-carbon chain length were shown remarkable activity (MIC) against tested other bacteria and fungi strains. To compare the efficiency

of our synthesized [alkyl-$^{t}$OHim][OMs], we compare the obtained MIC and MBC with previously reported non-halogenated IL bearing lactate anion (Pernak et al., 2004) (structure **C**, **Fig. 2**).

| **Strains** | | **1 ($C_1$)** | **2 ($C_3$)** | **5 ($C_8$)** | **6** ($C_{10}$) | **7** ($C_{12}$) | **IL-C[a]** | **Fluconazole** |
|---|---|---|---|---|---|---|---|---|
| *S. epidermidis* NCIM 2493 | MIC | >2000 | >2000 | **287 ± 6** | **9.5 ± 0.25** | **3.5± 0.8** | 12 | —**b** |
| | MBC | >2000 | >2000 | **587 ± 4** | **26.75 ± 0.5** | **15.2± 0.75** | 96 | — |
| *S. aureus NCIM* 5021 | MIC | >2000 | >2000 | >2000 | **107.5 ± 1.0** | **17.45± 1.5** | 24 | — |
| | MBC | >2000 | >2000 | >2000 | **215 ± 2.25** | **50.2±2.8** | 192 | — |
| *S. typhimurium* NCIM 2501 | MIC | >2000 | >2000 | >2000 | **107.5±0.56** | **81.5± 3.0** | — | — |
| | MBC | >2000 | >2000 | >2000 | **240 ± 1.25** | **157.5± 2.0** | — | — |
| *V. fischeri* NCIM 5269 | MIC | >2000 | >2000 | >2000 | **107.5±0.68** | **81.5± 0.25** | — | — |
| | MBC | >2000 | >2000 | >2000 | **240 ± 2.25** | **157.5± 0.3** | — | — |
| *F. moniliforme* NCIM 1100 | MIC | >2000 | >2000 | >2000 | **160.4±0.75** | **17.45± 1.5** | — | 417.95 |
| | MBC | >2000 | >2000 | >2000 | **267.5±0.85** | **25.1±2.2** | — | 835.9 |
| *F. oxysporum* NCIM 1103 | MIC | >2000 | >2000 | >2000 | **160.4±0.23** | **17.45± 1.2** | — | 417.95 |
| | MBC | >2000 | >2000 | >2000 | **267.5±0.42** | **25.1±2.4** | — | 835.9 |
| *C. albicans* NCIM 3471 | MIC | >2000 | >2000 | >2000 | **267.5±6.5** | **17.45±2** | 11 | 417.95 |
| | MBC | >2000 | >2000 | >2000 | **1335.5±0.42** | **25.1±4.5** | 88 | 835.9 |
| *C. albicans* NCIM 3628 | MIC | >2000 | >2000 | >2000 | **667.6±15** | **17.45±5** | - | >2000 |
| | MBC | >2000 | >2000 | >2000 | **1335.5±20** | **25.1±6.5** | - | >2000 |

[a]MIC and MBC values of 3l* lactate-IL (C, Fig. 1) taken from ref. (Pernak et al., 2004). [b]Not determined.

**Table 1.** MIC and MBC in µM of microorganisms with respect to [alkyl-$^{t}$OHim][OMs].

Microbial activity with similar type of microbial strains, results suggested that our synthesised IL bearing *tert*-BuOH moiety and mesylate anion has superior

antimicrobial activity. In case of fungi, ILs **6** and **7** showed similar activity (MIC and MBC) on *F. moniliforme* and *F. oxysporum* as they are belonging from the same genus. Further we compare the antifungal activity with fluconazole, is well known antifungal drug which inhibit the ergosterol biosynthesis pathway by targeting 14-α-lanosterol demethylase enzyme and also disturb the fungal membrane (Nucci and Colombo, 2007). Imidazolium salts has similar ability to disturb the membrane regeneration by decreasing the quantity of sterol in the fungal cell (Nweze et al., 2012). It's noteworthy that, IL **7** shown more than 20 folds antifungal activity comparatively to fluconazole. Finally in case of two strains of *C. albicans* has shown similar MIC to that of fungi. Surprisingly, strain NCIM 3628 was resistant to fluconazole as well as most of tested ILs except ILs **6** and **7**.

Due to the neutral character of fluconazole, it does not adjust to the surroundings with different hydrophilic–hydrophobic conditions it may trapped into the biofilm framework, thus it may have less effective antifungal activity compare to the [$C_{12}$-$^{t}$OHim][OMs] (**7**). This highly potential antifungal activity due to the unique physicochemical properties of [alkyl-$^{t}$OHim][OMs] perfectly matches the amphipathicity of the fungi. Our obtained result completely agreement with previously reported, role of imidazolium ILs in antifungal activity (Bergamo et al., 2015; Schrekker et al., 2013). Moreover, antifungal data clearly suggesting that *tert*-BuOH functionalized ILs **6** and **7** may consider as alternative to fluconazole.

All these ILs **1-7** were checked for their inhibitory effect against four bacteria in saline condition over 10 h of exposure time. As shown in **Fig. 4**, CFU/ml was declined in ILs 5-7 over time. It indicated that almost killing of 99.9 % of organisms after 10 h of incubation. The calculated average MIC values for ILs such as [$C_6$-$^{t}$OHim][OMs] (**4**), [$C_8$-$^{t}$OHim][OMs] (**5**), [$C_{10}$-$^{t}$OHim][OMs] (**6**) and [$C_{12}$-$^{t}$OHim][OMs] (**7**) for Gram positive, Gram negative pathogens and fungi are plotted in **Fig. 5** as the relationship between $\log_{10}$ MIC (μM) and ILs. The Gram positive bacteria and fungi showed most sensitive to [alkyl-$^{t}$OHim][OMs] whilst Gram negative bacteria was less susceptible, it also relevant to previous studies(Carson et al., 2009; Pernak et al., 2003).

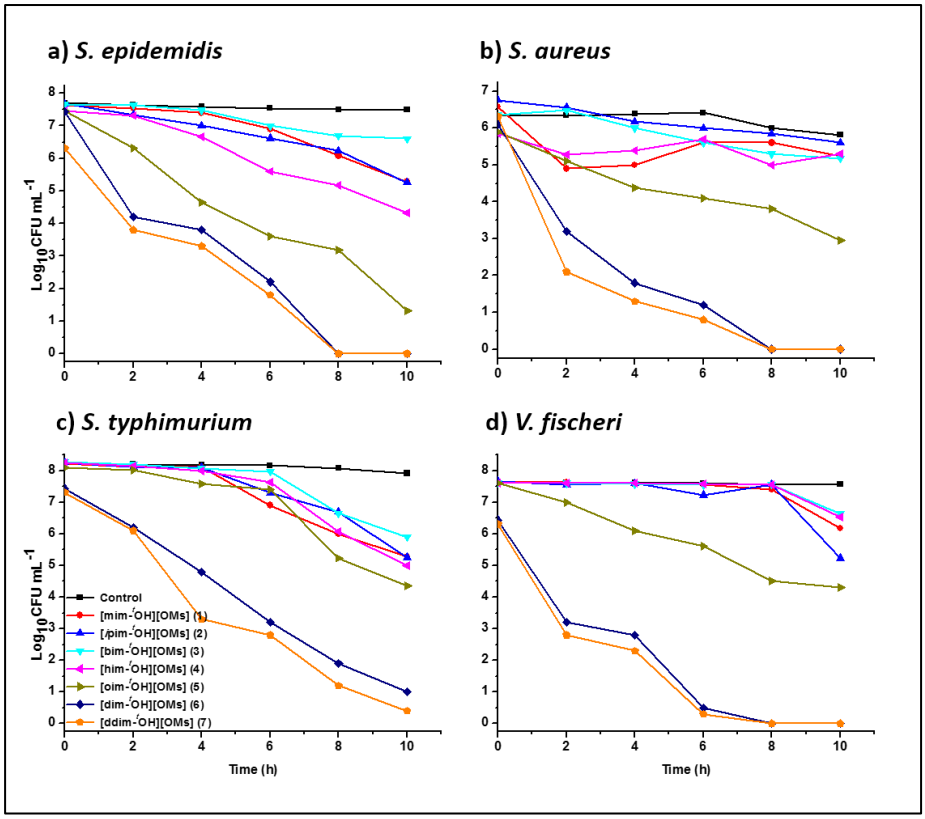


**Figure 4**. Inhibitory effect [alkyl-$^{t}$OH][OMs] ILs against four bacteria over 10 h of exposure time. Each data point represents a log of an average of colony forming units (CFU per mL).

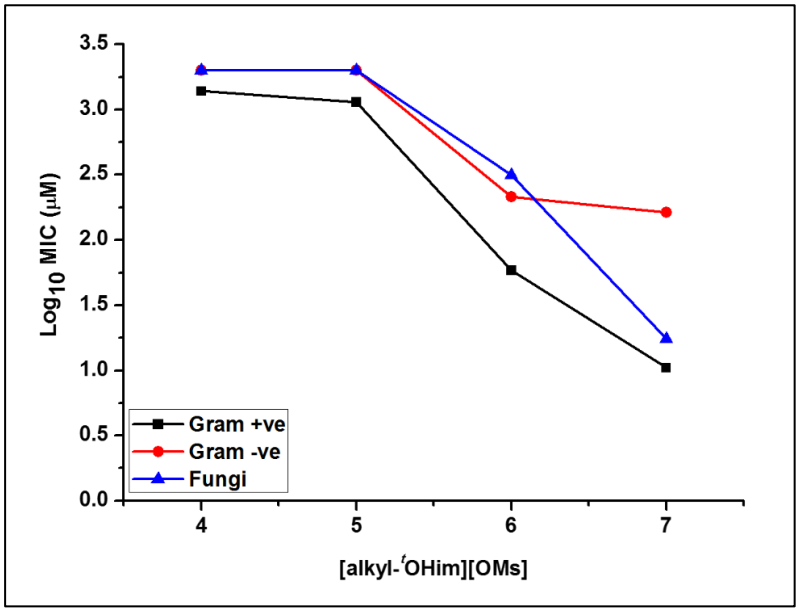


**Figure 5.** Comparison of mean MIC values ($log_{10}$) of [alkyl-$^{t}$OHim][OMs] **4**–**7** against Gram positive and Gram negative bacteria and fungi.

## 2.2 Antibiofilm activity of ILs

In order to measure the antibiofilm activity of series of [alkyl-$^{t}$OHim][OMs] against of clinically significant nosocomial pathogen and biofilm forming *S. epidermidis* strain was grown in 24 well plate as described in Experimental sections. This applied method can permit reproducible and quantitative assaying of biofilm susceptibility to antimicrobial and biocidal agents include imidazolium ILs. Biofilms were grown for 24 h in TSB medium supplemented with 0.5% glucose as described, and 24 h biofilm was treated with six different IL's with concentrations of (0, 50, 100, 250 and 500 µM) for 4 h. After 4 h of treatment, viable cells of biofilm were evaluated by determining average viable cell counts (CFU $mL^{-1}$) for each concentration along with control (without ILs). The percentage (%) of viable biofilm has shown in **Fig. 6**,

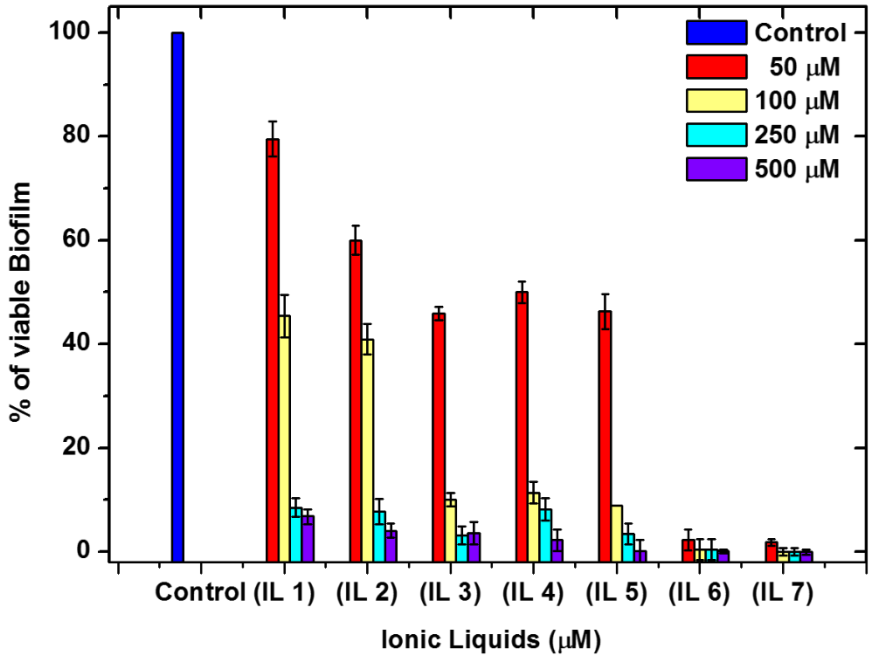


**Figure 6**. Percent (%) of viable biofilm of S. epidermidis after 4 h treatment of all [alkyl-$^{t}$OHim][OMs]. Value % calculated on the basis of Colony Forming Units (CFU $mL^{-1}$). Error bars denotes the standard deviation.

As alkyl chain length increases the activity of ILs against biofilm also increases. Above the concentration of 100 µM showed more than 55 ± 4.5% and 85 ± 5.5% preventing biofilm formation in ILs **1**, **2** and **3–5,** respectively. In other hand, **6** and **7** have showed excellent death effects on biofilm, at lowest concentration (50 µM), killed biofilm more than 97 ± 2.7%, which showed promising activity among the all tested

ILs. We believed that the significantly influenced antimicrobial and biofilm activity of IL-$C_{12}$ could be due to amphipathic nature of IL, in which longer alkyl chains possess high lipophilicity properties and the cationic *tert*-butanol contained imidazolium moiety may increase membrane permeability properties of the molecule. Once membrane become permeable, the ionic liquid will enter into the cells and thereby lead to killing phenotype.

The optical microscope images of morphological changes in the biofilm formation after treatment with ILs **1-7** (100 µM) as shown in **Fig. 7.** As seen in biofilm grown control image (a) of **Fig. 7** was more significantly disrupted by ILs **7** than **6.** As the alkyl chains increases the bacterial biofilm cell membrane was highly disrupted, as indicated by red arrow. Biofilm disrupted was not limited to **6**, **7** but also seen in lower alkyl chain length ILs **1–5**.

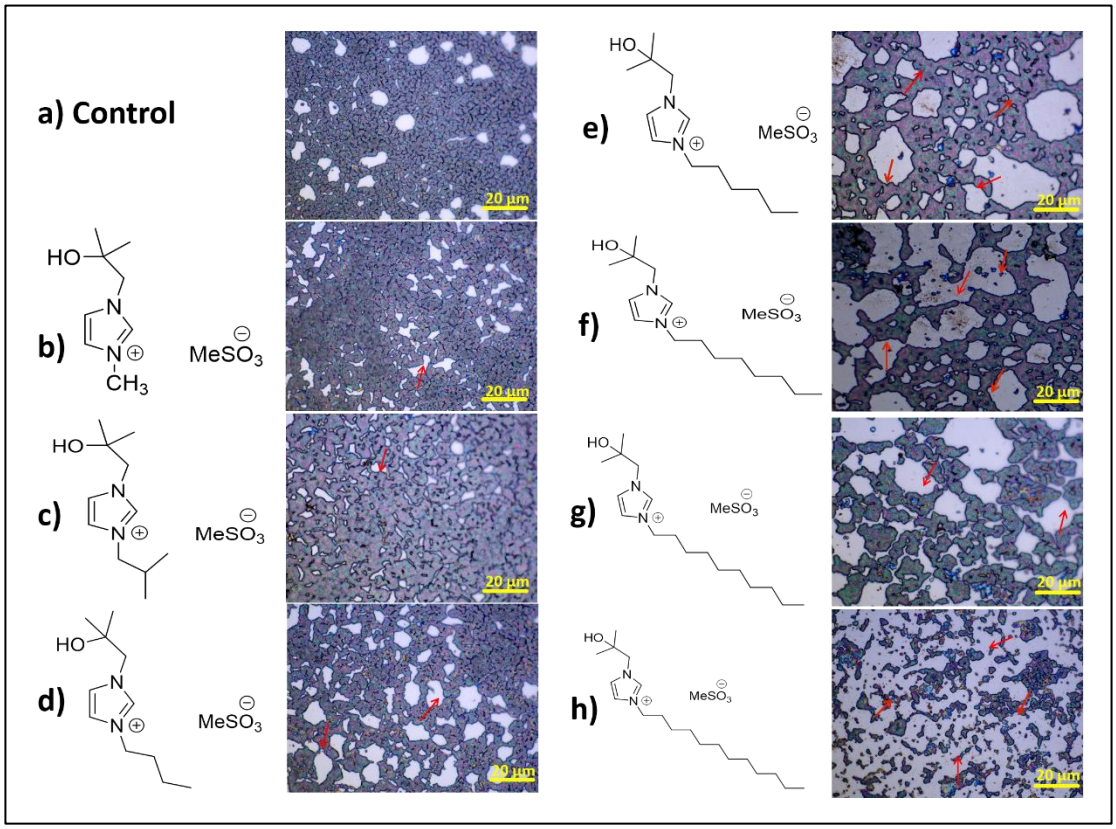


**Figure 7**. Optical microscopic images distorted morphology (indicated by red arrows) of *S. epidermidis* biofilm after exposure of 100 µM concentration ILs; (a) control (without ILs), (b-h) **1-7** [alkyl-$^{t}$OHim][OMs] ILs.

### 2.3 Haemolytic activity of ILs

Finally, the haemolytic activity of [alkyl-$^{t}$OHim][OMs] (**1–7**) was evaluated against fresh goat erythrocytes and results depicted in **Fig. 8**. Haemolytic assay indicated that the tested ILs did not show significant haemolytic activity up to using 100 µM concentration, except [$C_{12}$-$^{t}$OHim][OMs] (**7**) caused 48.4 ± 2.5% haemolysis. This was expected considering the high antimicrobial activity of **7**, which is most likely due to the ability to disrupt cellular membranes. Interestingly, the increased concentration of ILs **1–5** at 500 µM didn't exhibit the haemolytic activity. Overall, the concentrations of all ILs at MIC would not be expected to produce haemolysis, since these concentrations are inhibitory to microbial growth rather than producing a killing phenotype (of erythrocytes) which was observed at and above the MIC values.

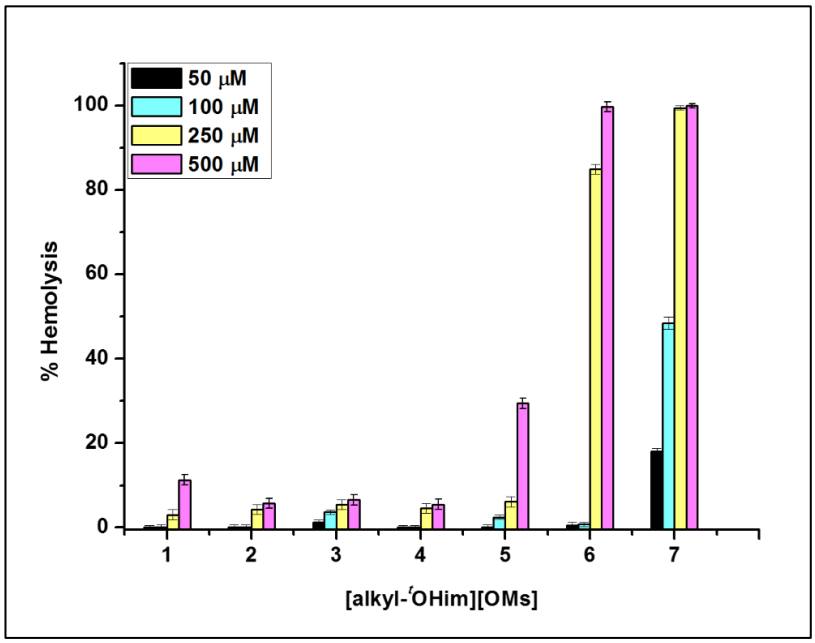


**Figure 8.** Haemolytic activity (%) of [alkyl-$^{t}$OHim][OMs] ILs against fresh erythrocytes. Each value is expressed as the mean of six replicates.

Our observations are in accordance with Busetti et al., wherein quinolinium bromide ILs also exhibited similar relationship between of haemolysis and MIC (Busetti et al., 2010). In case of both IL **6** and **7**, observed haemolysis at above 250 µM concentration, which is not surprising given the average MICs for the range of tested microorganisms was below 250 µM concentration **(Fig. 3)**. This haemolysis data clearly suggested that [alkyl-$^{t}$OHim][OMs] are highly membrane active and showed cidal activity *via* disruption of the cell membrane.

# Section 3B

# Stability and catalytic activity of *epi*-cedrol synthase in *tert*-BuOH functionalized ionic liquids

## 1. Methodology

### 1.1 Expression and purification of the recombinant *ECS* proteins

Plasmid ECS-pET28 transfer into competent cells of *E. coli Rosetta* (DE3 $\alpha$) by heat shock method (preparation of competent cells was carried out by rubidium chloride method as detailed protocol mentioned in chapter 2. Recombinant *E. coli Rosetta* (DE3 $\alpha$) harboring a recombinant plasmid, was grown overnight at 37 ◦C in 5 ml LB medium supplemented with 50 µg/ml kanamycin and 34 µg/ml chloramphenicol until the $OD_{600}$ reached 1.2 - 1.5. Then, the culture was diluted into 50 ml of the same fresh medium and cultivated at 37 ºC until the $OD_{600}$ reached 1.2 -1.5. Then this culture finally diluted into 1 L of fresh Terrific broth (TB) medium containing same antibiotics, incubated at 37°C until the $OD_{600}$ reached 0.7-0.8, IPTG was added to give a final concentration of 1 mM, and the culture was incubated for an additional 12 h at 16°C. The cells were harvested by centrifugation at 6000×*g* for 10 min, suspended in 15 ml different lysis buffer (A, B and C) containing Tris/Phosphate/HEPES pH-7.8. For further lysis, lysozyme (1 mg/mL), CHAPS (0.01%) and 1mM PMSF (proteinase inhibitor) were added. incubated for 30 min for membrane lysis on rocker. The cells were disrupted by sonication (Braun-Sonic 2000 microprobe) at 75% amplitude, 30 sec on, 45 Sec off, and total 6 Cycle. The sonicated crude was centrifuged at 10,000×g for 15 min at 4 °C for removing cell debris and remaining intact cells. The supernatant was collected and optimized for better buffer for solubilisation of enzyme by using 12 % SDS-polyacrylamide gel electrophoresis (SDS-PAGE).

Further optimized buffer was selected and same step were followed as mentioned above, the supernatant was taken and used for His-Tag $Ni^{2+}$-NTA affinity purification by using HEPES buffer. Wash buffer C containing 35 mM imidazole was used for washing undesired proteins and elution buffer C was used to eluting the final pure proteins. Fractions of 0.4 mL were collected and checked by using 12 % SDS-PAGE. Gels were stained with Coomassie Brilliant Blue R 250. Further enzyme was desalted by using desalting bag 3-15 kDa (Himedia)/10 kDa cut-off filter (Merck). Desalted proteins were stored at -80 °C. Protein concentrations and purified recombinant enzymes were determined according to Bradford using BSA as standard (Bradford, 1976).

### 1.2 Characterization of ECS enzyme by enzyme assay

Enzyme activity of ECS was assayed using Farnesyl pyrophosphate (FPP) as a substrate, and was monitored by GC-MS analysis of sesquiterpene *epi*-cedrol released from FPP by the enzymatic reaction. In a typical assay, a 200 µL enzymatic reaction mixture containing, assay buffer pH 8.5, 20 µg purified ECS, 150 µM FPP was incubated in shaker bath incubator (Spire, India) at 30 ºC for 1 h (30 ºC commonly used for terpene cyclase enzymes according to previous reports). The enzymatic reaction was stopped and quenched by an addition of 10 µl of absolute ethanol (95 %) followed by vortex it for 30 sec, extract product by adding thrice 300 µL hexane. Hexane layer was removed and transferred in a 1.5 mL GC-vial. Hexane was evaporated by passing $N_2$ gas. The e*pi*-cedrol was identified by GC-MS analysis by using Agilent Technology 5975-7890 GC-MS system with a HP-5MS capillary column (30 m x 0.250 mm x 0.25 µ coating of 5 % phenyl methyl siloxane). Injections were made cool on-column at 40°C with oven programming from 40 °C (50 °C/min) to 50 °C (5-min hold), then 10 °C/min to 250 °C, then 50 °C/min to 300 °C. Separations were made under a constant flow of 1 ml He y min. Mass spectral data were collected at 70 eV and analyzed by using MSD Chem station software. One unit of enzyme activity was defined as the amount of enzyme required to liberate 1 µmol of *epi*-cedrol/min under the assay conditions.

### 1.3 Divalent metal activity

To check the effect of divalent metal effect on terpene cyclase enzyme activity, different metal ions were selected such as $Mg^{2+}$, $Mn^{2+}$, $Zn^{2+}$, $Cu^{2+}$, $Ni^{2+}$, and $Cr^{2+}$. Two different concentrations (5 mM and 10 mM) of all divalent ions was used in enzymatic assay. The assay were kept as mention above for 1 h at 30 ºC and analyzed by GC-MS analysis according to mentioned protocol.

### 1.4 Temperature effect on enzyme activity

Effect of temperature on activity of ECS was assayed by using different temperature conditions (0 ºC, 10 ºC, 15 ºC, 20 ºC, 25 ºC, 30 ºC, 35 ºC and 40 ºC). All temperature conditions were maintained in shaker water bath in same assay buffer.

### 1.5 Enzyme Kinetics

Enzyme kinetics were studied by taking farnasol as a standard and verified by GC-FID analysis. Enzyme assay of different concentrations of FPP was used (1µM, 2µM, 5µM, 10µM, 15µM, 20µM, 25µM and 50 µM) with constant concentrations of ECS proteins (2.2 µg) in a same assay buffer (pH 8.5) as previously described (chapter 2). The Km and Vmax were plotted and calculated by Origin® software. And other specific activity calculated by Michalis Menten equation.

### 1.6 Enzyme activity in imidazolium ILs

A stock of substrate FPP (26 mM, 3mg/mL) was prepared in 25 mM of ammonium bicarbonate aqueous solution. To check the catalytic activity study of ECS enzyme in ILs, different concentrations of (1-20 µg OR 10, 50 and 100 µM) of each various imidazolium ILs having alkyl chains (IL**1**, [$C_1$-$^t$OHim][OMs]**;** IL**2**, [$C_3$-$^t$OHim][OMs]; IL**3**, [$C_4$-$^t$OHim][OMs], IL**4**, [$C_6$-$^t$OHim][OMs]; IL**5**, [$C_8$-$^t$OHim][OMs], and IL**6**, [$C_{10}$-$^t$OHim][OMs]) were incubated with purified ECS enzyme. In a typical enzymatic reaction, 400 µL assay buffer pH 8.5, containing individual different concentrations of all 6 ILs (0, 10, 50, and 100 µg) supplied with 100 µM FPP and 25 µg of purified ECS enzyme (15 µL) were incubated in shaker bath incubator at 30 ºC for 2 h at 70 rpm. The control enzyme assay (positive) was also kept without any ILs. The enzymatic reaction was analysed by above mentioned GCMS protocol (methodology section 1.3).

To check the stability study of enzyme (ECS) with ILs in various temperature conditions, 50 µM of each imidazolium ILs (IL**1**, [$C_1$-$^t$OHim][OMs]**;** IL**2**, [$C_3$-$^t$OHim][OMs]; IL**3**, [$C_4$-$^t$OHim][OMs], IL**4**, [$C_6$-$^t$OHim][OMs]; IL**5**, [$C_8$-$^t$OHim][OMs], and IL**6**, [$C_{10}$-$^t$OHim][OMs]) were mixed with 50 µg of ECS enzyme in 50 µL Tris buffer (pH 7.4, 50 mM Tris, 100 mM KCl, 10% glycerol), and incubated at 4 ºC, 28 ºC, 37 ºC, and 50 ºC for 12 h. After incubation reaction were cooled down at 4 ºC and enzyme assay was kept by adding assay buffer and 100 µM FPP and analysed as per above section 1.3.

### 1.7 Circular Dichroism Analysis

Circular dichroism spectroscopy was used to gain insights of secondary structure of proteins. Far-UV CD spectra from 190 to 290 nm wavelength were

recorded on a Jasco J-720 spectropolarimeter using 1 mm path length cuvette. The step resolution of measurement was 1 nm with a scan speed of 200 nm/min and bandwidth of 1 nm. Initially, ECS was destabilized by addition of various concentrations of GuHCl (0.1-6 mM) and incubated for 1 h. Stability of ECS in ILs was analyzed by adding various concentrations of (10, 50, 100 µM) ILs in enzyme ECS and incubated for 6 h of incubation at various temperatures (4, 28, 37 and 50 ºC). The CD spectra were recorded for destabilized ECS enzyme in GuHCl as well as mixture of ECS in various ILs, where the concentration of peptide and IL was 50 and 500 µM, respectively. All the spectra were taken over three scans (triplicates), and background measurements for Tris-buffer were subtracted.

### 1.8 Transmission Electron Microscopy

TEM measurements enzyme ECS with ILs were carried out for better understanding (Jha et al., 2018)(Jha et al., 2018)protein textures. In brief, ECS and ILs mixture samples passed through 0.22 µm filtered water and further incubated at 37 ºC for 12 h, such that the final concentration of enzyme and ILs was 50 µg and 20 µg, respectively. After incubation, each sample was further diluted to 10-fold in MilliQ water. For imaging, carbon-coated 200-mesh copper grids (Tedpella co.) were used where 20 µL of the diluted sample was placed and air-dried. For negatively staining, 10 µL of 2 % uranium acetate in Milli-Q water was added to each grid and incubated for 1 min at room temperature, and air-dried prior to examine under an electron microscope TEM images were collected using FEI TECNAI TF-30 (FEG) instrument.

### 1.9 *In-silico* Molecular Docking Analysis

*In-silico* molecular docking analysis was done only for **IL-4, IL-5** and **IL-6**, which gives better *In-vitro* activity among the all ILs. (NOTE: CD-spectra analysis, TEM images and *In-silico* docking has not been done yet due to the sudden announcement of lockdown in Covid-19 outbreak).

## 2. Results and discussion

The gene encoding 8-*Epi-cedrol* Synthase (ECS) (*Genbank* No. AF157059) EPCS a sesquiterpene cyclase protein contained an ORF of 1641 bp and encoded a protein of 547 amino residues was cloned into pET-28a (+) expression vector. Then the

pET-28a (+) expression vector was transformed in *E. coli* Topo 10 host for cloning purposes and *E.coli Rosetta DE3 α* host for expression by heat shock method. Expression of ECS enzyme carried out in *E. coli* Rosetta DE3 cells with 1 mM IPTG induction and further purified by affinity chromatography, (**Fig. 1)** as mentioned in previous *chapter 2*.

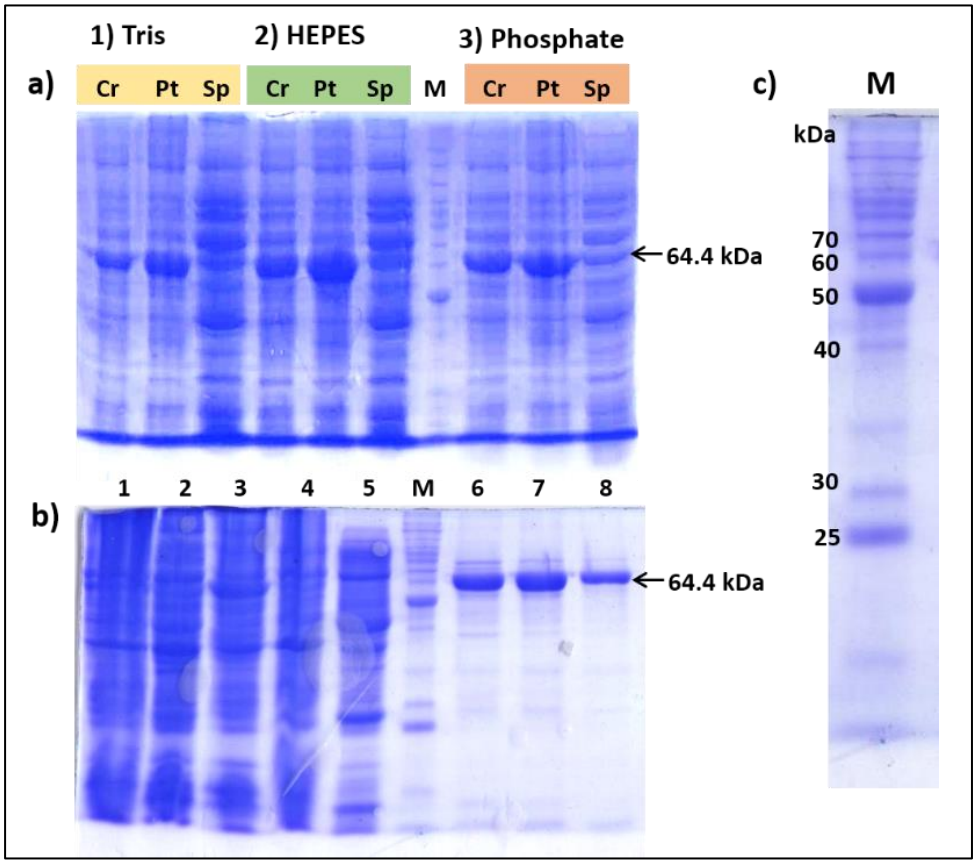


**Figure 1.** a) Expression and solubility of ECS in 1. Tris, 2. HEPS, and 3. Phosphate buffer; b. SDS-PAGE of ECS enzyme, 1. Crude fraction, 2. Supernatant, 3. Pellet, 4. Unbound fraction, 5. Wash fraction, 6-8. Purified ECS fractions; c. Protein marker (M) (Invitrogen)

Out of three buffer system, the Hepes buffer (pH 7.8) showed the maximum solubility and protein concentration as compare to Tris and Phosphate buffer. Total 4.2 mg per liter of ECS was obtained which is quite higher than Tris and Phosphate buffer as shown in **Table 1**. Purified fractions were desalted by 10 kDa cut-off filter by using desalting buffer and store in -80 ºC.

| Sr. No. | Buffer | ECS (mg/L) | Stability (pH) |
|---|---|---|---|
| 1 | Hepes | 4.22 | 7-11 |
| 2 | Phosphate | 3.40 | 7-10 |
| 3 | Tris | 3.54 | 7-9 |

**Table 1**. ECS enzyme concentrations in different buffer system.

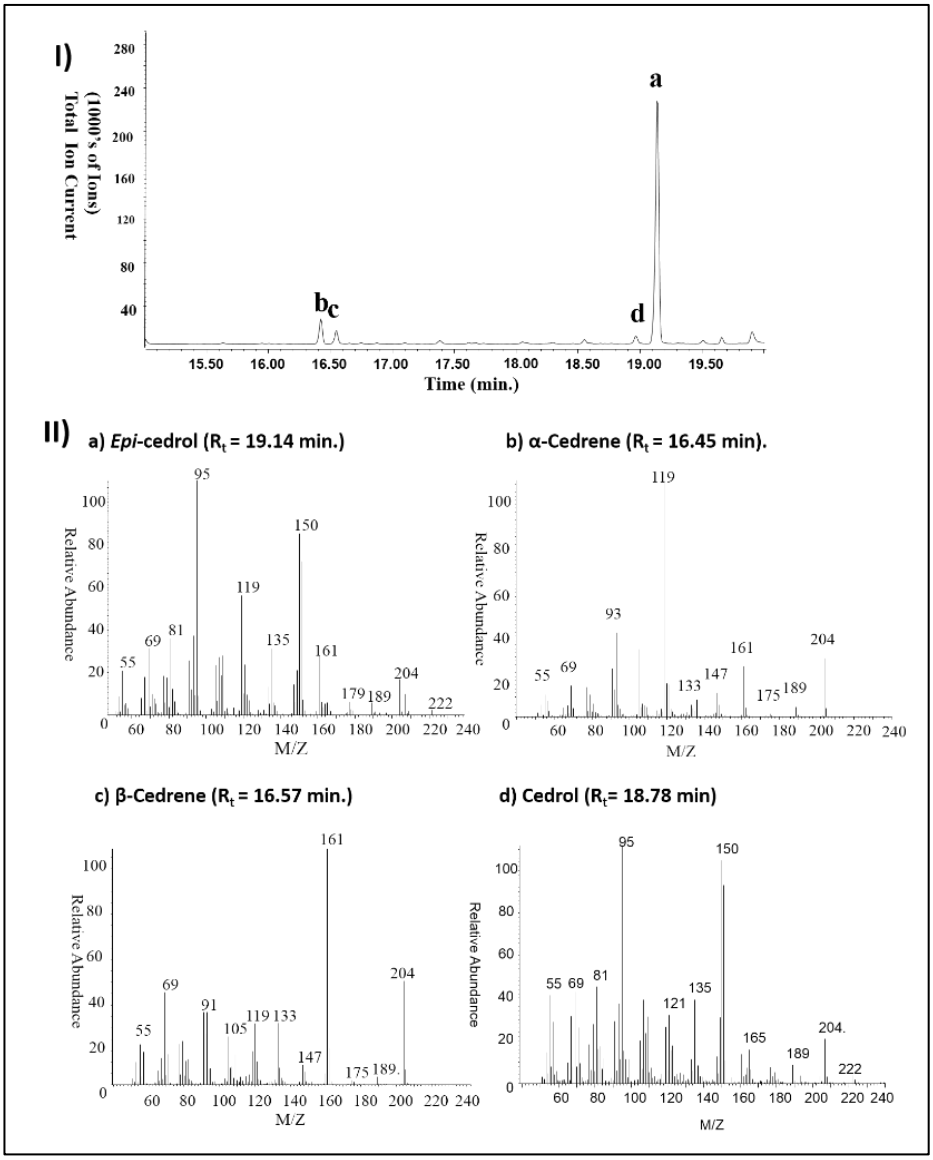


**Figure 2. I)** TIC of ECS enzyme assay. **II**) MS of product from enzyme assay: a) *epi*-cedrol, b) α- cedrene, c) β-cedrene, and d) cedrol.

The characterization of enzyme was done by enzymatic assay with FPP as a substrates as mentioned in methodology section. The recombinant, purified ECS

exhibited a maximum activity at relatively high pH (8.5–9.0). This optimum was the same when enzyme activity is measured as pure *epi*-cedrol produced. The ratio of the pure *epi*-cedrol, α-cedrol and β-cedrol olefin formation remains essentially constant throughout the pH range 8.0 – 9.0. GC-MS analysis showed the maximum product of *epi*-cedrol with few bi-products as shown in **Fig 2-I**. It was identified as α-cedrene (57% of the olefins), β-cedrene (13%), (*E*)-alpha-bisabolene (8%). The oxygenated sesquiterpenes as cedrol (~4 %) and epi-cedrol (~96 %). The major product was *epi*-cedrol **a** ($R_t$ 19.14 min) and two bi-products were α-Cedrene **b** ($R_t$ 16.45 min), β-Cedrene **c** ($R_t$ 16.57 min) (**Fig. 2-II**).

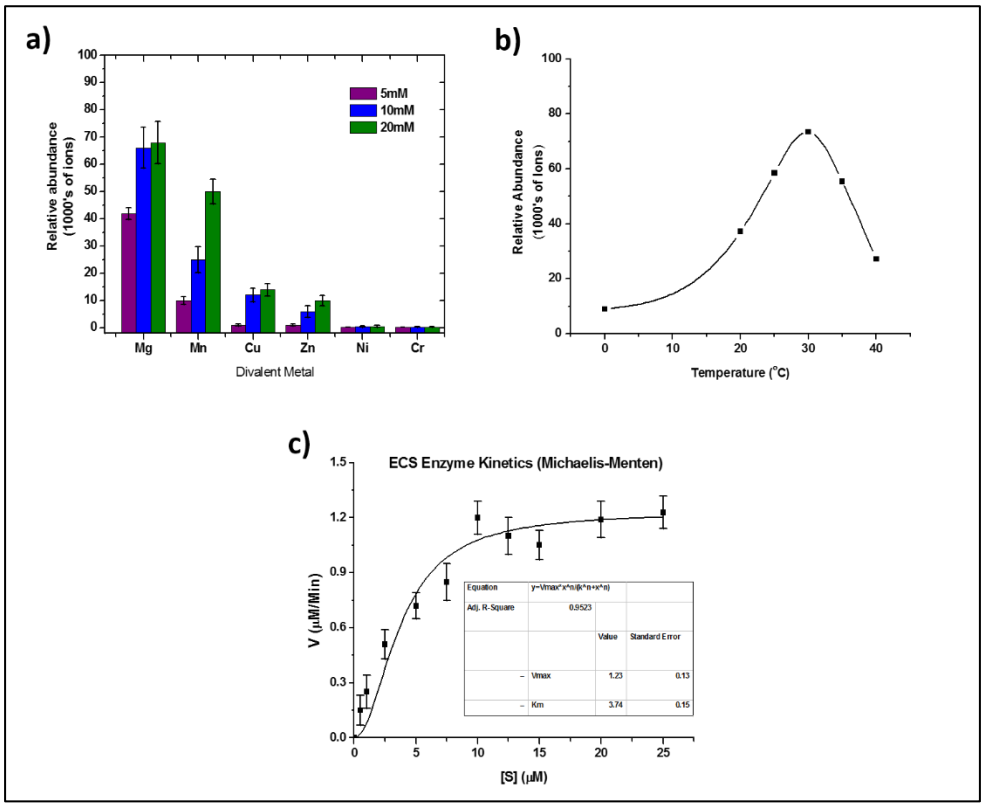


**Figure 3** a) Effect of different concentrations of divalent metal ions on ECS activity. b) Optimization of temperature condition for ECS enzyme assay. c) ECS enzyme kinetics for FPP.

The enzyme assay was carried in various divalent metals salts ($Mg^{2+}$, $Mn^{2+}$, $Zn^{2+}$, $Cu^{2+}$, $Ni^{2+}$, and, $Cr^{2+}$. **Fig. 3a** showed the divalent metal effect on ECS enzyme activity. As reported previously $Mg^{2+}$ are the essential co-factor for the terpene cyclase enzyme activity (Harms et al., 2020). The concentrations of 10 mM and 20 mM $MgCl_2$

showed the highest activity among the all the metal ions. The activity order of all metal ions was $Mg^{2+}$> $Mn^{+2}$> $Zn^{+2}$ >$Cu^{+2}$ >$Ni^{+2}$ >$Cr^{+2}$. The optimum temperature for the activity of ECS was 30 ºC as most of the enzymes were shown the good activity at this temperature (**Fig, 3b**). The optimum pH have been reported previously was 6.5-8.5. We observed the pH optimum condition was 8.5 for enzymatic assay (Luo et al., 2019). The Km value for FPP with the pure recombinant *epi*-cedrol synthase was calculated to be 3.74 µM at pH 8.5, a value typical of other sesquiterpene synthases of plant origin **Fig. 3c**. At pH 9.0, the Km for FPP is somewhat higher 1.3 mM. The specific activity of ECS was calculated as 8 µM per min. per mg of enzyme. One unit of enzyme activity was defined as the amount of enzyme required to liberate 1 µmol of *epi*-cedrol/min under the assay conditions.

## 2.2 Enzyme activity in ILs

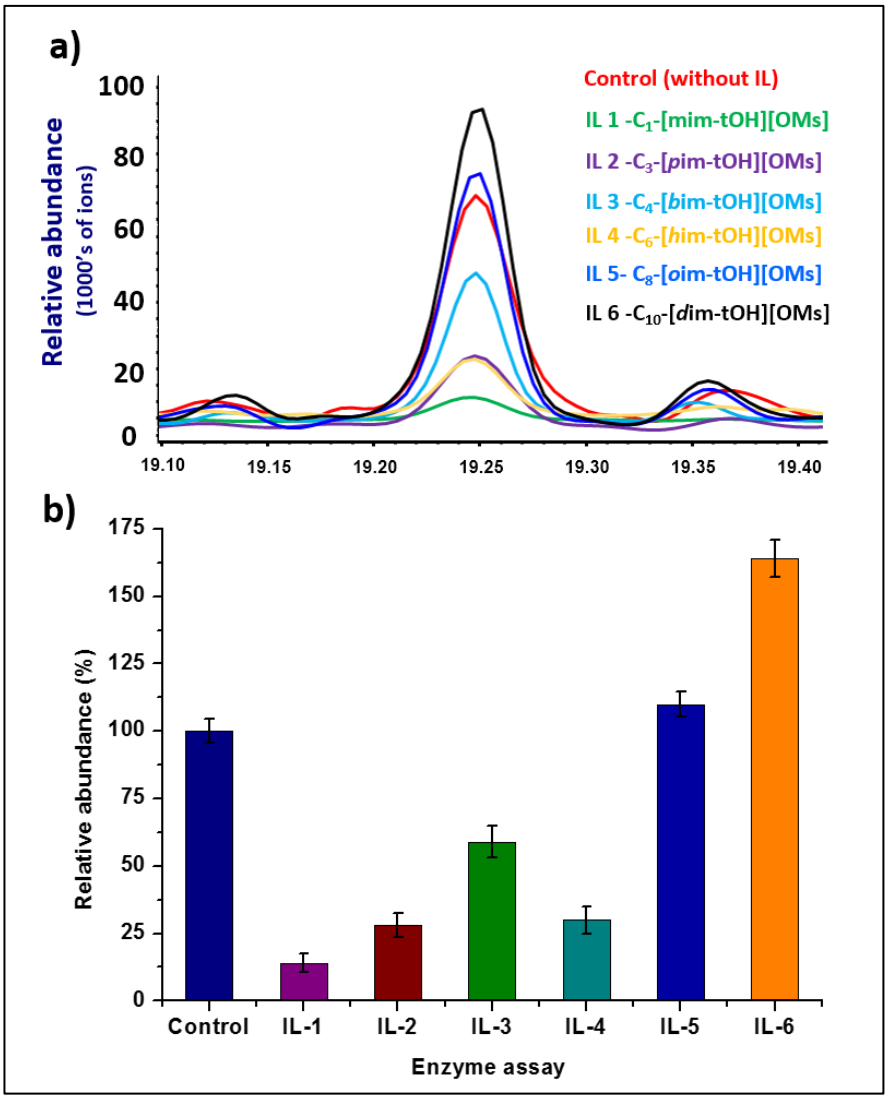

**Figure 4.** GC-FID analysis of *epi*-cedrol production after enzymatic assay in the presence of six ILs.

Several imidazolium ILs are reported for stabilizing enzymes and enhancing the enzyme activity (Sivapragasam et al., 2016). Initially, all the six ILs (methyl-$C_1$, propyl-$C_3$, butyl-$C_4$, hexyl-$C_6$, octyl-$C_8$ and decyl-$C_{10}$) were screened for the support in activity of ECS enzyme. When these ILs added in the enzymatic assay without incubation at various temperature, decyl containing enzymatic assay showed highest catalytic activity (1.6 fold compared to control assay, **Fig. 4**). Followed by octyl and hexyl group containing ILs showed good activity as compared to control (without ILs) experiments.

Out of six imidazolium ILs, total four ILs ($C_4$, $C_6$, $C_8$ and $C_{10}$) showed some positive activity. These four ILs were used in the different combinations to get optimized stability and catalytic activity in *epi*-cedrol production. In the first experiment, these four ILs incubated with four different temperature for 12 h. After incubation activity were compared with control enzyme assay (without ILs). As shown in **Fig. 5,** hexyl containing ILs showed higher stability among all the ILs followed by octyl and decyl imidazolium ILs. $C_6$ ILs consistently showed stability in all temperature while octyl and decyl only showed better stability at 37 ºC and 50 ºC. CD spectra of native structure of three enzymes and destabilized ECS enzyme spectra by GuHCl has shown in **Fig. 6**.

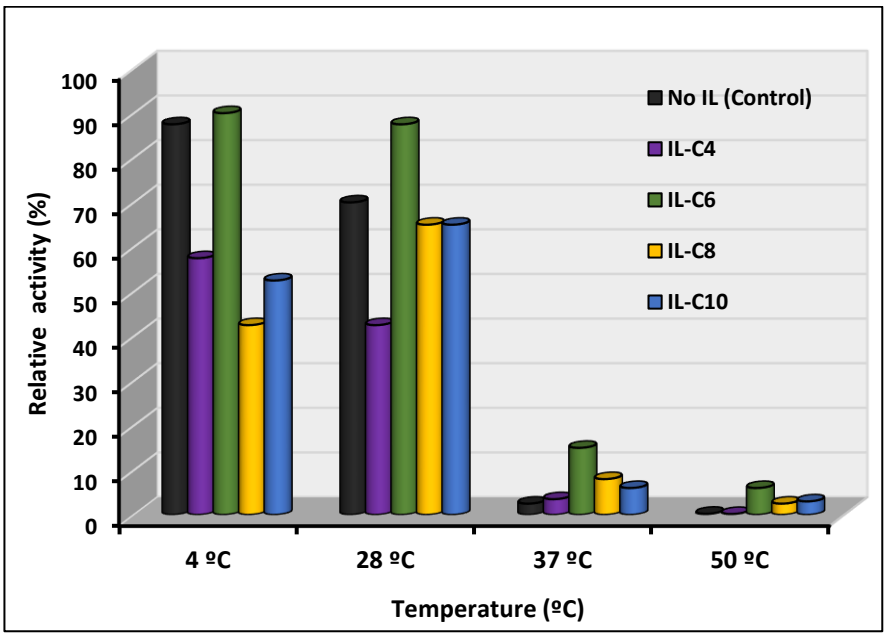

**Figure 5.** Relative enzyme activity (ECS) in presence of four ILs after incubation at various temperature conditions. (This experiment are performed in 2 times, and the error are ±5)

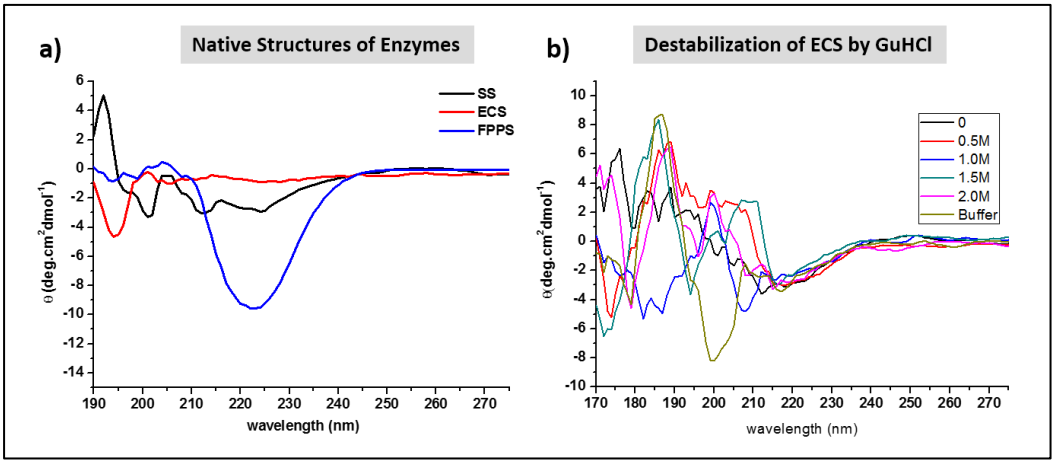


**Figure 6.** CD-spectra analysis of enzymes a) Native structure of SS, FPPS and ECS (SS & FPPS added just for information) b) Destabilization of ECS enzyme by various concentrations of gaunidium HCl.

Overall, *ter*-BuOH functioning imidazolium ILs might be a good option over other costly compounds for increasing stability and catalytic efficacy of enzyme, since this study was our first attempt over the increasing terpene cyclase enzyme activity and stability. In future, this study can help to researchers who are working with enzymology and their stability study.

## Conclusion

In conclusion, this chapter study provided a detailed account of *tert*-BuOH-functionalized-imidazolium mesylate ILs for biological activities and applications. These ILs displayed excellent, broad spectrum antimicrobial and antibiofilm activity against broad spectrum of microorganisms (bacteria, fungi, and yeast). These ILs [alkyl-$^{t}$OHim][OMs] showed better stability effect to ECS terpene cyclase enzyme at 100 mM concentration. Our study revealed that the hexyl, octyl, decyl substituted imidazolium ILs showed good stability at various higher temperature conditions and also helped in enhanced activity of ECS at various temperature condition. We conclude that the ILs bearing chain lengths higher than the hexyl ($C_6$) length were found to be less effective in ECS activity. In instant enzymatic assay decyl could be the best enhancer for enzymatic activity, in future these ILs could be applied in the industrial sector.

**NMR spectra of ionic liquids**

**$^{1}$H NMR (400 MHz, CDCl3) and $^{13}$C NMR (100 MHz, $CDCl_3$)**

**1). 1-(2-Methyl-2-hydroxy-n-propyl) imidazole (1)**

$^{1}$H NMR (400 MHz, CDCl3**)**

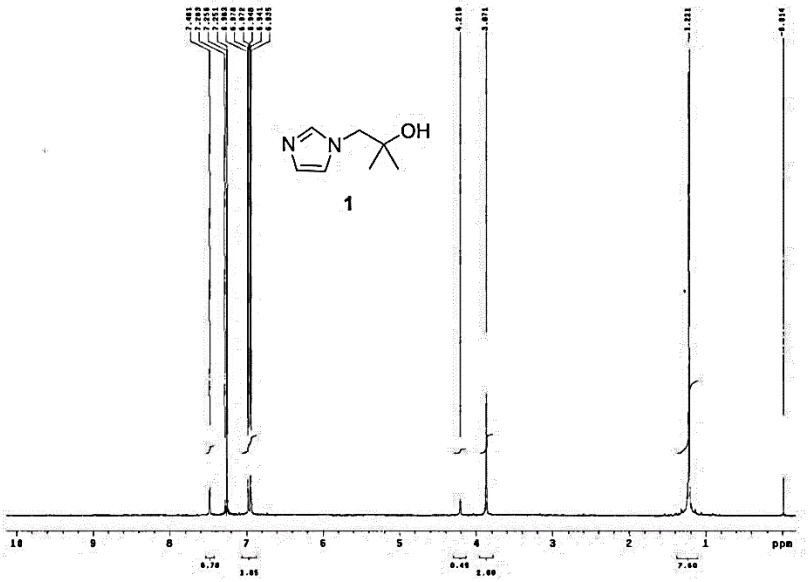


$^{13}$C NMR (100 MHz, $CDCl_3$)

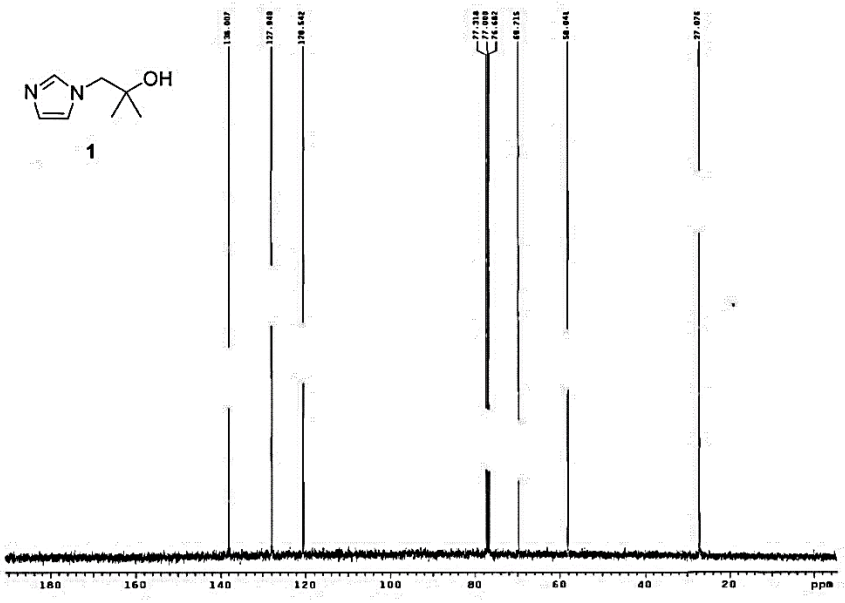

**2). 1-(2-Hydroxy-2-methyl-*n*-propyl)-3-methylimidazolium Mesylate [$C_1$-$^t$OH][OMs]**

$^1$H NMR (400 MHz, $CDCl_3$)

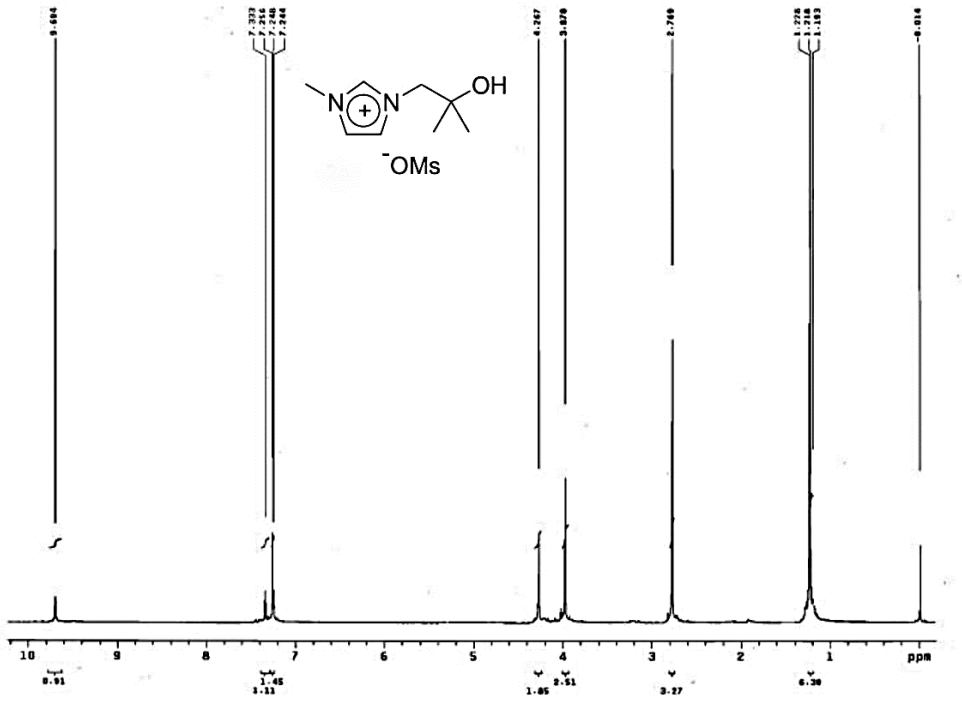


$^{13}$C NMR (100 MHz, $CDCl_3$)

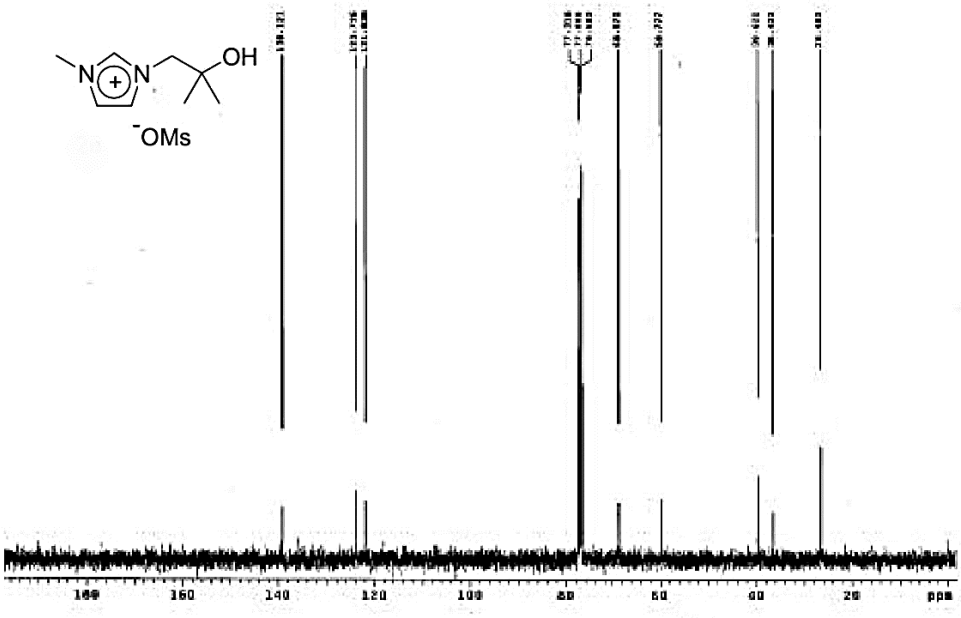

**3). 1-(2-Hydroxy-2-methyl-*n*-propyl)-3-isopropylimidazolium Mesylate [$C_3$-$^t$OH][OMs]**

$^1$H NMR (400 MHz, $CDCl_3$)

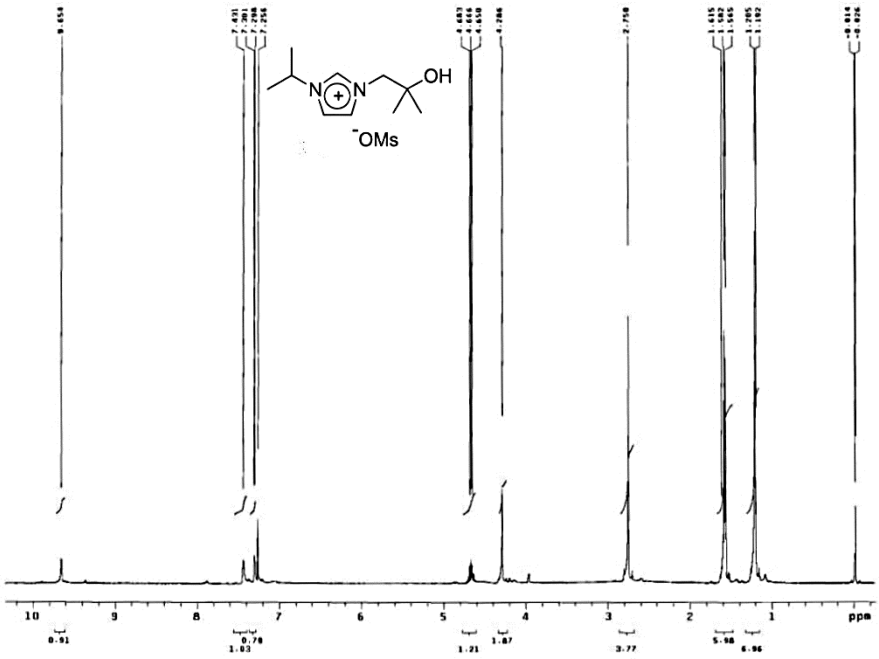


$^{13}$C NMR (100 MHz, $CDCl_3$)

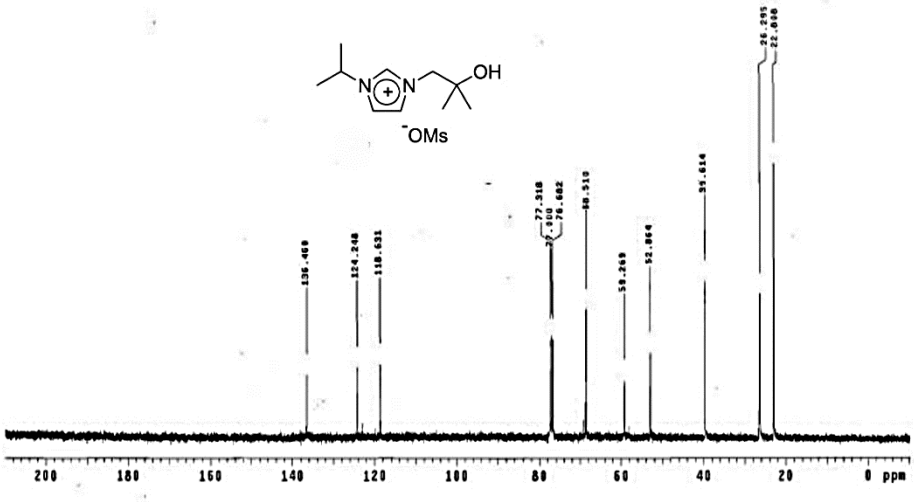

**4). 1-(2-Hydroxy-2-methyl-*n*-propyl)-3-*n*-butylimidazolium Mesylate [$C_4$-$^t$OH][OMs]**

$^1$H NMR (400 MHz, $CDCl_3$)

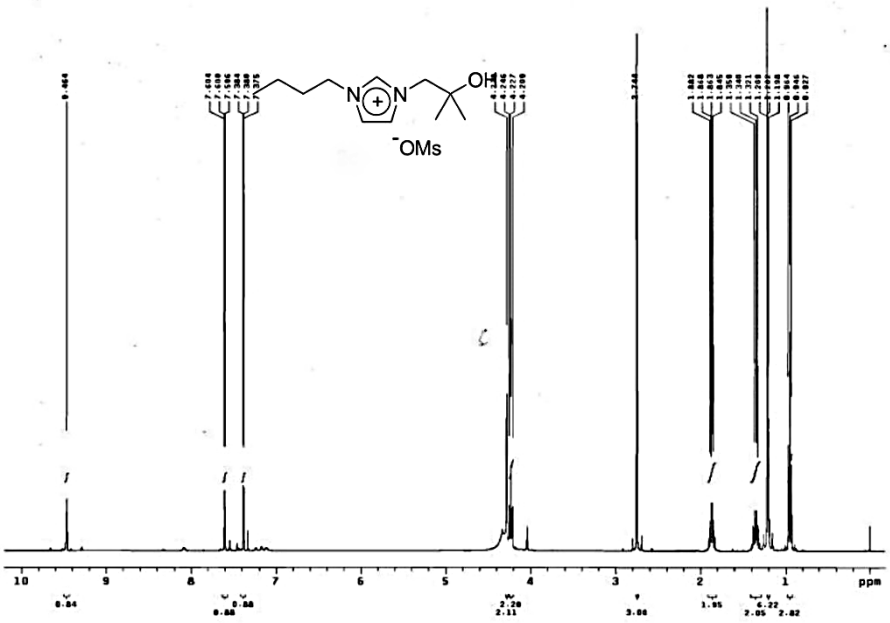


$^{13}$C NMR (100 MHz, $CDCl_3$)

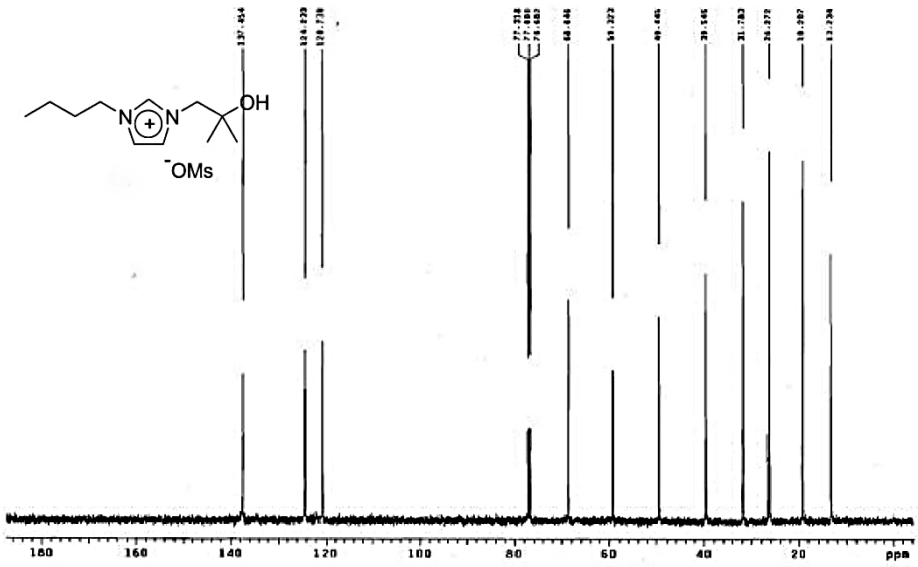

**5). 1-(2-Hydroxy-2-methyl-*n*-propyl)-3-*n*-hexylimidazolium Mesylate [$C_6$-$^t$OH][OMs]**

$^1$H NMR (400 MHz, CDCl3**)**

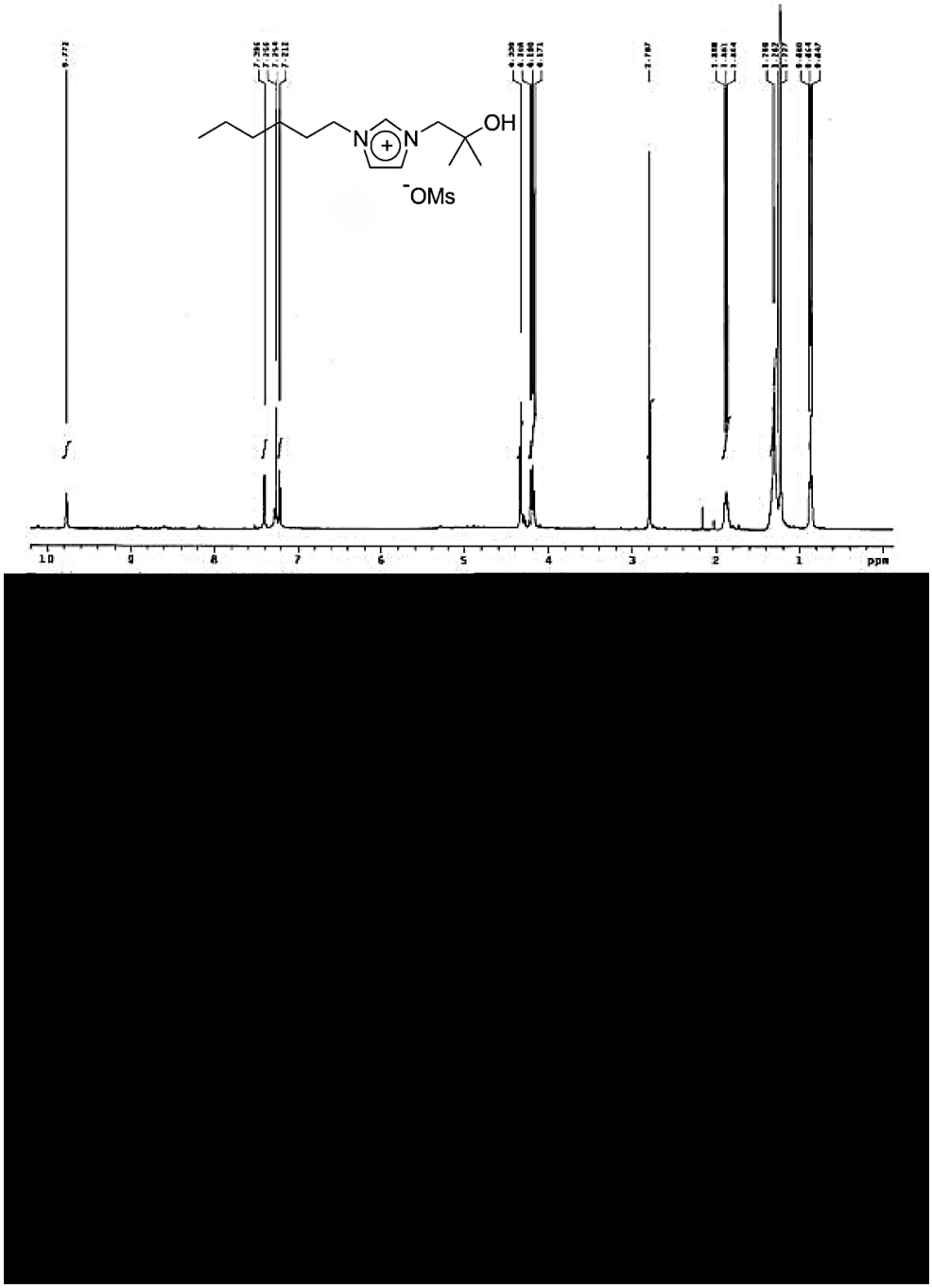

**6). 1-(2-Hydroxy-2-methyl-*n*-propyl)-3-*n*-octyllimidazolium Mesylate [$C_8$- $^t$OH][OMs]**

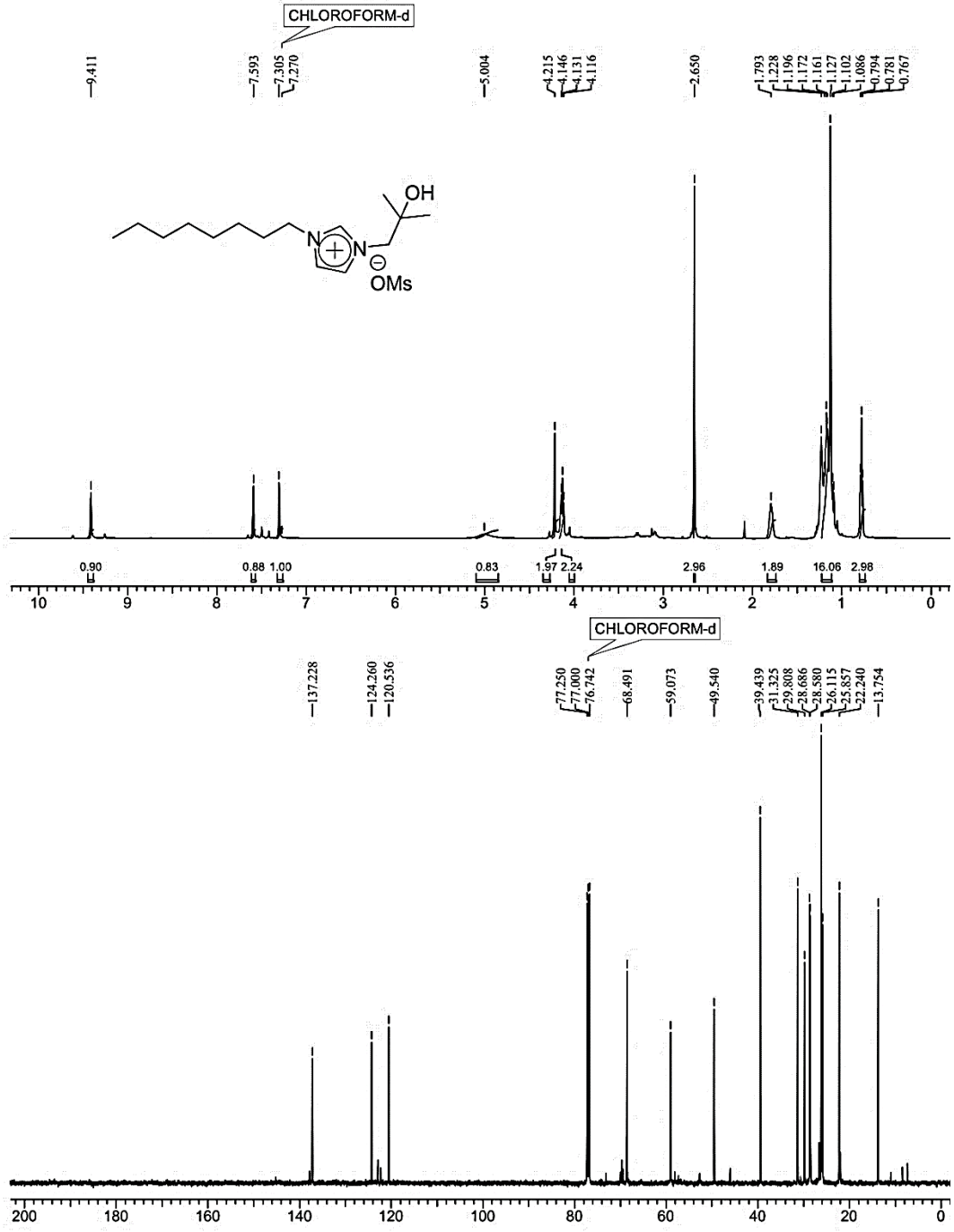

**7). 1-(2-Hydroxy-2-methyl-*n*-propyl)-3-*n*-decyliimidazolium Mesylate [$C_{10}$- $^{t}$OH][OMs]**

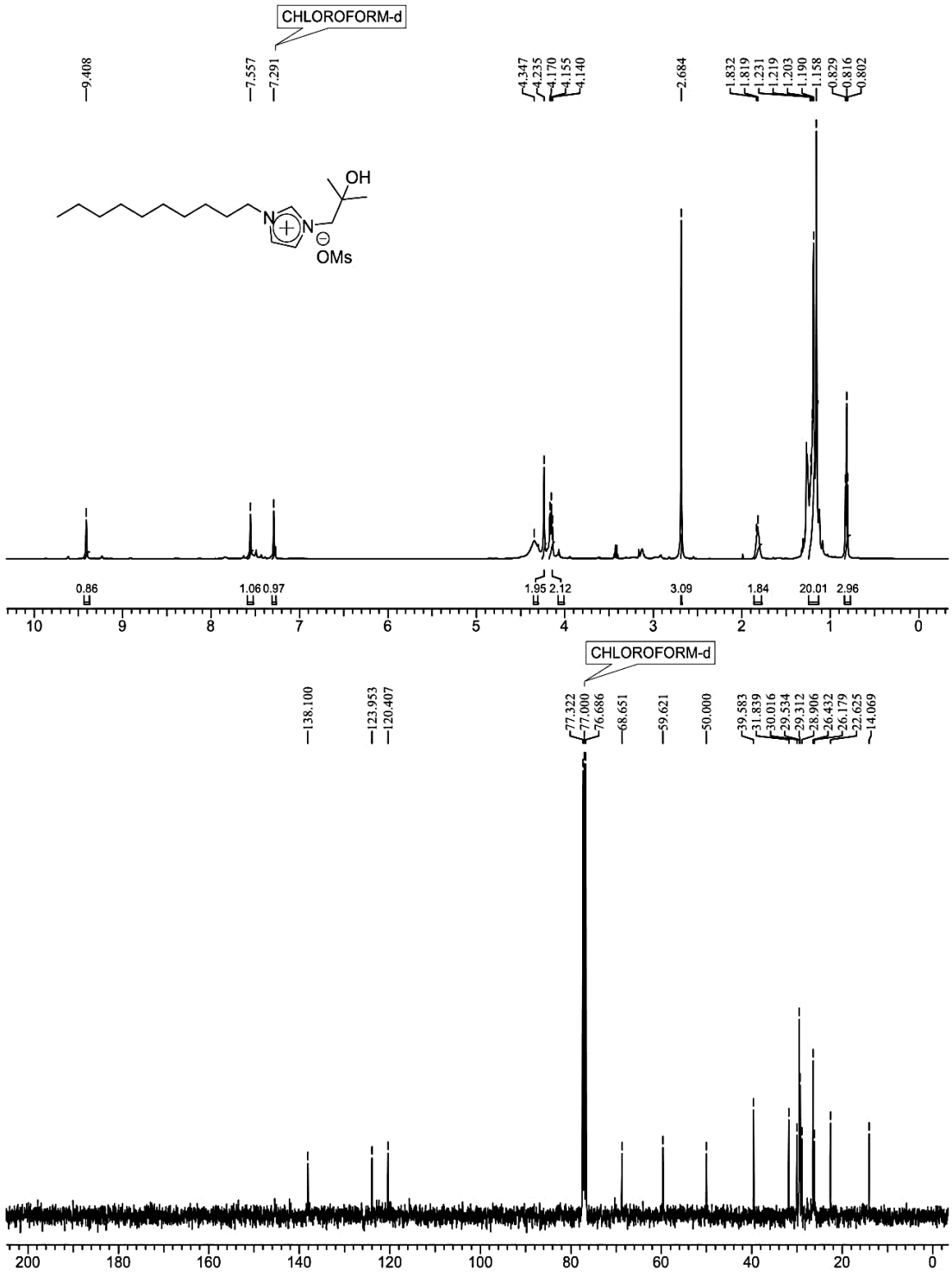

**8). 1-(2-Hydroxy-2-methyl-*n*-propyl)-3-*n*-dodecyliimidazolium Mesylate [$C_{12}$- $^{t}$OH][OMs]**

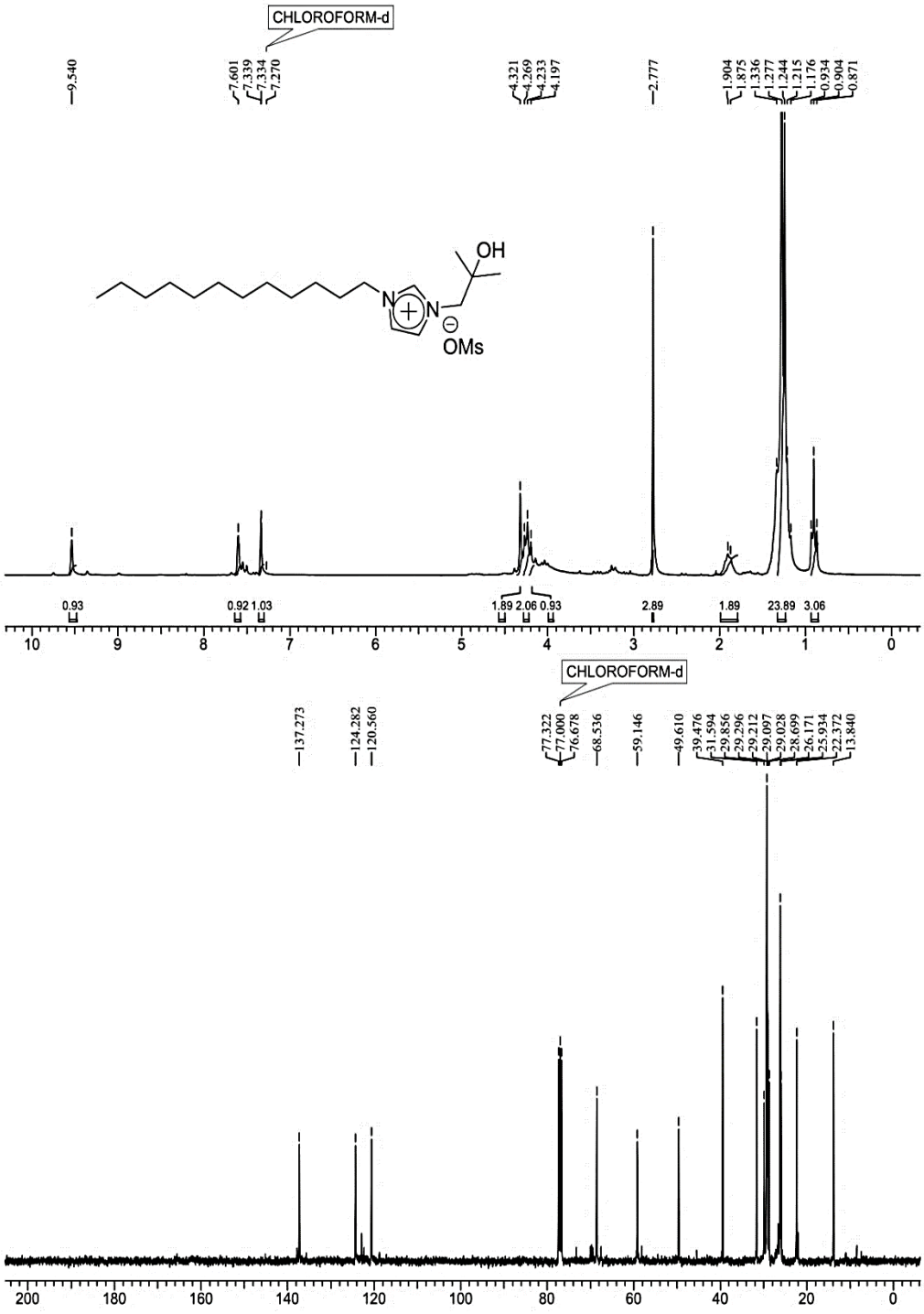

# Chapter 4
# Elucidation of Epi-cedrol cyclase mechanism

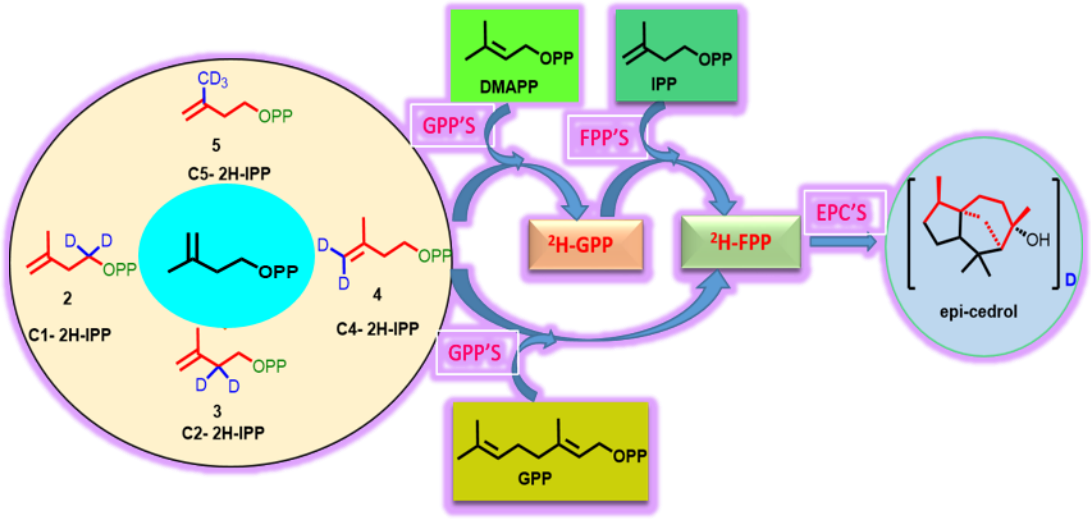

**Abstract**

*Epi*-cedrol synthase catalyzes the cyclization of (*E*,*E*)-farnesyl diphosphate (FPP) into *epi*-cedrol. In this chapter, we elucidated the source of oxygen in epi-cedrol biosynthesis by incubating FPP with *epi*-cedrol synthase in 21.6 atom % $H_2{}^{18}O$ buffer and GC-MS of assay extracts analysis. Further complete cyclization mechanism of *epi*-cedrol biosynthesis was elucidate based on the gas chromatography coupled to electron impact mass spectrometry fragmentation data of deuterated ($^2H$) *epi*-cedrol analogues. The chemo-enzymatically method was applied for the specific synthesis of 8-position labelled farnesyl pyrophosphate and epi-cedrol. Overall, these results showed that the molecular ion 224 *m/z*, instead of 222 *m/z* for *epi*-cedrol in GC-MS analysis when in $H_2{}^{18}O$ was supplied in assay buffer. These labeled oxygen study, revealed that the hydroxyl group of *epi*-cedrol cyclase enzymatic product, *epi*-cedrol was derived from water molecule, not from the phosphate moiety of the FPP. In the final elucidation of cyclization mechanism, we labelled 8-positions of FPP and *epi*-cedrol with deuterium by using four labelled IPPs. The EI-MS fragmentation ions were compared with non-labelled ions. These isotopic mass shift fragments suggested that the $^2H$ of C6 migrates to the C7 position during the cyclization mechanism.

## Introduction

More than 70,000 terpenoid molecules were isolated or synthesized, which has diverse chemical structures and possess numerous biological activities such as antibiotics, toxins, and pheromones (Bohlmann and Keeling, 2008; Kirby and Keasling, 2009; Vickers et al., 2017). Numerous terpene cyclase enzymes are isolated from bacteria, fungi, and plants, but only few have been investigated and characterized (Dickschat, 2016; Singh and Sharma, 2015). Isopentenyl pyrophosphate (IPP) is the universal precursor for the biosynthesis of isoprenoids. IPP plays a key role in extending linear alkyl pyrophosphates, such as geranyl pyrophosphates (GPP), farnesyl pyrophosphates (FPP) and geranylgeranyl pyrophosphates (GGPP), which finally triggered by terpene cyclase leads to the production of diverse hydrocarbon skeletons (Christianson, 2006; Christianson, 2017).

Few of sesquiterpene cyclase catalyse the cyclization of the linear substrate, FPP into complex hydrocarbon skeletons (Fraga, 2013; Matejić et al., 2010; O'Maille et al., 2006). Further pathway enzymes, mainly cytochrome P450 mono-oxygenase functionalize the metabolites, which will get the highly stereo- and regio-specific diverse class of molecule (Baunach et al., 2015). The cyclic cascade involved various reaction mechanism such as specific rearrangements; multiple cascade cyclisation, Wagner-Meerweinre arrangements, hydride shifts, and stereo-selective reactions *via* cationic intermediates to achieve unique diverse complex cyclic hydrocarbon skeletons (Mander and Liu, 2010; Townsend and Ebizuka, 2010). However there are many instances that, the cyclization of FPP leads to the formation of alcohol as a products.

Indeed sesquiterpene synthases, such as *epi*-cubanol synthase from *Streptomycetes spp.*, patchoulol synthase from *Pogostemoncablin* (patchouli), *epi*-cedrol synthase from *Artemisia annua*, τ-cadinol synthase from *Lavandula angustifolia* are known to produce sesquiterpenoid alcohols *epi*-cubanol (Cane et al., 1993; Cane and Ke, 2000; Cane and Tandon, 1995), patchoulol (Croteau et al., 1987; Faraldos et al., 2010; Hartwig et al., 2014), *epi-cedrol* (Brodelius et al., 2002; Mercke et al., 1999), and τ-cadinol (Jullien et al., 2014), respectively by quenching the respective final carbocation with oxygen nucleophile in stereospecific manner (**Fig. 1**).

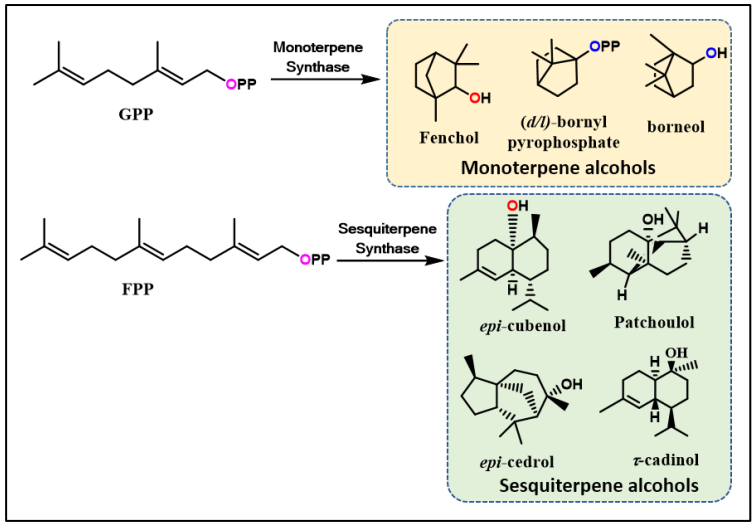


**Figure 1.** Few monoterpene and sesquiterpene alcohols from corresponding linear prenyl pyrophosphate.

Cane *et.al.*, explicitly showed the quenching of intermediate carbocation by pyrophosphate moiety in formation of monoterpene bornyl pyrophosphate and borneol (Cane et al., 1982)(**Fig. 1**) and also demonstrated that the pyrophosphate ester oxygen of geranyl pyrophosphate (GPP) is the original source of the both *d*- or *l*-bornyl pyrophosphate formation. Further conversion of the pyrophosphate to its corresponding secondary alcohols products (+)- and (-)-borneol derived by phospho-hydrolase-catalyzed hydrolysis of pyrophosphate ester moiety (Croteau et al., 1985; Whittington et al., 2002; Wise et al., 1998). Oikawa and co-worker investigated the cyclization mechanism of various terpenoids biosynthesis (Oikawa et al., 2001; Wise et al., 2001). Despite the active site of sesquiterpene synthase usually hydrophobic in nature to avoid improper quenching of the cationic intermediate with an external nucleophile including water (Oikawa et al., 2001; Wise et al., 2001). Few of them are exceptional, whose source of oxygen examined by isotopic labelling assay at the enzyme level includes the sesquiterpenes *epi*-cubenol (Cane and Ke, 2000), patchoulol (Faraldos et al., 2010) and monoterpene alcohol fenchol (Croteau et al., 1984). The example of fenchol and *epi*-cubenol clearly revealed that the unusual efficient quench of the carbocation involves the stereo-selective capture of oxygen nucleophile water.

The complete biosynthesis mechanism of enzymes mostly investigated by feeding isotope-labelled precursors to terpene cyclase reaction. The commonly used

isotopes are deuterium, ($^{2}$H), carbon ($^{13}$C) and tritium ($^{3}$H), for the characterization of enzymes and study the biosynthesis pathway. This including patchouli alcohol synthase, cadinene synthase, and geosmin synthase *etc.* (Faraldos et al., 2010; Faraldos et al., 2012; Gatto et al., 2015; Jiang and Cane, 2008; Savage and Croteau, 1993; Scholte and Vederas, 2006). Among this, deuterium ($^{2}$H or D) is most common due to its physicochemical properties such as naturally-occurring, stable, non-radioactive isotope of hydrogen. Hydrogen (H) having one electron and one proton and final atomic Mass 1.0 AMU while deuterium (D) having one electron and its nucleus contains one neutron and one proton, which results an atomic mass of approx. 2.0 AMU (Shao et al., 2014). We have selected these D-labelled substrates for study because of D-C bonds are about 6 to 10 times more stable than the corresponding C-H. It is used for to determine the reaction mechanism as well as identification of drug targets (**Figure 2**) (Djerassi and Tökés, 1966; Gant, 2014).

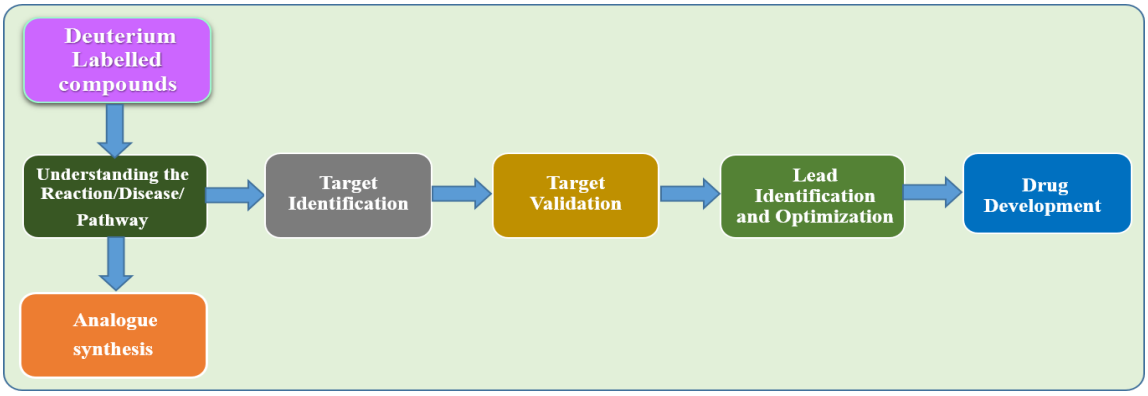


**Figure 2.** Various applications of deuterium labelled compounds.

There are many conventional method are reported to trace isotopically-labelled products derived from enzyme catalysts, such as nuclear magnetic resonance (NMR) spectroscopy, which is generally requires milligram amounts of product for complete analysis. Thus to synthesis a sufficient amount of product required high quantities of labelled precursors and enzymes (Meguro et al., 2015). Recently, the cyclization mechanisms of complex cyclic terpenes such as epicubebol, iso-dauc-8-en-11-ol (Rabe and Dickschat, 2016), pristinol synthase (Klapschinski et al., 2016), phomopsene (Shinde et al., 2017), spiro-albatene (Rinkel et al., 2018) and 18-hydroxydo labella-3,7-diene (Dickschat et al., 2017) have been studied by gas chromatography coupled to electron impact mass spectrometry (GC/EI-MS). The key advantage of GC-MS

analysis, is that it requires less amount of product compared to NMR spectroscopy, and is also a highly sensitivity, rapid method of analysis (Miller et al., 2007; Rabe et al., 2015). The chemical synthesis of specific position labelled linear prenyl pyrophosphate is time consuming, laborious, and requires a multistep reaction process (Ito et al., 1987; Kobayashi et al., 1985). To overcome these problems, a chemo-enzymatic strategy can be considered as an alternative protocol for the rapid synthesis of a specific precursor (Shinde et al., 2017).

As discussed in chapter 3, *epi*-cedrol synthase enzyme has been cloned and functionally characterized from *A. annua*, a source of the potent anti-malarial drug, Artemisinin, and is known to catalyzes the electrophilic cyclization of achiral universal diphosphate substrate FPP to *epi*-cedrol as a major enzymatic product with traces of cedrol and some hydrocarbons (Klayman, 1985; Mercke et al., 1999). Although, *epi*-cedrol synthase has been well studied, very little is known regarding the mechanism involved in *epi*-cedrol biosynthesis and the source of the oxygen atom.

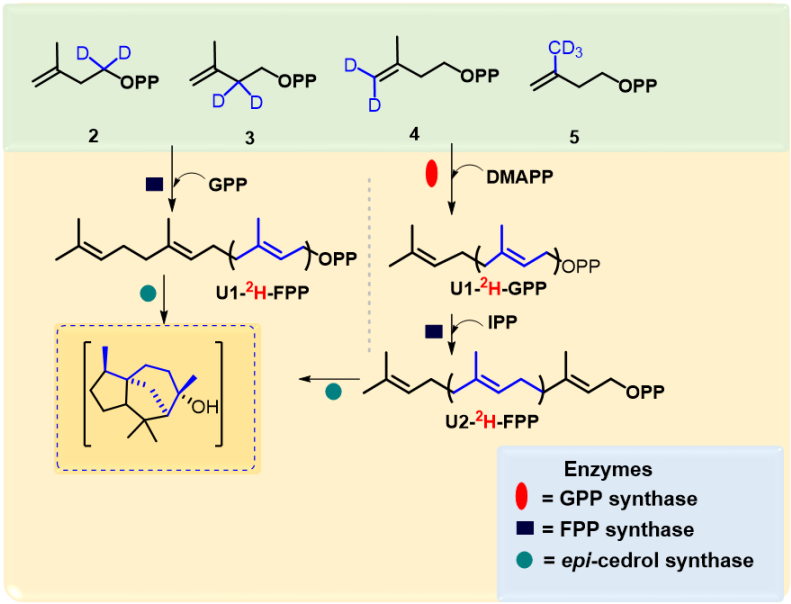


**Figure 3**.Strategy to specifically synthesize deuterium-labelled *epi*-cedrol using a chemo-enzymatic method

Our group studied the interface of chemistry and biology with a particular emphasis on reaction mechanism (Navale et al., 2015a; Shinde et al., 2017). In this chapter, in *section A*, we studied the source of oxygen atom in *epi*-cedrol biosynthesis by carrying out the enzyme assay in $H_2{}^{18}O$ labelled water. In *Section B*, a chemo-

enzymatic strategy was applied to synthesise ($^2$H)-labelled-*epi*-cedrol and investigated the cyclisation mechanism of *epi*-cedrol synthase (ECS) by EI-MS fragmentation ions compared with non-labelled species and isotopic mass shift fragments (**Fig. 3**). In this strategy, the chemically prepared synthetic four (D)-IPPs **2–5** were used for the elongation to ($^2$H)-FPP with dimethylallyl pyrophosphate (DMAPP) and GPP through sequential terpene cyclase reactions. The subsequent cyclisation by ECS yielded specific 8-position labelled *epi*-cedrol analogues, which were analysed by GC-MS.

## Materials and Reagents

- Dimethylallyl pyrophosphate (DMAPP) (Sigma-Aldrich)
- Isopentyl pyrophosphate (IPP)
- Deuterium labelled Isopentyl pyrophosphate (D-IPP)
- Geranyl diphosphate (GPP)
- Farnesyl diphosphate (FPP)
- Nuclease Free Water (Himedia, India)
- $H_2{}^{18}O$ water (97% $^{18}O$ atom, Sigma-Aldrich)
- BenchMark® Prestrained Protein ladder (Invitrogen-Thermo Fisher Scientific)
- Tris-HCl (Himedia, India)
- Ammonium bicarbonate (Himedia, India)
- Magnesium chloride (Merck)
- Dithiothreitol, DTT (Sigma-Aldrich)
- Glycerol (Himedia, India)
- Hexane (Spectrochem Lab)
- Isopropyl thio-β-D-thiogalactopyranoside (IPTG) Sigma-Aldrich
- Antibiotics (*viz.* Kanamycin, Chloramphenicol) Sigma-Aldrich
- Terrific Broth (TB) (Himedia, India)
- *Epi*-cedrol synthase-pET28a (*Genbank* No. AF157059, *Life Technology, Germany*)
- *Escherichia coli*

  Strains: Top10, Rosetta DE3 (Invitrogen-Thermo Fisher Scientific)
- Assay Buffer pH 8.5 (25 mM Tris-HCl, 5 mM DTT, 10 mM $MgCl_2$, 10% glycerol)

# Section 4A

# Elucidation of source of oxygen atom in epi-cedrol biosynthesis

## 1. Methodology

### 1.1 Expression, characterization of e*pi-cedrol* synthase (ECS)

The gene encoding *epi-cedrol* synthase (*Genbank* AF157059) ECS, contained an open reading frame of 1641bp and encoded a protein of 547 amino residues was cloned into pET-28a (+) bacterial expression vector by Life Technologies, Germany. The gene was expressed in *E. coli* Rosetta DE3 host cells and soluble form of recombinant ECS was purified by using $Ni^{2+}$-NTA agarose affinity chromatography using HEPES buffer containing 35 mM imidazole, homogeneity of the purified enzyme analysed by SDS-polyacrylamide gel electrophoresis (SDS-PAGE) as detailed methodology mentioned in Chapter **3**.

### 1.2 *Epi*-cedrol synthase enzyme assay in presence of $O^{18}$ atom

Enzyme activity was assayed using FPP as a substrate, and was monitored by measuring the amount of sesquiterpene *epi*-cedrol released from FPP by the enzymatic reaction. In a typical, control enzyme assay, 200 µL reaction mixture containing assay buffer pH 8.5, purified ECS (2.2 µg, specific. act. 8 µmol/min/mg protein), 130 µM FPP and, while in $H_2{}^{18}O$ enzyme assay experiment, 36.5µL (21.6 atom%) $H_2{}^{18}O$ was incubated in shaker bath incubator (Brunswick, Eppendorf) at 30 ºC for 1 h 30 min at 60 rpm. The enzymatic reaction was stopped by an addition of 10 µl of absolute ethanol (95%) followed by vortex it for 30 sec, was extracted with hexane (3 × 0.5 mL), and concentrated by passing it with $N_2$ gas and the *epi*-cedrol was identified by GC-MS analysis analyzed as per mentioned protocol (Chapter 3). One unit of enzyme activity was defined as the amount of enzyme required to liberate 1 µmol of *epi*-cedrol/min under the assay conditions.

## 2. Results and Discussion

A sesquiterpene cyclase, *epi*-cedrol synthase from *A. annua* (*Aa*ECS) was expressed in *E.coli* Rosetta DE3 and purified by affinity chromatography, protein appeared expected molecular weight around 64.4 kDa. Pure ECS was eluted in HEPES buffer containing 35 mM imidazole. Purified fractions were pooled and concentration was 1.8 mg/mL, which was determined by Bradford method (**Fig. 4A**). GC-MS analysis of the enzyme assay containing purified *epi*-cedrol synthase and (*E*,*E*)-FPP indicated

the formation of *epi*-cedrol as a major metabolite (>92%) along with small traces α/β-cedrene and cedrol as shown in **Fig. 4B**.

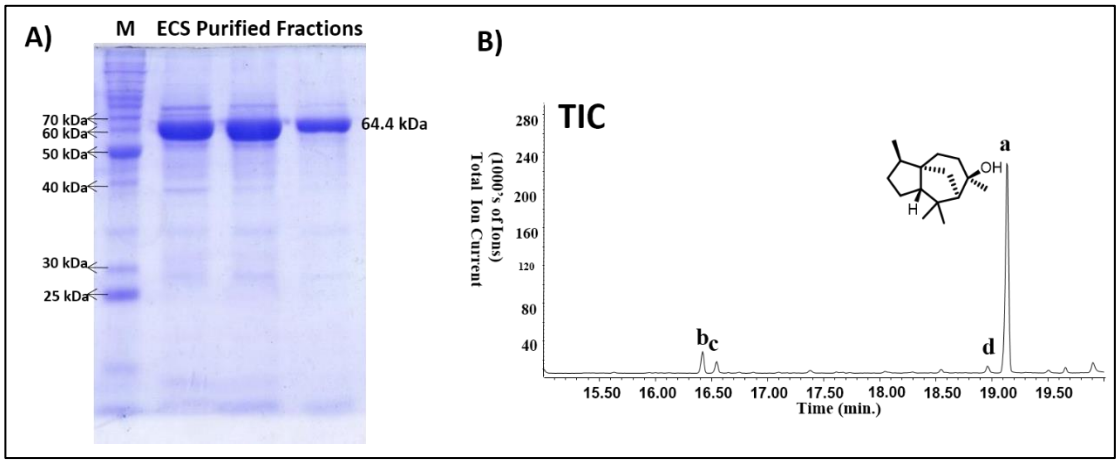


**Figure 4. A)** Marker and purified epicedrol synthase. **B**) GC–MS analysis (TIC) of *epi*-cedrol synthase enzyme assay (same for $H_2{}^{18}O$ and $H_2O$). Products: a) *epi*-cedrol, b) α-cedrene, c) β-cedrene, d) cedrol.

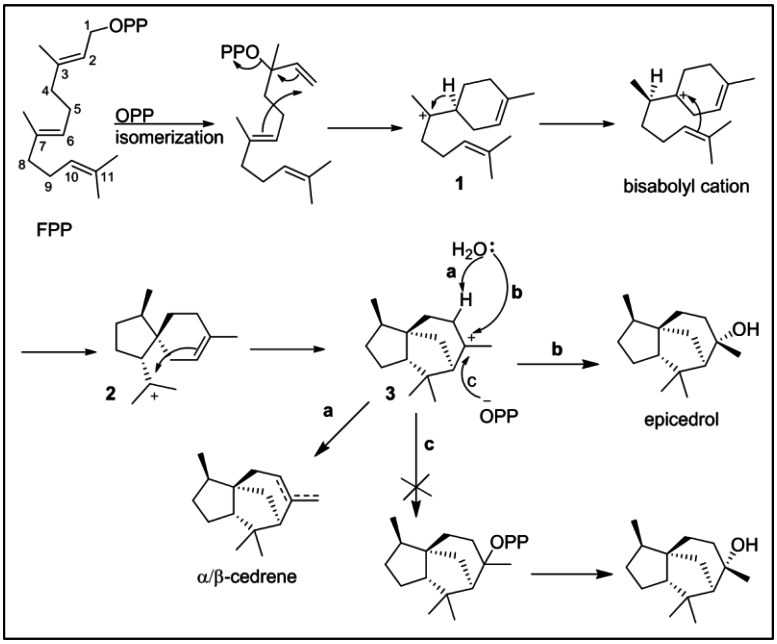


**Scheme 1.** Proposed mechanisms of *epi*-cedrol synthase, path a) elimination of H; path b) addition of OH from water, and path c) by OPP addition then hydrolysis.

This divalent metal dependent cyclization mechanism initiate the reaction by ionization of FPP to delocalized farnesyl/nerolidyl carbocation followed by series of electrophilic cyclization including a hydride shift from C-6 to C-7 to generation of

bisabolyl cation (**Scheme 1**). Then *si*-face attack of the C-10 olefin initiated two subsequent cyclizations to form exo-cyclic acordane and tricyclic cedrane skeletons by C-10 to C-6 and C-2 to C-11 ring closure, respectively. Generated tricyclic intermediate carbocation **(3**, **Scheme 1**) may be quenched by following three pathways: (**a**) deprotonation of either 15-H or 4-Hwhich produces two sesquiterpene hydrocarbons α-cedrene and β-cedrene, respectively or (**b**) stereo-selective addition of water to form cedrol/*epi*-cedrol, or (**c**) capture pyrophosphate anion present in the active site followed by hydrolysis to generate cedrol /epi-cedrol.

| | ***Epi*-cedrol** | **Cedrol** | ***α*-cedrene** | **β –cedrene** |
|---|---|---|---|---|
| **Control** | 93.38% | 1.22% | 2.14% | 3.26% |
| **$H_2{}^{18}O$** | 80.75% | 0.98% | 7.18% | 11.09% |

**Table 1**. Comparision of sesquiterpene hydrocarbons and alcohols (%) in control ($H_2O$) and $H_2{}^{18}O$ assay.

To address this ambiguity on source of oxygen atom in epi-cedrol biosynthesis, *epi-cedrol* synthase was incubated with FPP in both isotopic labeled and unlabeled conditions, then obtained extracted product were characterized by GC and GC-MS analysis. GC and GC-MS analysis of the control assay extract obtained by incubating FPP with *epi-cedrol* synthase in normal buffer system indicated the formation of *epi*-cedrol as a major product along with traces of cedrol (1.2%), *α*-cedrene (2.1%) and β-cedrene (3.2%) (**Table 1**). The formation of these compounds was confirmed by comparing retention time and GC co-injection studies. EI MS of sesquiterpene alcohols, *epi-cedrol* and cedrol gave detectable molecular ion (M+) at *m*/*z* 222 along with other peaks including *m*/*z* 206 and *m*/*z* 204 formed from loss of hydroxyl fragment or water molecule, respectively. Notably, when *epi-cedrol* synthase was incubated with FPP in Tris-HCl buffer, pH 8.5, containing $MgCl_2$ in $H_2{}^{18}O$ (21.6 atom %), the product ratios were slightly changed as shown in **Table 2**. Interestingly, the enrichment of molecular ion at *m*/*z* 224 for both *epi*-cedrol and cedrol was observed, increased up to 32 fold in $H_2{}^{18}O$ compared to control assay. This results are correlated with the previously reported terpene cyclases, source of oxygen atom (Cane and Ke, 2000; Croteau et al., 1984).. This shift in the molecular ion clearly indicates the insertion of $^{18}O$ to *epi*-cedrol

and cedrol molecules. Furthermore, there was no shift observed for the peak at m/z 204 due to the loss of water molecule (**Fig. 5b**).

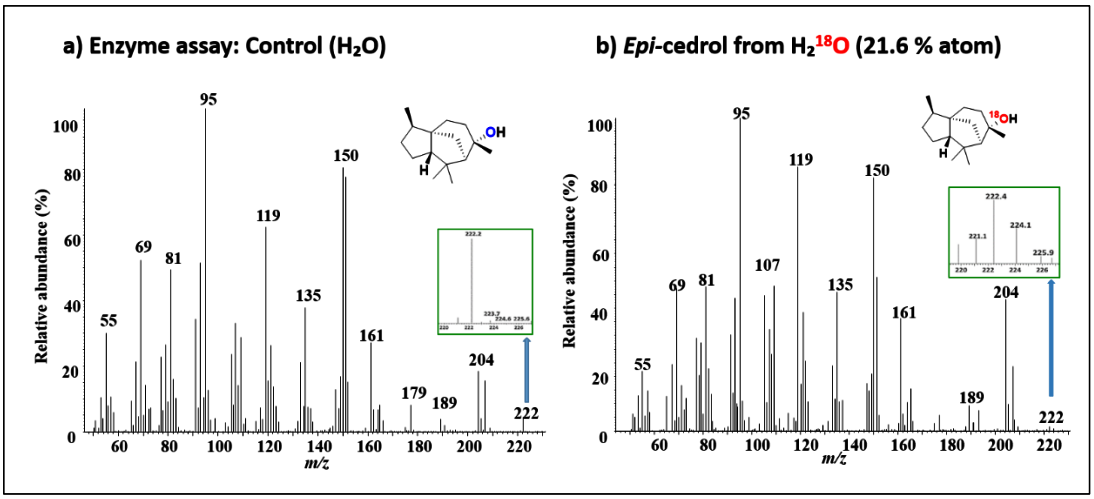


**Figure 5.** MS of product from FPP with control $H_2O$ (a), and $H_2{}^{18}O$ (b) enzyme assay. Inbox showed the enrichment of molecular ion *m/z* 222/224 in non-labelled and labelled *epi*-cedrol.

| EI mass (m/z) | 222 | 224 |
|---|---|---|
| Peak % (H216O) | 96.58 | 3.42 |
| Peak % (H218O) | 66.43 | 33.56 |

**Table 2.** Mass spectrometric analysis of molecular ion peaks of *Epi*-cedrol.

These results demonstrate that *epi*-cedrol and cedrol are formed through the quenching of cedryl carbocation **3** (**scheme 1**) by water molecule present in the active site either from *Si* or *Re*-face, respectively. However, Si-face seems to be more favorable as the epicedrol is the major enzymatic product. Furthermore, insertion of $^{18}O$ derived from $H_2{}^{18}O$ implies that both *epi*-cedrol and cedrol might not have formed through recapture of pyrophosphate anion present in the active site followed by the hydrolysis of corresponding diphosphate. The formation of corresponding sesquiterpene hydrocarbons α-cedrene and β-cedrene might be formed through deprotonation at 4-H and 15-H of cedryl carbocation (**3**), respectively.

# Section 4B

# Cyclization mechanism of epi-cedrol biosynthesis by Hydrogen ($^2H$) labelling

## 1. Methodology

### 1.1 Reagents

### 1.1 Synthesis of specific position labelled deuterium labelled IPP

To explore the structure-based mechanistic pathway of *epi*-cedrol biosynthesis, initially all four ($^2$H)-IPPs; (**2**-$^2H_2$)-IPP, (**3**-$^2H_2$)-IPP, (**4**-$^2H_2$)-IPP, and (**5**-C$^2H_3$)-IPP, as shown in **2–5** (**Scheme 1**), were synthesized from the starting material methyl acetoacetate (Han et al., 2017). The $^1$H, $^{13}$C and $^{31}$P NMR spectrum were recorded 500, 125 and 202 MHz on AV-500 and 400, 100 and 161 on AV-400 respectively on Bruker Avance-II. $CDCl_3$, D2O and TMS used as an internal standard ($CDCl_3$ at 7.27 ppm for $^1$H, 77.00 ppm for $^{13}$C and 4.75 ppm in $D_2O$ for $^1$H). Syntheses of this four d-IPP labelled at specific at positions deuterium, were synthesized in our chemistry laboratory by Dr. Madhukar Said, Organic Chemistry Division, NCL, Pune. All $^1$H and $^{13}$C NMR spectras analysis were added in the end of this chapter.

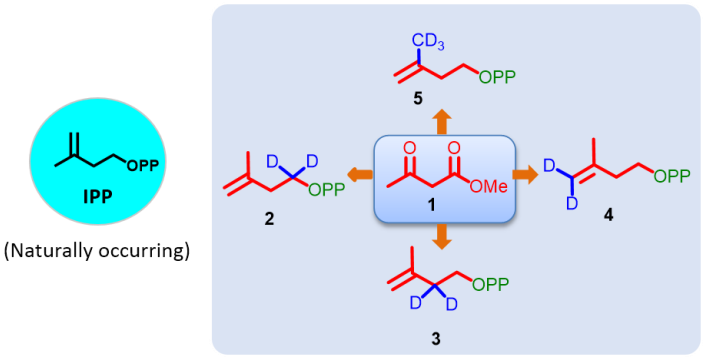


**Scheme 1.** Synthesized IPP, labelled with deuterium at various position.

### 1.2 Expression and purification of e*pi*-cedrol synthase (ECS), Farnesyl pyrophosphate synthase (FPPS)

The expression and purification of *Abis grandis*, Geranial pyrophosphate synthases (*Ag*GPPS, *Genbank* No. AF513112), farnesyl pyrophosphate synthase (FPPS, *Genbank* No. KF011939) and *epi*-cedrol synthase (ECS, *Genbank*. No. AF157059), reported previously (Shinde et al., 2016; Shinde et al., 2017; Srivastava et al., 2015) and detailed protocol same as mentioned in this chapter, *section A*.

### 1.3 *Epi*-cedrol synthase enzyme assay in presence D-labelled IPP

Enzyme assay was assayed using IPP and DMAPP as a basic substrate, and was monitored by measuring the amount of sesquiterpene *epi*-cedrol released from FPP by the sequential enzymatic reaction of GPPS and FPPS.

❖ **Labelling of first unit of FPP and *epi*-cedrol with deuterium**

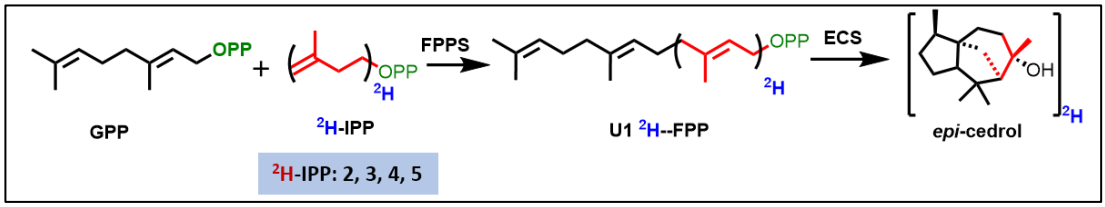


**Scheme 2.** Unit 1 labelling of FPP by feeding ($^2$H)-IPPs in enzyme assay.

In a typical, 250 µL of enzymatic reaction mixture containing Tris-Assay buffer pH 8.5 (25 mM Tris-HCl, 2.5 mM DTT, 10 mM $MgCl_2$, 10% glycerol), GPP (150 µM) 100 µM $^2$H-IPP (C**1**-$^2H_2$, C**2**-$^2$H, C**3**-$^2H_2$, C**4**-$^2H_3$), FPPS (25 µg) incubated at 30 ºC for 2 h at 60 rpm. After that *epi*-cedrol synthase (ECS, 25 µg) enzyme was added in each assay and keep it for another 1 h incubation at 30 ºC at 60 rpm (**Scheme 2**). All the enzymatic reaction was stopped by an addition of 10 µl of absolute ethanol (95%), and was extracted with hexane (3×500 µL), hexane layer was removed by passing it with $N_2$ gas. Labelled *epi*-cedrol was identified by GC/EI-MS analysis by using Agilent Technology 5975-7890 GC-MS system with a HP-5MS capillary column as mentioned in Chapter 2 & 3. Mass spectral data were collected at 70 eV and analysed by using MSD Chem station software.

❖ **Labelling of GPP, Second unit of FPP, and *epi*-cedrol with deuterium**

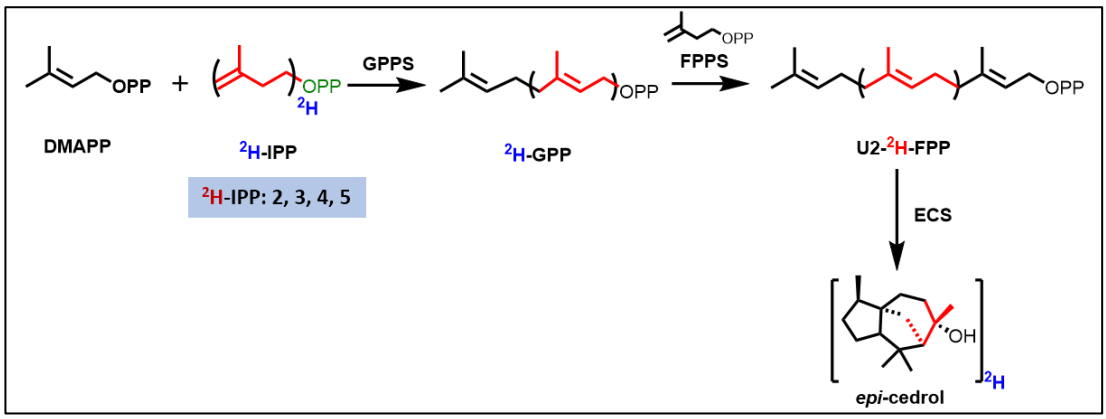


**Scheme 3.** Unit 2 labelling of FPP by feeding ($^2$H)-IPPs in enzyme assay.

For second unit labelling of FPP, a 250 µL enzymatic reaction mixture containing Tris assay buffer (pH 8.5) purified *Ag*GPPS (50 µg), 100 µM $^{2}$H-IPP (C2-$^{2}H_2$, C3-$^{2}H_2$, C4-$^{2}H_2$, C5-$^{2}H_3$) (for control non-labelled IPP used), 150 µM DMAPP incubated at 30 ºC for 12 h/overnight at 60 rpm (in water bath). After incubation GPPS was removed by using 10 kDa cut off filter to avoid double deuterium labelling. IPP (100 µM) was added along with FPPS (25 µg), and ECS (25 µg) enzymes in each enzyme assay tube. Again incubated it for 2 h at 30 ºC at 60 rpm (**Scheme 3**). All the enzymatic reaction was stopped by an addition of 10µl of absolute ethanol (95%) and proceed further and analyzed by GC/EI-MS, as per above mentioned protocols.

## 2. Results and Discussion

Deuterium ($^{2}$H or D) is a naturally-occurring, stable, non-radioactive isotope of hydrogen which are recently used in the elucidation of cyclization mechanism of several terpene cyclases (Cane et al., 1993; Shinde et al., 2017). The GC-EI-MS mass gave the accurate prediction of labelling of specific position of isoprenoids at very less product concentrations (Jin et al., 2005). The use of heavy isotope in enzymatic reactions changes the product ratio compared with non-labelled cyclic products. The kinetic isotope effects (KIE)s is considered to be one of the most essential and sensitive tools for the study of reaction mechanism, the knowledge of which allows the improvement of the desirable qualities of the corresponding reactions. Gatto *et al.*, 2015, observed KIEs, corresponding to a difference of 5 to 6 deuterium atoms between the substrates (GPP and FPP), were in the range of $k_H/k_D$ = 2.91–5.68. These values were similar to with those observed for terminating deprotonation reactions of other monoterpene cyclases. In case of substrates differing by only one deuterium atom, the observed KIEs were much smaller (within a range of kH/kD = 1.10–1.18) (Gatto et al., 2015). Our group were used 22 % of $H_2O^{18}$ water in enzymatic assay, the total isotopic mass ratio was also showed above 1 as only single heavy isotope was used.

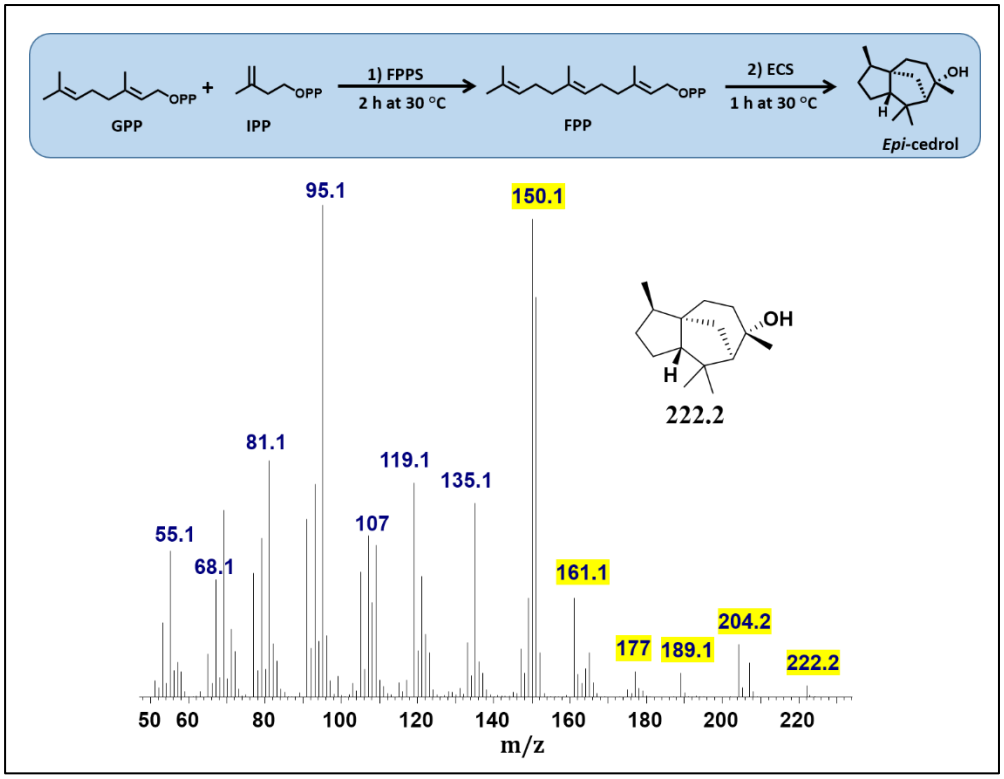


**Figure 1**. Non-labelled (control) mass spectra of *epi*-cedrol derived from GPP and unlabelled IPP by sequential enzymatic reactions.

For the analysis of complete cyclization mechanism of *epi*-cedrol, feeding ($^2$H)-IPPs **2**–**5** in enzyme assay were carried out with the help of GPP synthase, FPP synthase and EC synthase enzymes. The unit-1 (U1) in the FPP labelling was achieved by FPP synthase assay between GPP and 2–5, to give (2-$^2H_2$), (3-$^2$H), (4-$^2H_2$) and (5-C$^2H_3$)-FPP (as shown in **Scheme 2** and **Fig. 2**). Subsequent cyclisation by ECS yielded products to be analysed by GC/EI-MS. The obtained fragmentation ion data were compared with non-labeled *epi*-cedrol, as shown in **Fig. 1**. The other four positions of the U2 of FPP were labeled by (2-U2-$^2H_2$), (3-U2-$^2$H), (4-U2-$^2H_2$) and (5-U2-C$^2H_3$)-FPP by similar chemo-enzymatic methods using DMAPP, then subsequently exposed to FPP synthase, and ECS yielded deuterated EC analogues as shown in **Fig. 4**.The products were analyzed by GC/EI-MS as mentioned in methodology section. The comparative fragmentation patterns of unlabeled (**Fig. 1** and **3**) and ($^2$H)-*epi*-cedrols were studied. Their plausible structures were drawn after comparing the increased isotope mass shift fragments, as shown in **Fig. 5**.

**Figure 2.** Deuterium ($^2H_2$) labelled mass spectra of *epi*-cedrol derived from GPP and $^2H_2$-IPP's or (a) C1-$^2H_2$ FPP, (b) C2-$^2H$ FPP, (c) C3-$^2H_2$ FPP, and (d) C15-$^2H_3$ FPP by sequential enzymatic reactions.

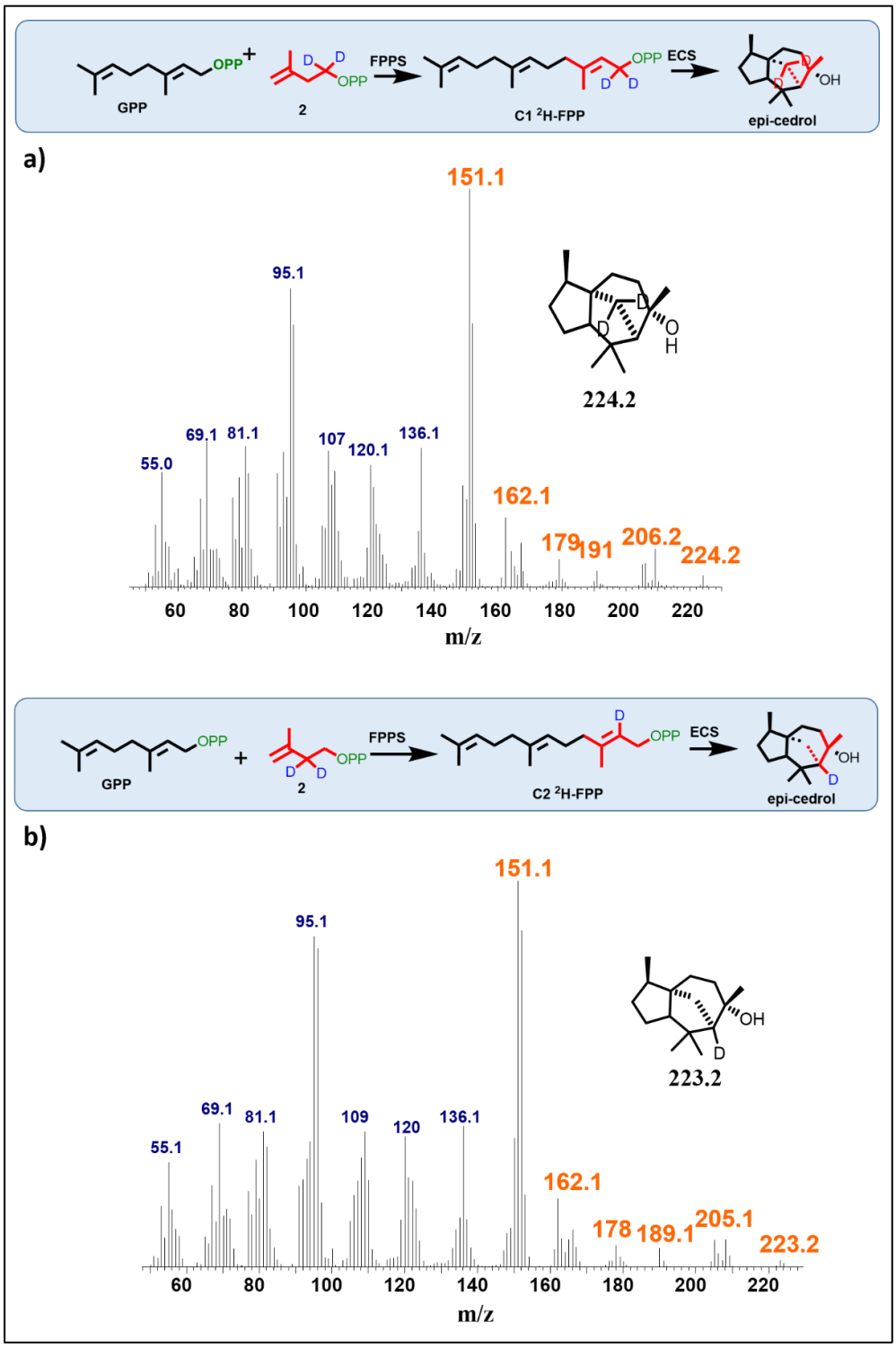

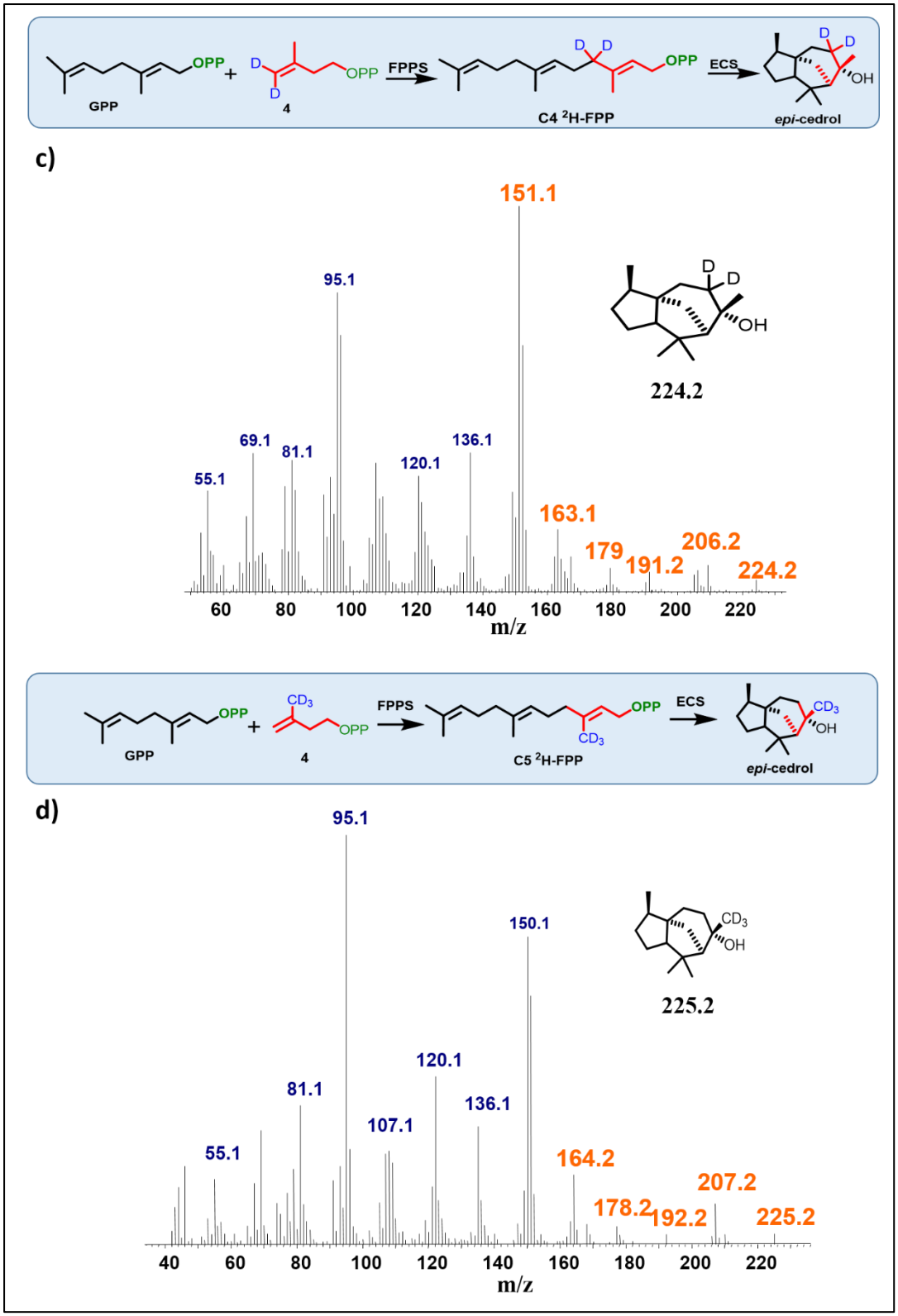


The selected major fragments of *epi*-cedrol for analysis was the molecular ion $[M]^+$ peak at m/z = 222 ($EC_{222}$), m/z = 95 ($EC_{95}$), m/z = 204 ($EC_{204}$), m/z = 161 ($EC_{161}$), m/z = 150 ($EC_{150}$) and m/z 119 ($EC_{119}$). The origin of fragment $EC_{204}$ reveals a

position-specific mass shift in the formation of m/z = 204 by the elimination of water molecules with the loss of hydrogen. The fragment ion was observed for all 8 position-labelled *epi*-cedrols with an increased mass of +1, as observed for m/z = 205 in the experiment with (2-$^{2}$H)-FPP. Mass shifts of +2 and +3 were observed at m/z = 206 and m/z = 207 in the spectra of (1-$^{2}H_2$), (4-$^{2}H_2$) and (15-C$^{2}H_3$)-FPP, as shown in **Fig. 2-5**. The electron impact ionization data of the *epi*-cedrols suggest the loss of an electron from the oxygen lone pairs to form $\mathbf{B}^{+\bullet}$, followed by hydrogen elimination with the loss of $H_2O$ to generate the fragment m/z = 204. This fragment ion structurally supports our $H_2{}^{18}O$ assay of *epi*-cedrol biosynthesis as mentioned in previous *section A*, where the tertiary cation intermediate was quenched with water molecule (Shinde et al., 2016).

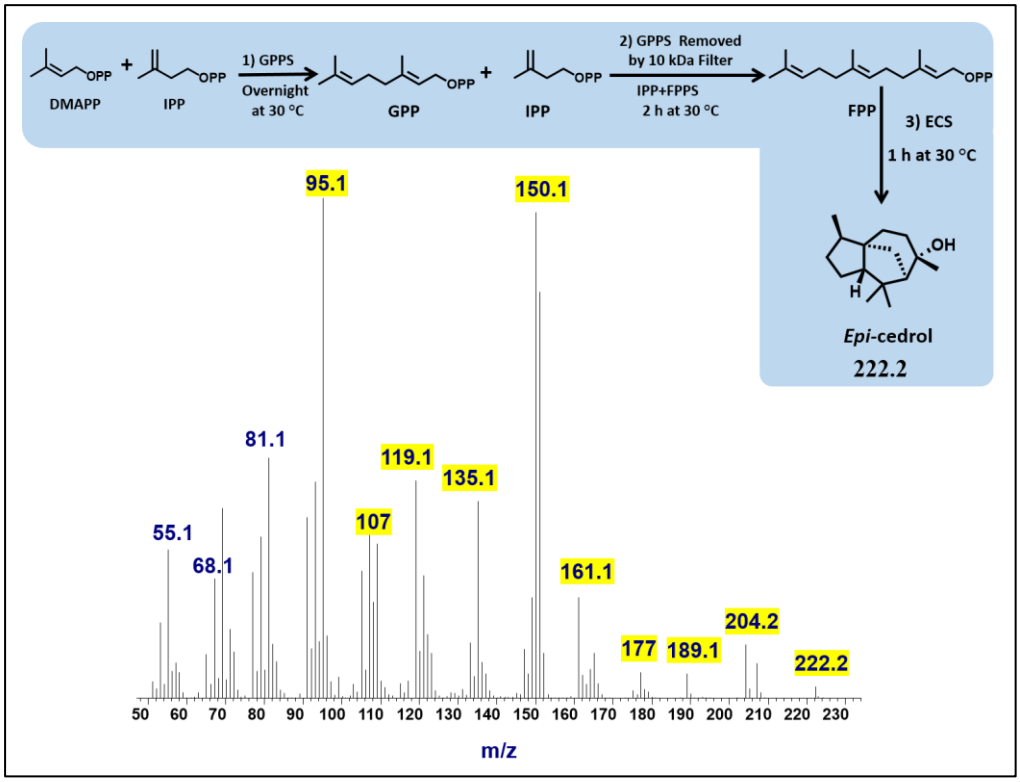


**Figure 3.** Un-labelled mass spectra (control) of *epi*-cedrol derived from IPP and DMAPP by sequential enzymatic reactions of GPPS, FPPS and ECS.

**Figure 4**. Deuterium ($^2H_2$) labelled mass spectra of *epi*-cedrol derived from DMAPP and $^2H_2$-IPP's or (a) $^2H_2$ GPP & FPP, (b) $^2H$ GPP & FPP, (c) $^2H_2$ GPP &FPP, and (d) $^2H_3$ GPP & FPP by sequential enzymatic reactions of GPPS, FPPS and ECS respectively.

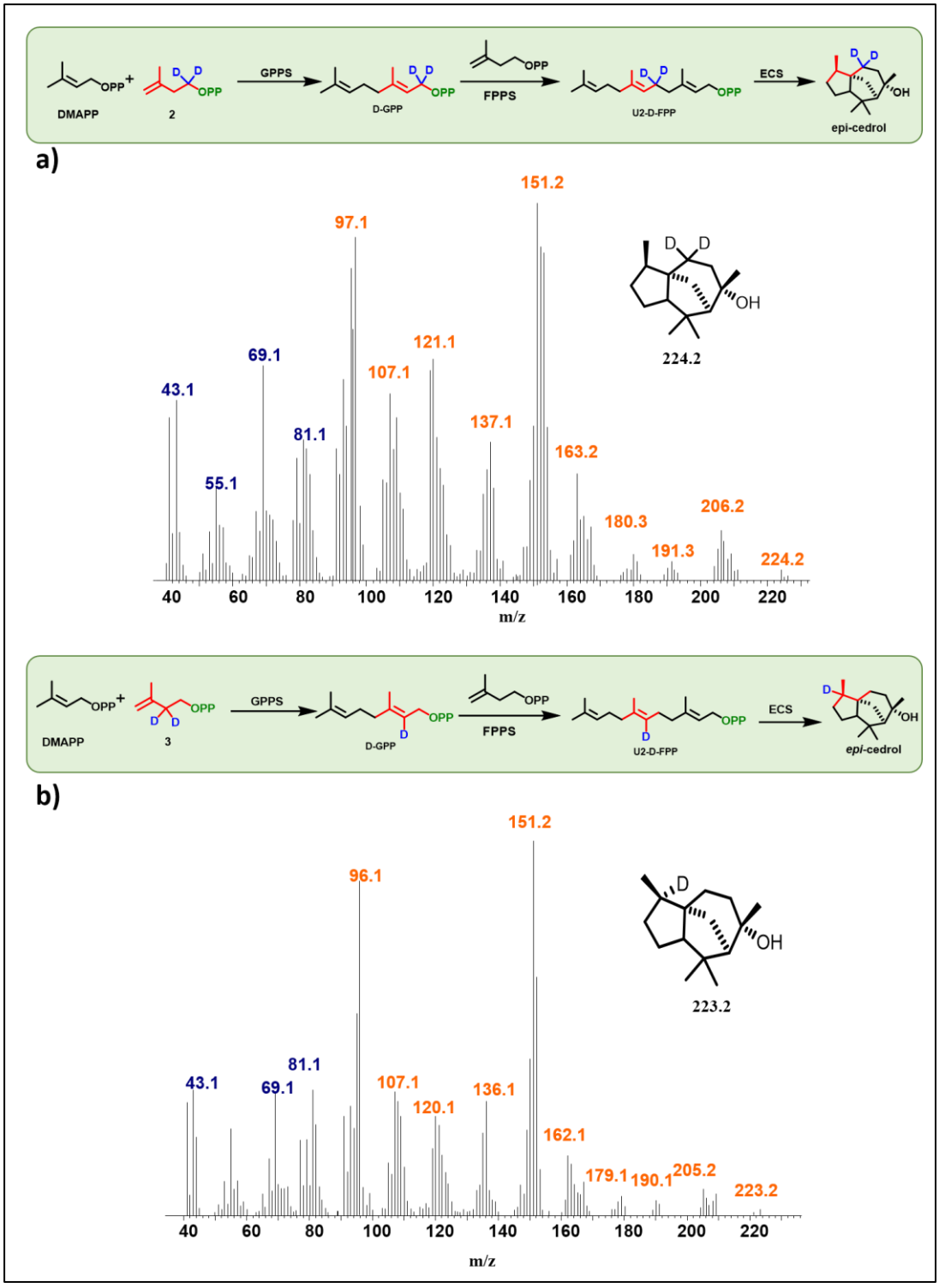

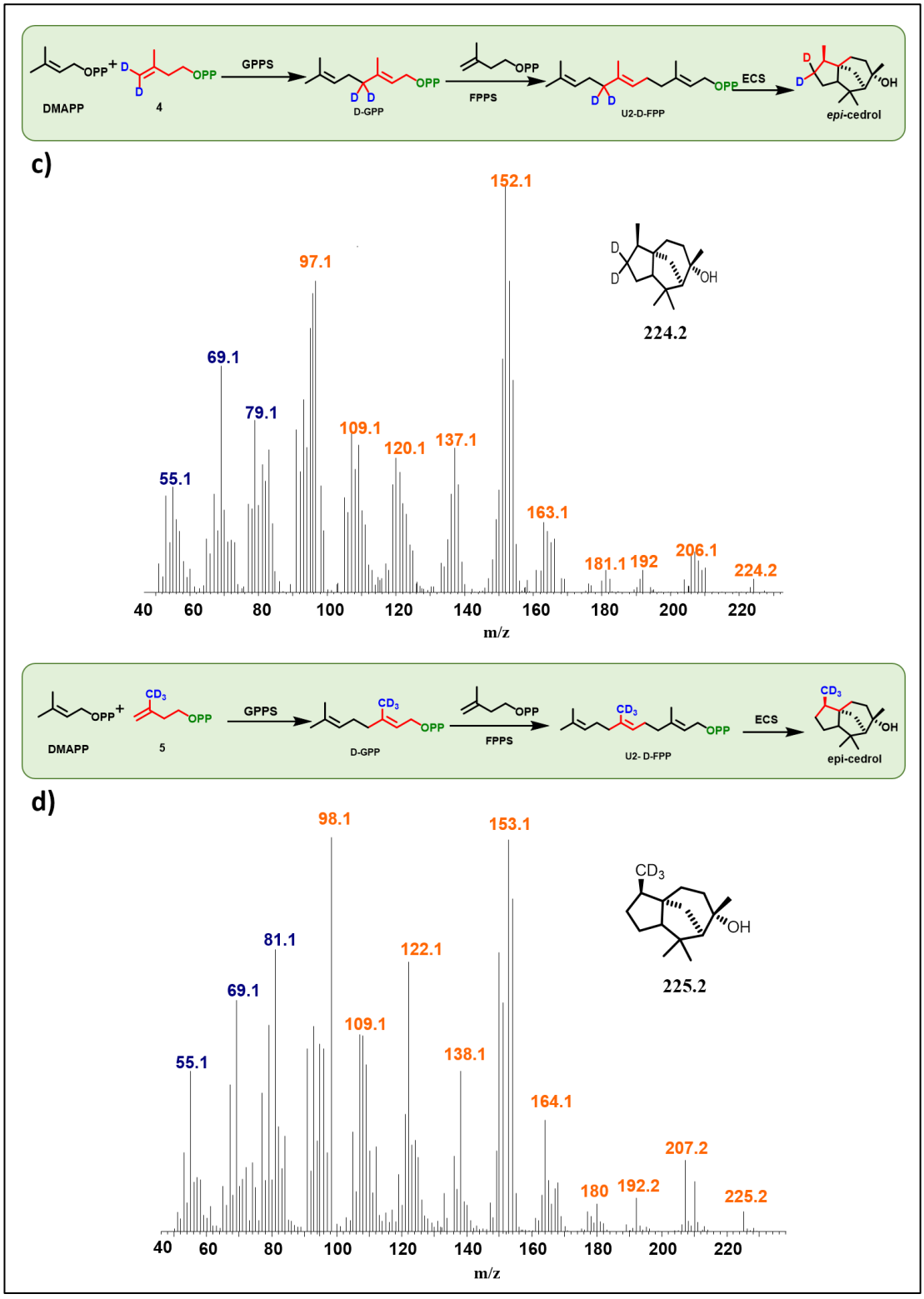


The structural fragment $EC_{189}$ suggests that the generation of the fragment ion m/z = 189 can be traced through the methyl groups of FPP. Thus, in the fragmentation generated from the experiments on (14-$C^2H_3$)-FPP and (15-$C^2H_3$)-FPP, we compared

the MS fragment ions to revealed that the labelled $CD_3$ group disappears from (15-$C^2H_3$)-FPP at C15, but this is not observed in (14-$C^2H_3$)-FPP. This fragment ion indicates that the fragment originates from precursor m/z = 204 via the loss of a methyl radical. The fragment m/z = 161 indicates the generation of the ion by the loss of a neutral iso-propyl group from fragment $EC_{189}$.

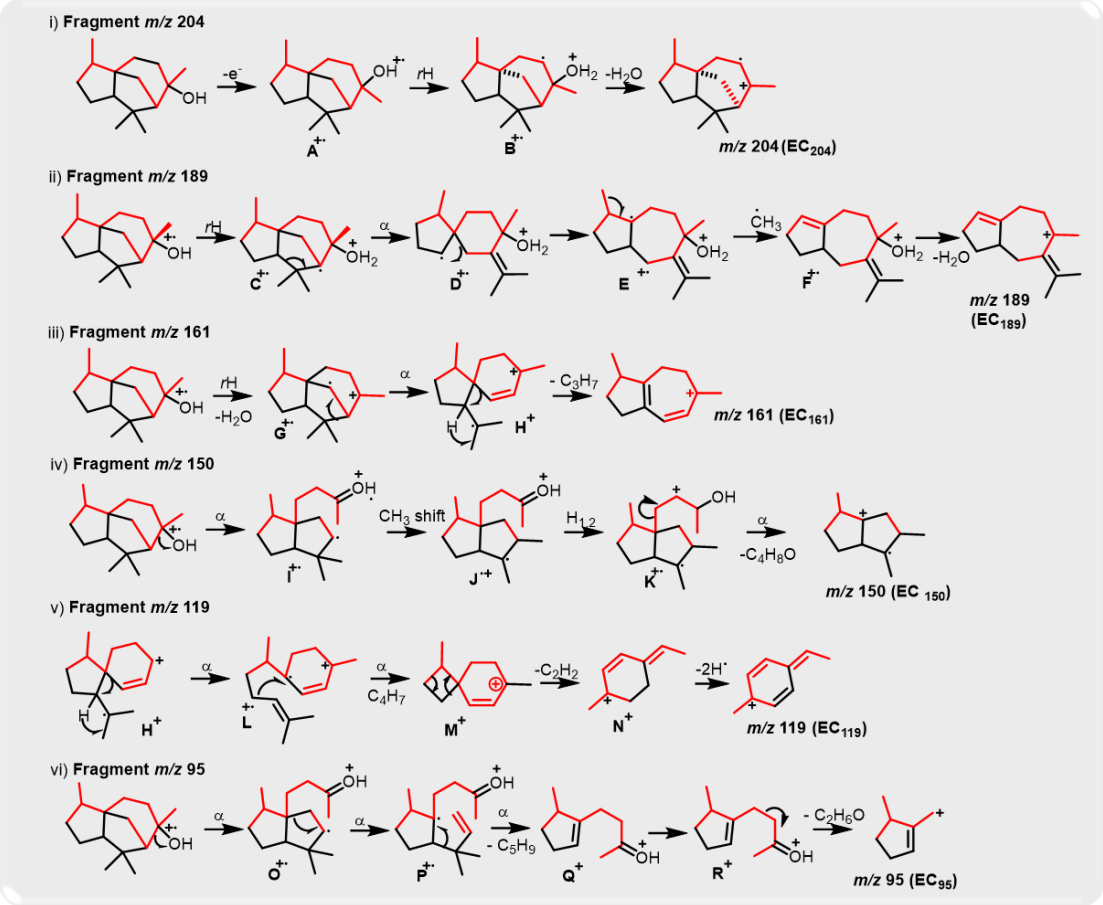


**Figure 5**. Possible fragmentation of *epi*-cedrol. The red lines indicate deuterium α-cleavage, rH: hydrogen rearrangement.

A plausible mechanism for this involves the sequential elimination of water then α-fragments from $\mathbf{H}^{+\cdot}$ followed by the loss of an iso-propyl group. An alternative possibility for the formation of $EC_{161}$ was via the cleavage of a C6–C10 bond to produce $\mathbf{H}^{+\cdot}$, which occurs during ring opening with the elimination of an isobutene unit, followed by an ethylene unit, with concomitant hydrogen rearrangement and multiple hydrogen eliminations to give $\mathbf{N}^{+}$ and the formation of ion m/z = 119. The mass

fragment ion m/z = 150 clearly indicates its formation from *epi*-cedrol by the α-cleavage of the C2–C3 bond followed by inductive cleavage with the neutral loss of iso-butyraldehyde. This cation intermediates were stabilizes *via* a tertiary carbocation and radical. After the initiation of $\mathbf{A}^{+\cdot}$ fragmentation, the formation of the structurally stable base ion fragment m/z = 95 is achieved after proton transfer to oxygen to yield $\mathbf{P}^{+\cdot}$ and subsequent hydrogen rearrangements via $Q^+$ and $R^+$ followed by inductive loss of acetone via a ring opening reaction. Furthermore, the B and C rings formed in *epi*-cedrol originate from isoprene U2 and U3-FPP (HR-MS shown in **Fig. 6** and NMR spectra shown in the end of this chapter)**.**

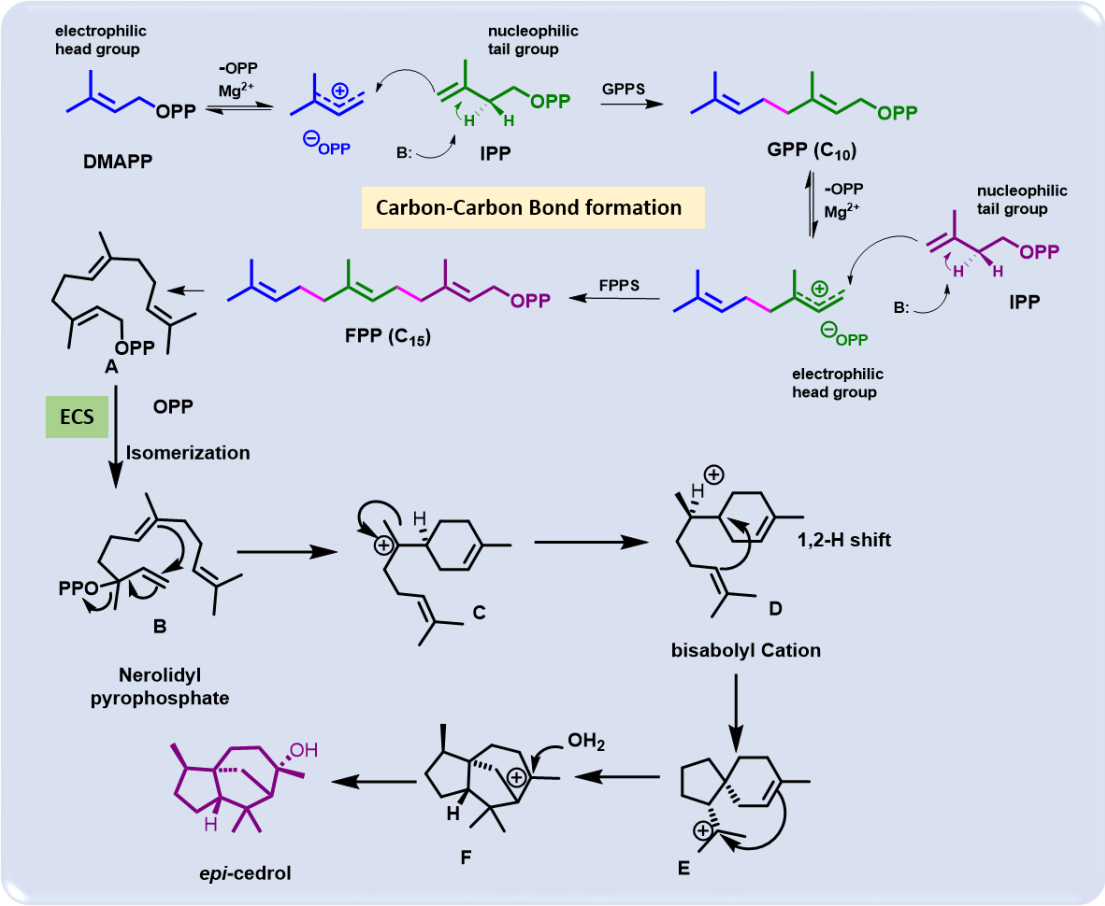


**Scheme 4.** Proposed mechanism of *epi*-cedrol biosynthesis.

The mechanism of hydride migration from C6 to C7 was studied by conversion of (6-$^2$H)-FPP to its corresponding *epi*-cedrol. The position-specific mass shift analysis of m/z = 95 shows an increase in the mass by +1 and even a loss of the C6 portion in the case of the fragment m/z = 161 (**Fig 4**). The extracted information from all the GC-

EI-MS spectra reveals that an exceptional labelling fragmentation pattern was observed in the MS analysis of the C7-containing fragment. These results suggested that the hydrogen migrated in a 1,2-hydride shift manner to quench bisabolyl cation **D**. Based on the comparative fragmentation analysis of the GC/EI-MS data of non-labeled and labelled *epi*-cedrol, we have proposed a possible mechanism for *epi*-cedrol biosynthesis, as mapped out in **scheme 4**. The isomerization of the OPP (O-pyrophosphate) group of FPP forms the stable isomer nerolidyl diphosphate intermediate **B.** The ring cyclisation of the C1 and C6 carbons generates intermediate **C**, then the axial hydride in the C6 position was transferred to C7 to generate bisabolyl carbocation **D**. The cyclisation driving force of the C10 double bond results in subsequent ring closure to form a new bond from C6-C10 and *spiro*-intermediate **E** followed by the formation of a third ring through the new bond between the C2 double bond and C11 carbocation *via* C-ring closure. Finally, carbocation **F** was quenched by an external water source to produce a stable *epi*-cedrol.

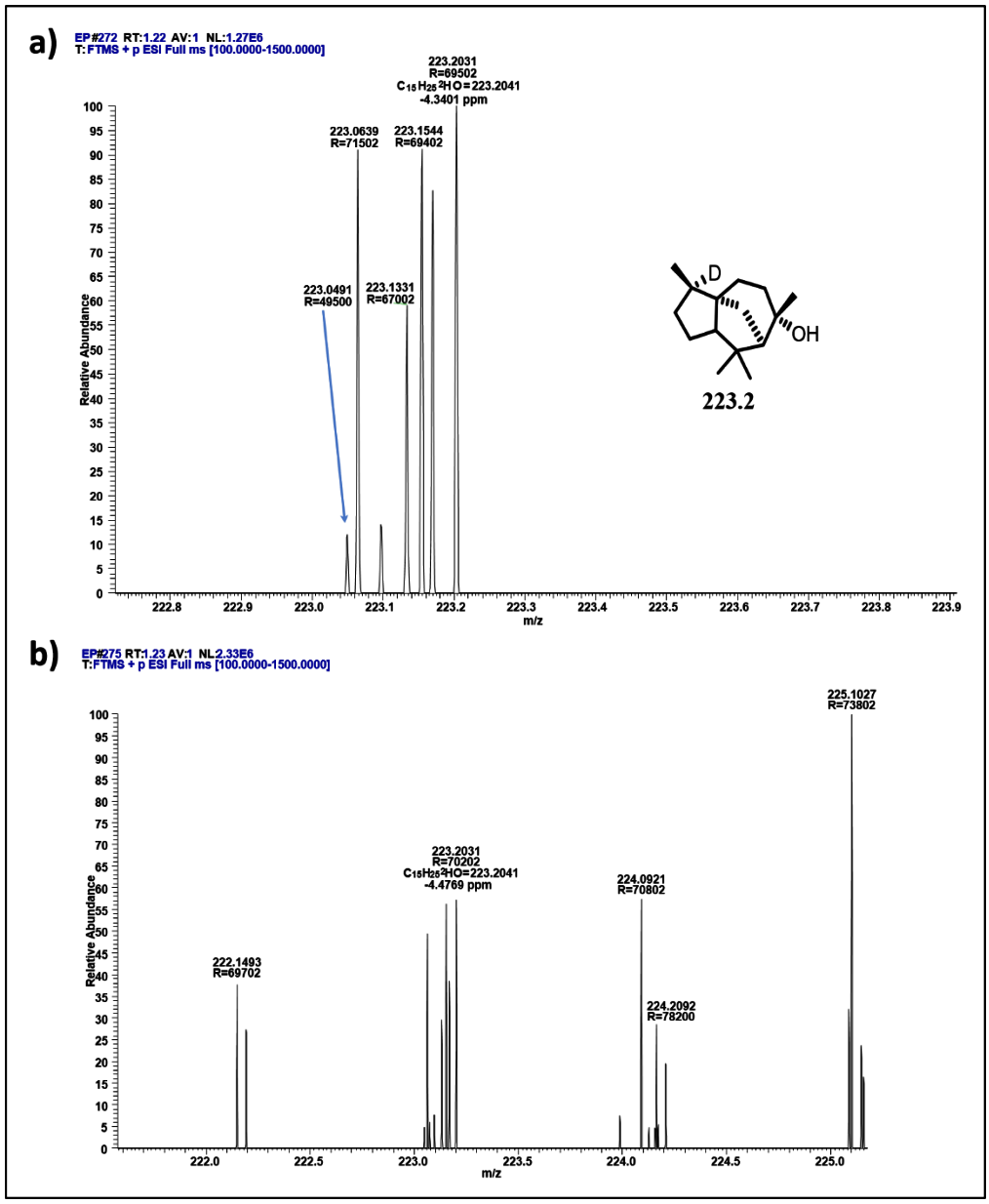


**Figure 6**. HR-MS spectra of labelled C2-$^{2}H_{2}$-*epi*-cedrol.

## Conclusions

In conclusion, we demonstrated that the hydroxyl functionality of sesquiterpene alcohols, *epi*-cedrol and cedrol formed through divalent metal dependent enzyme *epi*-cedrol synthase. The enzyme catalyzed electrophilic cyclization of achiral diphosphate substrate, farnesyl diphosphate from water molecule. GC and GC-MS analysis of the assay products obtained by incubation FPP with *epi*-cedrol synthase in presence of $H_2{}^{18}O$ (21.6 atom %) indicated the enrichment of molecular ion peak at m/z 224 for *epi*-cedrol is an evidence of that the hydroxyl group is derived from water by nucleophilic addition process. The attack of water to obtain the isotopically labelled *epi*-cedrol is preferred due to the steric blocking effects of the proximal geminal dimethyl groups in cedryl carbocation. The detection of traces of isotopically labelled cedrol implies that attack on the unbound carbocation is at least partially responsible for the observed product mixture. These results presented here clearly indicated that the *epi*-cedrol and cedrol might not be formed through recapturing of the original diphosphate anion present in the active site by cedryl carbocation followed by hydrolysis. In elucidation of final cyclization mechanism, four synthetic ($^2$H)-IPP isomers **2**–**5** were prepared from the common starting material methyl acetoacetate and successfully used for ($^2$H)-FPP synthesis through enzyme catalysts. The GC-EI-MS fragmentation based mechanism of *epi*-cedrol demonstrates that its biosynthesis proceeds *via* 1,2-hydride migration and cyclisation reactions. This strategy is highly sensitive and sufficient information on the proton/hydride rearrangement was obtained from the analysis of mass fragmented ions. Also, the rapid synthesis of any desired deuterium-labelled polyprenyl chain were achieved using the four IPPs **2–5**. Furthermore, we could use these deuterated-IPP for an application in a chemical and enzyme combination for elucidation of valuable terpenes biosynthesis.

**$^{1}$H, $^{13}$C and $^{31}$P NMR of synthesized deuterated IPP**

**1)**

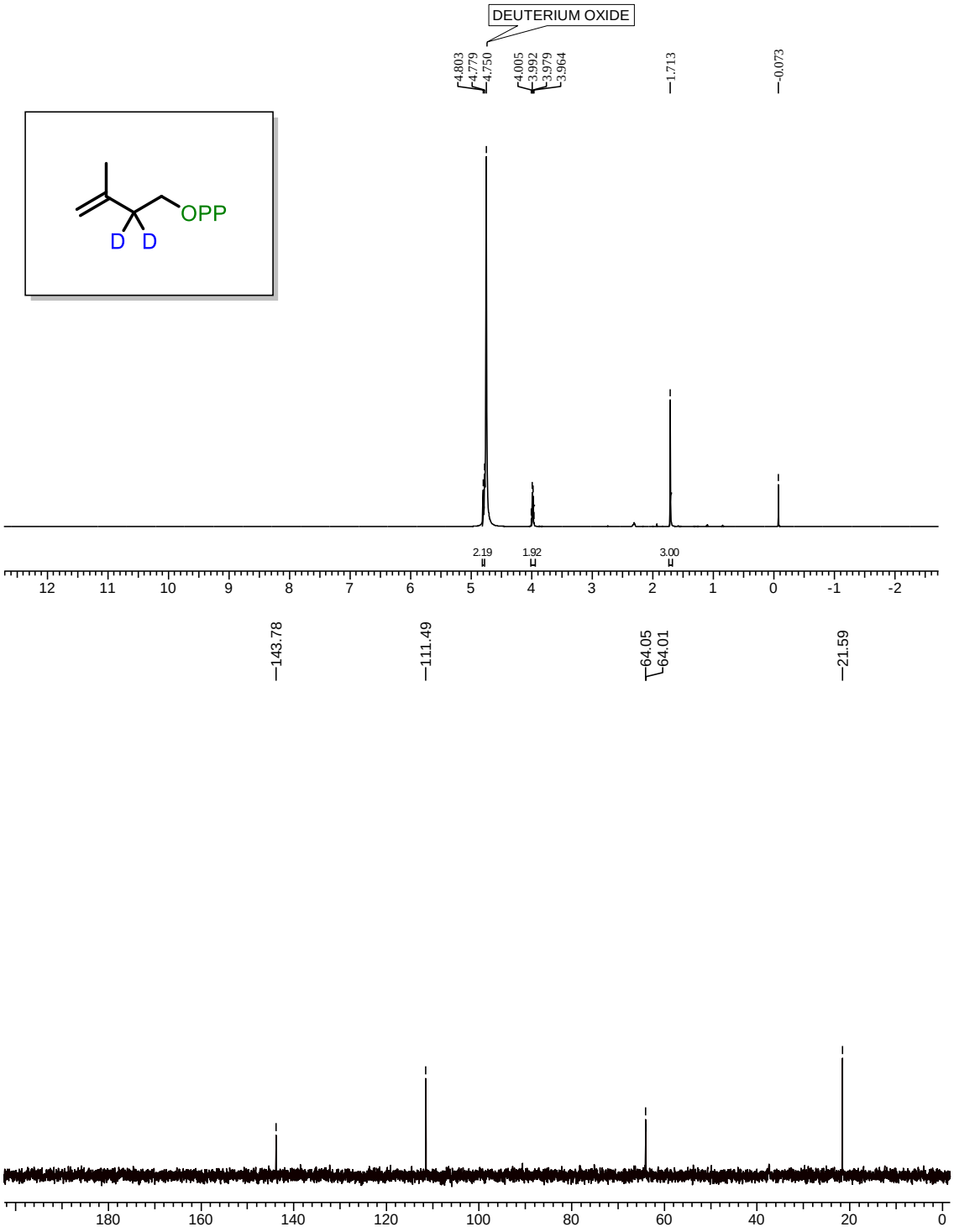

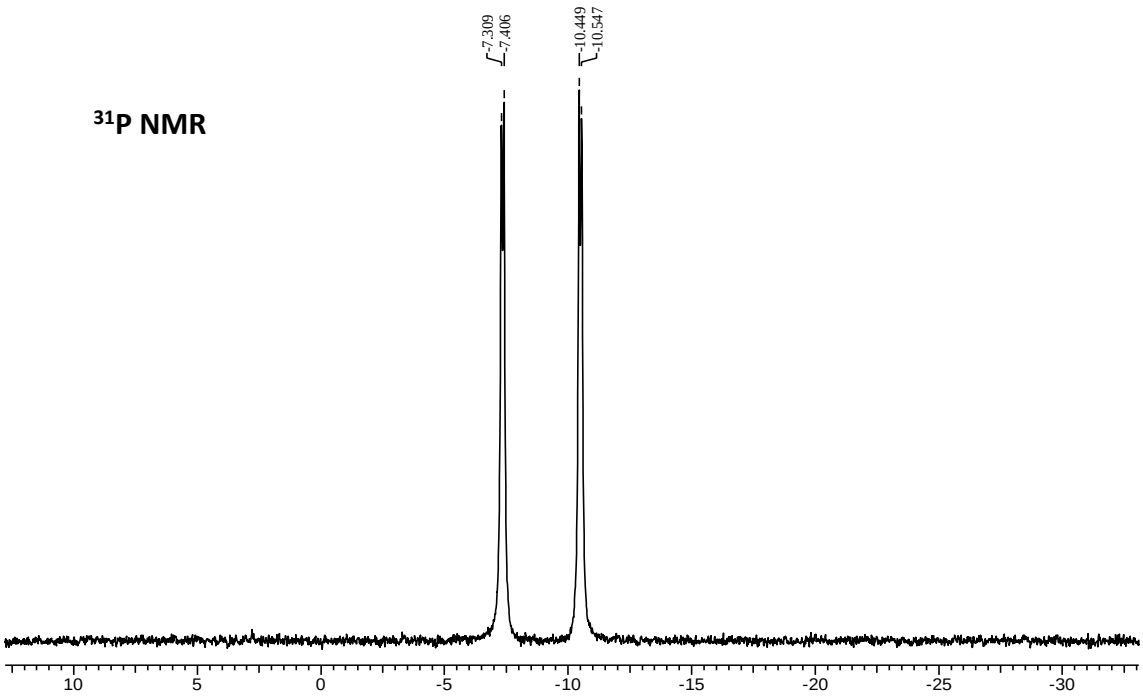
31P NMR
-7.309
-7.406
-10.449
-10.547
10
5
0
-5
-10
-15
-20
-25
-30

**2)**

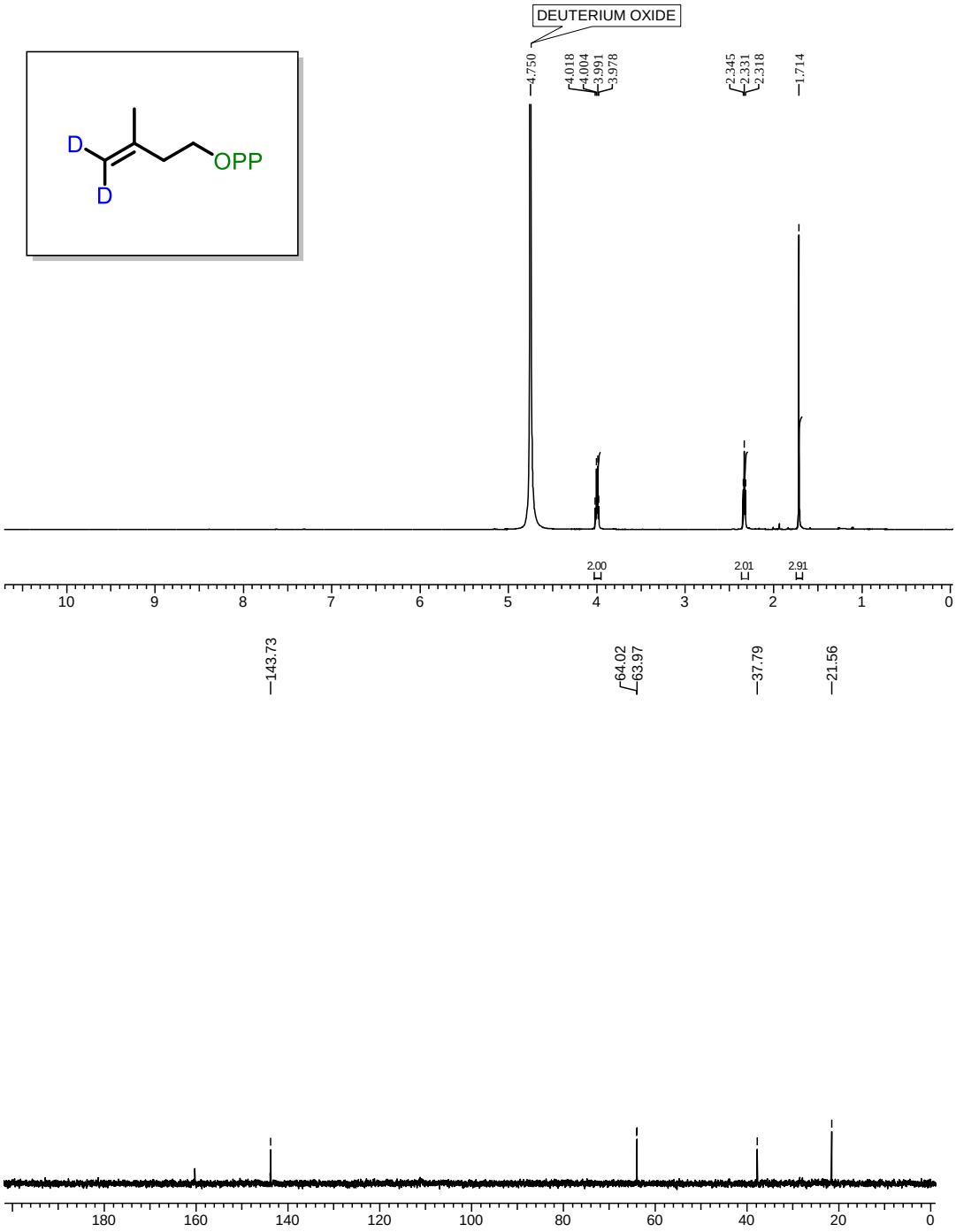
DEUTERIUM OXIDE
4.750
4.018
4.004
3.991
3.978
2.345
2.331
2.318
1.714
D
D
OPP
2.00
2.01
2.91
10
9
8
7
6
5
4
3
2
1
0
143.73
64.02
63.97
37.79
21.56
180
160
140
120
100
80
60
40
20
0

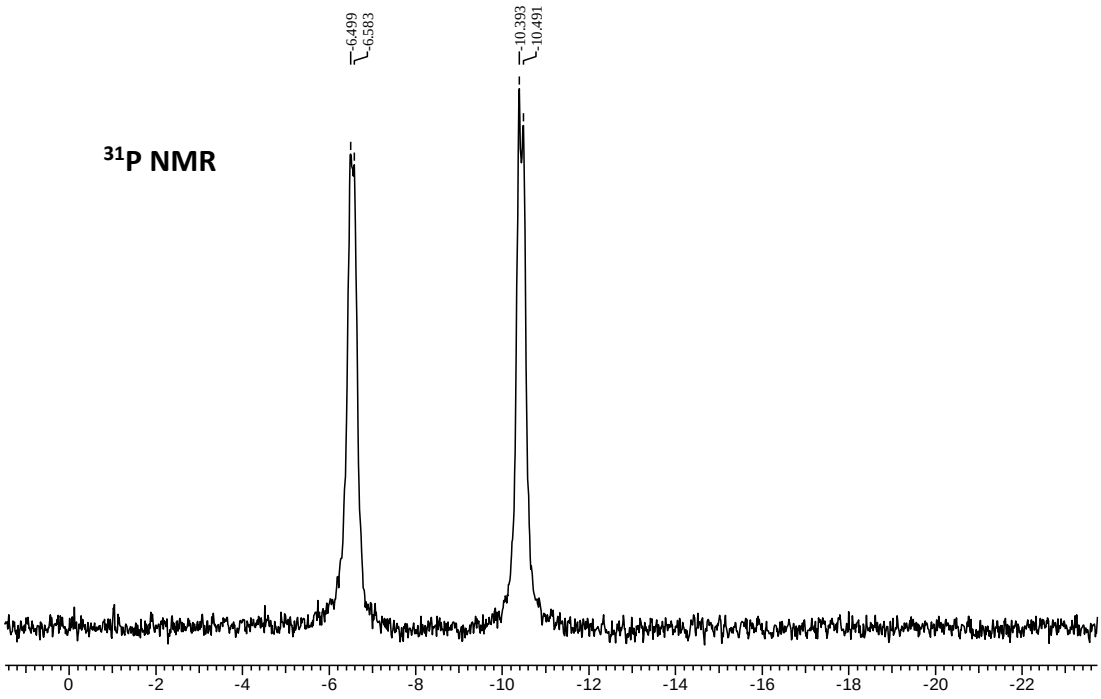
-6.499
-6.583
-10.393
-10.491
31P NMR
0
-2
-4
-6
-8
-10
-12
-14
-16
-18
-20
-22

**3)**

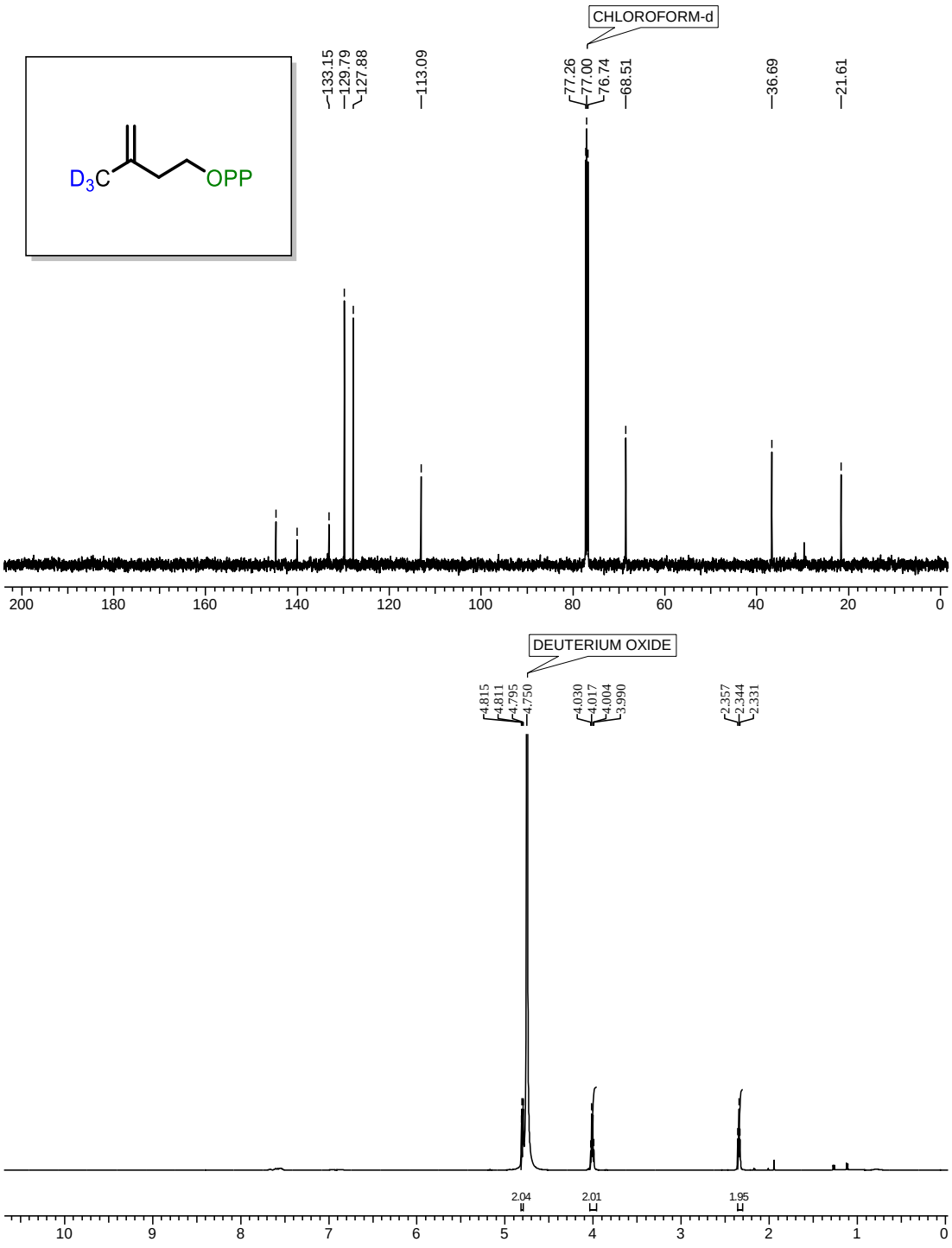
CHLOROFORM-d
133.15
129.79
127.88
113.09
77.26
77.00
76.74
68.51
36.69
21.61
$D_3C$
OPP
200
180
160
140
120
100
80
60
40
20
0
DEUTERIUM OXIDE
4.815
4.811
4.795
4.750
4.030
4.017
4.004
3.990
2.357
2.344
2.331
2.04
2.01
1.95
10
9
8
7
6
5
4
3
2
1
0

**$^{31}$P NMR**

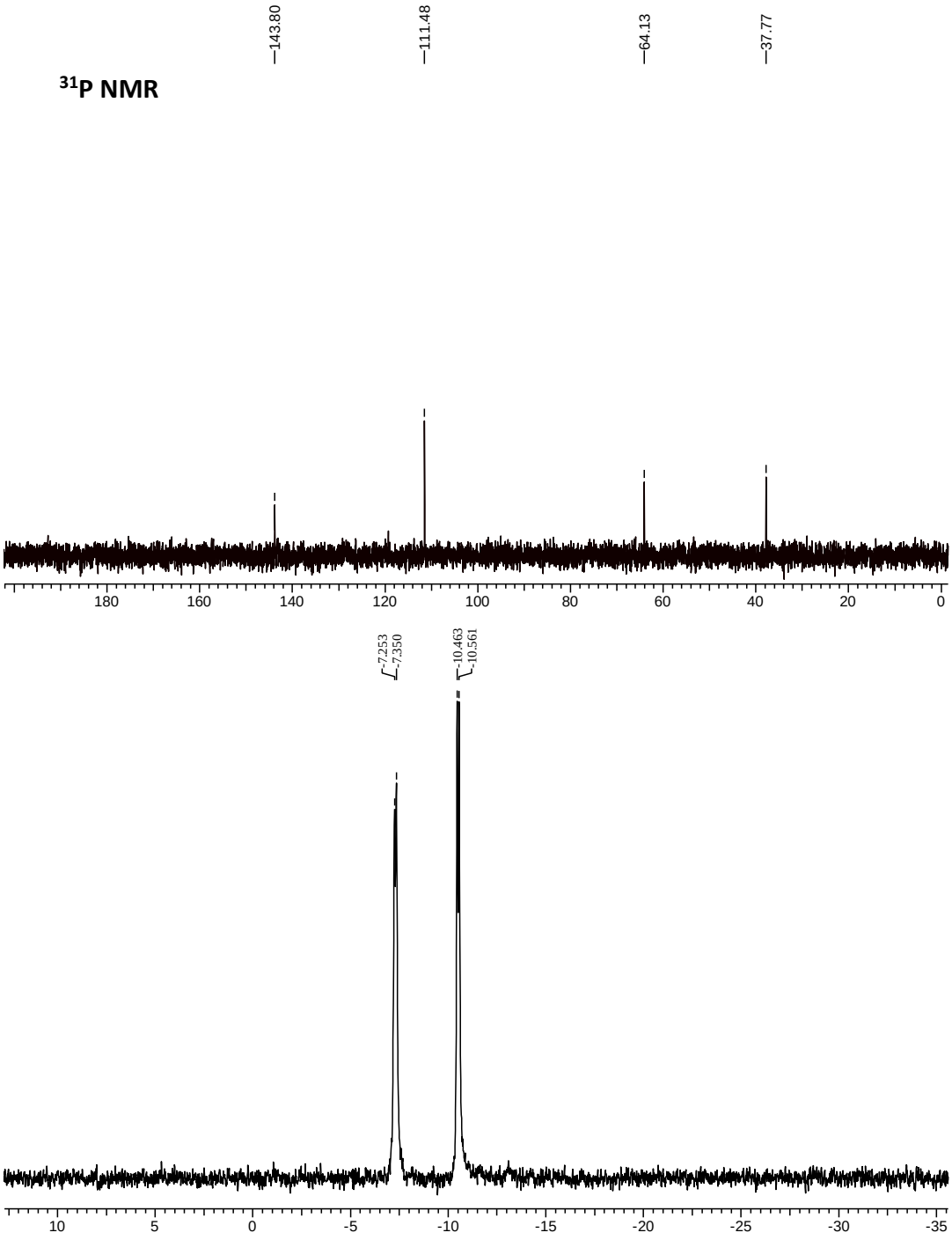
143.80
111.48
64.13
37.77
180
160
140
120
100
80
60
40
20
0
7.253
7.350
10.463
10.561
10
5
0
-5
-10
-15
-20
-25
-30
-35

**4) $^{2}$H-*epi*-cedrol**

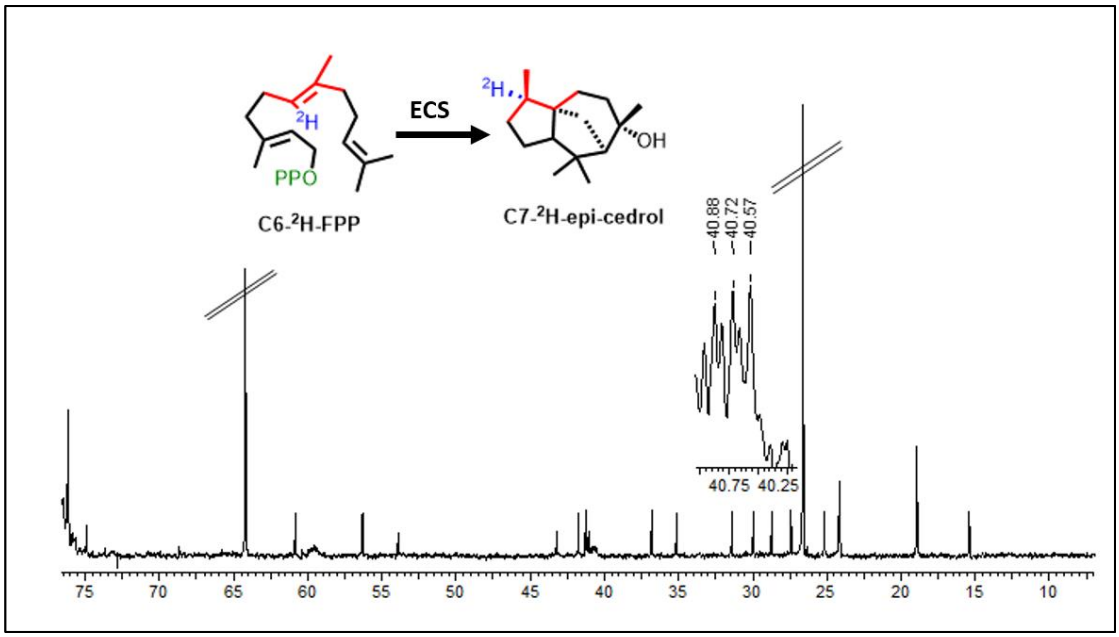

# Chapter 5
# Summary of thesis and future perspectives

In ***S***ummary, Isoprenoids are very diverse and complex natural products which are having important applications in various fields such as, fragrances, flavors, biofuel, rubber, high grade lubricants, agricultural products and traditional herbal medicines (Ayurveda). Since past two decades, synthetic biology and advanced metabolic engineering techniques helped in the microbial genetic manipulation along with the identification of their novel metabolic pathways. Mevalonate (MVA) and Methyl Erythritol phosphate (MEP) pathways play a crucial role in biosynthesis of isoprenoids in living things including plant and microbes. As per our literature review (till March 2020) several plant originated hemiterpenes (isoprene, isoprenol, isopentanol, and methylbutanol *etc*.); monoterpenes (geraniol, limonene, linalool, menthol, pinene, myrcene, and sabinene *etc*.); sesquiterpenes (amorphadiene, bisabolene, bisabolol, caryophyllene, cubebol, *epi*-cedrol, farnesene, farnesol, germacrene, humulene, nerolidol, nootkatone, patchoulol, protoilludene, santalene, valencene, and Valerenadiene *etc*.) has engineered by various scientific groups across the globe, in two microbial hosts *E. coli* and *S. cerevisiae* by heterologous expression as well as different metabolic engineering tools. Among the all available microbial hosts, *E. coli* and *S. cerevisiae* are the most attractive and economic platforms for the bulk production of value-added isoprenoids since they are editable, easy to manipulate, sustainable at ideal conditions. Apart from production of these isoprenoids the prediction of cyclization mechanism of these isoprenoid cyclases are the key factors for understanding enzyme functions. Overall, these literature survey suggested that there are many opportunities available for elaborating remaining un-engineered isoprenoid production and in future, expand the catalogue of isoprenoid biosynthesis.

*Epi*-cedrol and santalene are two sesquiterpenes ($C_{15}$) found in plant source. Till date *epi*-cedrol was reported from *A. annua* plant while santalene from two sources (*S. album* and *C. lansium*). Both the metabolites having their own value and applications. Among the two metabolites, *epi*-cedrol was less reported in literature and unexplored. While santalene and its derivatives were metabolically engineered and produced well by heterologous expression. For the production *epi*-cedrol and santalene, we applied fusion protein strategy with adjacent gene, to get maximum pool of substrate and channeling effect yields large quantity of desired products. We have successfully

constructed two unnatural multifunctional fusion proteins of sesquiterpenoid synthases which consumes maximum substrates in the microbial cell as well as in buffer condition. These constructs produces a higher amount of *epi*-cedrol and santalenes from basic building block of isoprenoid biosynthesis pathway, (IPP and DMAPP) as compared to utilizing two different enzymes together. *Epi*-cedrol was successfully produced by MEP as well as MVA pathway *via E. coli* and *S. cerevisiae*. *E. coli* produces maximum amount of *epi*-cedrol as compared to *S. cerevisiae*. Since amount of IPP and DMAPP, and cell density of *E. coli* are more as compared to yeast cell. We have reported three fold maximum production of e*pi*-cedrol by applying fusion protein strategy as compared to previous reports by Jackson *et al*., 2003. Production of another sesquiterpenes, santalene was improved by this strategy, but it was not up to the *epi*-cedrol yield. But, the santalene product yield was much higher than single enzyme construct. This construct needs codon and media optimisation (by adding some pathway intermediates). Overall, our study and its results suggested that the construction of fusion enzyme with the help of adjacent genes, has a great potential to improve natural product yield by utilizing maximum substrates of the biosynthetic pathways via sequential reactions. Fusion enzyme or bifunctional enzyme, brings two active pockets closing together and which helps in the substrate channeling and reduce the loss of substrates, resulted improved in the catalytic activity. Since, the isoprenoid products were secreted in growth medium, it can be promising industrially friendly harvesting system developed for downstream processing. Before constructing fusion enzyme, application of bioinformatics/structural models and docking studies could help in the developing desired protein which are having maximum enzyme activity.

In industries, enzymes are used as catalyst to convert desired product. Enzyme stability and activity at various condition are the crucial factors to decide whether application of these biocatalysts can be commercially successful or not. Enzymes can lost part of their activity when they are exposed to the action of heat, extreme pH or proteases conditions. Enzymes are protected by various way, like by immobilization, ionic liquid-microemulsion, IL coating etc. Till date terpene synthase enzyme was not immobilised or protected by any chemical methods. We synthesised various alkyl chains containing imidazolium based ILs having *ter*-BuOH and mesylate as counter anion. These ILs has significant biological activities including antimicrobial and

antibiofilm activity against broad spectrum of microorganisms. Theses ILs further screened for to enhance the stability and catalytic activity of terpene synthase enzyme *epi*-cedrol synthase. Among all ILs hexyl and octyl alkyl group containing ILs showed significant stability and catalytic activity to ECS enzyme. Our synthesized ILs are non-halogenated which make them environmentally-friendly and greener material character, methylsulfonate anion is well known for its non-toxic and pharmaceutically acceptable moiety. Overall, our study showed new opportunity to use of imidazolium based ILs in enhancing stability and activity of industrially important enzymes as well as to obtain secondary metabolites (isoprenoids) *via* terpene synthase enzymes at large scale.

Isoprenoid synthase has unique and specific catalytic activity, they catalyzes isoprenyl substrates into well characterized, complex structure or molecules. In this thesis, finally we demonstrated the mechanism of sesquiterpene synthase *epi*-cedrol synthase (ECS) by using GC and GC-MS technique. In this study, by feeding heavy water molecule and hydrogen ($^2$H)/deuterium labelled isoprene units (IPP) in enzymatic assay, cyclization mechanism and hydride shift were confirmed. In first study, we confirmed that the hydroxyl group of *epi*-cedrol and cedrol are formed from water molecules, not from achiral diphosphate substrate FPP by nucleophilic addition process, as the m/z 222 molecular ion was increased to m/z 224 in GC-MS analysis. The attack of water to obtain the isotopically labelled *epi*-cedrol is preferred due to the steric blocking effects of the proximal geminal dimethyl groups in cedryl carbocation. Finally, for complete elucidation of enzyme mechanism of ECS, four synthetic ($^2$H)-IPP isomers was synthesized and added in the sequential enzymatic assay. The eight different labelled *epi*-cedrol were chemo-enzymatically synthesized and further analyzed by GC-EI-MS. For the synthases of labelled *epi*-cedrol, fusion of ECS was also worked same as sequential feeding of various terpene cyclase enzymes. The GC-EI-MS fragmentation based mechanism of *epi*-cedrol showed that its biosynthesis proceeds *via* 1,2-hydride migration and cyclisation reactions **Scheme 1**. This analytical strategy are highly sensitive and gives sufficient information on the proton/hydride rearrangement. Also, we can rapidly synthesize any hydrogen ($^2$H)/ deuterium-labelled polyprenyl chain or isoprenoids by feeding these four unnatural IPPs.

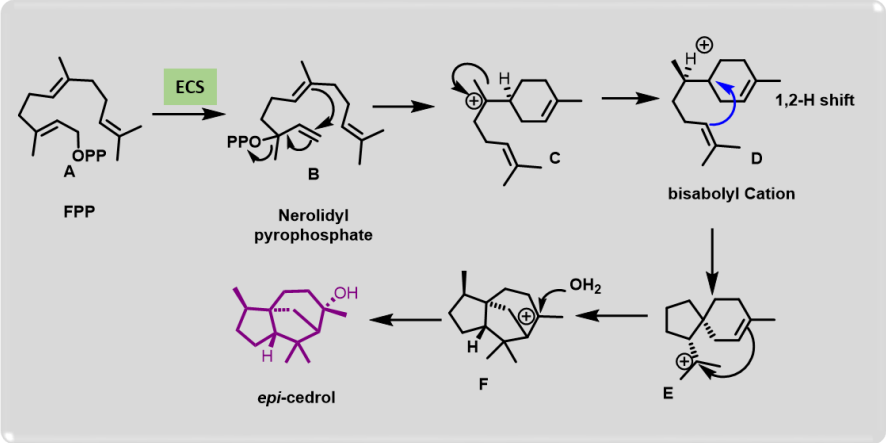


**Scheme 1**. Mechanism of *epi*-cedrol biosynthesis *via* 1,2-hydride shift.

**In *f*uture**, apart from fusion protein technique, these two metabolites can be produced by different way of heterologous expression in the same organism as we studied. For the more desirable production of *epi*-cedrol and santalene sesquiterpenes, following engineering approaches can be applied. In fermentation media, optimization of IPTG concentration, addition of pathway substrates (for MEP and MVA pathway) such as, mevalonic acid, acetyl coA can be used. Codon optimization and modification in MVA pathway of *S. cerevisiae*, by down-regulating squalene synthase (*ERG 9*) flux at FPP branch point or replacement with weak promoter, along with the use of variant HMG-CoA reductases can also improve yield of these sesquiterpenes. Overexpression of maximum enzymes in MEP and MVA pathway till FPP synthesis, would also result in a significant production of *epi*-cedrol and santalene. Fed-batch culture fermentation for 7-10 days would also help in large scale production. Optimization of extraction procedure, such as overlay of solvents dodecane or hexane would prevent the evaporation of volatile metabolites. Ionic liquids (ILs) are also called as future solvents, now they are widely applied in biological fields. Imidazolium IL's with *ter*-alcohol and mesylate moiety could be applied in many industrially important enzymatic reactions. They can retain the enzyme stability and activity at high temperature conditions. Since, they further need to be optimised for different ILs with different enzymes combinations. Finally, for enzymatic elucidating mechanism of hemiterpene synthase, monoterpene synthase, and sesquiterpene synthase, $^{2}H$ labelled IPP can be utilised *via* chemo-enzymatic reactions. They are the key factor in labelling or producing

deuterium/hydrogen labelled isoprenoids. This way of biosynthesis are rapid, specific and mechanistically easily interpretable.

## Overall challenges and novel strategies for metabolic engineering of isoprenoids

In chapter 1, we discussed many efforts have been taken for the improvement the production of $C_5$-$C_{20}$ isoprenoids in popular heterologous host *E. coli* and *S. cerevisiae* by the use of synthetic biology and metabolic engineering. A schematic representation of isoprenoid biosynthetic and its dynamic control depicted in **Fig. 1**.

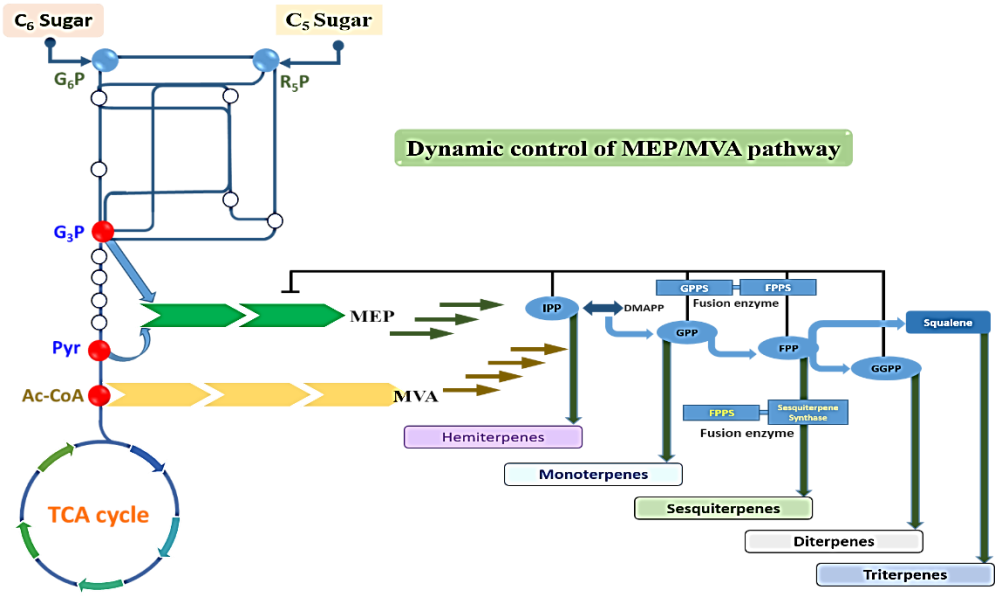


**Figure 1**. A schematic diagram of isoprenoids biosynthetic pathway. The central carbon incorporation and TCA cycle for the isoprene synthesis *via* MEP/MVA pathway. These IPP/DMAPP utilised for the biosynthesis of different types of isoprenoids. Fusion enzyme strategy could be used for enhancing substrate channeling effect. This two pathway could be assembled and engineered in microbial host for mass production by dynamic control of MEP/MVA pathway (Asadollahi et al., 2009; Zhao et al., 2013; Zhou et al., 2013).

Both the host requires certain balancing catalytic efficiencies, energy demands (ATP/CTP) and the availability of reducing cofactors (NADH, NADPH) and carbon supply, *i.e.* precursors or intermediates, are the crucial parameters for achieving high isoprenoid titres by MVA and MEP pathway (Gruchattka et al., 2013; Vranová et al., 2013). The central carbon metabolism provide the carbon to both the pathways, in which they have to compete with other pathway for the necessary precursors (Vickers

et al., 2017). Pyruvate and G3P supply is important for engineering MEP pathway. As per recent literature, overexpressing the Entner–Doudoroff pathway or using it in conjunction with the pentose phosphate pathway (PPP) instead of Embden– Meyerhof–Parnas pathway, better improves the G3P supply as well as it can also lead to increases in NADPH regeneration rates and finally increased isoprenoid titters (Liu et al., 2013). For improvement of MEP pathway another way is to bypass the pathway to direct DXP without using DXS enzyme. King *et al.*, proposed a new way to synthesized DXP in *E. coli* by using activity of fructose-6-phosphate aldolase to convert glycolaldehyde and hydroxyacetone phosphate to DXP (Kang et al., 2016).

In case of MVA pathway, acetyl-CoA availability necessary to carry forward further pathway by its entry point enzyme acetoacetyl-CoA thiolase (AACT). This enzyme plays an important role in regulation of isoprenoid production in response to abiotic stress and acetyl-CoA/CoA ratio in the tricarboxylic acid (TCA) cycle (Vögeli et al., 2018). In yeast, thiolytic activity are exhibited by *ERG*10 enzyme at high level of acetoacetyl-CoA (Tippmann et al., 2017). Free CoA also inhibited the thiolases AACT (Hemmerlin, 2013). Acetoacetate-CoA ligase enzyme used for conversion of acetoacetate to acetoacetyl-CoA, Harada *et al.*, reported the humulene production with the use of acetoacetate-CoA ligase and acetoacetate (Harada et al., 2009). Concerning energies, the MVA pathway requires 3 ATP molecules in two phosphorylation steps of mevalonate and one in decarboxylation step, and MVA also net consumes three ATP molecules. The consumption of redox agent NADPH is higher for MEP pathway (3 NADPH) compare to MVA pathway (2 NADPH). So the supply of these cofactor NADPH may affect the three steps of MEP pathway. This cofactor is largely provided by the PPP and affected by the redox state of the host system. To overcome this challenge several attempts were carried out including, overexpression of glutamate dehydrogenase, gdhA, and TCA cycle enzymes found to be increase cofactor supply in the cell (Asadollahi et al., 2009; Zhao et al., 2013; Zhou et al., 2013).

Another challenging factor is the accumulation of toxic intermediates or by-products, native intracellular pathway inhibitors. MVA/MEP pathway intermediates are playing a significant role in the overall pathway flux. Their complex regulation make them critical in overall balancing enzyme expression in the pathway (Yang et al.,

2016a). Overcoming each point of pathway regulation are the key for engineering both the MEP and MVA pathway. HMGR and HMGS are act as a regulator of the MVA pathway as per previous reports (Zhuang and Chappell, 2015). As it is inhibited by both its substrate, acetoacetyl-CoA, and by HMG-CoA and CoA, its products (Song et al., 2012). To overcome this, Tsuruta *et al*., reported the replacement of both the native HMGS and HMGR genes with the other equivalent genes from *S. aureus,* for the higher production of amorphadiene in *E. coli* (Tsuruta et al., 2009). Ma et al also used same strategy for amorphadiene production by using variant HMGR (Ma et al., 2011). Overexpression of truncated form of HMGS and HMGR also improves the titre of different isoprenoids (Hu et al., 2017; Ohto et al., 2009). Therefore the effective screening for more HMGS and HMGR homologs as well as plausible mutation could led to improve the pathway flux.

Simultaneously improving rate-limiting step and enzyme expression control are enough to optimization of any pathway. As discussed above DXS plays important role in MEP pathway flux, since thiamine is necessary cofactor for DXS activity but it act as feedback inhibitor for IPP and DMAPP which compete with thiamine pyrophosphate (Banerjee et al., 2013). To overcome this, two bypass pathways have been developed for avoiding DXS (Du et al., 2014; Kang et al., 2016; Kirby et al., 2015; Martin et al., 2003). However, the other MEP pathway enzymes Isp-FGH maintains the strict regulation of the MEP pathway. IspF enzyme is activated by MEP that forms ISP-F-complex which inhibited by FPP (Zhao et al., 2013). To overcome this issues, several isoprenoids such as Isopentanol, Protoilludene *etc*. has been produced by (Liu et al., 2014; Yang et al., 2016c). Increase flux of MEC may be carried out by the breakdown of IspG and IspH which contain iron-sulphur clusters sensitive to oxidative degradation. The catalytic efficiencies of these enzymes are highly dependent on these iron–sulphur clusters and availability of the NADPH flavodoxin reductase necessary for their regeneration (Rohdich et al., 2003).

For the production of oxygenated isoprenoids, such as taxanes from taxadiene and artemisinic acid from amorphadiene cytochrome P450 enzymes (cP450s) are required. These enzymes activity relies on NADPH- dependent CPR as a redox partner. Generation of these high value isoprenoids involves a co-expression of plant cP450 reductase in heterologous hosts to be the greatest challenge (Biggs et al., 2016; Tang et

al., 2017). Biggs *et al.,* overcome this by using overexpression of engineered cP450 and cytochrome reductase in *E. coli* which resulted up to 570 mg/L titre of oxygenated taxanes (Biggs et al., 2016). For more improvement various versatile P450 enzymes need to be developed and engineered for isoprenoid production in both host systems.

Once strains have been successfully engineered, the industrially economical production needed. For this cheap source of glucose biomass waste, such as hydrolysed molasses/sugar waste may be used to overcome this challenges. Since numerous pre-treatment and purification steps are required before its use (Bayer et al., 2007). Many isoprenoids are in the form of alcohols or volatiles, since the fermentation process are carried out in various temperature conditions. To overcome this issue several attempts were reported by overlaying solvents like octane, decane and dodecane. This alkanes prevents the volatile terpenes and help in the getting maximum titre (Newman et al., 2006). Recombinant plasmids have some limits, such as instability, metabolic burden on the cell were observed. As the combination of several genes may show adverse effect on cell growth in terms of large scale production. New techniques such as microbial cell immobilization (Rathore et al., 2013), genomic or chromosomal integration/deletion (Shi et al., 2016) may overcome plasmid instability issue. The requirement of inducer and antibiotics may affect the economical production of isoprenoids. In large scale production, to reduce the cost, expensive inducer/repressors could be eliminated. This could be the approach for increasing isoprenoid titres by developing inducer/repressor-free regulation systems which would be favourable for large-scale fermentations from the view of production cost. Liu *et al.,* developed an artificial genetic circuit which capable of sensing isoprene by incorporating a transcription regulator sensing isoprene, at least one reporter gene, together with desired promoters (Liu et al., 2018). In case of *E. coli* host, sometimes overexpression may accumulate as intracellular inclusion bodies, lack of post-traslational modification which resulted in improper protein folding (Young et al., 2012).

Compartmentalization of MVA pathway in the mitochondria (by utilizing mitochondrial intermediates) is another strategy to improve isoprenoid titre in the cytoplasm (Hammer and Avalos, 2017). Farhi *et al.,* reported these technique for boosting the heterologous production of valencene and amorphadiene (Farhi et al., 2011). These dual metabolic engineering strategy also used by various research groups

for the production of Isoprene and Isopentanol and amorphadiene. (Avalos et al., 2013; Lv et al., 2014; Lv et al., 2016b; Yuan and Ching, 2016). This strategy driven well because of the increased pool of enzymes, high redox potential, abundance energies (ATP), intermediates (acetyl-coA), and less competition with other pathway in mitochondria as compared to cytoplasm (Farhi et al., 2011; Klein-Marcuschamer et al., 2007). Another difficulties in better yield of isoprenoids is poor kinetics of isoprene synthases (IspS) which resulted low metabolic flux towards isoprene biosynthesis. To overcome this, several fusion enzyme approaches were reported (Chen et al., 2018; Weaver et al., 2015). Our group recently increased the production of sesquiterpenes in *E. coli* by improving catalytic efficiency by fusion of FPPS and ECS enzymes. This Fusion enzyme strategy could enhanced the substrate channeling effect and overall improved the production (Navale et al., 2019). Another strategy is overexpression of every enzyme of the MEP/MVA pathway up to desired terpene synthase can help in the higher yield. Westfall *eta al.*, used same strategy for highest production amorphadiene till date, in which they overexpressed each enzymes to ERG20 of MVA pathway in *S. cerevisiae* (Westfall et al., 2012).

Over the past two decades, the advances in emerging, knowledge, tools and technologies in synthetic biology and protein engineering can be combined to develop combinatorial engineering strategies to boost carbon flux into the desired isoprenoids. For achieving higher titre of isoprenoids, new enzymes screening, novel pathway discovery, protein engineering, conjugation of multiple pathway could be used. The new emerging techniques/tools for gene replacement/editing *eg.* CRISPR/CAS9 (Tian et al., 2019), pathway assembly methods CLIVA (Zou et al., 2013), pMRI-mediated decentralized assembly (Xie et al., 2014), traditional homologous recombination techniques, chromosomal integration techniques as well as the modular control systems (Liu et al., 2017; Shi et al., 2016; Zhou et al., 2012) (**Fig. 2**) would definitely boost the new developments in the biosynthesis of all types of isoprenoids. *In silico* comparative analysis for the heterologous expression also gave the promising metabolic engineering strategies for the production of various terpenoid.

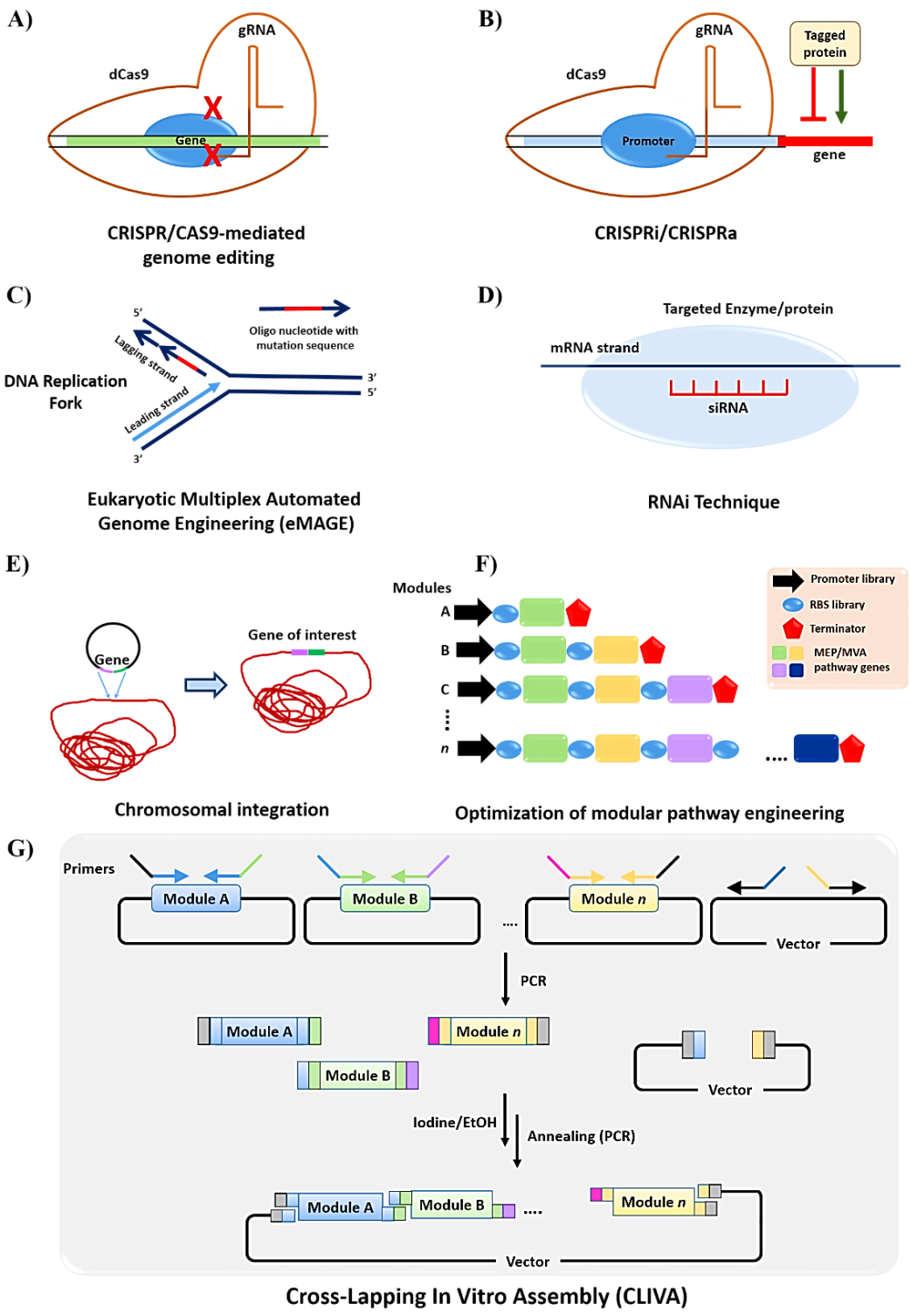


**Figure 2.** Microbial Genome editing tools for isoprenoid production: A) CRISPR/Cas9-mediated genome editing. A highly specific tool for deleting specific genes B) CRISPRi/CRISPRa mediated transcriptional regulation of genes used for the downregulation (interference) or upregulation (activation) of specific genes. C) Eukaryotic Multiplex Automated genome engineering (eMAGE) used for achieving specific chromosomal mutations

with high efficiency. D) RNAi mediated transcriptional regulation tool used to cleave specific mRNA sequences. E) Chromosomal integration technique for inserting new genes in the microbial genome *via* vector. F) Optimization of metabolic pathway by inserting various combinations of modules. G) Cross-Lapping-In Vitro assembly (CLIVA) used to insert multiple modules in single vector (Liu et al., 2017; Shi et al., 2016; Zhou et al., 2012).

The production of novel isoprenoid molecule faces several issues, the major difficulty are the lack of information about the complete biosynthetic pathways of molecules of interest. However, recent advances in technology and ease of transcriptome analysis have enabled, complete elucidation of metabolic pathways of medicinal plants or natural resources, thereby paving a way for further exploration into the field of isoprenoids.

# References

Abad MJ, Bedoya LM, Apaza L, Bermejo P. 2012. The Artemisia L. genus: a review of bioactive essential oils. *Molecules* **17**:2542–2566.

Ajikumar PK, Xiao WH, Tyo KEJ, Wang Y, Simeon F, Leonard E, Mucha O, Phon TH, Pfeifer B, Stephanopoulos G. 2010. Isoprenoid pathway optimization for Taxol precursor overproduction in Escherichia coli. *Science* **330**:70–74.

Albertsen L, Chen Y, Bach LS, Rattleff S, Maury J, Brix S, Nielsen J, Mortensen UH. 2011. Diversion of flux toward sesquiterpene production in Saccharomyces cerevisiae by fusion of host and heterologous enzymes. *Appl. Environ. Microbiol.* **77**:1033–40.

Alonso-Gutierrez J, Chan R, Batth TS, Adams PD, Keasling JD, Petzold CJ, Lee TS. 2013. Metabolic engineering of Escherichia coli for limonene and perillyl alcohol production. *Metab. Eng.* **19**:33–41.

Armand M, Endres F, MacFarlane DR, Ohno H, Scrosati B. 2009. Ionic-liquid materials for the electrochemical challenges of the future. *Nat. Mater.* **8**:621.

Arnold K, Bordoli L, Kopp J, Schwede T. 2006. The SWISS-MODEL workspace: A web-based environment for protein structure homology modelling. *Bioinformatics* **22**:195–201.

Asadollahi MA, Maury J, Patil KR, Schalk M, Clark A, Nielsen J. 2009. Enhancing sesquiterpene production in Saccharomyces cerevisiae through in silico driven metabolic engineering. *Metab. Eng.* **11**:328–334.

Avalos JL, Fink GR, Stephanopoulos G. 2013. Compartmentalization of metabolic pathways in yeast mitochondria improves the production of branched-chain alcohols. *Nat. Biotechnol.* **31**:335–341.

Baldovini N, Delasalle C, Joulain D. 2011. Phytochemistry of the heartwood from fragrant Santalum species: A review. *Flavour Fragr. J.*

Banerjee A, Sharkey TD. 2014. Methylerythritol 4-phosphate (MEP) pathway metabolic regulation. *Nat. Prod. Rep.* **31**:1043–1055.

Banerjee A, Wu Y, Banerjee R, Li Y, Yan H, Sharkey TD. 2013. Feedback Inhibition of Deoxy-d-xylulose-5-phosphate Synthase Regulates the Methylerythritol 4-Phosphate Pathway. *J. Biol. Chem.* **288**:16926–16936.

Baunach M, Franke J, Hertweck C. 2015. Terpenoid Biosynthesis Off the Beaten Track: Unconventional Cyclases and Their Impact on Biomimetic Synthesis. *Angew. Chemie Int. Ed.* **54**:2604–2626.

Bayer EA, Lamed R, Himmel ME. 2007. The potential of cellulases and cellulosomes for cellulosic waste management. *Curr. Opin. Biotechnol.* **18**:237–245.

Bergamo VZ, Donato RK, Dalla Lana DF, Donato KJZ, Ortega GG, Schrekker HS, Fuentefria AM. 2015. Imidazolium salts as antifungal agents: strong antibiofilm activity against multidrug-resistant Candida tropicalis isolates. *Lett. Appl. Microbiol.* **60**:66–71.

Besada-Lombana PB, McTaggart TL, Da Silva NA. 2018. Molecular tools for pathway engineering in Saccharomyces cerevisiae. *Curr. Opin. Biotechnol.* Elsevier Current Trends.

Bhatia SP, McGinty D, Letizia CS, Api AM. 2008. Fragrance material review on cedrol. *Food Chem. Toxicol.* **46**:S100–S102.

Biggs BW, Lim CG, Sagliani K, Shankar S, Stephanopoulos G, De Mey M, Ajikumar PK. 2016.

Overcoming heterologous protein interdependency to optimize P450-mediated Taxol precursor synthesis in Escherichia coli. *Proc. Natl. Acad. Sci. U. S. A.* **113**:3209–14.

BIOvIA DS. 2015. Discovery studio modeling environment, San Diego, Dassault Syst. Release.

Bisht M, Jha I, Venkatesu P. 2016. Comprehensive Evaluation of Biomolecular Interactions between Protein and Amino Acid Based-Ionic Liquids: A Comparable Study between [Bmim][Br] and [Bmim][Gly] Ionic Liquids. *ChemistrySelect* **1**:3510–3519.

Bohlmann J, Keeling CI. 2008. Terpenoid biomaterials. *Plant J.* **54**:656–669.

Bradford MM. 1976. A Rapid and Sensitive Method for the Quantitation Microgram Quantities of Protein Utilizing the Principle of Protein-Dye Binding. *Anal. Biochem.* **254**:248–254.

Brodelius M, Lundgren A, Mercke P, Brodelius PE. 2002. Fusion of farnesyldiphosphate synthase and epi -aristolochene synthase, a sesquiterpene cyclase involved in capsidiol biosynthesis in Nicotiana tabacum. *Eur. J. Biochem.* **269**:3570–3577.

Brogan APS, Bui-Le L, Hallett JP. 2018. Non-aqueous homogenous biocatalytic conversion of polysaccharides in ionic liquids using chemically modified glucosidase. *Nat. Chem.* **10**:859–865.

Burdock GA, Carabin IG. 2008. Safety assessment of sandalwood oil (Santalum album L.). *Food Chem. Toxicol.* **46**:421–432.

Busetti A, Crawford DE, Earle MJ, Gilea MA, Gilmore BF, Gorman SP, Laverty G, Lowry AF, McLaughlin M, Seddon KR. 2010. Antimicrobial and antibiofilm activities of 1-alkylquinolinium bromide ionic liquids. *Green Chem.* **12**:420–425.

Camesasca L, Minteguiaga M, Fariña L, Salzman V, Aguilar PS, Gaggero C, Carrau F. 2018. Overproduction of isoprenoids by Saccharomyces cerevisiae in a synthetic grape juice medium in the absence of plant genes. *Int. J. Food Microbiol.* **282**:42–48.

Cane DE, Ke N. 2000. Epicubenol synthase. Origin of the oxygen atom of a bacterial sesquiterpene alcohol. *Bioorg. Med. Chem. Lett.* **10**:105–7.

Cane DE, Tandon M. 1995. Epicubenol Synthase and the Stereochemistry of the Enzymatic Cyclization of Farnesyl and Nerolidyl Diphosphate. *J. Am. Chem. Soc.* **117**:5602–5603.

Cane DE, Tandon M, Prabhakaran PC. 1993. Epicubenol Synthase and the Enzymatic Cyclization of Farnesyl Diphosphate. *J. Am. Chem. Soc.* **115**:8103–8106.

Cane DE, Saito A, Croteau R, Shaskus J, Felton M. 1982. Enzymic cyclization of geranyl pyrophosphate to bornyl pyrophosphate. Role of the pyrophosphate moiety. *J. Am. Chem. Soc.* **104**:5831–5833.

Carson L, Chau PKW, Earle MJ, Gilea M a., Gilmore BF, Gorman SP, McCann MT, Seddon KR. 2009. Antibiofilm activities of 1-alkyl-3-methylimidazolium chloride ionic liquids. *Green Chem.* **11**:492.

Carter OA, Peters RJ, Croteau R. 2003. Monoterpene biosynthesis pathway construction in Escherichia coli. *Phytochemistry* **64**:425–433.

Catania TM, Branigan CA, Stawniak N, Hodson J, Harvey D, Larson TR, Czechowski T, Graham IA. 2018. Silencing amorpha-4,11-diene synthase Genes in Artemisia annua Leads to FPP Accumulation. *Front. Plant Sci.* **9**:547.

Ćavar S, Maksimović M, Vidic D, Parić A. 2012. Chemical composition and antioxidant and antimicrobial activity of essential oil of Artemisia annua L. from Bosnia. *Ind. Crops Prod.* **37**:479–

485.

Chan Y-T, Ko T-P, Yao S-H, Chen Y-W, Lee C-C, Wang AH-J. 2017. Crystal Structure and Potential Head-to-Middle Condensation Function of a *Z* , *Z* -Farnesyl Diphosphate Synthase. *ACS Omega* **2**:930–936.

Chappell J. 1995. Biochemistry and Molecular Biology of the Isoprenoid Biosynthetic Pathway in Plants. *Annu. Rev. Plant Physiol. Plant Mol. Biol.* **46**:521–547.

Chen H, Li M, Liu C, Zhang H, Xian M, Liu H. 2018. Enhancement of the catalytic activity of Isopentenyl diphosphate isomerase (IDI) from Saccharomyces cerevisiae through random and site-directed mutagenesis. *Microb. Cell Fact.* **17**:1–14.

Chen X, Zhang C, Zou R, Stephanopoulos G, Too HP. 2017. In Vitro Metabolic Engineering of Amorpha-4,11-diene Biosynthesis at Enhanced Rate and Specific Yield of Production. *ACS Synth. Biol.* **6**:1691–1700.

Chou HH, Keasling JD. 2012. Synthetic pathway for production of five-carbon alcohols from isopentenyl diphosphate. *Appl. Environ. Microbiol.* **78**:7849–55.

Christianson DW. 2006. Structural biology and chemistry of the terpenoid cyclases. *Chem. Rev.* **106**:3412–3442.

Christianson DW. 2017. Structural and Chemical Biology of Terpenoid Cyclases. *Chem. Rev.* **117**:11570–11648.

Conrado RJ, Varner JD, DeLisa MP. 2008. Engineering the spatial organization of metabolic enzymes: mimicking nature's synergy. *Curr. Opin. Biotechnol.* **19**:492–499.

Croteau R, Felton NM, Wheeler CJ. 1985. Stereochemistry at C-1 of geranyl pyrophosphate and neryl pyrophosphate in the cyclization to (+)-and (-)-bornyl pyrophosphate. *J. Biol. Chem.* **260**:5956–5962.

Croteau R, Munck SL, Akoh CC, Fisk HJ, Satterwhite DM. 1987. Biosynthesis of the sesquiterpene patchoulol from farnesyl pyrophosphate in leaf extracts of Pogostemon cablin (patchouli): Mechanistic considerations. *Arch. Biochem. Biophys.* **256**:56–68.

Croteau R, Shaskus J, Cane DE, Saito A, Chang C. 1984. Enzymatic Cyclization of [l-18O]Geranyl Pyrophosphate to 1-endo-Fenchol. *J. Am. Chem. Soc.* **106**:1142–1143.

Dahl RH, Zhang F, Alonso-Gutierrez J, Baidoo E, Batth TS, Redding-Johanson AM, Petzold CJ, Mukhopadhyay A, Lee TS, Adams PD, Keasling JD. 2013. Engineering dynamic pathway regulation using stress-response promoters. *Nat. Biotechnol.* **31**:1039–1046.

Daviet L, Schalk M. 2010. Factors affecting secondary metabolite production in plants: volatile components and essential oils. *Flavour Fragr. J.* **25**:123–127.

Davis EM, Croteau R. 2000. Cyclization Enzymes in the Biosynthesis of Monoterpenes, Sesquiterpenes, and Diterpenes. In: . Springer, Berlin, Heidelberg, pp. 53–95.

Dean PM, Turanjanin J, Yoshizawa-Fujita M, MacFarlane DR, Scott JL. 2009. Exploring an Anti-Crystal Engineering Approach to the Preparation of Pharmaceutically Active Ionic Liquids. *Cryst. Growth Des.* **9**:1137–1145.

Degenhardt J, Köllner TG, Gershenzon J. 2009. Phytochemistry Monoterpene and sesquiterpene

synthases and the origin of terpene skeletal diversity in plants. *Phytochemistry* **70**:1621–1637.

DeLano WL. 2002. The PyMOL molecular graphics system. *http//www. pymol. org*.

Deng Y, Sun M, Xu S, Zhou J. 2016. Enhanced (S)-linalool production by fusion expression of farnesyl diphosphate synthase and linalool synthase in Saccharomyces cerevisiae. *J. Appl. Microbiol.* **121**:187–195.

Dickschat JS. 2016. Bacterial terpene cyclases. *Nat. Prod. Rep.* **33**:87–110.

Dickschat JS, Rinkel J, Rabe P, Kashkooli AB, Bouwmeester HJ. 2017. 18-Hydroxydolabella-3,7-diene synthase - A diterpene synthase from Chitinophaga pinensis. *Beilstein J. Org. Chem.* **13**:1770–1780.

Djerassi C, Tökés L. 1966. Mass Spectrometry in Structural and Stereochemical Problems. XCIII.1 Further Observations on the Importance of Interatomic Distance in the McLafferty Rearrangement. Synthesis and Fragmentation Behavior of Deuterium-Labeled 12-Keto Steroids. *J. Am. Chem. Soc.*

Docherty KM, Kulpa, Jr. CF. 2005. Toxicity and antimicrobial activity of imidazolium and pyridinium ionic liquids. *Green Chem.* **7**:185.

Donohoue PD, Barrangou R, May AP. 2017. Advances in Industrial Biotechnology Using CRISPR-Cas Systems. *Trends Biotechnol.* **36**:134–146.

Du F-L, Yu H-L, Xu J-H, Li C-X. 2014. Enhanced limonene production by optimizing the expression of limonene biosynthesis and MEP pathway genes in E. coli. *Bioresour. Bioprocess.* **1:10**.

Dubey VS, Bhalla R, Luthra R. 2003. An overview of the non-mevalonate pathway for terpenoid biosynthesis in plants. *J. Biosci.* **28**:637–646.

Elleuche S. 2015. Bringing functions together with fusion enzymes — from nature's inventions to biotechnological applications. *Appl Microbiol Biotechnol.* **99**:1545–1556.

Elliott GD, Kemp R, MacFarlane DR. 2009. The development of ionic liquids for biomedical applications - Prospects and challenges. *ACS Symp. Ser.* **1030**:95–105.

Faraldos JA, Miller DJ, González V, Yoosuf-Aly Z, Cascón O, Li A, Allemann RK. 2012. A 1,6-ring closure mechanism for (+)-δ-cadinene synthase? *J. Am. Chem. Soc.* **134**:5900–5908.

Faraldos JA, Wu S, Chappell J, Coates RM. 2010. Doubly deuterium-labeled patchouli alcohol from cyclization of singly labeled [2-2H 1]farnesyl diphosphate catalyzed by recombinant patchoulol synthase. *J. Am. Chem. Soc.* **132**:2998–3008.

Farhi M, Marhevka E, Masci T, Marcos E, Eyal Y, Ovadis M, Abeliovich H, Vainstein A. 2011. Harnessing yeast subcellular compartments for the production of plant terpenoids. *Metab. Eng.* **13**:474–481.

Feder-Kubis J, Bryjak J. 2013. Laccase activity and stability in the presence of menthol-based ionic liquids. *Acta Biochim. Pol.* **60**:741–745.

Fraga BM. 2013. Natural sesquiterpenoids. *Nat. Prod. Rep.* **30**:1226–1264.

Gant TG. 2014. Using deuterium in drug discovery: Leaving the label in the drug. *J. Med. Chem.*

Garcia LC. 2015. A Review of Artemisia annua L .: Its Genetics , Biochemical Characteristics , and Anti-Malarial Efficacy. *Int. J. Sci. Technol.* **5**:38–46.

Gatto N, Vattekkatte A, Köllner T, Degenhardt J, Gershenzon J, Boland W. 2015. Isotope sensitive

branching and kinetic isotope effects to analyse multiproduct terpenoid synthases from Zea mays. *Chem. Commun.* **51**:3797–3800.

George KW, Thompson MG, Kang A, Baidoo E, Wang G, Chan LJG, Adams PD, Petzold CJ, Keasling JD, Soon Lee T. 2015. Metabolic engineering for the high-yield production of isoprenoid-based C5 alcohols in E. coli. *Sci. Rep.* **5**:11128.

Ghavre M, Byrne O, Altes L, Surolia PK, Spulak M, Quilty B, Thampi KR, Gathergood N. 2014. Low toxicity functionalised imidazolium salts for task specific ionic liquid electrolytes in dye-sensitised solar cells: a step towards less hazardous energy production. *Green Chem.* **16**:2252.

Ghimire GP, Lee HC, Sohng JK. 2009. Improved squalene production via modulation of the methylerythritol 4-phosphate pathway and heterologous expression of genes from Streptomyces peucetius ATCC 27952 in Escherichia coli. *Appl. Environ. Microbiol.* **75**:7291–3.

Giniger E, Varnum SM, Ptashne M. 1985. Specific DNA binding of GAL4, a positive regulatory protein of yeast. *Cell* **40**:767–774.

Gonzalez R, Clomburg JM, Cheong S. 2017. Engineered metabolic pathways for the fermentative production of isoprenoid precursors, isoprenoids and derivatives including prenylated aromatics compounds. *PCT Int. Appl.* William Marsh Rice University, USA .

Gore RG, Myles L, Spulak M, Beadham I, Garcia TM, Connon SJ, Gathergood N. 2013. A new generation of aprotic yet Brønsted acidic imidazolium salts: effect of ester/amide groups in the C-2, C-4 and C-5 on antimicrobial toxicity and biodegradation. *Green Chem.* **15**:2747.

Gruchattka E, Hädicke O, Klamt S, Schütz V, Kayser O. 2013. In silico profiling of Escherichia coli and Saccharomyces cerevisiae as terpenoid factories. *Microb. Cell Fact.* **12**:84.

Guo J, Cao Y, Liu H, Zhang R, Xian M, Liu H. 2019. Improving the production of isoprene and 1,3-propanediol by metabolically engineered Escherichia coli through recycling redox cofactor between the dual pathways. *Appl. Microbiol. Biotechnol.* **103**:2597–2608.

Hammer SK, Avalos JL. 2017. Harnessing yeast organelles for metabolic engineering. *Nat. Chem. Biol.* **13**:823–832.

Han GH, Kim SK, Yoon PK-S, Kang Y, Kim BS, Fu Y, Sung BH, Jung HC, Lee D-H, Kim S-W, Lee S-G. 2016. Fermentative production and direct extraction of (−)-α-bisabolol in metabolically engineered Escherichia coli. *Microb. Cell Fact.* **15**:185.

Han JY, Seo SH, Song JM, Lee H, Choi E-S. 2018. High-level recombinant production of squalene using selected Saccharomyces cerevisiae strains. *J. Ind. Microbiol. Biotechnol.* **45**:239–251.

Han M, Ma X, Yao S, Ding Y, Yan Z, Adijiang A, Wu Y, Li H, Zhang Y, Lei P, Ling Y, An J. 2017. Development of a Modified Bouveault-Blanc Reduction for the Selective Synthesis of α,α-Dideuterio Alcohols. *J. Org. Chem.* **82**:1285–1290.

Harada H, Yu F, Okamoto S, Kuzuyama T, Utsumi R, Misawa N. 2009. Efficient synthesis of functional isoprenoids from acetoacetate through metabolic pathway-engineered Escherichia coli. *Appl. Microbiol. Biotechnol.* **81**:915–925.

Harms V, Kirschning A, Dickschat JS. 2020. Nature-driven approaches to non-natural terpene analogues. *Nat. Prod. Rep.*

Harrison KW, Harvey BG. 2017. Renewable high density fuels containing tricyclic sesquiterpanes and alkyl diamondoids. *Sustain. Energy Fuels* **1**:467–473.

Hartwig S, Frister T, Alemdar S, Li Z, Krings U, Berger RG, Scheper T, Beutel S. 2014. Expression, purification and activity assay of a patchoulol synthase cDNA variant fused to thioredoxin in Escherichia coli. *Protein Expr. Purif.* **97**:61–71.

Hemmerlin A. 2013. Post-translational events and modifications regulating plant enzymes involved in isoprenoid precursor biosynthesis. *Plant Sci.* **203**:41–54.

Hu Y, Zhou YJ, Bao J, Huang L, Nielsen J, Krivoruchko A. 2017. Metabolic engineering of Saccharomyces cerevisiae for production of germacrene A, a precursor of beta-elemene. *J. Ind. Microbiol. Biotechnol.* **44**:1065–1072.

Ignea C, Cvetkovic I, Loupassaki S, Kefalas P, Johnson CB, Kampranis SC, Makris AM. 2011. Improving yeast strains using recyclable integration cassettes, for the production of plant terpenoids. *Microb. Cell Fact.* **10**:4.

Ignea C, Pontini M, Maffei ME, Makris AM, Kampranis SC. 2014. Engineering Monoterpene Production in Yeast Using a Synthetic Dominant Negative Geranyl Diphosphate Synthase. *ACS Synth. Biol.* **3**:298–306.

Ito M, Kobayashi M, Koyama T, Ogura K. 1987. Stereochemical Analysis of Prenyltransferase Reactions Leading to (Z)- and (E)-Polyprenyl Chains. *Biochemistry* **26**:4745–4750.

Jackson BE, Hart-Wells EA, Matsuda SPT. 2003. Metabolic engineering to produce sesquiterpenes in yeast. *Org. Lett.* **5**:1629–1632.

Jha A, Kumar MG, Gopi HN, Paknikar KM. 2018. Inhibition of β-Amyloid Aggregation through a Designed β-Hairpin Peptide. *Langmuir* **34**:1591–1600.

Jiang J, Cane DE. 2008. Geosmin biosynthesis. Mechanism of the fragmentation-rearrangement in the conversion of germacradienol to geosmin. *J. Am. Chem. Soc.* **130**:428–429.

Jin Q, Williams DC, Hezari M, Croteau R, Coates RM. 2005. Stereochemistry of the macrocyclization and elimination steps in taxadiene biosynthesis through deuterium labeling. *J. Org. Chem.* **70**:4667–4675.

Jones CG, Ghisalberti EL, Plummer JA, Barbour EL. 2006. Quantitative co-occurrence of sesquiterpenes; a tool for elucidating their biosynthesis in Indian sandalwood, Santalum album. *Phytochemistry* **67**:2463–2468.

Jones CG, Moniodis J, Zulak KG, Scaffidi A, Plummer JA, Ghisalberti EL, Barbour EL, Bohlmann J. 2011. Sandalwood fragrance biosynthesis involves sesquiterpene synthases of both the terpene synthase (TPS)-a and TPS-b subfamilies, including santalene synthases. *J. Biol. Chem.* **286**:17445–17454.

Joska TM, Mashruwala A, Boyd JM, Belden WJ. 2014. A universal cloning method based on yeast homologous recombination that is simple, efficient, and versatile. *J. Microbiol. Methods* **100**:46–51.

Jullien F, Moja S, Bony A, Legrand S, Petit C, Benabdelkader T, Poirot K, Fiorucci S, Guitton Y, Nicolè F, Baudino S, Magnard JL. 2014. Isolation and functional characterization of a τ-cadinol synthase,

a new sesquiterpene synthase from Lavandula angustifolia. *Plant Mol. Biol.* **84**:227–241.

Kang A, George KW, Wang G, Baidoo E, Keasling JD, Lee TS. 2016. Isopentenyl diphosphate (IPP)-bypass mevalonate pathways for isopentenol production. *Metab. Eng.* **34**:25–35.

Karuppiah V, Ranaghan KE, Leferink NGH, Johannissen LO, Shanmugam M, Ní Cheallaigh A, Bennett NJ, Kearsey LJ, Takano E, Gardiner JM, van der Kamp MW, Hay S, Mulholland AJ, Leys D, Scrutton NS. 2017. Structural Basis of Catalysis in the Bacterial Monoterpene Synthases Linalool Synthase and 1,8-Cineole Synthase. *ACS Catal.* **7**:6268–6282.

Katabami A, Li L, Iwasaki M, Furubayashi M, Saito K, Umeno D. 2015. Production of squalene by squalene synthases and their truncated mutants in Escherichia coli. *J. Biosci. Bioeng.* **119**:165–171.

Keasling JD. 2012. Synthetic biology and the development of tools for metabolic engineering. *Metab. Eng.* **14**:189–195.

Kim E-M, Eom J-H, Um Y, Kim Y, Woo HM. 2015. Microbial Synthesis of Myrcene by Metabolically Engineered *Escherichia coli*. *J. Agric. Food Chem.* **63**:4606–4612.

Kim J-H, Wang C, Jang H-J, Cha M-S, Park J-E, Jo S-Y, Choi E-S, Kim S-W. 2016. Isoprene production by Escherichia coli through the exogenous mevalonate pathway with reduced formation of fermentation byproducts. *Microb. Cell Fact.* **15**:214.

King JR, Edgar S, Qiao K, Stephanopoulos G. 2016. Accessing Nature's diversity through metabolic engineering and synthetic biology. *F1000Research* **5**:397.

Kirby J, Keasling JD. 2009. Biosynthesis of Plant Isoprenoids: Perspectives for Microbial Engineering. *Annu. Rev. Plant Biol.* **60**:335–355.

Kirby J, Nishimoto M, Chow RWN, Baidoo EEK, Wang G, Martin J, Schackwitz W, Chan R, Fortman JL, Keasling JD. 2015. Enhancing Terpene yield from sugars via novel routes to 1-deoxy-D-xylulose 5-phosphate. *Appl. Environ. Microbiol.* **81**:130–138.

Klapschinski TA, Rabe P, Dickschat JS. 2016. Pristinol, a Sesquiterpene Alcohol with an Unusual Skeleton from Streptomyces pristinaespiralis. *Angew. Chemie - Int. Ed.* **55**:10141–10144.

Klayman DL. 1985. Qinghaosu (artemisinin): an antimalarial drug from China. *Science (80-. ).* **228**:1049–1055.

Klein-Marcuschamer D, Ajikumar PK, Stephanopoulos G. 2007. Engineering microbial cell factories for biosynthesis of isoprenoid molecules: beyond lycopene. *Trends Biotechnol.* **25**:417–424.

Kobayashi M, Ito M, Koyama T, Ogura K. 1985. Stereochemistry of the Carbon to Carbon Bond Formation in the Biosynthesis of Polyprenyl Chains with Z Double Bonds. Studies with Undecaprenyl-Pyrophosphate Synthetase. *J. Am. Chem. Soc.* **107**:4588–4589.

Koziol A, Stryjewska A, Librowski T, Salat K, Gawel M, Moniczewski A, Lochynski S. 2015. An Overview of the Pharmacological Properties and Potential Applications of Natural Monoterpenes. *Mini-Reviews Med. Chem.* **14**:1156–1168.

Krivoruchko A, Nielsen J. 2015. Production of natural products through metabolic engineering of Saccharomyces cerevisiae. *Curr. Opin. Biotechnol.* **35**:7–15.

Kumar A, Bisht M, Venkatesu P. 2017. Biocompatibility of ionic liquids towards protein stability: A

comprehensive overview on the current understanding and their implications. *Int. J. Biol. Macromol.* **96**:611–651.

Lange BM, Croteau R, Herz S, Wungsintaweekul J, Hecht S, Schuhr CA, Fellermeier M, Sagner S, Zenk MH, Bacher A, Eisenreich W. 2000. Isopentenyl diphosphate biosynthesis via a mevalonate-independent pathway: Isopentenyl monophosphate kinase catalyzes the terminal enzymatic step. *Proc. Natl. Acad. Sci.* **97**:13172–13177.

Lange BM, Ahkami A. 2013. Metabolic engineering of plant monoterpenes, sesquiterpenes and diterpenes—current status and future opportunities. *Plant Biotechnol. J.* **11**:169–196.

Lei Z, Chen B, Koo Y-M, MacFarlane DR. 2017. Introduction: Ionic Liquids. *Chem. Rev.* **117**:6633–6635.

Lellouche J, Kahana E, Elias S, Gedanken A, Banin E. 2009. Antibiofilm activity of nanosized magnesium fluoride. *Biomaterials* **30**:5969–5978.

Li M, Chen H, Liu C, Guo J, Xu X, Zhang H, Nian R, Xian M. 2019. Improvement of isoprene production in Escherichia coli by rational optimization of RBSs and key enzymes screening. *Microb. Cell Fact.* **18**:4.

Li Y, Lin Z, Huang C, Zhang Y, Wang Z, Tang Y jie, Chen T, Zhao X. 2015. Metabolic engineering of Escherichia coli using CRISPR-Cas9 meditated genome editing. *Metab. Eng.* **31**:13–21.

Liu CL, Bi HR, Bai Z, Fan LH, Tan TW. 2019. Engineering and manipulation of a mevalonate pathway in Escherichia coli for isoprene production. *Appl. Microbiol. Biotechnol.* **103**:239–250.

Liu CL, Cai JY, Bi HR, Tan TW. 2018. A novel DMAPP-responding genetic circuit sensor for high-throughput screening and evolving isoprene synthase. *Appl. Microbiol. Biotechnol.*

Liu H, Sun Y, Ramos KRM, Nisola GM, Valdehuesa KNG, Lee W, Park SJ, Chung W-J. 2013. Combination of Entner-Doudoroff Pathway with MEP Increases Isoprene Production in Engineered Escherichia coli. Ed. Tanya Parish. *PLoS One* **8**:e83290.

Liu H, Wang Y, Tang Q, Kong W, Chung WJ, Lu T. 2014. MEP pathway-mediated isopentenol production in metabolically engineered Escherichia coli. *Microb. Cell Fact.* **13**:135.

Liu T, Khosla C. 2010. A Balancing Act for Taxol Precursor Pathways in E. coli. *Science* **330**:44–45.

Liu W, Xu X, Zhang R, Cheng T, Cao Y, Li X, Guo J, Liu H, Xian M. 2016. Engineering Escherichia coli for high-yield geraniol production with biotransformation of geranyl acetate to geraniol under fed-batch culture. *Biotechnol. Biofuels* **9**:58.

Liu Z, Liang Y, Ang EL, Zhao H. 2017. A New Era of Genome Integration - Simply Cut and Paste! *ACS Synth. Biol.* **6**:601–609.

Luo F, Ling Y, Li D Sen, Tang T, Liu YC, Liu Y, Li SH. 2019. Characterization of a sesquiterpene cyclase from the glandular trichomes of Leucosceptrum canum for sole production of cedrol in Escherichia coli and Nicotiana benthamiana. *Phytochemistry* **162**:121–128.

Lv X, Gu J, Wang F, Xie W, Liu M, Ye L, Yu H. 2016a. Combinatorial pathway optimization in *Escherichia coli* by directed co-evolution of rate-limiting enzymes and modular pathway engineering. *Biotechnol. Bioeng.* **113**:2661–2669.

Lv X, Wang F, Zhou P, Ye L, Xie W, Xu H, Yu H. 2016b. Dual regulation of cytoplasmic and

mitochondrial acetyl-CoA utilization for improved isoprene production in Saccharomyces cerevisiae. *Nat. Commun.* **7**:1–12.

Lv X, Xie W, Lu W, Guo F, Gu J, Yu H, Ye L. 2014. Enhanced isoprene biosynthesis in Saccharomyces cerevisiae by engineering of the native acetyl-CoA and mevalonic acid pathways with a push-pull-restrain strategy. *J. Biotechnol.* **186**:128–136.

Lv X, Xu H, Yu H. 2013. Significantly enhanced production of isoprene by ordered coexpression of genes dxs, dxr, and idi in Escherichia coli. *Appl Microbiol Biotechnol.* **97**:2357–2365.

Ma SM, Garcia DE, Redding-Johanson AM, Friedland GD, Chan R, Batth TS, Haliburton JR, Chivian D, Keasling JD, Petzold CJ, Soon Lee T, Chhabra SR. 2011. Optimization of a heterologous mevalonate pathway through the use of variant HMG-CoA reductases. *Metab. Eng.* **13**:588–597.

Mander L, Liu HW. 2010. Comprehensive Natural Products II: Chemistry and Biology. *Compr. Nat. Prod. II Chem. Biol.* Elsevier Ltd. Vol. 1 1–7451 p.

Markus Lange B, Ahkami A, Lange BM, Ahkami A, Kirby J, Keasling JD, Lange BM, Ahkami A. 2013. Metabolic engineering of plant monoterpenes, sesquiterpenes and diterpenes--current status and future opportunities. *Plant Biotechnol. J.* **11**:169–196.

Marrucho IM, Branco LC, Rebelo LPN. 2014. Ionic liquids in pharmaceutical applications. *Annu. Rev. Chem. Biomol. Eng.* **5**:527–46.

Martin VJJ, Pitera DJ, Withers ST, Newman JD, Keasling JD. 2003. Engineering a mevalonate pathway in Escherichia coli for production of terpenoids. *Nat. Biotechnol.* **21**:796–802.

Matejić J, Šarac Z, Ranđelović V. 2010. Pharmacological Activity of Sesquiterpene Lactones. *Biotechnol. Biotechnol. Equip.* **24**:95–100.

Meguro A, Motoyoshi Y, Teramoto K, Ueda S, Totsuka Y, Ando Y, Tomita T, Kim SY, Kimura T, Igarashi M, Sawa R, Shinada T, Nishiyama M, Kuzuyama T. 2015. An unusual terpene cyclization mechanism involving a carbon-carbon bond rearrangement. *Angew. Chemie - Int. Ed.* **54**:4353–4356.

Mendez-Perez D, Alonso-Gutierrez J, Hu Q, Molinas M, Baidoo EEK, Wang G, Chan LJG, Adams PD, Petzold CJ, Keasling JD, Lee TS. 2017. Production of jet fuel precursor monoterpenoids from engineered Escherichia coli. *Biotechnol. Bioeng.* **114**:1703–1712.

Mercke P, Crock J, Croteau R, Brodelius PE. 1999. Cloning, Expression, and Characterization of epi-Cedrol Synthase, a Sesquiterpene Cyclase from Artemisia annua L. *Arch. Biochem. Biophys.* **369**:213–222.

Miller DJ, Yu F, Allemann RK. 2007. Aristolochene synthase-catalyzed cyclization of 2-fluorofarnesyl-diphosphate to 2-fluorogermacrene A. *ChemBioChem* **8**:1819–1825.

Misra BB, Dey S. 2012. Comparative phytochemical analysis and antibacterial efficacy of in vitro and in vivo extracts from East Indian sandalwood tree (Santalum album L.). *Lett. Appl. Microbiol.* **55**:476–486.

Misra BB, Dey S. 2013. Quantitative and qualitative evaluation of sesquiter- penoids from essential oil and in vitro somatic em- bryos of east Indian Sandalwood (Santalum album) tree by HPTLC and GC. *J. Med. Aromat. plants* **4**:1–9.

Mitkare SS, Lakhane KG, Kokulwar PU. 2013. Ionic liquids: Novel applications in drug delivery. *Res. J. Pharm. Technol.* **6**:1367–1381.

Miziorko HM. 2011. Enzymes of the mevalonate pathway of isoprenoid biosynthesis. *Arch. Biochem. Biophys.* **505**:131–143.

Mótyán JA, Tóth F, Tőzsér J. 2013. Research applications of proteolytic enzymes in molecular biology. *Biomolecules* **3**:923–42.

Navale GR, Rout CS, Gohil KN, Dharne MS, Late DJ, Shinde SS. 2015a. Oxidative and membrane stress-mediated antibacterial activity of WS2 and rGO-WS2 nanosheets. *RSC Adv.* **5**:74726–74733.

Navale GR, Sharma P, Said MS, Ramkumar S, Dharne MS, Thulasiram H V., Shinde SS. 2019. Enhancing epi-cedrol production in Escherichia coli by fusion expression of farnesyl pyrophosphate synthase and epi-cedrol synthase. *Eng. Life Sci.* **19**:606–616.

Navale GR, Thripuranthaka M, Late, Dattatray J Shinde SS. 2015b. Antimicrobial Activity of ZnO Nanoparticles against Pathogenic Bacteria and Fungi. *JSM Nanotechnol. Nanomedicine* **3**:1033.

Newman JD, Marshall J, Chang M, Nowroozi F, Paradise E, Pitera D, Newman KL, Keasling JD. 2006. High-Level Production of Amorpha-4 , 11- Diene in a Two-Phase Partitioning Bioreactor of Metabolically Engineered Escherichia coli. *Biotechnol. Adv.* **95**:684–691.

Nguyen T-D, Macnevin G, Ro D-K. 2012. De Novo Synthesis of High-Value Plant Sesquiterpenoids in Yeast. In: . *Methods Enzymol.*, pp. 260–278.

Niu F-X, Lu Q, Bu Y-F, Liu J-Z. 2017. Metabolic engineering for the microbial production of isoprenoids: Carotenoids and isoprenoid-based biofuels. *Synth. Syst. Biotechnol.* **2**:167–175.

Nobile CJ, Johnson AD. 2015. Candida albicans Biofilms and Human Disease. *Annu. Rev. Microbiol.* **69**:71–92.

Noge K, Becerra JX. 2009. Germacrene D, A common sesquiterpene in the genus Bursera (Burseraceae). *Molecules* **14**:5289–5297.

Nosov AM, Popova E V., Kochkin D V. 2014. Isoprenoid production via plant cell cultures: Biosynthesis, accumulation and scaling-up to bioreactors. In: . *Prod. Biomass Bioact. Compd. Using Bioreact. Technol.* Dordrecht: Springer Netherlands, Vol. 9789401792, pp. 563–623.

Nowroozi FF, Baidoo EEK, Ermakov S, Redding-Johanson AM, Batth TS, Petzold CJ, Keasling JD. 2014. Metabolic pathway optimization using ribosome binding site variants and combinatorial gene assembly. *Appl Microbiol Biotechnol* **98**:1567–1581.

Nucci M, Colombo AL. 2007. Candidemia due to Candida tropicalis: clinical, epidemiologic, and microbiologic characteristics of 188 episodes occurring in tertiary care hospitals. *Diagn. Microbiol. Infect. Dis.* **58**:77–82.

Nweze EI, Ghannoum A, Chandra J, Ghannoum MA, Mukherjee PK. 2012. Development of a 96-well catheter-based microdilution method to test antifungal susceptibility of Candida biofilms. *J. Antimicrob. Chemother.* **67**:149–153.

Nybo SE, Saunders J, McCormick SP. 2017. Metabolic engineering of Escherichia coli for production of valerenadiene. *J. Biotechnol.* **262**:60–66.

O'Maille PE, Chappell J, Noel JP. 2006. Biosynthetic potential of sesquiterpene synthases: Alternative products of tobacco 5-epi-aristolochene synthase. *Arch. Biochem. Biophys.* **448**:73–82.

Ohto C, Muramatsu M, Obata S, Sakuradani E, Shimizu S. 2009. Overexpression of the gene encoding HMG-CoA reductase in Saccharomyces cerevisiae for production of prenyl alcohols. *Appl. Microbiol. Biotechnol.* **82**:837–845.

Oikawa H, Toyomasu T, Toshima H, Ohashi S, Kawaide H, Kamiya Y, Ohtsuka M, Shinoda S, Mitsuhashi W, Sassa T. 2001. Cloning and Functional Expression of cDNA Encoding Aphidicolan-16β-ol Synthase: A Key Enzyme Responsible for Formation of an Unusual Diterpene Skeleton in Biosynthesis of Aphidicolin. *J. Am. Chem. Soc.* **123**:5154–5155.

Orita I, Sakamoto N, Kato N, Yurimoto H, Sakai Y. 2007. Bifunctional enzyme fusion of 3-hexulose-6-phosphate synthase and 6-phospho-3-hexuloisomerase. *Appl. Microbiol. Biotechnol.* **76**:439–445.

Özaydin B, Burd H, Lee TS, Keasling JD. 2013. Carotenoid-based phenotypic screen of the yeast deletion collection reveals new genes with roles in isoprenoid production. *Metab. Eng.* **15**:174–183.

Paddon CJ, Westfall PJ, Pitera DJ, *et al*. 2013. High-level semi-synthetic production of the potent antimalarial artemisinin. *Nature* **496**:528–532.

Paradise EM, Kirby J, Chan R, Keasling JD. 2008. Redirection of flux through the FPP branch-point in saccharomyces cerevisiae by down-regulating squalene synthase. *Biotechnol. Bioeng.* **100**:371–378.

Paramasivan K, Mutturi S. 2017. Progress in terpene synthesis strategies through engineering of Saccharomyces cerevisiae. *Crit. Rev. Biotechnol.* Taylor & Francis.

Paul CE, Fernández VG. 2016. Biocatalysis and Biotransformation in Ionic Liquids. In: . *Ion. Liq. Lipid Process. Anal.* Elsevier, pp. 11–58.

Peng B, Nielsen LK, Kampranis SC, Vickers CE. 2018. Engineered protein degradation of farnesyl pyrophosphate synthase is an effective regulatory mechanism to increase monoterpene production in Saccharomyces cerevisiae. *Metab. Eng.* **47**:83–93.

Peng B, Plan MR, Chrysanthopoulos P, Hodson MP, Nielsen LK, Vickers CE. 2017. A squalene synthase protein degradation method for improved sesquiterpene production in Saccharomyces cerevisiae. *Metab. Eng.* **39**:209–219.

Peralta-Yahya PP, Ouellet M, Chan R, Mukhopadhyay A, Keasling JD, Lee TS. 2011. Identification and microbial production of a terpene-based advanced biofuel. *Nat. Commun.* **2**:483.

Pernak J, Goc I, Mirska I. 2004. Anti-microbial activities of protic ionic liquids with lactate anion. *Green Chem.* **6**:323.

Pernak J, Sobaszkiewicz K, Mirska I. 2003. Anti-microbial activities of ionic liquids. *Green Chem.* **5**:52–56.

Pickens LB, Tang Y, Chooi Y-H. 2011. Metabolic Engineering for the Production of Natural Products. *Annu. Rev. Chem. Biomol. Eng.* **2**:211–236.

Rabe P, Barra L, Rinkel J, Riclea R, Citron CA, Klapschinski TA, Janusko A, Dickschat JS. 2015. Conformational Analysis, Thermal Rearrangement, and EI-MS Fragmentation Mechanism of

(1(10)E,4E,6S,7R)-Germacradien-6-ol by 13C-Labeling Experiments. *Angew. Chemie - Int. Ed.* **54**:13448–13451.

Rabe P, Dickschat JS. 2016. The EIMS fragmentation mechanisms of the sesquiterpenes corvol ethers A and B, epi-cubebol and isodauc-8-en-11-ol. *Beilstein J. Org. Chem.* **12**:1380–1394.

Rani A, Ravikumar P, Reddy MD, Kush A. 2013. Molecular regulation of santalol biosynthesis in Santalum album L. *Gene* **527**:642–648.

Ranke J, Mölter K, Stock F, Bottin-Weber U, Poczobutt J, Hoffmann J, Ondruschka B, Filser J, Jastorff B. 2004. Biological effects of imidazolium ionic liquids with varying chain lengths in acute Vibrio fischeri and WST-1 cell viability assays. *Ecotoxicol. Environ. Saf.* **58**:396–404.

van Rantwijk F, Sheldon RA. 2007. Biocatalysis in Ionic Liquids. *Chem. Rev.* **107**:2757–2785.

Rathore S, Desai PM, Liew CV, Chan LW, Heng PWS. 2013. Microencapsulation of microbial cells. *J. Food Eng.* **116**:369–381.

Reiling KK, Yoshikuni Y, Martin VJJ, Newman J, Keasling JD. 2004. Mono and Diterpene Production in Escherichia coli. *Biotechnol. Bioeng.* **87**:200–2012.

Rinkel J, Lauterbach L, Rabe P, Dickschat JS. 2018. Two Diterpene Synthases for Spiroalbatene and Cembrene A from Allokutzneria albata. *Angew. Chemie - Int. Ed.* **57**:3238–3241.

Rodriguez S, Kirby J, Denby CM, Keasling JD. 2014. Production and quantification of sesquiterpenes in Saccharomyces cerevisiae, including extraction, detection and quantification of terpene products and key related metabolites. *Nat. Protoc.* **9**:1980–1996.

Rohdich F, Zepeck F, Adam P, Hecht S, Kaiser J, Laupitz R, Grawert T, Amslinger S, Eisenreich W, Bacher A, Arigoni D. 2003. The deoxyxylulose phosphate pathway of isoprenoid biosynthesis: Studies on the mechanisms of the reactions catalyzed by IspG and IspH protein. *Proc. Natl. Acad. Sci.* **100**:1586–1591.

Rohmer M, Knani TM, Simonin P, Sutter B, Sahmt H, Nationale E, Chimie S De, Werner A, Cedex FM. 1993. Isoprenoid biosynthesis in bacteria: a novel pathway for the early steps leading to isopentenyl diphosphate. *Biochem. J* **295**:517–524.

Rosano GL, Ceccarelli EA. 2014. Recombinant protein expression in Escherichia coli: advances and challenges. *Front. Microbiol.* **5**:172.

Rozkov A, Avignone-Rossa CA, Ertl PF, Jones P, O'Kennedy RD, Smith JJ, Dale JW, Bushell ME. 2004. Characterization of the metabolic burden onEscherichia coli DH1 cells imposed by the presence of a plasmid containing a gene therapy sequence. *Biotechnol. Bioeng.* **88**:909–915.

Rynkiewicz MJ, Cane DE, Christianson DW. 2001. Structure of trichodiene synthase from Fusarium sporotrichioides provides mechanistic inferences on the terpene cyclization cascade. *Proc. Natl. Acad. Sci. U. S. A.* **98**:13543–13548.

Sarria S, Wong B, Martín HG, Keasling JD, Peralta-Yahya P. 2014. Microbial synthesis of pinene. *ACS Synth. Biol.* **3**:466–475.

Savage TJ, Croteau R. 1993. Biosynthesis of Monoterpenes: Regio- and Stereochemistry of (+)-3-Carene Biosynthesis. *Arch. Biochem. Biophys.* **305**:581–587.

Scalcinati G, Partow S, Siewers V, Schalk M, Daviet L, Nielsen J. 2012. Combined metabolic

engineering of precursor and co-factor supply to increase α-santalene production by Saccharomyces cerevisiae. *Microb. Cell Fact.* **11**:117.

Scholte AA, Vederas JC. 2006. Incorporation of deuterium-labelled analogs of isopentenyl diphosphate for the elucidation of the stereochemistry of rubber biosynthesis. *Org. Biomol. Chem.*

Schrekker HS, Donato RK, Fuentefria AM, Bergamo V, Oliveira LF, Machado MM. 2013. Imidazolium salts as antifungal agents: activity against emerging yeast pathogens, without human leukocyte toxicity. *Medchemcomm* **4**:1457.

Sebesta J, Peebles C. 2017. Metabolic engineering of Synechocystis sp PCC 6803 for improved terpenoid production: Ribosome binding sites and codon optimization. In: . *Abstr. Pap. Am. Chem. Soc.* Amer Chemical Soc 1155 WASHINGTON, DC 20036 USA, Vol. 253, p.

Shao M, Keum J, Chen J, He Y, Chen W, Browning JF, Jakowski J, Sumpter BG, Ivanov IN, Ma YZ, Rouleau CM, Smith SC, Geohegan DB, Hong K, Xiao K. 2014. The isotopic effects of deuteration on optoelectronic properties of conducting polymers. *Nat. Commun.*

Sharma N, Anleu Gil M, Wengier D. 2017. A Quick and Easy Method for Making Competent Escherichia coli Cells for Transformation Using Rubidium Chloride. *Bio-protocol* **7**:1–5.

Shen HY, Li ZQ, Wang H, Ma LQ, Liu BY, Yan F, Li GF, Ye HC. 2007. Advances in Sesquiterpene Synthases (Cyclases) of Artemisia annua. *Chin. J. Biotechnol.* **23**:976–981.

Shi S, Liang Y, Zhang MM, Ang EL, Zhao H. 2016. A highly efficient single-step, markerless strategy for multi-copy chromosomal integration of large biochemical pathways in Saccharomyces cerevisiae. *Metab. Eng.* **33**:19–27.

Shin SY, Yang S-T, Park EJ, Eom SH, Song WK, Kim JI, Lee S-H, Lee MK, Lee DG, Hahm K-S, Kim Y. 2001. Antibacterial, antitumor and hemolytic activities of alpha-helical antibiotic peptide, P18 and its analogs. *J. Pept. Res.* **58**:504–514.

Shinde SS, Minami A, Chen Z, Tokiwano T, Toyomasu T, Kato N, Sassa T, Oikawa H. 2017. Cyclization mechanism of phomopsene synthase: Mass spectrometry based analysis of various site-specifically labeled terpenes. *J. Antibiot. (Tokyo).* **70**:632.

Shinde SS, Navale GR, Said MS, Thulasiram H V. 2016. Stereoselective quenching of cedryl carbocation in epicedrol biosynthesis. *Tetrahedron Lett.* **57**:1161–1164.

Shinde SS, Lee BS, Chi DY. 2008. Synergistic effect of two solvents, tert-alcohol and lonic liquid, in one molecule in nucleophilic fluorination. *Org. Lett.* **10**:733–735.

Shinde SS, Patil SN. 2014. One molecule of ionic liquid and tert-alcohol on a polystyrene-support as catalysts for efficient nucleophilic substitution including fluorination. *Org. Biomol. Chem.* **12**:9264–9271.

Shinde SS, Patil SN, Ghatge A, Kumar P. 2015. Nucleophilic fluorination using imidazolium based ionic liquid bearing tert-alcohol moiety. *New J. Chem.* **39**:4368–4374.

Shrivastava PL. 2014. Characterization of the Genes Involved in Santalene Biosynthetic Pathway in Indian Sandalwood Santalum album Linn. *(PhD Thesis) Univ. Pune*; (PhD. Thesis) Univerisity of Pune.

Singh B, Sharma RA. 2015. Plant terpenes: defense responses, phylogenetic analysis, regulation and

clinical applications. *3 Biotech* **5**:129–151.

Sivapragasam M, Moniruzzaman M, Goto M. 2016. Recent advances in exploiting ionic liquids for biomolecules: Solubility, stability and applications. *Biotechnol. J.* **11**:1000–1013.

Solhtalab M, Karbalaei-Heidari HR, Absalan G. 2015. Tuning of hydrophilic ionic liquids concentration: A way to prevent enzyme instability. *J. Mol. Catal. B Enzym.* **122**:125–130.

Song AA-L, Abdullah JO, Abdullah MP, Shafee N, Othman R, Tan E-F, Noor NM, Raha AR. 2012. Overexpressing 3-Hydroxy-3-Methylglutaryl Coenzyme A Reductase (HMGR) in the Lactococcal Mevalonate Pathway for Heterologous Plant Sesquiterpene Production. Ed. Paul Jaak Janssen. *PLoS One* **7**:e52444.

Srivastava PL, Daramwar PP, Krithika R, Pandreka A, Shankar SS, Thulasiram H V. 2015. Functional Characterization of Novel Sesquiterpene Synthases from Indian Sandalwood, Santalum album. *Sci. Rep.* **5**:10095.

Su X-Z, Miller LH. 2015. The discovery of artemisinin and the Nobel Prize in Physiology or Medicine. *Sci. China Life Sci.* **58**:1175–1179.

Swatloski RP, Holbrey JD, Rogers RD. 2003. Ionic liquids are not always green: hydrolysis of 1-butyl-3-methylimidazolium hexafluorophosphate. *Green Chem.* **5**:361.

Szczebara FM, Chandelier C, Villeret C, Masurel A, Bourot S, Duport C, Blanchard S, Groisillier A, Testet E, Costaglioli P, Cauet G, Degryse E, Balbuena D, Winter J, Achstetter T, Spagnoli R, Pompon D, Dumas B. 2003. Total biosynthesis of hydrocortisone from a simple carbon source in yeast. *Nat. Biotechnol.* **21**:143–149.

Takahashi S, Yeo Y, Greenhagen BT, McMullin T, Song L, Maurina-Brunker J, Rosson R, Noel JP, Chappell J. 2007. Metabolic engineering of sesquiterpene metabolism in yeast. *Biotechnol. Bioeng.* **97**:170–181.

Tang M-C, Zou Y, Watanabe K, Walsh CT, Tang Y. 2017. Oxidative Cyclization in Natural Product Biosynthesis. *Chem. Rev.* **117**:5226–5333.

Tashiro M, Kiyota H, Kawai-Noma S, Saito K, Ikeuchi M, Iijima Y, Umeno D. 2016. Bacterial Production of Pinene by a Laboratory-Evolved Pinene-Synthase. *ACS Synth. Biol.* **5**:1011–1020.

Tholl D. 2015. Biosynthesis and Biological Functions of Terpenoids in Plants. *Adv. Biochem. Eng. Biotechnol.* **148**:63–106.

Tian T, Kang JW, Kang A, Lee TS. 2019. Redirecting Metabolic Flux via Combinatorial Multiplex CRISPRi-Mediated Repression for Isopentenol Production in Escherichia coli. *ACS Synth. Biol.* **8**:391–402.

Tippmann S, Anfelt J, David F, Rand JM, Siewers V, Uhlén M, Nielsen J, Hudson EP. 2017. Affibody Scaffolds Improve Sesquiterpene Production in *Saccharomyces cerevisiae*. *ACS Synth. Biol.* **6**:19–28.

Tippmann S, Chen Y, Siewers V, Nielsen J. 2013. From flavors and pharmaceuticals to advanced biofuels: production of isoprenoids in Saccharomyces cerevisiae. *Biotechnol. J.* **8**:1435–1444.

Tippmann S, Scalcinati G, Siewers V, Nielsen J. 2016. Production of farnesene and santalene by Saccharomyces cerevisiae using fed-batch cultivations with RQ-controlled feed. *Biotechnol.*

*Bioeng.* **113**:72–81.

Tong Y, Weber T, Lee SY. 2019. CRISPR/Cas-based genome engineering in natural product discovery. *Nat. Prod. Rep.*

Toogood HS, Cheallaigh AN, Tait S, Mansell DJ, Jervis A, Lygidakis A, Humphreys L, Takano E, Gardiner JM, Scrutton NS. 2015. Enzymatic Menthol Production: One-Pot Approach Using Engineered Escherichia coli. *ACS Synth. Biol.* **4**:1112–1123.

Townsend CA, Ebizuka Y (Yutaka). 2010. Natural products structural diversity-I, secondary metabolites : organization and biosynthesis. *Compr. Nat. Prod. II Chem. Biol.* Vol. 1 1007 p.

Tsuruta H, Paddon CJ, Eng D, Lenihan JR, Horning T, Anthony LC, Regentin R, Keasling JD, Renninger NS, Newman JD. 2009. High-level production of amorpha-4, 11-diene, a precursor of the antimalarial agent artemisinin, in Escherichia coli. *PLoS One* **4**:e4489.

Tu Y. 2016. Artemisinin-A Gift from Traditional Chinese Medicine to the World (Nobel Lecture). *Angew. Chemie Int. Ed.* **55**:10210–10226.

Tyo KEJ, Ajikumar PK, Stephanopoulos G. 2009. Stabilized gene duplication enables long-term selection-free heterologous pathway expression. *Nat. Biotechnol.* **27**:760–765.

Vekariya RL. 2017. A review of ionic liquids: Applications towards catalytic organic transformations. *J. Mol. Liq.* **227**:44–60.

Venkatraman V, Evjen S, Lethesh KC, Raj JJ, Knuutila HK, Fiksdahl A. 2019. Rapid, comprehensive screening of ionic liquids towards sustainable applications. *Sustain. Energy Fuels* **3**:2798–2808.

Vickers CE, Williams TC, Peng B, Cherry J. 2017. Recent advances in synthetic biology for engineering isoprenoid production in yeast. *Curr. Opin. Chem. Biol.* **40**:47–56.

Vögeli B, Engilberge S, Girard E, Riobé F, Maury O, Erb TJ, Shima S, Wagner T. 2018. Archaeal acetoacetyl-CoA thiolase/HMG-CoA synthase complex channels the intermediate via a fused CoA-binding site. *Proc. Natl. Acad. Sci. U. S. A.* **115**:3380–3385.

Vranová E, Coman D, Gruissem W. 2013. Network Analysis of the MVA and MEP Pathways for Isoprenoid Synthesis. *Annu. Rev. Plant Biol.* **64**:665–700.

Wang C, Kim SW. 2015. Shaking up ancient scents: Insights into santalol synthesis in engineered Escherichia coli. *Process Biochem.* **50**:1177–1183.

Wang C, Liwei M, Park J Bin, Jeong SH, Wei G, Wang Y, Kim SW. 2018. Microbial platform for terpenoid production: Escherichia coli and Yeast. *Front. Microbiol.* **9**:1–8.

Wang C, Park J, Choi E, Kim S. 2016. Farnesol production in Escherichia coli through the construction of a farnesol biosynthesis pathway – application of PgpB and YbjG phosphatases. *Biotechnol. J.* **1297**:1291–1297.

Wang C, Yoon S, Jang H, Chung Y, Kim J-Y, Choi E, Kim S. 2011. Metabolic engineering of Escherichia coli for α-farnesene production. *Metab. Eng.* **13**:648–655.

Wang C, Yoon S, Shah AA, Chung Y, Kim J, Choi E, Keasling JD, Kim S. 2010. Farnesol Production From Escherichia coli by Harnessing the Exogenous Mevalonate Pathway. *Biotechnol. Bioeng.* **107**:421–429.

Wang C, Zada B, Wei G, Kim SW. 2017. Metabolic engineering and synthetic biology approaches

driving isoprenoid production in Escherichia coli. *Bioresour. Technol.* **241**:430–438.

Wang H, Han J, Kanagarajan S, Lundgren A, Brodelius PE. 2013. Studies on the Expression of Sesquiterpene Synthases Using Promoter-β-Glucuronidase Fusions in Transgenic Artemisia annua L. *PLoS One* **8**:1–17.

Wang J, Xu C, Wong YK, Li Y, Liao F, Jiang T, Tu Y. 2019. Artemisinin, the Magic Drug Discovered from Traditional Chinese Medicine. *Engineering* **5**:32–39.

Wang W, Oldfield E. 2014. Bioorganometallic chemistry with IspG and IspH: Structure, function, and inhibition of the [Fe4S4] proteins involved in isoprenoid biosynthesis. *Angew. Chemie - Int. Ed.* **53**:4294–4310.

Weathers PJ, Arsenault PR, Covello PS, McMickle A, Teoh KH, Reed DW. 2011. Artemisinin production in Artemisia annua: studies in planta and results of a novel delivery method for treating malaria and other neglected diseases. *Phytochem. Rev.* **10**:173–183.

Weaver LJ, Sousa MML, Wang G, Baidoo E, Petzold CJ, Keasling JD. 2015. A kinetic-based approach to understanding heterologous mevalonate pathway function in E. coli. *Biotechnol. Bioeng.* **112**:111–119.

Wells AS, Coombe VT. 2006. On the freshwater ecotoxicity and biodegradation properties of some common ionic liquids. *Org. Process Res. Dev.* **10**:794–798.

West Jr RW, Yocum RR, Ptashne M. 1984. Saccharomyces cerevisiae GAL1-GAL10 divergent promoter region: location and function of the upstream activating sequence UASG. *Mol. Cell. Biol.* **4**:2467–2478.

Westfall PJ, Pitera DJ, Lenihan JR, Eng D, Woolard FX, Regentin R, Horning T, Tsuruta H, Melis DJ, Owens A, Fickes S, Diola D, Benjamin KR, Keasling JD, Leavell MD, McPhee DJ, Renninger NS, Newman JD, Paddon CJ. 2012. Production of amorphadiene in yeast, and its conversion to dihydroartemisinic acid, precursor to the antimalarial agent artemisinin. *Proc. Natl. Acad. Sci. U. S. A.* **109**:E111-8.

Whited GM, Feher FJ, Benko DA, Cervin MA, Chotani GK, McAuliffe JC, LaDuca RJ, Ben-Shoshan EA, Sanford KJ. 2010. Development of a gas-phase bioprocess for isoprene-monomer production using metabolic pathway engineering. *Ind. Biotechnol.* **6**:152–163.

Whittington DA, Wise ML, Urbansky M, Coates RM, Croteau RB, Christianson DW. 2002. Bornyl diphosphate synthase: structure and strategy for carbocation manipulation by a terpenoid cyclase. *Proc. Natl. Acad. Sci.* **99**:15375–15380.

Willrodt C, David C, Cornelissen S, Bühler B, Julsing MK, Schmid A. 2014. Engineering the productivity of recombinant Escherichia coli for limonene formation from glycerol in minimal media. *Biotechnol. J.* **9**:1000–1012.

Wise ML, Pyun HJ, Helms G, Assink B, Coates RM, Croteau RB. 2001. Stereochemical disposition of the geminal dimethyl groups in the enzymatic cyclization of geranyl diphosphate to (+)-bornyl diphosphate by recombinant (+)-bornyl diphosphate synthase from Salvia officinalis. *Tetrahedron* **57**:5327–5334.

Wise ML, Savage TJ, Katahira E, Croteau R. 1998. Monoterpene synthases from common sage (Salvia

officinalis) cDNA isolation, characterization, and functional expression of (+)-sabinene synthase, 1, 8-cineole synthase, and (+)-bornyl diphosphate synthase. *J. Biol. Chem.* **273**:14891–14899.

Withers ST, Keasling JD. 2007. Biosynthesis and engineering of isoprenoid small molecules. *Appl. Microbiol. Biotechnol.* **73**:980–990.

Wong J, D'Espaux L, Dev I, van der Horst C, Keasling J. 2018. De novo synthesis of the sedative valerenic acid in Saccharomyces cerevisiae. *Metab. Eng.* **47**:94–101.

Wu J, Cheng S, Cao J, Qiao J, Zhao G-R. 2019. Systematic Optimization of Limonene Production in Engineered *Escherichia coli*. *J. Agric. Food Chem.*:acs.jafc.9b01427.

Wu W, Liu F, Davis RW. 2018. Engineering Escherichia coli for the production of terpene mixture enriched in caryophyllene and caryophyllene alcohol as potential aviation fuel compounds. *Metab. Eng. Commun.* **6**:13–21.

Wyne. 2008. Reference method for broth dilution antifungal susceptibility testing of yeasts: approved standard - third edition. *Clin. Lab. Stand. Inst.* 1–25 p.

Xie W, Liu M, Lv X, Lu W, Gu J, Yu H. 2014. Construction of a controllable β-carotene biosynthetic pathway by decentralized assembly strategy in Saccharomyces cerevisiae. *Biotechnol. Bioeng.*

Xu W-J, Huang Y-K, Li F, Wang D-D, Yin M-N, Wang M, Xia Z-N. 2018. Improving β-glucosidase biocatalysis with deep eutectic solvents based on choline chloride. *Biochem. Eng. J.* **138**:37–46.

Xu Y, Sheng S, Liu X, Wang C, Xiao W, Wang J, Wu FA. 2017. Cooperative reinforcement of ionic liquid and reactive solvent on enzymatic synthesis of caffeic acid phenethyl ester as an in vitro inhibitor of plant pathogenic bacteria. *Molecules* **22**:6–11.

Yamada Y, Kuzuyama T, Komatsu M, Shin-ya K, Omura S, Cane DE, Ikeda H. 2015. Terpene synthases are widely distributed in bacteria. *Proc. Natl. Acad. Sci.* **112**:857–862.

Yang C, Gao X, Jiang Y, Sun B, Gao F, Yang S. 2016a. Synergy between methylerythritol phosphate pathway and mevalonate pathway for isoprene production in Escherichia coli. *Metab. Eng.* **37**:79–91.

Yang J, Nie Q, Liu H, Xian M, Liu H. 2016b. A novel MVA-mediated pathway for isoprene production in engineered E. coli. *BMC Biotechnol.* **16**:5.

Yang J, Nie Q, Ren M, Feng H, Jiang X, Zheng Y, Liu M, Zhang H, Xian M. 2013. Metabolic engineering of Escherichia coli for the biosynthesis of alpha-pinene. *Biotechnol. Biofuels* **6**:60.

Yang J, Xian M, Su S, Zhao G, Nie Q, Jiang X, Zheng Y, Liu W. 2012a. Enhancing Production of Bio-Isoprene Using Hybrid MVA Pathway and Isoprene Synthase in E. coli. Ed. Spencer J. Williams. *PLoS One* **7**:e33509.

Yang J, Zhao G, Sun Y, Zheng Y, Jiang X, Liu W, Xian M. 2012b. Bio-isoprene production using exogenous MVA pathway and isoprene synthase in Escherichia coli. *Bioresour. Technol.* **104**:642–647.

Yang J, Yan R, Roy A, Xu D, Poisson J, Zhang Y. 2014. The I-TASSER Suite: protein structure and function prediction. *Nat. Methods* **12**:7–8.

Yang L, Jiang L, Li W, Yang Y, Zhang G, Luo Y. 2017. A homomeric geranyl diphosphate synthase-encoding gene from Camptotheca acuminata and its combinatorial optimization for production of

geraniol in Escherichia coli. *J. Ind. Microbiol. Biotechnol.* **44**:1431–1441.

Yang L, Wang C, Zhou J, Kim SW. 2016c. Combinatorial engineering of hybrid mevalonate pathways in Escherichia coli for protoilludene production. *Microb. Cell Fact.*:1–8.

Yang Z. 2009. Hofmeister effects: an explanation for the impact of ionic liquids on biocatalysis. *J. Biotechnol.* **144**:12–22.

Young CL, Britton ZT, Robinson AS. 2012. Recombinant protein expression and purification: A comprehensive review of affinity tags and microbial applications. *Biotechnol. J.* **7**:620–634.

Yu F, Harada H, Yamasaki K, Okamoto S, Hirase S, Tanaka Y, Misawa N, Utsumi R. 2008. Isolation and functional characterization of a β-eudesmol synthase, a new sesquiterpene synthase from Zingiber zerumbet Smith. *FEBS Lett.* **582**:565–572.

Yu K, Liu C, Kim B-GG, Lee D-YY. 2015. Synthetic fusion protein design and applications. *Biotechnol. Adv.* **33**:155–64.

Yuan J, Ching C-B. 2016. Mitochondrial acetyl-CoA utilization pathway for terpenoid productions. *Metab. Eng.* **38**:303–309.

Zhang C, Zou R, Chen X, Experimental HT, Link C, Zhang C, Zou R, Chen X. 2015. Experimental design-aided systematic pathway optimization of glucose uptake and deoxyxylulose phosphate pathway for improved amorphadiene Accessed Experimental design-aided systematic pathway optimization of glucose uptake and deoxyxylulose phosphate path. *App Microbiol Biotechnol* **99**:3825–3837.

Zhang H, Liu Q, Cao Y, Feng X, Zheng Y, Zou H, Liu H, Yang J, Xian M. 2014. Microbial production of sabinene-a new terpene-based precursor of advanced biofuel. *Microb. Cell Fact.* **13**:20.

Zhang K, Ou M, Wang W, Ling J. 2009. Effects of quorum sensing on cell viability in Streptococcus mutans biofilm formation. *Biochem. Biophys. Res. Commun.* **379**:933–938.

Zhang Y-HP. 2011. Substrate channeling and enzyme complexes for biotechnological applications. *Biotechnol. Adv.* **29**:715–725.

Zhang Y, Han L, Chen S-S, Guan J, Qu F-Z, Zhao Y-Q. 2016. Hair growth promoting activity of cedrol isolated from the leaves of Platycladus orientalis. *Biomed. Pharmacother.* **83**:641–647.

Zhang Y, Wang J, Cao X, Liu W, Yu H, Ye L. 2020. High-level production of linalool by engineered Saccharomyces cerevisiae harboring dual mevalonate pathways in mitochondria and cytoplasm. *Enzyme Microb. Technol.* **134**:109462.

Zhang Y, Wang Y, Wang S, Fang B. 2017a. Engineering bi-functional enzyme complex of formate dehydrogenase and leucine dehydrogenase by peptide linker mediated fusion for accelerating cofactor regeneration. *Eng. Life Sci.* **17**:989–996.

Zhang Y, Nielsen J, Liu Z, Nielsen J, Nielsen J, Liu Z. 2017b. Engineering yeast metabolism for production of terpenoids for use as perfume ingredients, pharmaceuticals and biofuels. *FEMS Yeast Res.* **17**:1–8.

Zhao H. 2012. Ionic Liquids as (Co-)Solvents for Hydrolytic Enzymes. In: . *Ion. Liq. Biotransformations Organocatalysis*. Hoboken, NJ, USA: John Wiley & Sons, Inc., pp. 151–227.

Zhao H, Harter GA, Martin CJ. 2019. “water-like” Dual-Functionalized Ionic Liquids for Enzyme

Activation. Research-article. *ACS Omega* **4**:15234–15239.

Zhao J, Li C, Zhang Y, Shen Y, Hou J, Bao X. 2017. Dynamic control of ERG20 expression combined with minimized endogenous downstream metabolism contributes to the improvement of geraniol production in Saccharomyces cerevisiae. *Microb. Cell Fact.* **16**:1–11.

Zhao L, Chang W, Xiao Y, Liu H, Liu P. 2013. Methylerythritol phosphate pathway of isoprenoid biosynthesis. *Annu. Rev. Biochem.* **82**:497–530.

Zhao Y, Yang J, Qin B, Li Y, Sun Y, Su S, Xian M. 2011. Biosynthesis of isoprene in Escherichia coli via methylerythritol phosphate (MEP) pathway. *Appl. Microbiol. Biotechnol.* **90**:1915.

Zheng Y, Liu Q, Li L, Qin W, Yang J, Zhang H, Jiang X, Cheng T, Liu W, Xu X, Xian M. 2013. Metabolic engineering of Escherichia coli for high-specificity production of isoprenol and prenol as next generation of biofuels. *Biotechnol. Biofuels* **6**:57.

Zhou J, Wang C, Yang L, Choi ES, Kim SW. 2015. Geranyl diphosphate synthase: An important regulation point in balancing a recombinant monoterpene pathway in Escherichia coli. *Enzyme Microb. Technol.* **68**:50–55.

Zhou J, Wang C, Yoon SH, Jang HJ, Choi ES, Kim SW. 2014. Engineering Escherichia coli for selective geraniol production with minimized endogenous dehydrogenation. *J. Biotechnol.* **169**:42–50.

Zhou J, Yang L, Wang C, Choi ES, Kim SW. 2017. Enhanced performance of the methylerythritol phosphate pathway by manipulation of redox reactions relevant to IspC, IspG, and IspH. *J. Biotechnol.* **248**:1–8.

Zhou Y, Nambou K, Wei L, Cao J, Imanaka T, Hua Q. 2013. Lycopene production in recombinant strains of Escherichia coli is improved by knockout of the central carbon metabolism gene coding for glucose-6-phosphate dehydrogenase. *Biotechnol. Lett.* **35**:2137–2145.

Zhou Y, Li G, Dong J, Xing X hui, Dai J, Zhang C. 2018. MiYA, an efficient machine-learning workflow in conjunction with the YeastFab assembly strategy for combinatorial optimization of heterologous metabolic pathways in Saccharomyces cerevisiae. *Metab. Eng.* **47**:294–302.

Zhou YJ, Gao W, Rong Q, Jin G, Chu H, Liu W, Yang W, Zhu Z, Li G, Zhu G, Huang L, Zhao ZK. 2012. Modular pathway engineering of diterpenoid synthases and the mevalonic acid pathway for miltiradiene production. *J. Am. Chem. Soc.* **134**:3234–3241.

Zhu F, Zhong X, Hu M, Lu L, Deng Z, Liu T. 2014. In vitro reconstitution of mevalonate pathway and targeted engineering of farnesene overproduction in Escherichia coli. *Biotechnol. Bioeng.* **111**:1396–1405.

Zhuang X, Chappell J. 2015. Building terpene production platforms in yeast. *Biotechnol. Bioeng.* **112**:1854–1864.

Zou R, Zhou K, Stephanopoulos G, Too HP. 2013. Combinatorial Engineering of 1-Deoxy-D-Xylulose 5- Phosphate Pathway Using Cross-Lapping In Vitro Assembly ( CLIVA ) Method. *PLoS One* **8**:1–12.

# *Publications*

# Publications

## ❖ List of Publications (from Thesis)

1. **Navale GR**, Sharma P, Said MS, Ramkumar S, Dharne MS, Thulasiram HV, Shinde SS. 2019. Enhancing *epi* -cedrol production in Escherichia coli by fusion expression of farnesyl pyrophosphate synthase and epi -cedrol synthase. *Eng. Life Sci.* **19**:606–616.

2. Shinde SS*, **Navale GR**, Said MS, Thulasiram HV. 2016. Stereoselective quenching of cedryl carbocation in epicedrol biosynthesis. *Tetrahedron Lett.* **57**:1161–1164.

3. **Navale GR**, Dharne MS, Shinde SS. 2015. Antibiofilm activity of tert-BuOH functionalized ionic liquids with methylsulfonate counteranions. *RSC Adv.* **5**:68136–68142.

4. **Navale GR**, Yadav AP, Shinde SS, Dharne MS, Improved stability and catalytic efficiency of Artemisia annua L. *epi*-cedrol synthase in ter-alcohol functionalised Imidazolium based ionic liquids. (Manuscript under communication)

5. **Navale GR**, Shinde SS, Dharne MS. Metabolic engineering of *Escherichia coli* and *Saccharomyces cerevisiae* for $C_5$-$C_{20}$ isoprenoids production: A Review. (Manuscript communicated)

6. **Navale GR**, PD Sharma, Dharne MS, Thulsiram HV, Shinde SS. Fusion expression of farnesyl pyrophosphate synthase and Santalene synthase for production of santalene in *Escherichia coli* and *Saccharomyces cerevisiae:* A Comparative study. ((Manuscript under writing)

❖ **List of Publications (other than Thesis)**

1. **Navale GR** †, Samson R.†, Dharne MS. 2020. Biosensors: Frontiers in Rapid Detection of COVID-19: Review, *3 Biotech*, **10**, 395.

2. Deshpande JB, **Navale GR**, Dharne MS, Kulkarni AA. 2020. Continuous Interfacial Centrifugal Separation and Recovery of Silver Nanoparticles. *Chem. Eng. Technol.* **43**:582–592.

3. **Navale GR**, Gohil KN, Puppala KR, Shinde SS, Umbarkar S, Dharne MS. 2019. Rapid and greener method for utilization of Plaster of Paris (POP) waste generated from biomedical samples. *Int. J. Environ. Sci. Technol.***24**:2475-2480.

4. **Navale GR**, Rout CS, Gohil KN, Dharne MS, Late DJ, Shinde SS. 2015. Oxidative and membrane stress-mediated antibacterial activity of WS2 and rGO-WS2 nanosheets. *RSC Adv.* **5**:74726–74733.

5. **Navale GR**, Thripuranthaka M, Late, Dattatray J Shinde SS. 2015. Antimicrobial Activity of ZnO Nanoparticles against Pathogenic Bacteria and Fungi. *JSM Nanotechnol. Nanomedicine* **3**:1033.

6. Shaikh MHMH, Subhedar DD, Shingate BB, Kalam Khan FA, Sangshetti JN, Khedkar VM, Nawale L, Sarkar D, **Navale GR**, Shinde SS. 2016. Synthesis, biological evaluation and molecular docking of novel coumarin incorporated triazoles as antitubercular, antioxidant and antimicrobial agents. *Med. Chem. Res.* **25**:790–804.

Received: 31 January 2019 | Revised: 19 June 2019 | Accepted: 8 July 2019

DOI: 10.1002/elsc.201900103

Engineering in Life Sciences

RESEARCH ARTICLE

# Enhancing *epi*-cedrol production in *Escherichia coli* by fusion expression of farnesyl pyrophosphate synthase and *epi*-cedrol synthase

**Govinda R. Navale[1,2,3] | Poojadevi Sharma[1] | Madhukar S. Said[1] | Sudha Ramkumar[1] | Mahesh S. Dharne[2,3] | H. V. Thulasiram[1,2] | Sandip S. Shinde[1,2]**

[1]Division of Organic Chemistry, CSIR-National Chemical Laboratory, Pune, Maharashtra, India

[2]Academy of Scientific and Innovative Research (AcSIR), Ghaziabad, India

[3]NCIM Resource Centre, CSIR-National Chemical Laboratory, Pune, Maharashtra, India

**Correspondence**
Dr. Sandip S. Shinde, Division of Organic Chemistry, CSIR-National Chemical Laboratory, Dr. Homi Bhabha Road, Pune, Maharashtra 411008, India.
Email: shinde88@gmail.com

H. V. Thulasiram, Division of Organic Chemistry, CSIR-National Chemical Laboratory, Dr. Homi Bhabha Road, Pune, Maharashtra 411008, India.
Email: hv.thulasiram@ncl.res.in

**Present Address**
Dr. Sandip S. Shinde, Department Industrial and Engineering Chemistry, Institute of Chemical Technology Mumbai Marathwada Campus, Jalna, India 431213.

Terpene synthase catalyses acyclic diphosphate farnesyl diphosphate into desired sesquiterpenes. In this study, a fusion enzyme was constructed by linking *Santalum album* farnesyl pyrophosphate synthase (*SaFPPS*) individually with terpene synthase and *Artemisia annua Epi*-cedrol synthase (*AaECS*). The stop codon at the N-terminus of *SaFPPS* was removed and replaced by a short peptide (GSGGS) to introduce a linker between the two open reading frames. This fusion clone was expressed in *Escherichia coli* Rosseta DE3 cells. The fusion enzyme *FPPS-ECS* produced sesquiterpene 8-*epi*-cedrol from substrates isopentenyl pyrophosphate and dimethylallyl pyrophosphate through sequential reactions. The $K_m$ values for *FPPS-ECS* for isopentyl diphosphate was 4.71 μM. The fusion enzyme carried out the efficient conversion of IPP to *epi*-cedrol, in comparison to single enzymes *SaFPPS* and *AaECS* when combined together in enzyme assay over time. Further, the recombinant *E. coli* BL21 strain harbouring fusion plasmid successfully produced *epi*-cedrol in fermentation medium. The strain having fusion plasmid (pET32a-FPPS-ECS) produced 1.084 ± 0.09 mg/L *epi*-cedrol, while the strain harbouring mixed plasmid (pRSETB-FPPS and pET28a-ECS) showed 1.002 ± 0.07 mg/L titre in fermentation medium by overexpression and MEP pathway utilization. Structural analysis was done by I-TASSER server and docking was done by AutoDock Vina software, which suggested that secondary structure of the N- C terminal domain and their relative positions to functional domains of the fusion enzyme was greatly significant to the catalytic properties of the fusion enzymatic complex than individual enzymes.

**KEYWORDS**
*epi*-cedrol synthase, fusion enzymes, recombinant expression

## 1 | INTRODUCTION

Sesquiterpenes ($C_{15}$) are chemically and structurally diverse class of terpenes which have found vast commercial applications in chemical, flavour, fragrance, pharmaceutical and, nutraceutical industries [1,2]. However, these are produced in very low concentrations by mevalonate (MVA)

Abbreviations: DMAPP, dimethylallyl pyrophosphate; DTT, dithiothreitol; DXP, deoxy-D-xylulose-5-phosphate; *ECS*, *epi*-cedrol synthase; FPP, farnesyl diphosphate; *FPPS*, farnesyl pyrophosphate synthase; GPP, geranyl diphosphate; IPP, isopentyl diphosphate; IPTG, isopropyl thio-β-D-thiogalactopyranoside; MEP, methyl D-erythritol 4-phosphate; MVA, mevalonate.

  

Tetrahedron Letters 57 (2016) 1161–1164

Contents lists available at ScienceDirect

Tetrahedron Letters

journal homepage: www.elsevier.com/locate/tetlet

# Stereoselective quenching of cedryl carbocation in epicedrol biosynthesis

Sandip S. Shinde *, Govinda R. Navale, Madhukar S. Said, Hirekodathakallu V. Thulasiram *

*Organic Chemistry Division, CSIR-National Chemical Laboratory (CSIR-NCL), Dr. Homi Bhabha Road, Pashan, Pune 411008, India*

ARTICLE INFO

*Article history:*
Received 8 January 2016
Revised 29 January 2016
Accepted 31 January 2016
Available online 1 February 2016

*Keywords:*
Epicedrol
Isotopic labeling
Sesquiterpenoid
Biosynthesis
Enzyme

ABSTRACT

Epicedrol synthase catalyzes the cyclization of achiral diphosphate substrate, (*E*,*E*)-farnesyldiphosphate (FPP) into epicedrol. GC–MS analysis of assay extracts obtained by incubating FPP with epicedrol synthase in 21.6 at % $H_2{}^{18}O$ buffer showed the molecular ion of 224 for epicedrol. The labeled oxygen study presented here unambiguously demonstrates that the hydroxyl group of the epicedrol synthase enzymatic product, epicedrol, is derived from a water molecule, not from the phosphate moiety of the FPP.


## Introduction

Over 70,000 isoprenoid compounds with diverse chemical structures are known to date and possess numerous biological activities such as antibiotics, toxins, and pheromones.[1,2] Usually, divalent metal dependent sesquiterpene synthases catalyze the cyclization of the linear substrate, farnesyl diphosphate (FPP) into complex hydrocarbon skeletons through a series of reactions involving electrophilic cyclizations, Wagner-Meerwein rearrangements, hydride/methyl shifts and oxidation then occur to synthesize the final terpenoid products.[3,4] Indeed many sesquiterpene synthases, such as *epi*-cubenol synthase from *Streptomycetes*, patchoulol synthase from *Pogostemon cablin*, epicedrol synthase from *Artemisia annua*, τ-cadinol synthase from *Lavandula angustifolia* are known to produce sesquiterpenoid alcohols *epi*-cubanol,[5] patchoulol,[6] epicedrol,[7] and τ-cadinol[8] respectively by quenching the respective final carbocation with an oxygen nucleophile in a stereoselective manner (Fig. 1).

Cane and co-workers[9] have demonstrated that the hydroxyl group of the borneol synthase product, borneol, is derived from the diphosphate moiety of the acyclic geranyl diphosphate substrate (GPP) (Fig 1).[10] The active site contour of terpene synthases usually is hydrophobic in nature to avoid improper quenching of the cationic intermediate with an external nucleophile such as water.[11] However, isotope labeling studies using *epi*-cubenol synthase,[12] patchoulol synthase,[13] and fenchol synthase[14] demonstrated that the oxygen atoms of the alcohol groups of these compounds are derived from water molecules present in the active site.

Epicedrol synthase[7,15] has been cloned and functionally characterized from *Artemisia annua*, a source of the potent anti-malarial drug, Artimisinin,[16] and is known to catalyze the electrophilic cyclization of achiral universal diphosphate substrate FPP to epicedrol as a major enzymatic product with traces of cedrol and corresponding hydrocarbons. Furthermore, studies have been carried out for the production of epicedrol in metabolically tractable heterologous systems such as *Saccharomyces cerevicea*.[17] Although, epicedrol synthase has been well studied, very little is known regarding the mechanism involved in epicedrol biosynthesis and the source of the oxygen atom.

Our continued interest to study the interface of chemical and biology with a particular emphasis on reaction mechanism[18] and protein function in biology.[19] Herein we studied the source of oxygen atom in epicedrol biosynthesis by carrying out the enzyme assay in $H_2{}^{18}O$.

## Results and discussion

Epicedrol synthase of *A. annua* was expressed in *Escherichia coli* and purified as reported elsewhere.[7] GC and GCMS analysis of the assay containing purified epicedrol synthase and (*E*,*E*)-FPP indicated the formation of epicedrol as a major metabolite (~90%)

* Corresponding authors. Tel.: +91 20 25902329; fax: +91 020 25902629.
*E-mail addresses:* ss.shinde@ncl.res.in (S.S. Shinde), hv.thulasiram@ncl.res.in (H.V. Thulasiram).

http://dx.doi.org/10.1016/j.tetlet.2016.01.109
0040-4039/

RSC Advances

PAPER

Cite this: *RSC Adv.*, 2015, **5**, 68136

# Antibiofilm activity of *tert*-BuOH functionalized ionic liquids with methylsulfonate counteranions†

Govinda R. Navale,[a] Mahesh S. Dharne*[b] and Sandip S. Shinde*[a]

Received 2nd July 2015
Accepted 30th July 2015

DOI: 10.1039/c5ra12854d

www.rsc.org/advances

A series of varying alkyl chain length substituted *tert*-BuOH-functionalized-imidazolium mesylate salts [alkyl-$^t$OHim][OMs] were synthesized and evaluated for antimicrobial activity and antibiofilm potential on selected pathogenic microorganisms including bacteria (Gram positive and Gram negative), yeast, and fungi. The dodecyl substituted ionic liquid [$C_{12}$-$^t$OHim][OMs] significantly prevented the biofilm formation of *S. epidermidis* at 100 μM concentration as well as showed noteworthy antimicrobial activity. We conclude that the ionic liquids (ILs) bearing chain lengths lower than the dodecyl length were found to be less effective against most of the tested pathogenic microorganisms.

## Introduction

Imidazolium-based ionic liquids (ILs) are widely applied in the academic and industry sector as greener solvents or catalysts.[1] Their physical, biological and chemical properties such as being liquids at room temperature, reasonable chemical stability, low flammability, insignificant vapor pressure and high ionic conductivity of ILs are the main motivating factor behind the vast interest in green chemistry applications. Tunability nature of ILs introduces an incomparable flexibility in the design of reagents for a specific functional role.[2] Since a decade, task-specific ILs gained vast interest in developing biological applications such as biocatalysis, biomass transformation, biodegradability, drug delivery, and gene delivery vector.[3]

Numerous studies have demonstrated the antimicrobial activity of various task-specific ionic liquids against both environmental and health concern microorganisms.[4] However, appropriate designing and reasonable application of task-specific ILs bearing toxicity evaluation creates valuable information and possibilities of developing new disinfectants, antiseptics and preservatives.[5] The task-specific imidazolium ILs containing an ester functional group with varying alkyl chain length possesses adsorption efficiency due to enhance the hydrophobicity of the amphiphilic nature of cation (**A**, Fig. 1).[6] Similarly the antimicrobial activity of ILs bearing more than C-10 chain length with alkoxymethyl moiety on other side (**B**, Fig. 1) has been studied against clinically important pathogens.[7] However, ILs bearing halogenated counter anion can produce volatile byproduct such as HF.[8]

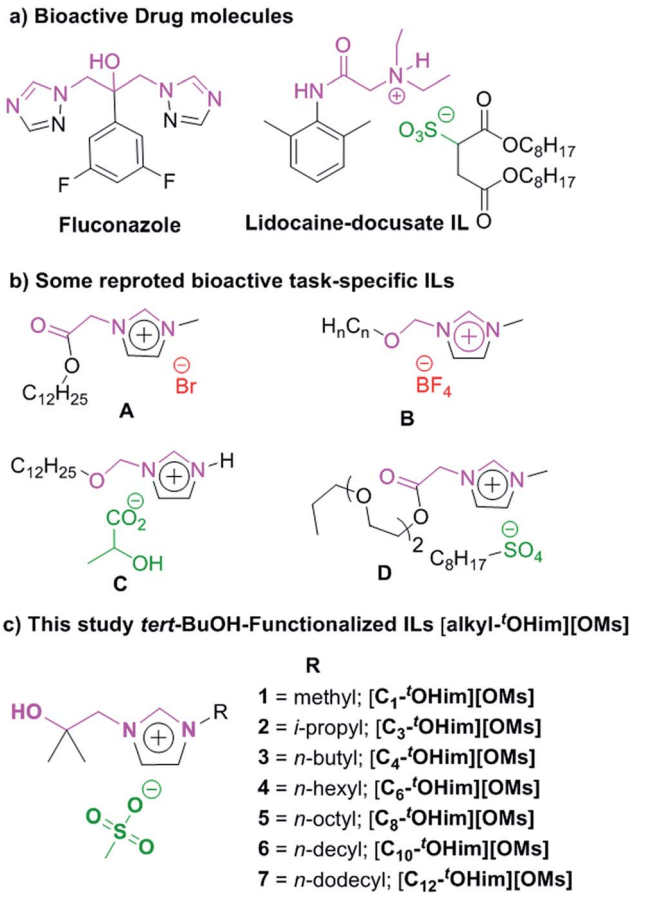


Fig. 1 Bioactive active molecules and task-specific-imidazolium ILs.

[a]*Organic Chemistry Division, National Chemical Laboratory (CSIR-NCL), Dr Homi Bhabha Road, Pashan, Pune-411008, India. E-mail: ss.shinde@ncl.res.in; Fax: +91-20-25902627; Tel: +91-20-25902329*

[b]*NCIM Resource Centre, CSIR-National Chemical Laboratory, Dr Homi Bhabha Road, Pune 411008, Maharashtra, India. E-mail: ms.dharne@ncl.res.in*

† Electronic supplementary information (ESI) available: $^1$H and $^{13}$C NMR of new IL, optical images of biofilm and ILs. See DOI: 10.1039/c5ra12854d

# *Appendix*

# *Terpene cyclase sequences*

- **Farnesyl diphosphate synthase from *Santalum album L.* (*SaFPPS*; *Genbank* No.KF011939.1) 1029 bp**

ATGGGCGATCGGAAAACCAAATTTCTCGAGGCCTACTCTGTCTTGAAATCGGAGCTCCTCCGGGACCCT
GCTTTCAATTTTACAGACGCTTCCCGTCAATGGGTCGACCGGATGCTGGACTACAATGTGCCTGGAGGG
AAACTGAATCGAGGGCTCTCAGTGATTGACAGCTATGAGTTGCTGAAAGAAGGAAAAGAGCTAACTGAT
GATGAAATATTTCTTGCATCTGCACTCGGTTGGTGCATTGAATGGCTTCAAGCATATTTTCTTGTTCTC
GATGATATTATGGATGGCTCTCATACACGCCGAGGTCAGCCTTGTTGGTTCAGGTTGCCTGAGGTTGGT
CTGATTGCTGTAAATGATGGCATAATGCTTCGCAACCACATCCCAAGAATTCTCAAGAAGCACTTCAAA
AATAAGCCTTATTATGTGGAACTGTTGGATTTATTTAATGAGGTCGAGTTCCAAACAACTTCAGGACAG
ATGATAGATTTGATAACCACGCTTGAAGGGCAGAAAGATCTTTCAAAGTATTCAATGCCTATTCACCAT
CGCATTGTTCAGTATAAAACTGCTTATTACTCCTTTTACCTTCCGGTTGCTTGTGCACTGCTTATGTCA
GGTGAGAATCTGGACAGCCACACTGAAGTGGAGAAAATCCTTGTTGAAATGGGAACCTATTTTCAAGTA
CAGGATGATTACCTGGACTGCTTTGGTCATCCTGATGTCATTGGAAAGATTGGAACAGATATTGAAGAT
TTTAAGTGTTCTTGGTTGGTTGTAAAAGCGTTGGAACTTTCCAACGAGGAACAGAAGAAATTATTATAT
GAGAACTATGGGAAAGCCGATGAAGCCAGCGTTGCAAAAGTAAAGGCACTTTATAAGGAACTTGACCTT
GAGGGTGCATTTGTGGAGTACGAGAATGCTAGTTATGAGAAGATAATCAGCTCAATTGAGGTGCAGCCA
AGCAAAGCAGTACAAGCAGTGCTGAAATCCTTTTTGGCGAAGATATACAAGCGGCAGAAGTAG

- **Protein sequence**

MGDRKTKFLEAYSVLKSELLRDPAFNFTDASRQWVDRMLDYNVPGGKLNRGLSVIDSYELLKEGKELTD
DEIFLASALGWCIEWLQAYFLVLDDIMDGSHTRRGQPCWFRLPEVGLIAVNDGIMLRNHIPRILKKHFK
NKPYYVELLDLFNEVEFQTTSGQMIDLITTLEGQKDLSKYSMPIHHRIVQYKTAYYSFYLPVACALLMS
GENLDSHTEVEKILVEMGTYFQVQDDYLDCFGHPDVIGKIGTDIEDFKCSWLVVKALELSNEEQKKLLY
ENYGKADEASVAKVKALYKELDLEGAFVEYENASYEKIISSIEVQPSKAVQAVLKSFLAKIYKRQK

- ***Epi*-cedrol Synthase from *Artemisia annua* (*AaECS*; *Genbank* No. AF157059) 1644 bp**

ATGAGCCTGATTGTTGAAGATGTTATTCGTCCGAATGCAAACTTTCCGAGCGAAATTTGGGGTGATCAG
TTTCTGGCATATGATCAGGATGAACAAGAAGGTGTTGAGCAGGTTATCAAAGATCTGAAAGAAGAAGTG
AAAAGCGAACTGCTGACCGCACTGAATAGCCCGACCCAGCATACCGAACTGCTGAAATTTATCGATGCA
ATTGAACGTCTGGGCATTGCCTATTATTTCGAAGAAGAAATCAACCAGGTCTTTCAGCATATGTATACC
GCCTATGGTGATAAATGGACCGGTGGTAATACCAGCCTGTGGTTTCGTCTGATGCGTCAGCATGGTTTT
TTTGTTAGCAGCGATATCTTCAGCACCTATAAAGATAAAGAGGGTCGCTTTAAAGAAAGCCTGGAAAAA
GATGTTCATGGTCTGCTGGAACTGTATGAAGCAGCATATATGTTTGTTCCGGGTGAAGGTATTCTGGAT
GATGCACTGGTTTTTACCCGTACCTGTCTGGATGAAATTGCAAAAAATCCGAGCCTGAGCAATAGCGCA
GTTAGCAGCCAGATTCGTGAAGCACTGACCCAGCCGCTGCATAAACGTCTGCCTCGTCTGGAAGCACTG
CGTTATATTCCGTTTTATCAGCAGCAGGCAAGCCATAGCGAAACCCTGCTGAAACTGGCAAAACTGGGT
TTTAATCAGCTGCAGAGCCTGCATAAAAAAGAACTGAGCATTATTAGCAAATGGTGGAAAAGCTTTGAT
GTGGCAAATAATCTGCCGTATGCACGTAATCGTCCGGTTGAATGTTATTTTTGGGCACTGGCAGTTTAT
TTTGAACCGCAGTATAGCGAAAGCCGTGTTTTTCTGAGCCGTTTTTTTAGCATTCAGACCTTTCTGGAT
GATACCTATGATGCATATGGCACCTATGAAGAACTGGAACAGTTTACCGAAGCAATTCAGCGTTGGAGC
ATTACCTGCCTGGATGGTCTGCCGGAAAGCATGAAACTGATTTTTCAGATGCTGGTGAAAATCTTTGAA
GAAATCGAAGAAATTCTGAGCAAAGACGGCAAACAGCATCATGTGAACTATATCAAAGAAACCCTGAAA
GAAGCCGTGCAGAGCTATATGACCGAAGCACGTTGGGCAAAAGAAGAATATATTCCGACCATTGAGGAA
CACACCAAAGTGAGCTATATTAGCATTGGTTATAAACTGGCACTGGTTGCAGGTTTTGCATGTATGGGT
GATGTTATTGCAGATGATAGCTTTGAATGGGTGTTTACCAATCCGCCTCTGGTTAATGCATGTTGTCTG
CTGTGTCGTACCATGGATGATCTGGGTAGCCATAAAGGTGAACAGGATCGTAAACATGTTGCAAGCACC
ATTGAGTGCTATATGAAACAGTTTGATGCAAGCGAACAGCAGGCATATGAAAGCCTGAACAAAAAAGTT
GAAGATGCCTGGAAAGAAATTAATCGCGAATTCATGATTACCTGCAAAGACGTGAATATTCATGTTGCA

ATGCGCGTGCTGAATTTTAGCCGTAGCGTTGATGTTCTGTATAAAAACAAAGATCACTTTACCCATGTG
GGCGTGGAAGTGATTAATCATATCAAAAGCCTGTTTGTGGATGCCATCATCACCTAA

- **Protein sequence**

MSLIVEDVIRPNANFPSEIWGDQFLAYDQDEQEGVEQVIKDLKEEVKSELLTALNSPTQHTELLKFIDA
IERLGIAYYFEEEINQVFQHMYTAYGDKWTGGNTSLWFRLMRQHGFFVSSDIFSTYKDKEGRFKESLEK
DVHGLLELYEAAYMFVPGEGILDDALVFTRTCLDEIAKNPSLSNSAVSSQIREALTQPLHKRLPRLEAL
RYIPFYQQQASHSETLLKLAKLGFNQLQSLHKKELSIISKWWKSFDVANNLPYARNRPVECYFWALAVY
FEPQYSESRVFLSRFFSIQTFLDDTYDAYGTYEELEQFTEAIQRWSITCLDGLPESMKLIFQMLVKIFE
EIEEILSKDGKQHHVNYIKETLKEAVQSYMTEARWAKEEYIPTIEEHTKVSYISIGYKLALVAGFACMG
DVIADDSFEWVFTNPPLVNACCLLCRTMDDLGSHKGEQDRKHVASTIECYMKQFDASEQQAYESLNKKV
EDAWKEINREFMITCKDVNIHVAMRVLNFSRSVDVLYKNKDHFTHVGVEVINHIKSLFVDAIIT

- **Santelene synthase from *Santelum album L.* ((*SaSS*, Acc. No.KF011938) 1686 bp**

ATGACAGCTCCATTCATTGATCCTACTGATCATGTGAATCTCAAAACTGATACGGATGCCTCAGAGAAT
CGAAGGATGGGAAATTATAAACCCAGCATTTGGAATTATGATTTTTTACAATCACTTGCAACTCATCAC
AATATTGTGGAAGAGAGGCATCTAAAGCTAGCTGAGAAGCTGAAGGGCCAAGTGAAGTTTATGTTTGGG
GCACCAATGGAGCCGTTAGCAAAGCTGGAGCTTGTGGATGTGGTTCAAAGGCTTGGGCTAAACCACCTA
TTTGAGACAGAGATCAAGGAAGCGCTGTTTAGTATTTACAAGGATGGGAGCAATGGATGGTGGTTTGGC
CACCTTCATGCGACATCTCTCCGATTTAGGCTGCTACGACAGTGTGGGCTTTTTATTCCCCAAGATGTG
TTTAAAACGTTCCAAAACAAGACTGGGGAATTTGATATGAAACTTTGTGACAACGTAAAAGGGCTGCTG
AGCTTATATGAAGCTTCATACTTGGGATGGAAGGGTGAAAACATCCTAGATGAAGCCAAGGCCTTCACC
ACCAAGTGCTTGAAAAGTGCATGGGAAAATATATCCGAAAAGTGGTTAGCCAAAAGAGTGAAGCATGCA
TTGGCTTTGCCTTTGCATTGGAGAGTCCCTCGAATCGAAGCTAGATGGTTCATTGAGGCATATGAGCAA
GAAGCGAATATGAACCCAACACTACTCAAACTCGCAAAATTAGACTTTAATATGGTGCAATCAATTCAT
CAGAAAGAGATTGGGGAATTAGCAAGGTGGTGGGTGACTACTGGCTTGGATAAGTTAGCCTTTGCCAGG
AATAATTTACTGCAGAGCTATATGTGGAGCTGCGCGATTGCTTCCGACCCGAAGTTCAAACTTGCTAGA
GAAACTATTGTCGAAATCGGAAGTGTACTCACAGTTGTTGACGATGGATATGACGTCTATGGTTCAATC
GACGAACTTGATCTCTACACAAGCTCCGTTGAAAGGTGGAGCTGTGTGGAAATTGACAAGTTGCCAAAC
ACGTTAAAATTAATTTTTATGTCTATGTTCAACAAGACCAATGAGGTTGGCCTTCGAGTCCAGCATGAG
CGAGGCTACAATAGCATCCCTACTTTTATCAAAGCGTGGGTTGAACAGTGTAAATCATACCAGAAAGAA
GCAAGATGGTTCCACGGGGGACACACGCCTCCATTGGAAGAATATAGCTTGAATGGACTTGTTTCCATA
GGATTCCCTCTCTTGTTAATCACGGGCTACGTGGCAATCGCTGAGAACGAGGCTGCACTGGATAAAGTG
CACCCCCTTCCTGATCTTCTGCACTACTCCTCCCTCCTTAGTCGCCTCATCAATGATATAGGAACGTCT
CCGGATGAGATGGCAAGAGGCGATAATCTGAAGTCAATCCATTGTTACATGAACGAAACTGGGGCTTCC
GAGGAAGTTGCTCGTGAGCACATAAAGGGAGTAATCGAGGAGAATTGGAAAATACTGAATCAGTGCTGC
TTTGATCAATCTCAGTTTCAGGAGCCTTTTATAACCTTCAATTTGAACTCTGTTCGAGGGTCTCATTTC
TTCTATGAATTTGGGGATGGCTTTGGGGTGACGGATAGCTGGACAAAGGTTGATATGAAGTCCGTTTTG
ATCGACCCTATTCCTCTCGGCGAGGAGTAG

- **Protein sequence**

MDSSTATAMTAPFIDPTDHVNLKTDTDASENRRMGNYKPSIWNYDFLQSLATHHNIVEERHLKLAEKLK
GQVKFMFGAPMEPLAKLELVDVVQRLGLNHLFETEIKEALFSIYKDGSNGWWFGHLHATSLRFRLLRQC
GLFIPQDVFKTFQNKTGEFDMKLCDNVKGLLSLYEASYLGWKGENILDEAKAFTTKCLKSAWENISEKW
LAKRVKHALALPLHWRVPRIEARWFIEAYEQEANMNPTLLKLAKLDFNMVQSIHQKEIGELARWWVTTG
LDKLAFARNNLLQSYMWSCAIASDPKFKLARETIVEIGSVLTVVDDGYDVYGSIDELDLYTSSVERWSC
VEIDKLPNTLKLIFMSMFNKTNEVGLRVQHERGYNSIPTFIKAWVEQCKSYQKEARWFHGGHTPPLEEY
SLNGLVSIGFPLLLITGYVAIAENEAALDKVHPLPDLLHYSSLLSRLINDIGTSPDEMARGDNLKSIHC
YMNETGASEEVAREHIKGVIEENWKILNQCCFDQSQFQEPFITFNLNSVRGSHFFYEFGDGFGVTDSWT
KVDMKSVLIDPIPLGEE

| Items | Concentration / Volume |
|---|---|
| Ampicillin (100 mg/mL) | add 1 g ampicillin to 10 mL $dH_2O$, sterilize solution transfer through syringe filter (0.2 mm), prepare 1.0 mL aliquots in individual Eppendorf tubes, and store at –20º C. |
| Chloramphenicol (35 mg/mL) | add 0.35 g Chloramphenicol to 10 mL $dH_2O$, sterilize solution transfer through syringe filter (0.2 mm), prepare 1.0 mL aliquots in individual Eppendorf tubes, and store at –20º C. |
| Kanamycin ((50 mg/mL)) | add 0.50 g Kanamycin to 10 mL $dH_2O$, sterilize solution transfer through syringe filter (0.2 mm), prepare 1.0 mL aliquots in individual Eppendorf tubes, and store at –20º C. |
| IPTG (1 M stock) | 2.38 g IPTG in 10 mL $dH_2O$ (sterilize solution through syringe filter (0.22 mm) |
| Lysis buffer (50 mL) | Tris (50 mM) - 0.6 gm.<br>NaCl (300 mM)- 0.87 gm.<br>Glycerol (10%)<br>pH- 8.0 |
| Wash buffer (100 mL) | Tris (50 mM)- 1.2 gm.<br>NaCl (300mM)- 1.74 gm.<br>Glycerol (10%)<br>Imidazole (40 mM)- 0.272 gm. |
| Elution buffer (50 mL) | Tris (50 mM) - 0.6 gm.<br>NaCl (300 mM)- 0.87 gm.<br>Glycerol (10%)<br>Imidazole (40 mM)- 0.85 gm |
| 5x Tris- SDS buffer (1000 mL) | Tries base (25 mM)- 15.1 gm<br>Glycine (190 mM)- 90 gm<br>SDS (10 %)- 50 mL<br>adjust with Milli Q water to final volume 1000 mL |

| | |
|---|---|
| Destining solution (100 mL) | Methanol (50 %)- 50 mL<br>Acetic accid-10 %<br>Water- 40 % |
| **SDS Gel** | |
| Resolving gel (5mL) | 30% Acrylamide – 2 mL<br>Water- 1.6 mL<br>1.5 M Tris (pH-8.8)- 1.3 mL<br>10 % SDS- 0.05 mL<br>10 % APS- 0.05 mL<br>TEMED- 0.002 mL |
| Stacking gel (2mL) | 30% Acrylamide- 0.33 mL<br>Water- 1.4 mL<br>1M Tris (pH-6.8) -0.25 mL<br>10% SDS- 0.02 mL<br>10% APS- 0.02 mL<br>TEMED- 0.002 mL |
| Tris-Glycine running buffer (5x) | Tris- 15 g<br>Glycine- 72 g<br>SDS- 5 g |
| Coomassie Blue Stain | Acetic acid- 10% (v/v)<br>Coomassie Blue dye- 0.006% (w/v)<br>90 % dd$H_2O$ |
| SDS sample loading buffer (40 mL) | dd$H_2O$ 16 ml<br>0.5 M Tris - 5 ml<br>pH 6.8<br>50 % Glycerol<br>10 % SDS- 8 ml<br>2-βmercaptoethanol- 2 ml<br>bromophenol blue – 0.25 g<br>acetic acid- 10 % (v/v) |
| Terrific Broth preparation (1L) | Tryptone- 12 g<br>Yeast extract- 24 g |

| | |
|---|---|
| | Potassium phosphate monobasic- 2.2 g<br>Potassium phosphate Dibasic- 9.4 g<br>pH- 7.2 (at 25 °C)<br>Glycerol- 4 mL |
| Luria Broth (Himedia) | 40 g/1 |
| CSM-w/o URA broth (Himedia) | 790 mg in 1 L distilled water. Sterilize by autoclaving at 10 lbs pressure (115 ºC) for 20 minutes. Mix well and dispense as desired. |
| Yeast nitrogen base w/o ammonium sulphate (Himedia) | 6.75 g in 1 L distilled water. Sterilize by autoclaving at 10 lbs pressure (115 ºC) for 20 minutes. Mix well and dispense as desired |
| Yeast Peptone dextrose broth (YPD) | 10 g of Yeast extract in 500 ml water.<br>20g of Peptone in the above solution<br>20 g Dextrose in the above solution<br>Make it up to 1000 mL with water and Autoclave it. |
| MGYP medium | Malt extract- 0.3 g<br>Glucose – 1 g<br>Yeast extract- 0.3 g<br>Peptone 0.5 g<br>Distilled water 1 L<br>Adjust pH to 6.4-6.8 |
| 20 % Galactose | 20 g galactose in 100 mL distilled water. Sterilize by autoclaving at 10 lbs pressure (115 ºC) for 20 minutes. Mix well and dispense as desired |
| 20 % Raffinose | 20 g raffinose in 100 mL distilled water. Sterilize by autoclaving at 10 lbs pressure (115 ºC) for 20 minutes. Mix well and dispense as desired |
| 20 % Glucose | 20 g glucose in 100 mL distilled water. Sterilize by autoclaving at 10 lbs pressure (115 ºC) for 20 minutes. Mix well and dispense as desired |
| EDTA (50 mM) | 18.60 g added in 500 mL distilled water |

| | |
|---|---|
| Nickel-chloride hexahydrate (8mg/mL) | 8 g added in 1 L Milli Q water |
| **Phosphate buffer** | |
| Lysis buffer (500 mL) | $Na_2HPO_4$ (50 mM) - 3.525g<br>NaCl(300mM)- 8.7g<br>Glycerol (10 %)- 50 mL<br>Imidazole (10 mM)- 0.34g<br>pH- 7.4 |
| Wash buffer (1L) | $Na_2HPO_4$ (50mM)- 7.05 g<br>NaCl (300mM)- 17 g<br>Glycerol-10 %<br>Imidazole (35mM)- 2.38<br>pH-7.4 |
| Elution buffer (200 mL) | $Na_2HPO_4$ (50mM)- 1.41 g<br>NaCl (300mM)- 3.48 g<br>Glycerol- 10 %<br>Imidazole (250 mM)- 3.43 g<br>pH- 7.4 |
| **HEPES buffer** | |
| Lysis buffer (200 mL) | HEPES (50 mM)- 2.38<br>NaCl (300 mM)- 3.48g<br>Glycerol- 10 %<br>Imidazole (10 mM)- 0.13g<br>pH- 7.8 |
| Wash buffer (1 L) | HEPES (50mM)- 11.9g/1L<br>NaCl (300 mM)- 17.4g/1L<br>Glycerol- 10%<br>Imidazole (35 mM)- 2.38g/1L<br>pH- 7.8 |
| Elution buffer (200 mL) | HEPES (50 mM)- 2.38 g<br>NaCl (300 mM)- 3.48 g<br>Glycerol- 10 %<br>Imidazole (250 mM) - 3.43g<br>pH- 7.8 |

| | |
|---|---|
| **Desalting buffers** | |
| Phosphate buffer | $Na_2HPO_4$ (50 mM)- 7.0 g/L<br>NaCl (100 mM)- 5.8 g/L<br>Glycerol- 10 %<br>pH- 7.4 |
| HEPES buffer | HEPES (50 mM)- 11.9 g/L<br>NaCl (100 mM) – 5.8 g/L<br>Glycerol- 10 %<br>pH- 7.4 |
| Enzyme Assay buffer (50 mL) | Tries (25 mM)- 0.07 g<br>$Mgcl_2$ (10 mM)- 0.04 g<br>Glycerol- 10 %<br>Adjust volume up to 50 mL with Milli Q water. |
| Lysozyme | 10 mg/mL stock |
| 10 % SDS (100 mL) | 10 g SDS in 90 mL Milli Q, filter the solution using 0.45µ filter unit |
| 10 % APS | 1 g APS in 9 mL Milli Q, filter the solution using 0.45µ filter unit |